REPUBLIC OF CAMEROON
Peace- Work- Fatherland

THE UNIVERSITY OF YAOUNDE I

POSTGRADUATE SCHOOL OF SCIENCE, TECHNOLOGY AND GEOSCIENCES

RESEARCH AND DOCTORAL TRAINING UNIT IN CHEMISTRY AND APPLICATIONS

REPUBLIQUE DU CAMEROUN
Paix- Travail- Patrie

UNIVERSITE DE YAOUNDE I

CENTRE DE RECHERCHE ET DE FORMATION DOCTORALE EN SCIENCES, TECHNOLOGIE ET GEOSCIENCES

UNITE DE RECHERCHE ET DE FORMATION DOCTORALE EN CHIMIE ET APPLICATIONS

DEPARTMENT OF ORGANIC CHEMISTRY
DEPARTEMENT DE CHIMIE ORGANIQUE

LABORATORY OF NATURAL PRODUCTS AND APPLIED ORGANIC SYNTHESIS (LANAPOS)
LABORATOIRE DE SUBSTANCES NATURELLES ET DE SYNTHESES ORGANIQUE APPLIQUEE

Phytochemical studies of *Diospyros gilletii* De Wild and *Diospyros fragrans* Gürke (Ebenaceae), chemical transformations and antibacterial, antioxidant and cytotoxic activities of extracts and isolated compounds

Thesis submitted and publicly defended for the award of Doctorat / Ph.D in Chemistry

Option : Organic Chemistry

By :

JOUWA TAMEYE Nathalie Samantha

Matricule : 17T5845

D.E.A. in Chemistry-Biology

Under the co-Direction of:

MVOT AKAK Carine

Associate Professor

University of Yaoundé I

NKENGFACK Augustin Ephrem

Professor

University of Yaoundé I

Academic Year 2021-2022

RÉPUBLIQUE DU CAMEROUN
Paix - Travail - Patrie
UNIVERSITÉ DE YAOUNDÉ I
Faculté des sciences

REPUBLIC OF CAMEROON
Peace- Work-Fatherland
THE UNIVERSITY OF YAOUNDE I
Faculty of Science

DEPARTEMENT DE CHIMIE ORGANIQUE
DEPARTMENT OF ORGANIC CHEMISTRY

ATTESTATION DE CORRECTION DU MEMOIRE DE THESE DE DOCTORAT/Ph.D DE MADAME JOUWA TAMEYE Nathalie Samantha, matricule 17T5845

Titre de la these : « Phytochemical studies of *Diospyros gilletii* De Wild and *Diospyros fragrans* Gürke (Ebenaceae), chemical transformations and antibacterial, antioxidant and cytotoxic activities of extracts and isolated compounds ».

Nous soussignés, enseignants ci-dessous nommés, membres du jury de soutenance de thèse de Doctorat/Ph.D de Madame **JOUWA TAMEYE Nathalie Samantha**, matricule **17T5845** attestons que cette candidate a bel et bien pris en compte dans la mouture finale de sa thèse, toutes les corrections et recommandations qui lui ont été faites au cours de sa soutenance en date du **21 Décembre 2021**.

En foi de quoi, la présente attestation de correction lui est délivrée pour servir et valoir ce que de droit.

Fait à Yaoundé, le 13 Janvier 2022

Le Jury:

Le President:

NGADJUI TCHALEU Bonaventure, *Professeur*

Les Rapporteurs:

NKENGFACK AUGUSTIN Ephrem, *Professeur*

MVOT AKAK Carine, *Maître de Conférences*

Examinateur:

NOUNGOUE TCHAMO Diderot, *Maître de Conférences*

PROTOCOL LIST

THE UNIVERSITY OF YAOUNDE I **Faculty of Science** Division of Programming and Follow-up of Academic Affaires		*UNIVERSITE DE YAOUNDE I* *Faculté des Sciences* *Division de la Programmation et du Suivi des Activités Academiques*
LIST OF PERMANENT TEACHING STAFF		**LISTE DES ENSEIGNANTS PERMANENTS**

OFFICIAL LIST OF LECTURERS OF THE FACULTY OF SCIENCE

ACADEMIC YEAR 2021/2022

(*by Department and by Grade*)

LAST UPDATED: July 12, 2021

ADMINISTRATION

Dean: TCHOUANKEU Jean- Claude, Associate Professor

Vice Dean in Charge of Academic Affairs: ATCHADE Alex de Théodore, Associate Professor

Vice Dean in Charge of Student Affairs: NYEGUE Maximilienne Ascension, Professor

Vice Dean in Charge of Research and Cooperation: ABOSSOLO Monique, Associate Professor

Head of Administrative and Financial Division: NDOYE FOE Marie C. F., Associate Professor

Head of Academic Affairs division, Keeping of Terms and Research: AJEAGAH Gideon AGHAINDUM, Professor

1- DEPARTMENT OF BIOCHEMISTRY (BCH) (37)			
N°	**NAME AND SURNAME**	**GRADE**	**OBSERVATIONS**
1	BIGOGA DIAGA Jude	Professor	In service
2	FEKAM BOYOM Fabrice	Professor	In service
3	FOKOU Elie	Professor	In service
4	KANSCI Germain	Professor	In service
5	MBACHAM FON Wilfried	Professor	In service

6	MOUNDIPA FEWOU Paul	Professor	**Head of Department**
7	NINTCHOM PENLAP V. épse BENG	Professor	In service
8	OBEN Julius ENYONG	Professor	In service
9	ACHU Merci BIH	Associate Professor	In service
10	ATOGHO Barbara Mma	Associate Professor	In service
11	AZANTSA KINGUE GABIN BORIS	Associate Professor	In service
12	BELINGA née NDOYE FOE M. C. F.	Associate Professor	**Chief DAF / FS**
13	BOUDJEKO Thaddée	Associate Professor	In service
14	DJUIDJE NGOUNOUE Marcelline	Associate Professor	In service
15	EFFA NNOMO Pierre	Associate Professor	In service
16	NANA Louise épouse WAKAM	Associate Professor	In service
17	NGONDI Judith Laure	Associate Professor	In service
18	NGUEFACK Julienne	Associate Professor	In service
19	NJAYOU Frédéric Nico	Associate Professor	In service
20	MOFOR née TEUGWA Clotilde	Associate Professor	**Insp. Serv. MINESUP**
21	TCHANA KOUATCHOUA Angèle	Associate Professor	In service
22	AKINDEH MBUH NJI	Senior Lecturer	In service
23	BEBOY EDZENGUELE Sara N.	Senior Lecturer	In service
24	DAKOLE DABOY Charles	Senior Lecturer	In service
25	DJUIKWO NKONGA Ruth Viviane	Senior Lecturer	In service
26	DONGMO LEKAGNE Joseph Blaise	Senior Lecturer	In service
27	FONKOUA Martin	Senior Lecturer	In service
28	BEBEE Fadimatou	Senior Lecturer	In service
29	KOTUE KAPTUE Charles	Senior Lecturer	In service
30	LUNGA Paul KEILAH	Senior Lecturer	In service
31	MANANGA Marlyse Joséphine	Senior Lecturer	In service
32	MBONG ANGIE M. Mary Anne	Senior Lecturer	In service
33	PECHANGOU NSANGOU Sylvain	Senior Lecturer	In service
34	Palmer MASUMBE NETONGO	Senior Lecturer	In service
35	MBOUCHE FANMOE Marceline J.	Assist. Lecturer	In service
36	OWONA AYISSI Vincent Brice	Assist. Lecturer	In service
37	WILFRIED ANGIE Abia	Assist. Lecturer	In service
2- DEPARTMENT OF ANIMAL BIOLOGY AND PHYSIOLOGY (A. B. P.) (48)			

1	AJEAGAH Gideon AGHAINDUM	Professor	**DAASR**
2	BILONG BILONG Charles-Félix	Professor	**Head of Department**
3	DIMO Théophile	Professor	In service
4	DJIETO LORDON Champlain	Professor	In service
5	ESSOMBA née NTSAMA MBALA	Professor	**Vice dean/FMSB/UYI**
6	FOMENA Abraham	Professor	In service
7	KAMTCHOUING Pierre	Professor	In service
8	NJAMEN Dieudonné	Professor	In service
9	NJIOKOU Flobert	Professor	In service
10	NOLA Moïse	Professor	In service
11	TAN Paul VERNYUY	Professor	In service
12	TCHUEM TCHUENTE Louis Albert	Professor	**Insp. Serv. Coord. Progr. in HEALTH**
13	ZEBAZE TOGOUET Serge Hubert	Professor	In service
14	BILANDA Danielle Claude	Associate Professor	In service
15	DJIOGUE Séfirin	Associate Professor	In service
16	DZEUFIET DJOMENI Paul Désiré	Associate Professor	In service
17	JATSA BOUKENG Hermine épse M.	Associate Professor	In service
18	KEKEUNOU Sévilor	Associate Professor	In service
19	MEGNEKOU Rosette	Associate Professor	In service
20	MONY Ruth épse NTONE	Associate Professor	In service
21	NGUEGUIM TSOFACK Florence	Associate Professor	In service
22	TOMBI Jeannette	Associate Professor	In service
23	ALENE Désirée Chantal	Senior Lecturer	In service
26	ATSAMO Albert Donatien	Senior Lecturer	In service
27	BELLET EDIMO Oscar Roger	Senior Lecturer	In service
28	DONFACK Mireille	Senior Lecturer	In service
29	ETEME ENAMA Serge	Senior Lecturer	In service
30	GOUNOUE KAMKUMO Raceline	Senior Lecturer	In service
31	KANDEDA KAVAYE Antoine	Senior Lecturer	In service
32	LEKEUFACK FOLEFACK Guy B.	Senior Lecturer	In service
33	MAHOB Raymond Joseph	Senior Lecturer	In service
34	MBENOUN MASSE Paul Serge	Senior Lecturer	In service

35	MOUNGANG LucianeMarlyse	Senior Lecturer	In service
36	MVEYO NDANKEU Yves Patrick	Senior Lecturer	In service
37	NGOUATEU KENFACK Omer Bébé	Senior Lecturer	In service
38	NGUEMBOK	Senior Lecturer	In service
39	NJUA Clarisse Yafi	Senior Lecturer	**Chief of Division/UBA**
40	NOAH EWOTI Olive Vivien	Senior Lecturer	In service
41	TADU Zephyrin	Senior Lecturer	In service
42	TAMSA ARFAO Antoine	Senior Lecturer	In service
43	YEDE	Senior Lecturer	In service
44	BASSOCK BAYIHA Etienne Didier	Assist. Lecturer	In service
45	ESSAMA MBIDA Désirée Sandrine	Assist. Lecturer	In service
46	KOGA MANG DOBARA	Assist. Lecturer	In service
47	LEME BANOCK Lucie	Assist. Lecturer	In service
48	YOUNOUSSA LAME	Assist. Lecturer	In service
3- DEPARTMENT OF PLANT BIOLOGY AND PHYSIOLOGY (P. B. P.) (33)			
1	AMBANG Zachée	Professor	**Chief of Division/UYII**
2	BELL Joseph Martin	Professor	In service
3	DJOCGOUE Pierre François	Professor	In service
4	MOSSEBO Dominique Claude	Professor	In service
5	YOUMBI Emmanuel	Professor	**Head of Department**
6	ZAPFACK Louis	Professor	In service
7	ANGONI Hyacinthe	Associate Professor	In service
8	BIYE Elvire Hortense	Associate Professor	In service
9	KENGNE NOUMSI Ives Magloire	Associate Professor	In service
10	MALA Armand William	Associate Professor	In service
11	MBARGA BINDZI Marie Alain	Associate Professor	**CT/ MINESUP**
12	MBOLO Marie	Associate Professor	In service
13	NDONGO BEKOLO	Associate Professor	**CE/MINRESI**
14	NGODO MELINGUI Jean Baptiste	Associate Professor	In service
15	NGONKEU MAGAPTCHE Eddy L.	Associate Professor	In service
16	TSOATA Esaïe	Associate Professor	In service
17	TONFACK Libert Brice	Associate Professor	In service
18	DJEUANI Astride Carole	Senior Lecturer	In service

19	GOMANDJE Christelle	Senior Lecturer	In service
20	MAFFO MAFFO Nicole Liliane	Senior Lecturer	In service
21	MAHBOU SOMO TOUKAM G.	Senior Lecturer	In service
22	NGALLE Hermine BILLE	Senior Lecturer	In service
23	NGOUO Lucas Vincent	Senior Lecturer	In service
24	NNANGA MEBENGA Ruth Laure	Senior Lecturer	In service
25	NOUKEU KOUAKAM Armelle	Senior Lecturer	In service
26	ONANA JEAN MICHEL	Senior Lecturer	In service
27	GODSWILL NTSOMBAH N.	Assist. Lecturer	In service
28	KABELONG BANAHO Louis-P.-R.	Assist. Lecturer	In service
29	KONO Léon Dieudonné	Assist. Lecturer	In service
30	LIBALAH Moses BAKONCK	Assist. Lecturer	In service
31	LIKENG-LI-NGUE Benoit C	Assist. Lecturer	In service
32	TAEDOUNG Evariste Hermann	Assist. Lecturer	In service
33	TEMEGNE NONO Carine	Assist. Lecturer	In service
4- DEPARTMENT OF INORGANIC CHEMISTRY (I. C.) (35)			
1	AGWARA ONDOH Moïse	Professor	**Head of Department**
2	ELIMBI Antoine	Professor	In service
3	Florence UFI CHINJE épouse MELO	Professor	**Rector Univ. Ngaoundere**
4	GHOGOMU Paul MINGO	Professor	**Minister in charge of mission. P.R.**
5	NANSEU Njiki Charles Péguy	Professor	In service
6	NDIFON Peter TEKE	Professor	**C.T. MINRESI**
7	NGOMO Horace MANGA	Professor	**Vice Chancellor/U.B.**
8	NDIKONTAR Maurice KOR	Professor	**Vice-Dean Un. Bamenda**
9	NENWA Justin	Professor	In service
10	NGAMENI Emmanuel	Professor	**Dean F.S. U. Ds**
11	BABALE née DJAM DOUDOU	Associate Professor	**Mission manager P.R.**
12	DJOUFAC WOUMFO Emmanuel	Associate Professor	In service
13	KAMGANG YOUBI Georges	Associate Professor	In service
14	KEMMEGNE MBOUGUEM Jean C.	Associate Professor	In service
15	KONG SAKEO	Associate Professor	In service

16	NDI NSAMI Julius	Associate Professor	In service
17	NJIOMOU C. épse DJANGANG	Associate Professor	In service
18	NJOYA Dayirou	Associate Professor	In service
19	YOUNANG Elie	Associate Professor	In service
20	ACAYANKA Elie	Senior Lecturer	In service
21	BELIBI BELIBI Placide Désiré	Senior Lecturer	**CS/ ENS Bertoua**
22	CHEUMANI YONA Arnaud M.	Senior Lecturer	In service
23	EMADACK Alphonse	Senior Lecturer	In service
24	KENNE DEDZO GUSTAVE	Senior Lecturer	In service
25	KOUOTOU DAOUDA	Senior Lecturer	In service
26	MAKON Thomas Beauregard	Senior Lecturer	In service
27	MBEY Jean Aime	Senior Lecturer	In service
28	NCHIMI NONO KATIA	Senior Lecturer	In service
29	NEBA nee NDOSIRI Bridget N.	Senior Lecturer	**CT/ MINFEM**
30	NYAMEN Linda Dyorisse	Senior Lecturer	In service
31	PABOUDAM GBAMBIE A.	Senior Lecturer	In service
32	TCHAKOUTE KOUAMO Hervé	Senior Lecturer	In service
33	NJANKWA NJABONG N. Eric	Assist. Lecturer	In service
34	PATOUOSSA ISSOFA	Assist. Lecturer	In service
35	SIEWE Jean Mermoz	Assist. Lecturer	In service
5- DEPARTMENT OF ORGANIC CHEMISTRY (O. C.) (40)			
1	DONGO Etienne	Professor	**Vice Dean/CSA/ *F. SED***
2	GHOGOMU TIH Robert Ralph	Professor	**Director B. A. I Foumban**
3	NGOUELA Silvère Augustin	Professor	**Head of Department UDs**
4	NKENGFACK Augustin Ephrem	Professor	In service
5	NYASSE Barthélemy	Professor	In service
6	PEGNYEMB Dieudonné Emmanuel	Professor	**Director MINESUP/ Head of Department**
7	WANDJI Jean	Professor	In service
8	Alex de Théodore ATCHADE	Associate Professor	**Vice-Dean/PSAA**
9	EYONG Kenneth OBEN	Associate Professor	In service
10	FOLEFOC Gabriel NGOSONG	Associate Professor	In service

11	FOTSO WABO Ghislain	Associate Professor	In service
12	KEUMEDJIO Félix	Associate Professor	In service
13	KEUMOGNE Marguerite	Associate Professor	In service
14	KOUAM Jacques	Associate Professor	In service
15	MBAZOA née DJAMA Céline	Associate Professor	In service
16	MKOUNGA Pierre	Associate Professor	In service
17	NOTE LOUGBOT Olivier Placide	Associate Professor	**Chief Service/MINESUP**
18	NGO MBING Joséphine	Associate Professor	**Sous/Direct. MINERESI**
19	NGONO BIKOBO Dominique Serge	Associate Professor	**Study charge Ass. n°3/MINESUP**
20	NOUNGOUE TCHAMO Diderot	Associate Professor	In service
21	TABOPDA KUATE Turibio	Associate Professor	In service
22	TCHOUANKEU Jean-Claude	Associate Professor	**Dean/FS/ UY1**
23	TIH née NGO BILONG E. Anastasie	Associate Professor	In service
24	YANKEP Emmanuel	Associate Professor	In service
25	MVOT AKAK Carine	Associate Professor	In service
26	AMBASSA Pantaléon	Associate Professor	In service
27	TAGATSING FOTSING Maurice	Associate Professor	In service
28	ZONDENDEGOUMBA Ernestine	Associate Professor	In service
29	KAMTO Eutrophe Le Doux	Senior Lecturer	In service
30	NGNINTEDO Dominique	Senior Lecturer	In service
31	NGOMO Orléans	Senior Lecturer	In service
32	OUAHOUO WACHE Blandine M.	Senior Lecturer	In service
33	SIELINOU TEDJON Valérie	Senior Lecturer	In service
34	MESSI Angélique Nicolas	Assist. Lecturer	In service
35	TSEMEUGNE Joseph	Assist. Lecturer	In service
36	TCHAMGOUE Joseph	Assist. Lecturer	In service
37	TSAFACK Maurice	Assist. Lecturer	In service
38	TSAMO Armelle	Assist. Lecturer	In service
39	NONO Eric Carly	Assist. Lecturer	In service
40	OUETE Judith	Assist. Lecturer	In service
6- DEPARTMENT OF COMPUTER SCIENCE (C. S.) (25)			
1	ATSA ETOUNDI Roger	Professor	**Chief Div.MINESUP**

2	FOUDA NDJODO Marcel Laurent	Professor	**Head of Dpt HTTC/Chief IGA. MINESUP**
3	NDOUNDAM Réné	Associate Professor	In service
4	AMINOU Halidou	Senior Lecturer	**Head of Department**
5	DJAM Xaviera YOUH - KIMBI	Senior Lecturer	In service
6	EBELE Serge Alain	Senior Lecturer	In service
7	KOUOKAM KOUOKAM E. A.	Senior Lecturer	In service
8	MELATAGIA YONTA Paulin	Senior Lecturer	In service
9	MOTO MPONG Serge Alain	Senior Lecturer	In service
10	TAPAMO Hyppolite	Senior Lecturer	In service
11	ABESSOLO ALO'O Gislain	Senior Lecturer	In service
12	MONTHE DJIADEU Valery M.	Senior Lecturer	In service
13	OLLE OLLE Daniel Claude Delort	Senior Lecturer	**C/D Enset. Ebolowa**
14	TINDO Gilbert	Senior Lecturer	In service
15	TSOPZE Norbert	Senior Lecturer	In service
16	WAKU KOUAMOU Jules	Senior Lecturer	In service
17	BAYEM Jacques Narcisse	Assist. Lecturer	In service
18	DOMGA KOMGUEM Rodrigue	Assist. Lecturer	In service
19	EKODECK Stéphane Gaël Raymond	Assist. Lecturer	In service
20	HAMZA Adamou	Assist. Lecturer	In service
21	JIOMEKONG AZANZI Fidel	Assist. Lecturer	In service
22	MAKEMBE. S. Oswald	Assist. Lecturer	In service
23	MESSI NGUELE Thomas	Assist. Lecturer	In service
24	MEYEMDOU Nadège Sylvianne	Assist. Lecturer	In service
25	NKONDOCK. MI. BAHANACK.N.	Assist. Lecturer	In service
7- DEPARTMENT OF MATHEMATICS (MAT) (30)			
1	EMVUDU WONO Yves S.	Professor	**CD Info/Inspecteur MINESUP**
2	AYISSI Raoult Domingo	Associate Professor	**Head of Department**
3	NKUIMI JUGNIA Célestin	Associate Professor	In service
4	NOUNDJEU Pierre	Associate Professor	**Chief serv. certif. prog.**
5	MBEHOU Mohamed	Associate Professor	In service

6	TCHAPNDA NJABO Sophonie B.	Associate Professor	**Director/AIMS Rwanda**
7	AGHOUKENG JIOFACK Jean G.	Senior Lecturer	**Chief Cell MINPLAMAT**
8	CHENDJOU Gilbert	Senior Lecturer	In service
9	DJIADEU NGAHA Michel	Senior Lecturer	In service
10	DOUANLA YONTA Herman	Senior Lecturer	In service
11	FOMEKONG Christophe	Senior Lecturer	In service
12	KIANPI Maurice	Senior Lecturer	In service
13	KIKI Maxime Armand	Senior Lecturer	In service
14	MBAKOP Guy Merlin	Senior Lecturer	In service
15	MBANG Joseph	Senior Lecturer	In service
16	MBELE BIDIMA Martin Ledoux	Senior Lecturer	In service
17	MENGUE MENGUE David Joe	Senior Lecturer	In service
18	NGUEFACK Bernard	Senior Lecturer	In service
19	NIMPA PEFOUNKEU Romain	Senior Lecturer	In service
20	POLA DOUNDOU Emmanuel	Senior Lecturer	In service
21	TAKAM SOH Patrice	Senior Lecturer	In service
22	TCHANGANG Roger Duclos	Senior Lecturer	In service
23	TCHOUNDJA Edgar Landry	Senior Lecturer	In service
24	TETSADJIO TCHILEPECK M. E.	Senior Lecturer	In service
25	TIAYA TSAGUE N. Anne-Marie	Senior Lecturer	In service
26	MBIAKOP Hilaire George	Assist. Lecturer	In service
27	BITYE MVONDO Esther Claudine	Assist. Lecturer	In service
28	MBATAKOU Salomon Joseph	Assist. Lecturer	In service
29	MEFENZA NOUNTU Thiery	Assist. Lecturer	In service
30	TCHEUTIA Daniel Duviol	Assist. Lecturer	In service
8- DEPARTMENT OF MICROBIOLOGY (MIB) (18)			
1	ESSIA NGANG Jean Justin	Professor	**Head of Department**
2	NYEGUE Maximilienne Ascension	Professor	**Vice Dean/DSSE**
3	BOYOMO ONANA	Associate Professor	In service
4	NWAGA Dieudonné M.	Associate Professor	In service
5	RIWOM Sara Honorine	Associate Professor	In service
6	SADO KAMDEM Sylvain Leroy	Associate Professor	In service

7	ASSAM ASSAM Jean Paul	Senior Lecturer	In service
8	BODA Maurice	Senior Lecturer	In service
9	BOUGNOM Blaise Pascal	Senior Lecturer	In service
10	ESSONO OBOUGOU Germain G.	Senior Lecturer	In service
11	NJIKI BIKOÏ Jacky	Senior Lecturer	In service
12	TCHIKOUA Roger	Senior Lecturer	In service
13	ESSONO Damien Marie	Assist. Lecturer	In service
14	LAMYE Glory MOH	Assist. Lecturer	In service
15	MEYIN A EBONG Solange	Assist. Lecturer	In service
16	NKOUDOU ZE Nardis	Assist. Lecturer	In service
17	SAKE NGANE Carole Stéphanie	Assist. Lecturer	In service
18	TOBOLBAÏ Richard	Assist. Lecturer	In service
9- DEPARTMENT OF PHYSICS (PHY) (42)			
1	BEN-BOLIE Germain Hubert	Professor	In service
2	ESSIMBI ZOBO Bernard	Professor	In service
3	EKOBENA FOUDA Henri Paul	Associate Professor	**Chief of Division. UN**
4	KOFANE Timoléon Crépin	Professor	In service
5	NANA ENGO Serge Guy	Professor	In service
6	NDJAKA Jean Marie Bienvenu	Professor	**Head of Department**
7	NOUAYOU Robert	Professor	In service
8	NJANDJOCK NOUCK Philippe	Professor	**Under Director/ MINRESI**
9	PEMHA Elkana	Professor	In service
10	TABOD Charles TABOD	Professor	**Dean Univ. Bda**
11	TCHAWOUA Clément	Professor	In service
12	WOAFO Paul	Professor	In service
13	BIYA MOTTO Frédéric	Associate Professor	**G. D./HYDRO Mekin**
14	BODO Bertrand	Associate Professor	In service
15	DJUIDJE KENMOE épouse A.	Associate Professor	In service
16	EYEBE FOUDA Jean sire	Associate Professor	In service
17	FEWO Serge Ibraïd	Associate Professor	In service
18	HONA Jacques	Associate Professor	In service
19	MBANE BIOUELE César	Associate Professor	In service

20	NANA NBENDJO Blaise	Associate Professor	In service
21	NDOP Joseph	Associate Professor	In service
22	SAIDOU	Associate Professor	**MINRESI**
23	SIEWE SIEWE Martin	Associate Professor	In service
24	SIMO Elie	Associate Professor	In service
25	VONDOU Derbetini Appolinaire	Associate Professor	In service
26	WAKATA née BEYA Annie	Associate Professor	**Under Dir./ MINESUP**
27	ZEKENG Serge Sylvain	Associate Professor	In service
28	ABDOURAHIMI	Senior Lecturer	In service
29	EDONGUE HERVAIS	Senior Lecturer	In service
30	ENYEGUE A NYAM épse BELINGA	Senior Lecturer	In service
31	FOUEDJIO David	Senior Lecturer	**Chief of Cell MINADER**
32	MBINACK Clément	Senior Lecturer	In service
33	MBONO SAMBA Yves Christian U.	Senior Lecturer	In service
34	MELI'I Joelle Larissa	Senior Lecturer	In service
35	MVOGO ALAIN	Senior Lecturer	In service
38	OBOUNOU Marcel	Senior Lecturer	**DA/U. Int. Etat/Sangma.**
39	WOULACHE Rosalie Laure	Senior Lecturer	In service
40	AYISSI EYEBE Guy François V.	Assist. Lecturer	In service
41	CHAMANI Roméo	Assist. Lecturer	In service
42	TEYOU NGOUPOU Ariel	Assist. Lecturer	In service
10- DEPARTMENT OF EARTH SCIENCES (E. S.) (43)			
1	BITOM Dieudonné	Professor	**Dean/FASA/UDs**
2	FOUATEU Rose épse YONGUE	Professor	In service
3	KAMGANG Pierre	Professor	In service
4	NDJIGUI Paul Désiré	Professor	**Head of Department**
5	NDAM NGOUPAYOU Jules-Remy	Professor	In service
6	NGOS III Simon	Professor	**DAAC/Uma**
7	NKOUMBOU Charles	Professor	In service
8	NZENTI Jean-Paul	Professor	In service
9	ABOSSOLO née ANGUE Monique	Associate Professor	**Vice-Dean/DRC**
10	GHOGOMU Richard TANWI	Associate Professor	**CD/Uma**
11	MOUNDI Amidou	Associate Professor	**CT/ MINIMDT**

12	NGUEUTCHOUA Gabriel	Associate Professor	**CEA/MINRESI**
13	NJILAH Isaac KONFOR	Associate Professor	**In service**
14	ONANA Vincent Laurent	Associate Professor	**Chief serv. Mater. Maint.**
15	BISSO Dieudonné	Associate Professor	**Director/Project Barrage Memve'ele**
16	EKOMANE Emile	Associate Professor	In service
17	GANNO Sylvestre	Associate Professor	In service
18	NYECK Bruno	Associate Professor	In service
19	TCHOUANKOUE Jean-Pierre	Associate Professor	In service
20	TEMDJIM Robert	Associate Professor	In service
21	YENE ATANGANA Joseph Q.	Associate Professor	**Chief Div. /MINTP**
22	ZO'O ZAME Philémon	Associate Professor	**G. D./ART**
23	ANABA ONANA Achille Basile	Senior Lecturer	In service
24	BEKOA Etienne	Senior Lecturer	In service
25	ELISE SABABA	Senior Lecturer	In service
26	ESSONO Jean	Senior Lecturer	In service
27	EYONG JOHN TAKEM	Senior Lecturer	In service
28	FUH Calistus Gentry	Senior Lecturer	**Sec. D'Etat/MINMIDT**
29	LAMILEN BILLA Daniel	Senior Lecturer	In service
30	MBESSE CECILE OLIVE	Senior Lecturer	In service
31	MBIDA YEM	Senior Lecturer	In service
32	METANG Victor	Senior Lecturer	In service
33	MINYEM Dieudonné-Lucien	Senior Lecturer	**CD/Uma**
34	NGO BELNOUN Rose Noël	Senior Lecturer	In service
35	NGO BIDJECK Louise Marie	Senior Lecturer	In service
36	NOMO NEGUE Emmanuel	Senior Lecturer	In service
37	NTSAMA ATANGANA Jacqueline	Senior Lecturer	In service
38	TCHAKOUNTE J. épse NOUMBEM	Senior Lecturer	**Chief of cell/MINRESI**
39	TCHAPTCHET TCHATO De P.	Senior Lecturer	In service
40	TEHNA Nathanaël	Senior Lecturer	In service
41	TEMGA Jean Pierre	Senior Lecturer	In service
42	FEUMBA Roger	Assist. Lecturer	In service
43	MBANGA NYOBE Jules	Assist. Lecturer	In service

Classification of teaching staff at the faculty of Science of the University of Yaoundé 1

NUMBER OF LECTURERS					
Department	**Professor**	**Associate Professor**	**Senior Lecturer**	**Assist. Lecturer**	**Total**
BCH	9 (1)	13 (09)	14 (06)	3 (2)	**39 (18)**
A. B. P.	13 (1)	09 (06)	19 (05)	05 (2)	**46 (14)**
P. B. P.	06 (0)	11 (02)	9 (06)	07 (01)	**33 (9)**
I. C.	10 (1)	09 (02)	12 (02)	03 (0)	**34 (5)**
O. C.	7 (0)	19 (06)	09 (03)	06 (01)	**40 (10)**
C. S.	2 (0)	1 (0)	13 (01)	09 (01)	**25 (2)**
MAT	1 (0)	5 (0)	19 (01)	05 (02)	**30 (3)**
MIB	1 (0)	5 (02)	06 (01)	06 (02)	**18 (5)**
PHY	12 (0)	15 (02)	10 (03)	03 (0)	**40 (5)**
E. S.	8 (1)	14 (01)	19 (05)	02 (0)	**43 (7)**
Total	**69 (4)**	**99 (28)**	**130 (33)**	**45 (10)**	**348 (78)**

A total of: **348 (78)** including:

Professors **69 (4)**

Associate Professors **101 (30)**

Senior Lecturers **130 (33)**

Assist. Lecturers **48 (11)**

( ) = Number of women **78**

The Dean of the Faculty of Science

Prof. TCHOUANKEU Jean-Claude

DECLARATION

We, the undersigned, Mr. **NKENGFACK Augustin Ephrem** (Professor) and Mrs. **MVOT AKAK Carine** (Associate Professor), certify that the work presented in this thesis and entitled « **Phytochemical studies of *Diospyros gilletii* De Wild and *Diospyros fragrans* Gürke (Ebenaceae), chemical transformations and antibacterial, antioxidant and cytotoxic activities of extracts and isolated compounds**» was carried out by Mrs. **JOUWA TAMEYE NATHALIE SAMANTHA** (Master in Chemistry-Biology, Registration number 17T5845), in Laboratory of Natural Products and Applied Organic Synthesis (**LANAPOS**), at the University of Yaoundé I.

This work has not yet been the subject to any submission for the acquisition of any academic degree.

Student

JOUWA TAMEYE Nathalie Samantha

Director **Supervisor**

MVOT AKAK Carine **NKENGFACK Augustin Ephrem**

Associate Professor *Professor*

DEDICATION

To my parents...

Mr. and Mrs. TAMEYE

ACKNOWLEDGEMENTS

This work carried out jointly at the Department of Organic Chemistry, Faculty of Science of the University of Yaoundé I, Cameroon and the Department of Organic and Bioorganic Chemistry, Faculty of Chemistry of the University of Bielefeld, Germany was made possible thanks to the financial and material support of the **DAAD** (German Academic Exchange Service) through **YaBiNaPA** (Yaoundé-Bielefeld Graduate School of Natural Products with Antiparasite and Antibacterial activities) project. I would like to express my gratitude for receiving this scholarship.

My deepest gratitude goes also to all those who, from near and far, have each contributed in their own way to the realization of this work, demonstrating at the same time their attachment to my humble person. I am addressing in particular:

To my research supervisor, Professor **Augustin Ephrem NKENGFACK**, Professor at the Department of Organic Chemistry, Faculty of Science, University of Yaoundé I, for welcoming and giving me the opportunity to carry out my work within his research team. Be assured, Dear Professor, of my deep respect for having given me the benefit of your professional experience, your knowledge, your zeal for the task, your critical spirit and your scientific rigour.

To my research director, Doctor **Carine MVOT AKAK**, Associate Professor at the Department of Organic Chemistry, Faculty of Science, University of Yaoundé I, who throughout this work has given me her unfailing support and availability. Your sense of work well done, your ardour for the task, your scientific rigour and your kindness have allowed me to give the best of myself. This work is the fruit of all the follow-up I have benefited from you, I would like to say thank you.

To Professor **Norbert SEWALD**, Head of the research team Organic Chemistry III (OCIII) of the Department of Organic and Bioorganic Chemistry, Faculty of Chemistry, University of Bielefeld and co-coordonator of the YaBiNaPA project, for the trust he placed in me by welcoming and giving me the opportunity to carry out my work within his research team in Bielefeld, for facilities placed at my disposal and for his precious advice. I am very grateful.

To Professor **Bruno LENTA**, Professor at the Higher Teacher Training College of the University of Yaoundé I and co-coordonator of the YaBiNaPA project, for the opportunity he gave to me by choosing me as a student of this prestigious graduate school, for his encouragement and guidance throughout my fellowship. Dear Professor, I would like to express my infinite gratitude to you.

To Doctor **Pierre MKOUNGA**, Associate Professor at the Department of Organic Chemistry, Faculty of Science, University of Yaoundé I, for his assistance, availability and support during my work thesis.

To Doctor **Blandine OUAHOUO**, Senior Lecturer at the Department of Organic Chemistry, Faculty of Science, University of Yaoundé I for her precious advice and encouragement.

To Doctors **Marcel FRESE** and **Veronica DODERO**, Senior Lecturers and members of the research team Organic Chemistry III (OCIII) of the Department of Organic and Bioorganic Chemistry, Faculty of Chemistry, University of Bielefeld for their guidance and availabilities during my research stay at Bielefeld University.

To all the teachers of the Department of Organic Chemistry of the Faculty of Science of the University of Yaoundé I and all the teachers of the Department of Chemistry of the Faculty of Sciences of the University of Douala for the solid intellectual training they gave to me during my studies.

To Doctors **Julio PAGNA, Hermine MAZA, Jean Pierre ABDOU, Pamela NANGMO**, **Maurice TSAFFACK, Valerie TEDJON SIELINOU, Edwige FODJA, Armelle TSAMO, Hugues FOUOTSA, Jean Paul TSOPMEJIO, Aristide MFIFEN, William FEUDJIO, Jean Robert NGUEMEVING, Eric Carly NONO** and **Eric Gustave GOMPE** for their help, support and judicious advice for the realization of this work.

To all the members of the laboratory of natural products and applied organic synthesis (LANAPOS) of the Department of Organic Chemistry of the Faculty of Sciences of the University of Yaoundé I, I am thinking in particular to Mrs. **Christelle NOUBISSI YONGA,** Mrs. **Beauvarine KOUCHELE**, Mrs. **Sandra FENKAM,** Mr. **Emar TCHAPO,** Mrs. **Stephanie NGUEGUIM,** Mr. **Einstein GUIZOKO TOKO,** Mr. **Stephane FOKOU,** Mr. **Paul MBARGA,** Mrs. **Sandra KAMTCHOUM** for the friendly atmosphere they have created in the laboratory.

To my friends Mrs. **Sorel NITCHEU**, Mr. **Sylvanis TEGOUMTSOP,** Mr. **Cedric NOULALA,** Mr. **Armand TAIZOUMBE**, Mrs. **Ines MOUAFO,** Mr. **Florent TCHAMEZI,** Mr. **Maxime NANGMO,** Doctors **Bellier TABEKOUENG, Willifred DONGMO**, **Judith MBOUGNIA,** who have always been there and supported me during difficult times, your unconditional support has allowed me to move forward despite the difficulties I was facing. Thank you very much.

To all my family members, in particular my father Mr. **Andre TAMEYE**, my mother Mrs. **Pauline MACHE spouse TAMEYE**, my sisters Doctor **Stevine POPWO TAMEYE spouse NGANTCHA,** Mrs. **Edith GUELOH TAMEYE spouse SOWE,** Mrs. **Cynthia MAWOUT TAMEYE,** Mrs. **Michelle FONGANG TAMEYE**, for their patience, understanding, encouragements and support during these years of study. Thank you to have always believed in me.

To all those who were not mentioned by name and whose moral support and presence by my side have been a great contribution to the realization of this work, thank you very much.

SUMMARY

LIST OF ABBREVIATIONS AND SIGGLES

AACR :	American Association for Cancer Research
Ac_2O :	Acetic anhydride
CC :	Column Chromatography
$CDCl_3$:	Deuterated Chloroform
C_5D_5N :	Deuterated Pyridin
CI_{50} :	Concentration Inhibitrice médiane
°C :	degree Celsius
^{13}C :	Carbon 13
CMI:	Concentration Minimale Inhibitrice
CoA:	Coenzyme-A
COSY :	Correlation Spectroscopy
D.	*Diospyros*
d :	Doublet
dd :	Doublet dedoubled
dt :	Doublet of triplet
DEPT:	Distortionless Enhancement by Polarization Transfer
DMAP :	4-(Dimethylamino)pyridin
DMSO:	Dimethylsulfoxide
DMSO-d_6	Deuterated Dimethylsulfoxide
DPPH:	2,2-DiPhenyl-1-PicrylHydrazyl
ESI :	Electrospray Ionization
ED_{50}	50% Effective Dose
EtOAc:	Ethyl Acetate
Fig.:	Figure
Hex:	Hexane
^1H :	Proton
HMBC:	Heteronuclear Multiple Bond Connectivity
HMQC :	Heteronuclear Multi Quantum Coherence
HR-ESIMS :	High Resolution Electrospray Ionization Mass Spectrometry
Hz :	Hertz
IC_{50} :	50% Inhibitory Concentration
IR:	Infra Red

J :	Coupling constant
KOAc :	Potassium acetate
m :	Multiplet
MeOH:	Methanol
MIC :	Minimal Inhibitory Concentration
MS :	Mass Spectrometry
m/z :	Mass/atomic charge ratio
NADPH :	Nicotinamide Adenine Dinucleotide Phosphate Hydrogenase
NMR :	Nuclear Magnetic Resonance
n-BuOH :	*n*- butanol
NOESY:	Nuclear Overhauser Effect Spectroscopy
PE :	Petroleum Ether
ppm :	Part Per Million
pyr :	Pyridin
Ref. :	References
ROS	Reactive Oxygen Species
s :	Singlet
SAM :	s-adenosyl methionine
t :	Triplet
tBu :	tert-Butyl
Tf_2O :	Trifluoromethanesulfonic anhydride
THF :	Tetrahydrofuran
TLC :	Thin Layer Chromatography
TMSOTf :	Trifluoromethane sulfonate
UV :	Ultra Violet
WHO:	World Health Organization

LIST OF TABLES

LIST OF FIGURES

LIST OF SCHEMES

ABSTRACT

The present thesis focused on the isolation, characterization and chemical transformations of some secondary metabolites of the species *Diospyros gilletii* De Wild and *Diospyros fragrans* Gürke, two Cameroonian medicinal plants belonging to the Ebenaceae family, followed by a subsequent evaluation of the antioxidant, antibacterial and cytotoxic properties of extracts and isolates.

From these two plants, thirty-four compounds were isolated using liquid phase chromatographic methods, twenty eight of which were fully characterized and belong to various classes of secondary metabolites. These include five (05) isocoumarins among which two (02) new assigned as 4-*O*-*p*-hydroxybenzoylnorbergenin and 11-*O*-*(E)*-cinnamoylnorbergenin and three known identified as norbergenin, 4-*O*-galloylnorbergenin and 11-*O*-*p*-hydroxybenzoylnorbergenin; one (01) new naphthalene derivative, the 3,6-dihydroxy-8-methyl-3,4-dihydronaphthalen-1(2H)-one or fragranone, Twelve (12) pentacyclic triterpenes identified as ursolic acid, oleanolic acid, corosolic acid, rotundic acid, myrtifolic acid, betulinic acid, vismiaefolic acid, uvaol, lupeol, betulin, hederagenin and *β*-amyrin acetate; one (01) polyterpene, the *α*-tocopherol; one monoglyceride (01), the 1-*O*-(28-hydroxyoctacosanoyl) glycerol; one carotenoid, the luteine; four sterols (04) identified respectively as a mixture of stigmasterol + *β*-sitosterol and a mixture of 3-*O*-*β*-*D*-glucopyranoside of stigmasterol + *β*-sitosterol; three (03) polyols, identified as quercitol, 5-*O*-methyl-myo-inositol and methyl-*β*-*D*-glucopyranoside.

The structures of these compounds were established by means of spectroscopic techniques including IR, UV, MS, NMR 1D and 2D, by X-ray diffraction for some and by comparison of their spectral data with those reported in the literature.

4-*O*-*p*-hydroxybenzoylnorbergenin, ursolic acid, betulinic acid and vismiaefolic acid underwent chemical transformation by acetylation and allylation, leading to their acetylated and allylated derivatives, among which those of 4-*O*-*p*-hydroxybenzoylnorbergenin were new derivatives.

Crude extracts and some of the isolated and hemisynthetic compounds were evaluated for their antibacterial activities against five strains of microorganisms using agar disk diffusion and microdilution method, for their cytotoxic effect on human cervix carcinoma cell

line KB-3-1 and human colon cancer cell line HT-29 using resazurin reduction assay and for their antioxidant activities using DPPH method.

The results from antibacterial activities showed that the most active compounds were myrtifolic acid and acetylated betulinic acid against *Bacillus subtilis* with MIC values of 31.3 and 250 µg/ mL respectively.

The results from cytotoxic activities showed that corosolic acid was the most active compound on both cancer cells KB-3-1 and HT-29 with IC_{50} values of 14.6 and 16.5 µM respectively.

The antioxidant activity showed that all the five isocoumarins exhibited good activities with IC_{50} values between 8.2-144 µg/mL.

Keywords: *Diospyros*; isocoumarin; naphthalene derivative; antioxidant; antibacterial; cytotoxic.

RESUME

La présente thèse porte sur l'isolement et la caractérisation des métabolites secondaires de *Diospyros gilletii* De Wild et *Diospyros fragrans* Gürke, deux plantes médicinales Camerounaises appartenant à la famille des Ebenaceae, sur quelques transformations chimiques sur les composés isolés ainsi que l'évaluation des activités biologiques antioxydante, antibacterienne et cytotoxique des extraits, isolats et produits de réaction.

De ces deux plantes ont été isolés, au moyen de méthodes chromatographiques en phase liquide, trente-quatre (34) composés parmis lesquels vingt-huit (28) ont été entièrement caractérisés comme appartenant à diverses classes de métabolites secondaires. Il s'agit de cinq (05) isocoumarines parmi lesquelles deux (02) nouvelles auxquelles ont été attribuées les noms triviaux 4-*O*-*p*-hydroxybenzoylnorbergenine et 11-*O*-*(E)*-cinnamoylnorbergenine, et trois connues (03) identifiées à la norbergenine, la 4-*O*-galloylnorbergenine et la 11-*O*-*p*-hydroxybenzoylnorbergenine ; un (01) dérivé nouveau de naphtalène, le 3,6-dihydroxy-8-methyl-3,4-dihydronaphthalen-1(2H)-one et auquel nous avons donné le nom trivial fragranone, douze (12) triterpenes pentacycliques connus identifiés à l'acide ursolique, l'acide oléanolique, l'acide bétulinique, l'acide corosolique, l'acide rotundique, l'acide vismiaefolique, l'acide myrtifolique, l'uvaol, le lupéol, la bétuline, l'hédéragenine et la *β*-amyrin acetate ; un (01) polyterpène connu, le *α*-tocopherol ; un (01) monoglyceride connu, le 1-*O*-(28-hydroxyoctacosanoyl) glycerol ; un (01) caroténoïde connu, la luteine; quatre (04) stérols connus, le mélange de stigmastérol + *β*-sitostérol et le mélange du 3-*O*-β-*D*-glucopyranoside de stigmastérol + *β*-sitostérol, et trois (03) polyols connus, le quercitol, le 5-*O*-methyl-myo-inositol et le methyl-*β*-*D*-glucopyranoside.

L'élucidation structurale de tous ces composés s'est faite sur la base d'une interprétation de leurs données spectrales, en particulier, la RMN ^{1}H et ^{13}C à une et deux dimensions en conjonction avec la spectrométrie de masse, l'IR et l'UV, et quelques fois par analyse aux rayons X.

La 4-*O*-*p*-hydroxybenzoylnorbergenine, l'acide ursolique, l'acide betulinique et l'acide vismiaefolique ont fait l'objet de deux transformations chimiques : les réactions d'acétylation et d'allylation, ayant conduit à leurs dérivés acetylés et allylés correspondants. Ces dérivés ont été à leur tour entièrement caractérisés à partir de leurs données spectrales et

parmis eux, ceux provenant de la 4-*O*-*p*-hydroxybenzoylnorbergenine ont été identifiés comme étant nouveaux.

Sur le plan biologique les extraits provenant des différentes parties de ces deux plantes ainsi que les composés isolés et hemisynthétiques ont été évalués pour leurs activités antibacterienne contre cinq souches de microorganismes par les méthodes de diffusion de disques et de microdilution, cytotoxique contre les lignées cellulaires KB-3-1 du carcinome du col de l'utérus et les lignées cellulaires HT-29 du cancer du côlon par la methode de reduction de la resazurine, et enfin antioxydante en utilisant la méthode au DPPH.

S'agissant de l'activité antibactérienne, l'acide myrtifolique et le dérivé acetylé de l'acide betulinique ont présenté une bonne activité contre *Bacillus subtilis* avec des CMI de 31,3 et 250 µg/ mL respectivement.

En ce qui concerne l'activité cytotoxique, l'acide corosolique s'est avéré actif sur les deux lignées de cellules cancereuses KB-3-1 and HT-29 avec des CI_{50} de 14,6 et 16,5 µM respectivement.

Pour ce qui est de l'activité antioxydante, les cinq isocoumarines testées ont présenté de bonnes activités avec des valeurs de CI_{50} comprises entre 8,2-144 µg/ mL.

Mots clés : *Diospyros*; isocoumarine; derivé du naphtalène ; antioxydante; antibactérienne; cytotoxique.

GENERAL INTRODUCTION

Originally, plants were used as food by animals and people living on earth. In addition to this nutritional function, man discovered their healing power. That healing power function, known by our ancestors since time immemorial, especially in India, China and Africa have been used in the manufacture of traditional remedies without knowing their composition and origin of that healing power. It is estimated that an approximate range of the total number of plants growing worldwide may vary between 310000 and 422000, among which 20000 to 25000 are used in human pharmacopeia (Chorghade, 2007; Newman et *al.*, 2000). However, because of a "relative" knowledge of plants and their environment, man is still sometimes victim of accidental poisoning due to them.

The commonly uses of plants in traditional medicine have led pharmacological industries to produce plants derivate drugs. In fact, about 60 to 70% of antibacterial and anti-cancer drugs are from natural origin and more than 61% of new drugs developed between 1981 and 2002 were based on natural product (Cragg et Newman, 2005). But due to improper use of antibacterial drugs in the area of infectious diseases, microorganisms have developed resistance. This, combined to the side effects observed sometimes when taking existing drugs or the aggressiveness and non-selectivity of drugs used in chemotherapy, creates an ongoing need for new active molecules that could potentially lead in the development of new antibacterial or anticancerous drugs.

For few years now, our laboratory has focused part of his research work in the discovery of molecules derived plants with antibacterial and anticancer potentials, as bacterial infections and cancer are major health concern worldwide in general and in Cameroon in particular. In fact, very high incidence and mortality rates have been reported concerning these two health problems, with more than 10 million death each year for cancer worldwide among which nearly 8000 in Cameroon (WHO, 2021) and more than 700000 death each year worldwide due to drug-resistant diseases (WHO, 2019). Among the family of plants that make the Cameroonian flora, our attention was dramn to the Ebenaceae family, especially genus *Diospyros*, the most abundant genus on the family with a large number of species used to treat infectious diseases such as gonorrhea, tuberculosis and leprosis (Tangmouo et *al.*, 2005, 2006; Dzoyem et *al.*, 2007), cardiovascular diseases and cancer (Rauf et *al.*, 2017). Thus the present work on the phytochemical study of two Cameroonian medicinal plants, *Diospyros gilletii* and *Diospyros fragrans* and evaluation of their antibacterial, antioxidant and cytotoxic activities.

Our general objective is to identify secondary metabolites from our selected plants as potential antibacterial, antioxidant and anticancer agents. To achieve this goal, we will extract, isolate and purify the chemical constituents of these plants through chromatographic methods, then elucidate their structures using spectral data, literature data or laboratory samples, perform hemisynthesis of some isolates and finally evaluate the antioxidant, antibacterial and cytotoxic activities of compounds, extracts and reaction products.

Our work will be divided into three chapters:

- The first chapter, devoted to a literature review, will include generalities on oxidative stress and cancer, a botanical overview of our two plants followed by a presentation of previous phytochemical and pharmacological work already done on plants of the genus *Diospyros*.
- The second chapter will present the results of our work.
- The third chapter will be on the experimental part. Here, the equipment, the plant and biological material, the different protocols for the extraction and isolation of compounds, their physicochemical data and the protocols used for the evaluation of biological activities will be presented.

CHAPTER I: LITERATURE REVIEW

I.1. OXIDATIVE STRESS

I.1.1. Generalities

Oxidation reactions are usual and essential reactions within our cells, as they contribute to the proper functioning of cell metabolism. Indeed, the oxidation reactions take place in many biological processes which aim to maintain a cellular balance or synthesize essential molecules. Concentration of reactive oxidizing species produced during these oxidation reactions is regulated in the cells by the balance between their production rate and their elimination rate by antioxidant systems and a disruption in this redox homeostasis is the cause of oxidative stress (Inoue et *al.*, 2003).

Oxidative stress is defined as an imbalance between the production of reactive oxygen species (ROS) and the antioxidant capacity of the cell (**Figure 1)**. This imbalance may be due to an increased production of reactive oxygen (ROS) and / or to a depletion of enzymes or antioxidant molecules due to physio-pathological factors (inflammation, sports activity ...) or environmental (tobacco, alcohol, medication, gamma or ultraviolet rays) (Inoue et *al.*, 2003; Sies et *al.*, 2017).

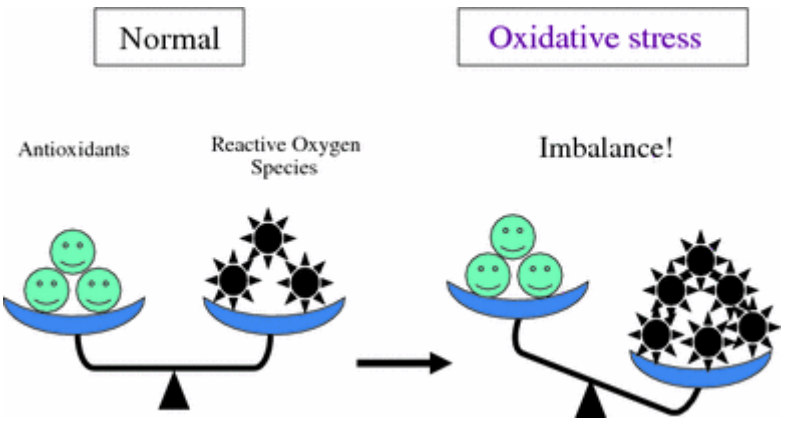

Figure 1: Normal and imbalance antioxidant and pro-oxidant (Inoue et *al.*, 2003)

The term ROS refers to reactive oxygen species having in their structure one or more unpaired electrons. This includes:

- Free radical of oxygen: that is atoms, molecules or ions with one or more unpaired electrons such as superoxide anion ($O_2^{\bullet -}$), hydroxyl radical ($^{\bullet}OH$);
- Molecules of significant toxicity such as hydrogen peroxide (H_2O_2) and singlet oxygen $^1O_2$ (Wiseman et Halliwell, 1996).

ROS have a very short lifespan and are very reactive. Low and moderate amounts of ROS have beneficial effects on several physiological processes including killing of invading pathogens, wound healing and tissue repair processes. However, their disproportionated generation can cause oxidation of surrounding molecules (Bhattacharyya et *al.*, 2014).

I.1.2. Origin of ROS and free radicals

ROS which are the cause of oxidative stress generation can be produced endogenously (intracellularly) or exogenously (Klaunig, 2018).

I.1.2.1. Endogenous sources

Endogenous mechanisms that can induce ROS production are generally processes biologically useful within cells. For instance, ROS are mainly formed during the oxidation of lipids to produce acetyl coenzyme-A (acetyl-CoA) fuel of the Krebs cycle and in the mitochondrial electron transport chain which aims to produce energy. Several different enzymes have been implicated in the generation of ROS, for example xanthine oxidase, NADPH oxidases and cytochromes P450 are capable of producing superoxide anion.

I.1.2.2. Exogenous sources

There are also exogenous sources producing ROS as photochemical pollutants, tobacco, drugs, and ionizing radiation entering the body through respiration, food, or mucous membranes (Kohen et Nyska, 2002). Transition metal ions (such as iron or copper) which are key elements of various biological processes and can also be brought in exogenously, at high levels, generate ROS by participating in Fenton's reaction (Halliwell et Gutteridge, 1990). Indeed, these transition metals can react with hydrogen peroxide (H_2O_2) and generate ROS according to the following reaction:

$$Fe^{2+} + H_2O_2 \longrightarrow Fe^{3+} + HO^{\bullet} + OH^-$$

$$Fe^{3+} + H_2O_2 \longrightarrow Fe^{2+} + HOO^{\bullet} + H^+$$

$$2H_2O_2 \longrightarrow HO^{\bullet} + HOO^{\bullet} + H_2O$$

Figure 2: Fenton reaction (Halliwell et Gutteridge, 1990)

I.1.3. Diseases affected by oxidative stress

ROS and free radicals can cause severe damage to the normal cells of the body. This damage can be to the DNA, proteins, and other macromolecules of the cell and therefore,

forms the basis of a wide variety of diseases, most notably neurodegenerative diseases, cardiovascular diseases, and cancers.

I.1.3.1. Neurodegenerative diseases

Oxidative stress is suspected to play an important role in neurodegenerative diseases. Indeed, Neurodegenerative diseases comprise a condition in which nerve cells from brain and spinal cord are lost, leading to either functional loss (ataxia) or sensory dysfunction (dementia). Neural tissue may be particularly susceptible to oxidative damage, because the brain receives a disproportionately large percentage of oxygen and has large amounts of polyunsaturated fatty acids that are highly prone to oxidation. Mitochondrial dysfunctions, excitotoxicity and finally apoptosis have been reported as pathological causes for aging on neurodegenerative diseases such as Parkinson's and Alzheimer's diseases, and multiple and amyolotrophic lateral sclerosis. Neurodegeneration has been speculated to be interplay of a number of factors including environmental and genetic predisposition, but redox metal abuse occupies central role as most of symptoms stems out from abnormal metal metabolism (Mattson, 2004). Oxidative stress and free radical generation catalyzed by redox metals have been shown to play pivotal role in regulating redox reactions *in vivo* contributing ROS, main culprits in neurodegeneration (Emerit et Edeas, 2004).

I.1.3.2. Cardiovascular diseases

Heart disease risk is raised by several factors including high cholesterol levels, high blood pressure, cigarette smoking, and diabetes which promote atherosclerosis. Atherosclerosis refers to formation of hardened walls of the arteries that impairs blood flow to the heart and other vital organs. It is speculated that a critical step in development of atherosclerosis is oxidation of low-density lipoprotein (LDL) (a type of bad cholesterol in blood) within the arterial wall, which conduct to oxidative stress. Several studies show an association between low intakes of dietary antioxidants to an increased frequency of heart disease (Nijs et *al*., 2006).

I.1.3.3. Cancers

Pro-oxidants, or those who generate free radicals, stimulate cell division and these form the beginnings of mutagenesis and tumor formation. When a cell with a damaged DNA strand divides, it gives rise to disturbed and deformed clusters of cells that form the cancer. In addition, cigarette smoking and chronic inflammation lead to strong free radical generation that seems to be the reason for many cancers. Some research has indicated that people who

smoke tend to have lower antioxidant levels than non-smokers and this makes smokers more at risk of cancers (Ruano-Ravina et *al*., 2006).

I.1.4. defence systems against oxidative stress: antioxidants

The body is constantly protecting itself against the formation and aggression of these oxidants through various enzymatic and non-enzymatic defense mechanisms. Antioxidants can be defined as substances that can neutralize the active forms of oxygen and which help to maintain, at the level of the cell and the organism, non-cytotoxic levels of free radicals.

Antioxidants have different modes of action: they can stop free radical reaction chains (anti-radical), inhibit specific oxidizing enzymes, or react with oxidizing substances before they damage biological molecules (Halliwell, 1994). They can come either from endogenous or exogenous sources of the body.

I.1.4.1. Endogenous sources of antioxidants

These are different enzymes that can metabolize free radicals. The best known are the superoxide dismutase (SOD), glutathione peroxidase (GSH) and catalase. SOD are metallo-proteins that catalyze dismutation of the superoxide anion ($O_2^{\bullet -}$) in hydrogen peroxide (H_2O_2) and O_2 (Darley-Usmar et Halliwell, 1996). Glutathione peroxidase (GSH) catalyses reduction of H_2O_2 and organic peroxides, while catalase allows elimination of excess H_2O_2 from the body (Harris, 1991). These endogenous antioxidants therefore participate in ROS detoxification reactions.

.

$$2O_2^{\bullet -} + 2H^+ \xrightarrow{SOD} O_2 + H_2O_2$$

$$2H_2O_2 \xrightarrow{Catalyse} O_2 + 2H_2O$$

$$H_2O_2 + NADH,H+ \xrightarrow{Peroxidase} 2H_2O + NAD+$$

Figure 3: Detoxification reactions (Harris, 1991)

Under the effect of high oxidative stress, the ability of these antioxidants to eliminate ROS is often exceeded and as a result, other exogenous sources of antioxidants are necessary.

I.1.4.2. Exogenous sources of antioxidants

Various antioxidants are supplied to the human body through diet, both vegetarian as well as non-vegetarian. Vitamin C **1**, coenzyme Q **2**, β-carotene **3** and vitamin E are the most famous antioxidants of diet, out of which, Vitamin E is present in vegetable oils and found abundantly in wheat germ. It is a fat soluble vitamin, absorbed in the gut and carried in the

plasma by lipoproteins. Out of the eight (8) natural state isomeric forms of vitamin E, *α*-tocopherol **4** is the most common and potent isomeric form. Being lipid soluble, vitamin E can effectively prevent lipid peroxidation of plasma membrane (Burton et Ingold, 1989). Plants (fruits, vegetables, medicinal herbs) can contain a wide variety of free radical scavenging molecules such as phenolic compounds (Phenolic acids, flavonoids, quinons, coumarins, lignans, stilbenes, tannins etc.), nitrogen compounds (alkaloids, amines, betalains etc.), vitamins, terpenoids (including carotenoids) and some other endogenous metabolites which are rich in antioxidant activity (Cai et *al*., 2003; Cotelle et *al*., 1996). **Figures 4** and **5** below are presenting the state of a normal and stressed cell membrane, as well as some natural antioxidants.

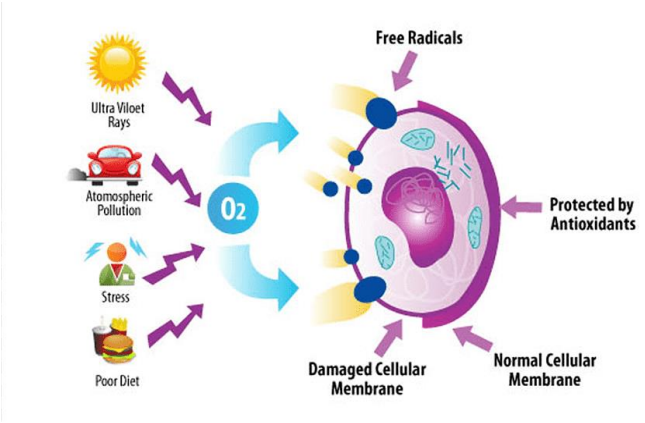

Figure 4: oxidative stress and antioxidant protection on cells membrane

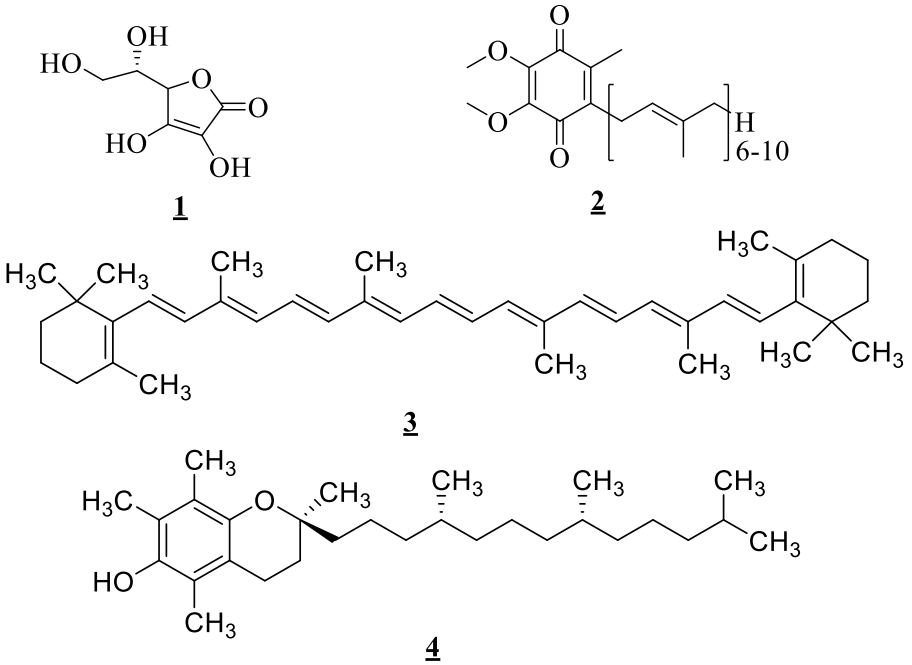

Figure 5: **Some natural antioxidant compounds**

I.2. CANCERS

I.2.1. Generalities

Cancer is the second leading cause of death worldwide, amongst the non-communicable diseases. One in 5 men and one in 6 women worldwide develop cancer during their lifetime, and one in 8 men and one in 11 women die from the disease (WHO, 2018) and the number of cancer deaths is projected to increase from 7.1 million in 2002 to 11.5 million in 2030 (Mathers et Loncar, 2006). Cancers are a large family of diseases that involve abnormal cell growth (WHO, 2018). A tumor develops when cells reproduce too quickly but not all tumors are cancerous. There are benign ones that develop locally and can not spread; others are premalignant (not yet cancerous but can become so) and the last are malignant which means cancerous. Abnormal cells termed cancer cells or malignant tumour have the ability to spread and invade other tissues.

The hallmarks of cancer comprise six biological capabilities acquired during the multistep development of human tumors. They include sustaining proliferative signaling, evading growth suppressors, resisting cell death, enabling replicative immortality, inducing angiogenesis, and activating invasion and metastasis (Hanahan et Weinberg, 2000).

Frequently, cancer cells can break away from this original mass of cells, travel through the blood and lymph systems, and lodge in other organs where they can again repeat the uncontrolled growth cycle. This process of cancer cells leaving an area and growing in another body area is termed metastatic spread or metastasis. As an example, if breast cancer cells spread to a bone, it means that the individual has metastatic breast cancer to bone. This is not the same as "bone cancer," which would mean the cancer had started in the bone (Hanahan et Weinberg, 2000). These metastatic tumors are "secondary cancers" because they arise from the primary tumor. The metastasis process is shown by **Figure 6** below.

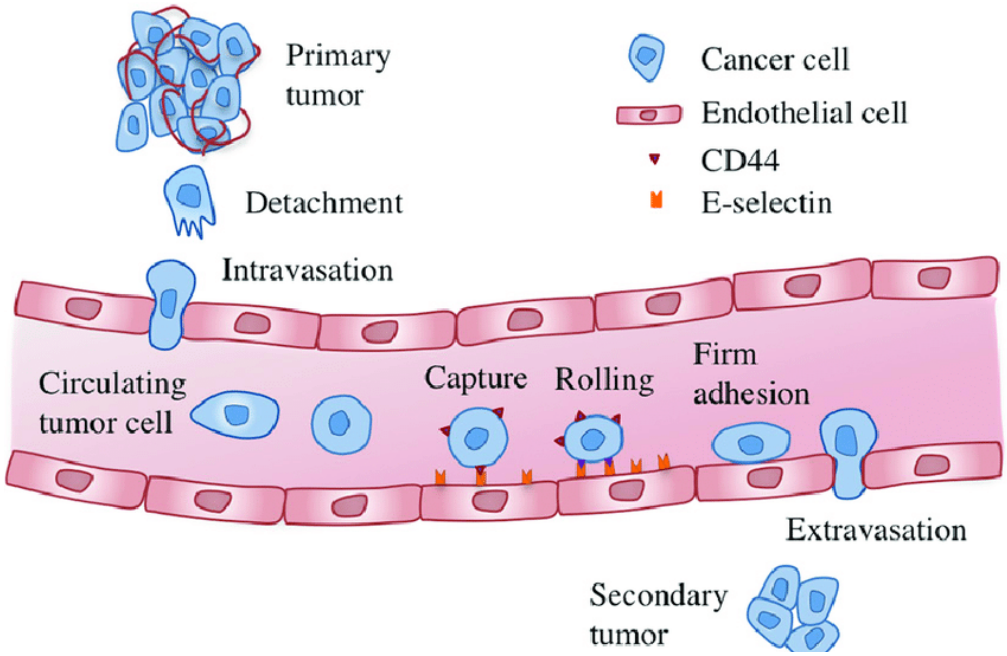

Figure 6: Invasion of cancer cells: Metastasis process (Hanahan et Weinberg, 2000)

I.2.2. Causes of cancers

Many factors that can cause cell abnormalities have been linked to cancer development. Most cancer causes remain unknown while other cancers have environmental or lifestyle triggers or may develop from more than one known cause. Although it is often difficult or impossible to determine the initiating event(s) that cause a cancer to develop in a specific person, the following is a listing of major causes (Anand et *al*., 2008; Kuper et *al*., 2002)

- Chemical or toxic compound exposures: Benzene, asbestos, nickel, cadmium, vinyl chloride, benzidine, N-nitrosamines, aflatoxin and tobacco or cigarette smoke which contains at least 66 known potential carcinogenic chemicals and toxins.
- Ionizing radiation: Uranium, radon, ultraviolet rays from sunlight, radiation from alpha, beta, gamma, and X-ray-emitting sources
- Pathogens: Human papillomavirus (HPV), EBV or Epstein-Barr virus, hepatitis viruses B and C, Kaposi's sarcoma-associated herpes virus (KSHV), Merkel cell polyomavirus, Schistosoma spp., and Helicobacter pylori; other bacteria are being researched as possible agents.

- Genetics. Indeed, a number of specific cancers have been linked to human genes and are as follows: breast, ovarian, colorectal, prostate, skin and melanoma.

Recently, other risk factors have been added to the list of items that may increase cancer risk. Specifically, red meat, obesity, lack of exercise, chronic inflammation, Non-ionizing radio frequency radiation from mobile phones and hormones used for replacement therapy were placed on the carcinogenic list by the World Health Organization's International Agency for Research on Cancer (WHO, 2011). **Figure 7** below is presenting the estimated percentage of identifiable cancer factors.

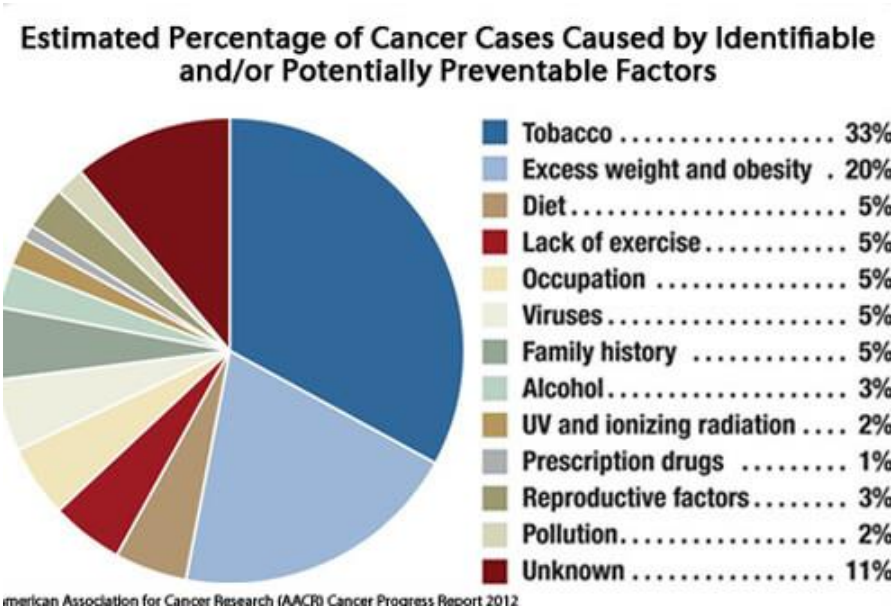

Figure 7: Estimated percentage of cancer due to identifiable factors (AACR, 2012).

I.2.3. Symptoms and diagnosis

When cancer begins, it produces no symptoms. Signs and symptoms appear as the mass grows or ulcerates and depend on the type of cancer, where it is located, and/or where the cancer cells have spread (Kufe et *al*., 2003). A few patients show no signs or symptoms until the cancer is far advanced. Cancer can be difficult to diagnose and can be considered a "great imitator". Generally, when advanced, cancer's symptoms can be classified in two main groups: local symptoms and systemic symptoms

I.2.3.1. Local symptom

Local symptoms may occur due to the mass of the tumor or its ulceration. Ulceration can cause bleeding that can lead to symptoms such as coughing up blood (lung cancer),

anemia or rectal bleeding (colon cancer), blood in the urine (bladder cancer), or abnormal vaginal bleeding (endometrial or cervical cancer) (Kufe et *al*., 2003).

I.2.3.2. Systemic symptoms

Systemic symptoms (affecting the entire body, rather than a single organ or body part) may occur due to the body's response to the cancer. This include: unexplained loss of weight or loss of appetite, persistent fatigue, nausea, vomiting, unexplained low-grade fevers which may be either persistent or come and go, recurring infections which will not clear with usual treatment (Dimitriadis et *al*., 2017).

Many cancers will present with some of the above general symptoms but often have one or more symptoms that are more specific for the cancer type. People with suspected cancer are investigated with medical tests. These commonly include blood tests, X-rays, contrast scans and endoscopy. The tissue diagnosis from the biopsy indicates the type of cell that is proliferating, its histological grade, genetic abnormalities, and other features. Together, those informations are useful to evaluate the prognosis and to choose the best treatment (Kufe et *al*., 2003).

I.2.4. Types of cancers

There are over 200 types of cancer classified in general categories. These types include:

- Carcinoma: Cancer that begins in the skin or in tissues that line or cover internal organs. This group includes many of the most common cancers, among which skin, lung, colon, breast, prostate, pancreatic, ovarian cancers.
- Sarcoma: Cancer that begins in bone, cartilage, fat, muscle, blood vessels, or other connective or supportive tissue.
- Lymphoma and Leukemia: Cancer that starts in blood-forming tissue such as the bone marrow and causes large numbers of abnormal blood cells to be produced and enter the blood.
- Blastoma: Cancers derived from immature precursor cells or embryonic tissue

I.2.5. Treatments

Cancer treatment depends on the type and the stage of the cancer. In some people, diagnosis and treatment may occur at the same time if the cancer is entirely surgically removed when the surgeon removes the tissue for biopsy.

Although patients may receive a unique sequenced treatment, or protocol, for their cancer, most treatments have one or more of the following components: surgery, chemotherapy, radiation therapy, ionotherapy, hormonotherapy immunotherapy or combination treatments (a combination of two or three treatments). The treatment intent may or may not be curative.

I.2.5.1. Surgery

It is the primary method of treatment for most isolated, solid, and localized cancer. Surgery typically attempts to remove the entire tumor mass and for some types of cancer it is sufficient to eliminate the cancer (King et Primrose, 2003; Kufe et *al*., 2003). But the inability to kill microscopic disease around the edges of the tumor may leave tumor cells in the patient after surgery.

I.2.5.2. Radiation therapy

Radiation therapy is used in about half of cases. It involves the use of ionizing radiation in an attempt to either cure or improve symptoms (Fong et *al*., 2005). This treatment works by damaging the DNA of cancerous tissue, killing it. Radiation is typically used in addition to surgery and/or chemotherapy, but for certain types of cancers like head and neck cancer, it may be used alone.

I.2.5.3. Chemotherapy

Chemotherapy is the treatment of cancer with one or more cytotoxic anti-neoplastic drugs (chemotherapeutic agents) as part of a standardized regimen. This treatment works by stopping or slowing the growth of cancer cells, which grow and divide quickly (Shu et *al*., 2010). Chemotherapy can either treat cancer or ease cancer symptoms. When used with other treatments, chemotherapy can:

- Make a tumor smaller before surgery or radiation therapy. This is called neoadjuvant chemotherapy.
- Destroy cancer cells that may remain after treatment with surgery or radiation therapy. This is called adjuvant chemotherapy.
- Help other treatments work better.
- Kill cancer cells that have returned or spread to other parts of your body.

There is a huge list of chemotherapy drugs which are specifically used for different types of cancers. For example, drugs for breast cancer commonly used are cyclophosphamide **5**, methotrexate **6** and drugs for lung cancer are carboplatin **7**, gemcitabine **8**. Structures of these drugs are shown by **figure 8** below.

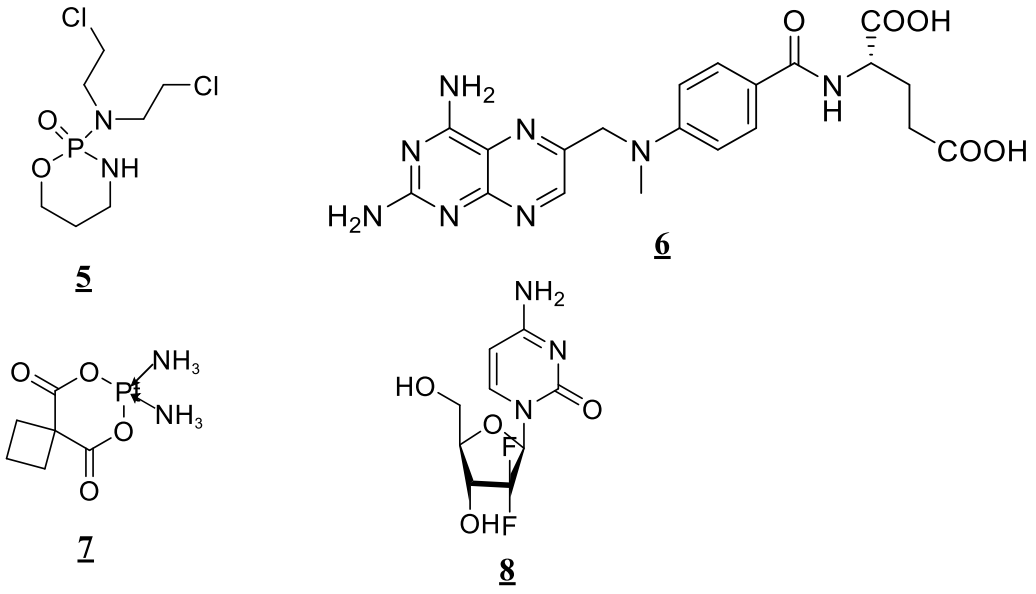

Figure 8: Structure of some drugs used in chemotherapy

These drugs can be given orally, intravenously, intrathecally or topically. But while killing cancerous cells, they can also damage the functioning of the other rapidly growing cells too, like white blood cells, red blood cells and platelets. Hence all the chemotherapy drugs have side effects which vary according to the dosage, type of cancer, type of drug and the person's resistance power. These side effects commonly include: nausea, vomiting, diarrhea, hair loss, loss of appetite, fatigue, fever, mouth sores, pain, constipation and easy bruising. Even when chemotherapy does not provide a permanent cure, it may be useful to reduce symptoms such as pain or to reduce the size of an inoperable tumor in the hope that surgery will become possible in the future.

I.2.6. Alternative treatment of cancers: Medicinal plants

The toxicity of chemotherapeutic drugs sometimes creates a significant problem in the treatment of cancer using allopathy or established medicine. Various therapies have been propounded for the treatment of cancer, many of which use plant-derived products. There are four classes of plant-derived anticancer agents in the market today, the vinca alkaloids

(vinblastine **9**, vincristine **10** and vindesine **11**), the epipodophyllotoxins (etoposide **12** and teniposide), the taxanes (paclitaxel **13** and docetaxel **14**) and the camptothecin derivatives (camptotecin **15** and irinotecan) (Taneja and Qazi, 2007).

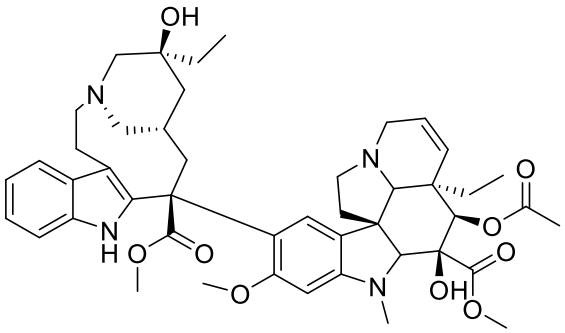

9

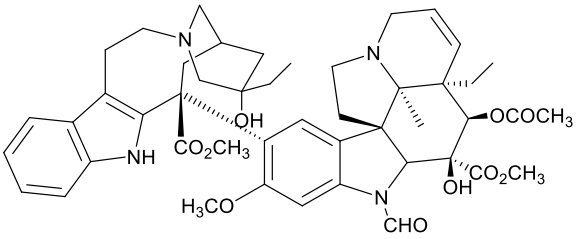

10

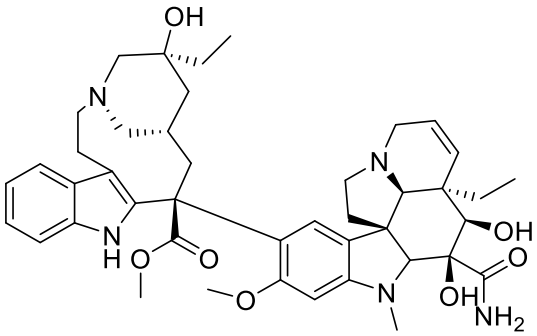

11

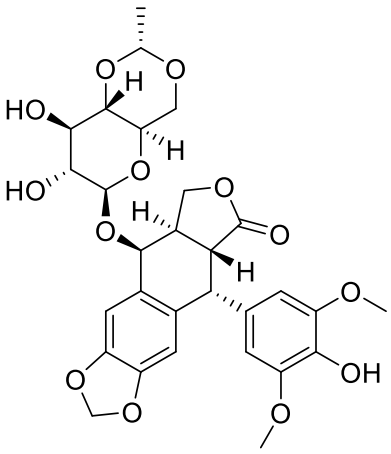

12

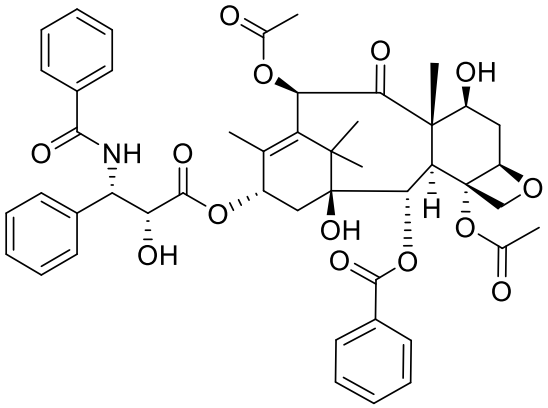

13

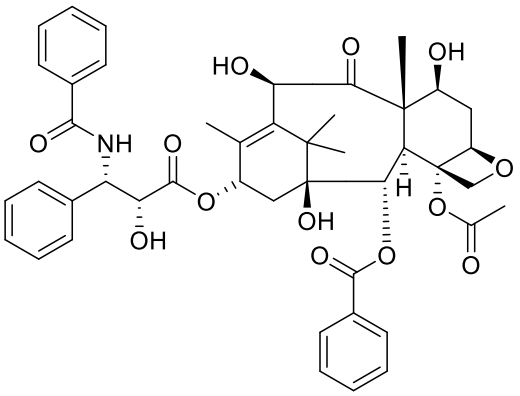

14

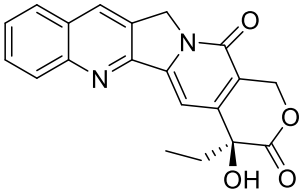

15

Figure 9: Some plant derived anticancer agents (Taneja and Qazi, 2007).

Plants still have enormous potential to provide newer drugs and as such are a reservoir of natural chemicals that may provide chemoprotective potential against cancer.

I.3. BOTANY

I.3.1. Generalities on Ebenaceae family

I.3.1.1. Systematic classification

Ebenaceae are a family of dicotyledonous plants belonging to the Ericale order and whose position in evolutionary classification systems is given in the **scheme 1** below:

Kingdom ⟶ *Plantae*

Subkingdom ⟶ *Tracheobionta*

Superdivision ⟶ *Spermatophyta*

Division ⟶ *Magnoliophyta*

Class ⟶ *Magnoliopsida*

Subclass ⟶ *Dilleniidae*

Order ⟶ *Ericale*

Suborder ⟶ *Ebenineae*

Family ⟶ *Ebenaceae*

Genus ⟶ ***Diospyros***
Euclea
Royena
Lassiocarpa

Species ⟶ ***Diospyros gilletii*** De Wild
Diospyros fragrans Gürke
Euclea natalensis White
Euclea multiflora Hiern

Scheme 1 : Systematic classification of Ebenaceae

I.3.1.2. Description

The Ebenaceae are a family of flowering plants consisting of about 500 to 600 species of trees and shrubs mostly distributed across the tropical and warmer temperate regions of the world (Wallnöfer, 2001; Mallavadhani et *al.*, 1998). They are mostly found in Africa, Asia and South America, with the majority of species in Asia and the Indo-Pacific region, but the greatest morphological diversity is in Africa and Madagascar (Wallnöfer, 2001; Samuel et *al*., 2019). Earlier classifications of genera of this family based on the morphological and anatomical characters have been problematic, changing from two to eight from one author to the other (Dungjai et *al.,* 2006). Some studies, based this time on phylogenetic analysis, reduced the number of genera into four: *Diospyros*, *Euclea*, *Royena* and *Lissocarpa*, divided in two subfamilies, Lissocarpoideae and Ebenoideae (Dungjai et *al.*, 2006; Samuel et *al*., 2019). The genus *Lissocarpa* is the smallest with 9 species (Geeraerts et *al.,* 2009) and the genus *Diospyros* the largest with more than 500 species (Dungjai et *al.*, 2006; Wallnöfer, 2001). Plants belonging to this family are characterized by alternate and evergreen leaves, persistent calyx, absence of latex, berry-like or capsular fruits with 1 to 16 seeds, black wood and bark, unisexual flowers with 3 to 8 petals which are joined at the bases (Dungjai et *al.*, 2006). In Africa, the Ebenaceae family is represented by the genera *Diospyros* and *Euclea* while in Cameroon only the genus *Diospyros* is found (Letouzey et white, 1970).

I.3.2. Generalities on genus *Diospyros*

The genus *Diospyros* is numerically and economically the most important genus of Ebenaceae family. Approximately 300 species of *Diospyros* are found in Asia and Pacific area, 100 species in the Americas, 15 species in Australia, 31 species in New Caledonia, 98 species in Madagascar and the Comoros, and 94 species in mainland Africa (Dungjai et *al.*, 2009). They are mostly trees and shrubs up to 30 m high and 50 cm of diameter growing in tropical area but also in some warm temperate zones (Wallnöfer, 2001). The characteristic features of the species belonging to this genus are: alternate leaves; white, green or yellow unisexual flowers with 3-7 lobes and campanulate corolla; male flowers always a little smaller than female flowers; large fruits, usually berries up to 10 cm of diameter with 1-10 seeds; white and soft sap wood with black and hard heartwood (Mallavadhani et *al.*, 1998; Letouzey et white, 1970; Wallnöfer, 2001). In Africa they occur in dry and humid areas and the following map gives a brief overview of their distribution.

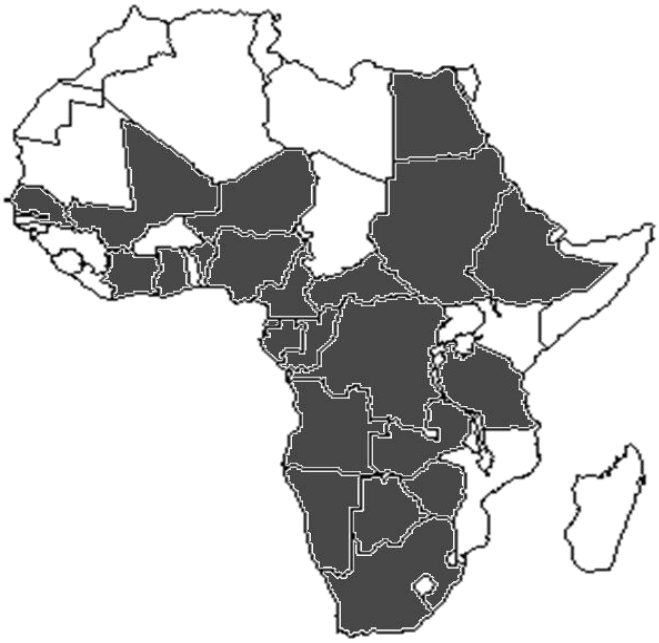

Diospyros species in Africa

Figure 10 : Distribution of *Diospyros* species in Africa

36 species belonging to this genus are reported to be present in Cameroon in dense and evergreen or semi-deciduous forests of Center, Littoral, South, South-East, and East regions as indicated by the table below**.**

Table 1: Distribution of *Diospyros* species in Cameroon (Letouzey et White, 1970).

Species	Authors	Regions	Localities
D. abyssinica	White	East.	Mont Sangembam.
D. alboflavescens	White	South.	Bipindi, Mimfia.
D. barteri	Hiern	Littoral, South.	Mangombé, Bipindi, Mimfia.
			Banga, Eséka, Nkoemvone, Masok, Koumou,

D. bipindensis	Gürke	Center, Littoral, South.	Mangombé, Yaoundé, Bipindi.
D. boala	De Wild	South	Ongongondjé.
D. canaliculata	De Wild	Center, East.	Bertoua, Yaoundé, Ntam, Yokadouma, Ndikiniméki.
D. cinnabarina	Gürke	Littoral, South.	Banga, Douala, Bipindi, Mimfia, Nkuambe.
D. conocarpa	Gürke and Schumann	Center, South, South-west.	Bityé, Kumba, Banga, Nkolebunde, Essong, Mekassi, Nkane, Lolodorf, Ejagham lake, Bipindi, Yaoundé.
D. crassiflora	Hiern	Center, East, South-west and South.	Yaoundé, Bityé, Mbet, Pouté, Essaoulo, Mbalmayo, Abong Mbang, Batouri, Mamfé.
D. dendo	Welwitsh	South-west, South.	Kumba, Kribi, Likomba, Bakumbo, Mamfé, Bipindi.
D. ferrea	Bakhuizen	South-west.	Bambuko, Kumba
D. fragrans	Gürke	South, Center, South-west.	Kribi, Grand Batanga, Ejagham lake, Mimfia hills, Abang.
D. gabunensis	Gürke	Center, South, South-west	Eséka, Bambuko, Kumba, Mimfia Mimiaca, Bipindi.
D. gilletii	De Wild	Littoral, East, South.	Edge of Sanaga, edge of Nyong, Mbalmayo, Ebolowa, Abong Mbang, Yaoundé.
D. gracilescens	Gürke	Center, Littoral.	Eséka, Colline Nkolakaye, Badjob, Mangombé.
D. hoyleana	White	Littoral, Center, South, South-west	Bakundu, Eséka, Douala, Ongongondjé hills, Kembong, Ejagham.
D. iturensis	Letouzey and White	Center, Littoral, East, South, South-west	Edge of Nyong, Eséka, Douala, Edéa, Ongongondjé hills, Ebolowa, Ejagham lake.
D. kamerunensis	Gürke	South, Center.	Kribi, Bipindi, Mimfia, Eséka.
D. longiflora	Letouzey and White	Center	Edge of Nyong.
D. mannii	Hiern	Center, East, Littoral, west, South.	Yaoundé, Ambam, Mélong, Edea, Kribi, Eséka, Mimfia, Deng-Deng, Yokadouma.
D. melocarpa	White	Littoral, South, South-west.	Mamfé, Douala, Kolakaye hills.
D. mespiliformis	Hochst	Extreme North, Adamaoua, North.	Maroua, Moutouroua hills, Hoyo hills, Ngaoundéré, Garoua, Mogodé.
D. monbuttensis	Gürke	Center, Adamaoua, East, west, North-west.	Mendougué, Mont Fébé, Gounté, Bambui, Dimako, Baleng lake, Meïganga, Ngaoundéré.
D. obliquifolia	White	South-west, South, Littoral.	Ndifo, Banga, Fenda, Batanga.
D. physocalycina	Gürke	South.	Yokadouma, Campo, Bipindi, Mbiave.
D. piscatoria	Gürke	Littoral, South, South-west.	Bidjoka, Douala, Muyuka, Bambuko, Bipindi, Kumba.
D. platanoïdes	Letouzey and White	South-west.	Lac Ejagham.

D. polystemon	Gürke	South.	Kuke Boua, Masok, Makak, Valley of Lokundjé, Nkuambe, Bipindi.
D. preussii	Gürke	South.	Bakundu, Grand Batanga, Kribi, Njabilobé, Bipindi.
D. pseudomespilus	Mildbraed	Center, South.	Yaoundé, Grand Batanga
D. sanza-minika	Chevalier	Littoral, South.	Douala, Mangombé forest, Badjob, Bonépoupa, Bipindi, Nsambi, Manoka
D. simulans	White	South.	Banga, Nkolomeyan, Bipindi
D. soyauxii	Gürke et K. Schumann	South.	Zingui
D. suaveolens	Gürke	Center, South, South-west.	Yaoundé, Eseka, Bipindi, Ejagham lake, Lolodorf, Ndengué, Mbalmayo, Limbé, Bambuko, Mangombé
D. viridicans	Hiern	South-west.	Bambuko, Limbé
D. zenkeri	White	Center, Littoral, South.	Eséka, Douala, Bambuko, Masok, Nkolebunde, Edéa, Kumba, Bipindi

I.3.3. Generalities on the species *Diospyros gilletii* De Wild

Synonym: *Diospyros potamophyla* Mildbraed (Letouzey et White, 1970).

I.3.3.1. Botanical description

Diospyros gilletii is a shrub that can reach about 6 to 8 m high with a bark measuring up to 30 cm in diameter (Letouzey et White, 1970). Its 20 x 9 cm long leaves have 10-12 mm long petioles, sharply channeled above the upper part and with an elliptical-lanceolate blade, often somewhat falcate. The young leaves, red in colour, have scattered hairs at the base. The bark is very thin, with an oblique section, brownish-black outside, and egg-yellow inside (Letouzey et White, 1970). Its male axillary influorescence of about 2 cm in diameter can group up to 50 fragrant flowers, not exceeding 1 mm in length, hinged at the top and also pubescent, while its female one has only 5-8 flowers. The fruits exceed the lobes of the calyx, globular, of 10-15 mm in diameter, glabrous, smooth, green, then yellow, then dark red, glossy, with 4 seeds maximum of 8 x 5 x 4 mm size (Letouzey et White, 1970). Some parts of *Diospyros gilletii* De Wild are presented in **Figure 11** below.

1: leaves; 2: bark; 3: fruits; 4: stem bark

Figure 11: *Diospyros gilletii* De Wild (Harris et *al*., 2011).

I.3.3.2. Geographical repartition

Diospyros gilletii De Wild is found in Cameroon, Central African Republic, Congo and Gabon. In Cameroon this plant is reported mainly along rivers and is found in the high valleys of Sanaga, Nyong, Dja and at the East longitude of yaounde (Letouzey et White, 1970). The following map is presenting the distribution of this species in Cameroon.

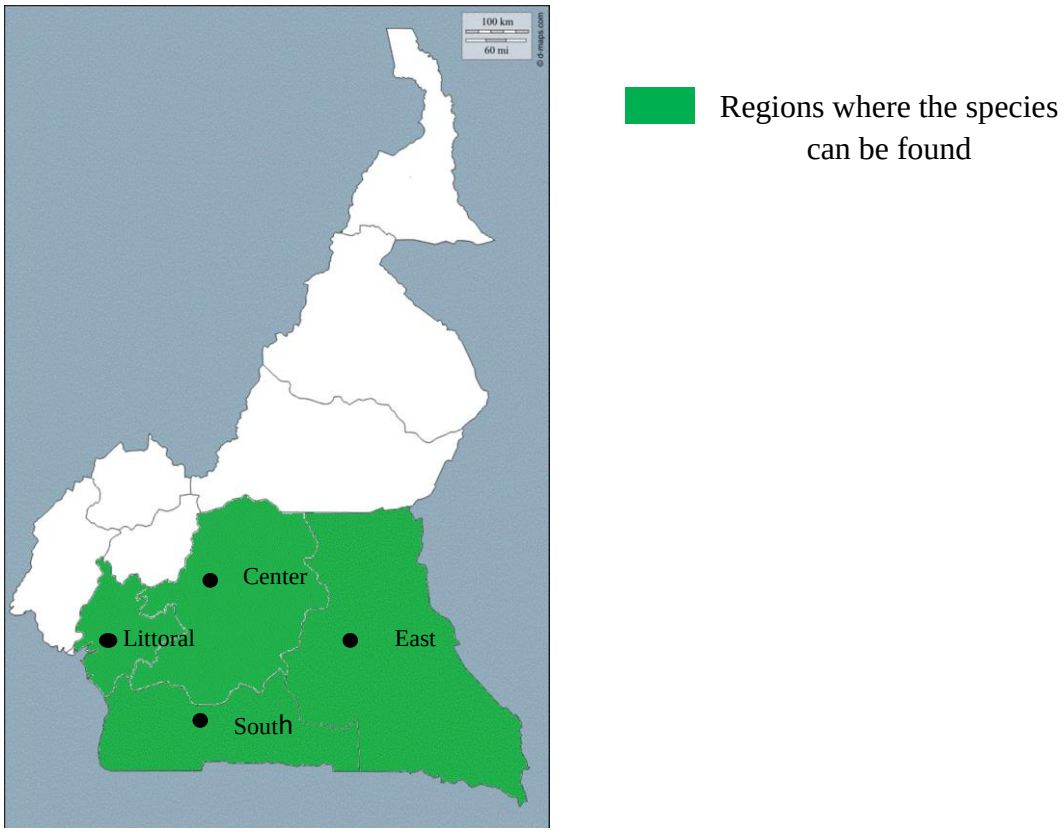

Figure 12 : Distribution of *Diospyros gilletii* De Wild in Cameroon (Letouzey et White, 1970).

I.3.4. Generalities on the species *Diospyros fragrans* Gurke

Synonym: *Maba fragrans* Hiern**;** *Diospyros mucronata* Pierre (Letouzey et White, 1970).

I.3.4.1. Botanical description

Diospyros fragrans is a small tree of height about 15 m, sometimes consists of several vertical twigs. Its sapwood is yellowish cream-coloured with slices black on the outside and dark ochre on the inside. The leaves are briefly petiolate **(Figure 13**), with an oblong-lanceolate blade of 7-11.5 x 3-4 cm obtuse or broadly rounded at the base. The male influorescences consist of 6-15 flowers born on the old wood, almost down to the ground, lined with bracts and lanceolate bracteoles of 2-3 mm long and pubescent on the outside while the female influorescence have 5-8 flowers. The Globular ovoid fruit is about 3-4 cm in diameter, scattered with silky hairs, surrounded at the base by a calyx up to 1.5 cm in diameter and have approximately 10 seeds of 30 x 13 x 8 mm size.

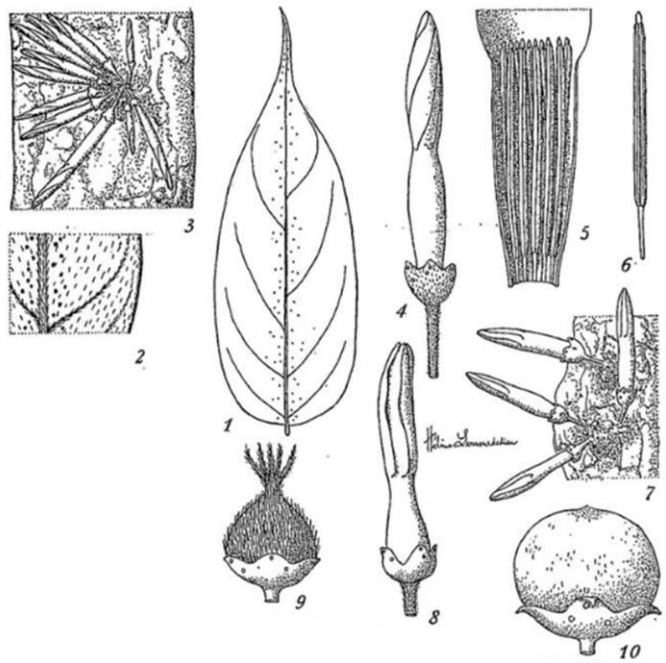

1: leaves; 2: leaf fragment; 3: male influorescence; 4: male flower; 5 and 6: corolla; 7: female influorescence; 8: female flower; 9: calice; 10: fruit

Figure 13 : *Diospyros fragrans* Gürke (Letouzey et White, 1970; Jouwa, 2018)

I.3.4.2. Geographical repartition

Diospyros fragrans is found in Cameroon, Equatorial Guinea, Gabon and Congo Brazzaville in the wettest areas of dense forest. In Cameroon this species is present at Kribi, Kumba, Manoka, Bipindi, Oveng and Mamfe (Letouzey et White, 1970), as shown by the map below.

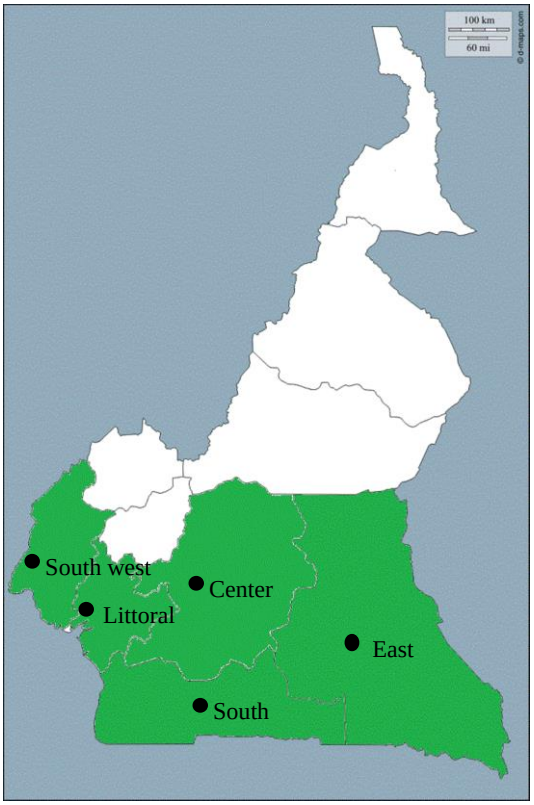

Figure 14 : Distribution of *Diospyros fragrans* Gürke in Cameroon

I.4. USES OF GENUS *DIOSPYROS*

I.4.1. Uses in traditional medicine

Diospyros species are widely used in many traditional medicinal systems of the world such as Ayurveda, the African folklore and Chinese medicine for the treatment of various diseases including leprosy, fungal infections, dysentery, whooping cough, hemorrhages, incontinence, rheumatoid arthritis, cardiovascular disorder and various cancer types (Maroyi, 2018; Rauf et *al*., 2017; Ravikumar et *al*., 2014). Naoxinqing, a standardized extract of the leaves of *D. kaki* is a patented neural drug of traditional Chinese medicine (TCM) (Rauf et *al*., 2017). A decoction of the dried fruits and leaves of this same specie is traditionally used as a folk medicine in Korea for hiccups, reduction of internal bleeding, blood clotting, and

dispelling of pathogenic heat, while its traditionally fermented fruits vinegar is used against hangovers caused by excessive alcohol consumption (Titto et *al*., 2009). The dried flowers of *D. melanoxylon* are recorded in Yunani medicine for urinary discharges, inflammation of the spleen and enrichment of blood, while its bark extract is used in Ayurveda medicine as an astringent lotion for eyes (Mallavadhani et *al.*, 1998). In Nigeria the dried leaves of *D. melanoxylon* are used for the treatment of malaria, sleeping sickness and headache (Adzu et *al.*, 2002). *D. mespiliformis* leaves decoction is used in central Africa for the treatment of fever, whooping cough, wounds and a decoction of its barks and roots are used for infections such as malaria, pneumonia, syphilis, leprosy, and dermatomycoses (Mohamed et *al*., 2009). The juice of the fresh leaves of *D. hoyleana* is sucked up or the powder of the dried leaves snuff in case of severe or persistent cephalgy (Bouquet, 1969). In Cameroon, the baka pygmies used the infusion of the stem barks of *D. bipindesis* to treat the diseases "that attacks both sides and makes difficult the breathing" (Brisson, 1999). The roots decoction of *D. fischeri* is taken in Tanzania against stomach aches, chest complaints, gonorrhea, and dry cough, whereas the one of *D. usambarensis* is used for the treatment of stomach pain, constipation, rashes, cervical prolapse, epilepsy, malaria, measles, psychiatric disorders, sterility, and joint pain (Chhabra et *al*., 1989). In Côte d'Ivoire the leaves of *D. soubreana* are used as wound healing (Bouquet et Debray, 1974). The thin twigs of *D. lycioides* are used in Namibia as chewing sticks to clean the teeth (Cai et *al*., 2000). In West Africa boiled leaves of *D. barteri* are applied as poultices to treat vaginal discharges (Oluremi et *al*., 2010). Unripe fruits of *D. peregrina* are used in India for the treatment of diarrhoea, dysentery, cholera, ulcer of mouth and wounds (Saikat et *al*., 2009). In pharmacopeia and medical books, these plants are cited as indigenous therapies (Rauf et *al*., 2017).

I.4.2. Nutritional uses

The name *Diospyros* comes from an old Greek denomination consisting of "*Dios*" which means divine and "*pyros*" referring to wheat, hence the name "divine food" given to *Diospyros* species. Indeed, plants belonging to this genus among which *D. virginiana, D. ebenaster, D. lotus, D. mespiliformis* and *D. melanoxylon* have edible fruits that are very appreciated for their taste (Mallavadhani et *al.*, 1998). The thin yellow fruit-pulp of *D. barteri* is edible and is a minor item of diet (Oluremi et *al*., 2010). Soft sweet fruit-pulp of *D. mespiliformis* is used in some parts of Sudan to make a fermented drink (Adzu et *al*., 2002). Mature fruits of *D. peregrina* are highly nutritious and contribute to household food security of rural populations in India (Saikat et *al*., 2009). The most consumed fruit is the kaki or Japanese persimmon, a large orange-red berry from *D. kaki* cultivated in Japan for several

centuries and which produces sweet and palatable juice when fully ripe (Mallavadhani et *al.*, 1998).

I.4.3. Economical and socio-cultural uses

The genus *Diospyros* is of great economic importance with many species yielding edible fruits, ebony, valuable timbers, and ornamental trees. Japanese persimmon is the most cultivated fruit of this genus with a global production totaling 2,429,840 t in 2003 and 3,300,000 t in 2007 (Rauf et *al*., 2017). Indeed, this fruit is mainly grown in China, Korea, Japan, Brazil, Italy, Israel, and New Zealand and exported all over the world (Yamagishi et *al*., 2005). In China, the leaves of *D. kaki* are used to manufacture a variety of functional health food and cosmetics, such as health protection tea, milky tea, other beverages granules and freckle cream (Huang et *al*., 2016). In India the leaves of *D. melanoxylon* are greatly valued in wrapping cigarettes because of their flavour, flexibility and resistance to decay (Mallavadhani et *al*., 1998). Many species yield useful and valuable wood. So are *D. dendo, D. mespiliformis, D. crassiflora, D. ebenum, D. melanoxylon* and *D. celebica* which produced ebony used in ornamental works and musical instruments. In Japan, the wood of *D. kaki* is of decorative class with an exceptionally smooth surface and a marble like coldness to the touch. This wood is also used for ornamental to make boxes, desks and mosaics (Mallavadhani et *al*., 1998). The wood of *D. barteri* is used in Nigeria to make clubs, spear shafts, walking sticks and as house building materials (Oluremi et *al*., 2010).

I.5. PREVIOUS PHARMACOLOGICAL WORKS ON GENUS *DIOSPYROS*

Many *Diospyros* species have been reported to exhibit interesting biological and pharmacological activities. Indeed, the activities such as antioxidant, antiinflammatory, analgesic, antipyretic, anti-diabetic, antibacterial, anthelmintic, antihypertensive, cosmeceutical, anti-protozoal, fungicidal, anthelmintic, insecticidal, molluscicidal, cytotoxicity, anti-tumor, multidrug resistance reversal, sedative and enzyme-inhibitory of these plants have been validated by means of an *in vitro, in vivo,* and clinical tests (Rauf et *al*., 2017). As a rich reserve of pharmacologically important constituents, this genus can quicken the pace of drug discovery.

I.5.1. Antioxidant activities

A methanolic extract of *D. lotus* exhibited antioxidant activity. Indeed, Treatment of cisplatin-injected rats with *D. lotus* extract led to a significant increase in superoxide

dismutase and glutathione levels (Sagar et *al*., 2016). The reducing power of an extract of total flavonoids from persimmon leaves (TFPL) on total antioxidant activity, 1,1-diphenyl-2-picrylhydrazyl (DPPH$^{\bullet}$) radical scavenging, superoxide anion ($O_2^{\bullet-}$) radical scavenging, hydroxyl ($^{\bullet}$OH) radical scavenging and metal chelating activities was examined by Sun et *al*. Results showed that the effect of this extract in total antioxidant activity, scavenging activity of superoxide anion and hydroxyl radical was significantly better than that of rutin (Sun et *al*., 2011). Furthermore, it was reported that tannin isolated from *D. kaki* at a dose of 200 mg/mL exerts radioprotective effect on 8 Gy gamma-radiation-exposed HEK 293T cells. The anti-radiation effect is achieved by preventing formation of oxygen reactive species (Zhou et *al*., 2016).

I.5.2. Antimicrobial activities

Several extracts of *D. ebenum*, including ether, ethyl acetate, methanol, and aqueous extracts were tested to assess their antibacterial potential against various Gram-positive and Gram-negative bacteria. All the tested extracts, except the aqueous one, displayed significant activity against *Staphylococcus aureus*. Furthermore, the methanol extract was more active against *Pseudomonas aeruginosa* and *Salmonella Typhimurium* than amikacin, an antibiotic used to treat different bacterial infections (Baravalia et *al*., 2009). The methanol extract of *D. lycioides* was found to inhibit growth of selected oral pathogens (*Streptococcus mutans*, *Streptococcus sanguis*, *Porphyromonas gingivalis*, and *Prevotella intermedia*) (Cai et *al*., 2000). The ethanol extracts of stems and leaves of *D. gracilipes* Hiern exhibited moderate antimicrobial activity against *Staphylococcus aureus,* and *Klebsiella pneumonia (*Rasamison et *al*., 2016). Furthermore, the methanol extract of *D. sylvatica* was reported to be active against *P. falciparum* strains (Kantamreddi et Wright, 2008). Similarly, stem bark methanol/ dichloromethane (1:1) extract of *D. crassiflora* were tested against several strains of fungi and were found to inhibit the growth of strains such as *Candida albicans, Candida tropicalis, Cryptococcus neoformans, Aspergillus niger, Aspergillus flavus, Fusarium sp.,* and *Penicillium sp.*(Dzoyem et *al*., 2007).

I.5.3. Cytotoxic activities

The acetone fraction from *D. kaki* peel extract showed cytotoxic activity against human oral squamous cell carcinoma HSC-2 and human submandibular gland tumor HSG cells (Kawase et *al*., 2003). The effect of acetone extract of *D. lycioides* leaves on MCF-7 cell viability reduction was studied and the cytotoxicity was demonstrated to be due to apoptosis

(Pilane et *al.*, 2015). The cytotoxic effect of crude methanolic extract of seeds (CMES) and peels (CMEP) and crude ethyl acetate extract of seeds (CEAES) and peels (CEAEP) of *Diospyros blancoi* was evaluated by brine shrimp (*Artemia salina*) lethality bioassay procedures. The ED_{50} values of the CMES, CEAES, CMEP, CEAEP were 40, 20, 20 and 10 mg/mL respectively, compared with the standard vincristine sulphate with an ED_{50} value of 1.04 mg/mL (Setu et *al*., 2017).

I.5.4. Antidiabetic activities

The methanolic extracts of the stem and leaves of *D. buxifolia* were evaluated for their antidiabetic activities by measuring in vitro α-amylase and amyloglucosidase inhibitory activities at four different extract concentrations (0.125, 0.250, 0.500 and 1.000 mg/mL) and the results showed a significant α-amylase inhibitory activity for the stem (Pasupuleti et *al*., 2016). Rathore et al. discovered that the ethanol extract of *D. melanoxylon* could serve as a good adjuvant to other oral hypoglycemic agents and seems to be promising for the development of phytomedicines for diabetes mellitus. In addition, *D. melanoxylon* leaves petroleum ether extract was found to exhibit antiadipogenic, antidiabetic, and hypolipidemic activity both in vitro 3T3-L1 cell line and in rats. These blood glucose controlling effects might be promising for diabetes treatment (Rathore et *al*., 2014).

I.6. PREVIOUS PHYTOCHEMICAL WORK ON GENUS *DIOSPYROS*

The extraordinary uses in traditional pharmacopoeia of *Diospyros* species have attracted the attention of researchers who wanted to know their chemical composition and identify the compounds responsible for their many virtues. Thus, more than 130 species were investigated chemically, which led to the isolation and the characterization of a wide range of secondary metabolites among which triterpenes, naphtoquinones, coumarins and isocoumarins (Mallavadhani et *al*., 1998).

I.6.1. Triterpenes

I.6.1.1. Generalities

Triterpenes are a class of secondary metabolites widely distributed in *Diospyros* species. In fact, more than 90% of these species screened so far were found to contain this class of secondary metabolites in almost all parts of the plants (Mallavadhani et *al*., 1998). Approximately 4000 structures of triterpenes are known in the free, esterified or heterosidic state, represented by nearly 40 different skeletons (Bruneton, 1999). They are hydrocarbons or

their derivatives formed by the condensation of six isoprene units (equivalent to three terpene units) and containing, thus, 30 carbon atoms. These compounds rarely derive from squalene ‘and more often from 2,3-epoxysqualene and are therefore almost always hydroxylated in position C-3 due to the opening of this epoxide. Triterpenes exist in several forms, including acyclic, monocyclic, bicyclic, tricyclic, tetracyclic, pentacyclic and hexacyclic, but most of the triterpenes isolated from *Diospyros* species have a basic pentacyclic skeleton and belongs to the classes of lupane, ursane, oleanane, friedelane and taraxerane. Amongst the pentacyclic triterpenes isolated from *Diospyros* species, lupane, ursane and oleanane are more prevalent (Mallavadhani et *al*., 1998).

I.6.1.2. Common triterpenes isolated from *Diospyros* species

- **Lupane**

It is the most common triterpene skeleton found in *Diospyros* species, evident from the fact that out of 54 publications of *Diospyros* terpenoids, more than 24 papers reported the exclusive isolation of the lupane group **16**. They are characterized by the presence in the pentacyclic skeleton of an E ring with five vertices substituted by an isopropyl group and six angular methyl. The major metabolites of this class encountered in *Diospyros* species are lupeol **17**, betulin **18** and betulinic acid **19**, mostly accumulate in bark and heartwood (Mallavadhani et *al*., 1998).

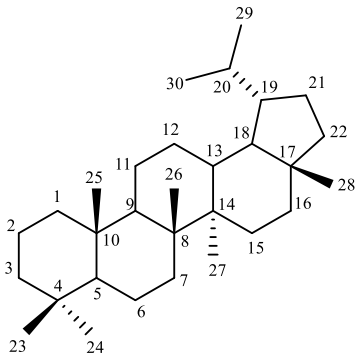

16

- **Ursane**

Pentacyclic triterpenes type ursanes **20** are the second common skeleton found in *Diospyros* species. Contrary to lupanes **16**, the five cycles present in their structures have six vertices and seven methyl including one gem dimethyl at C-4. In *Diospyros* species, both urs-12-ene and urs-7ene skeletons have so far been isolated, with few urs-7-ene representatives.

Ursolic acid **21**, *α*-amyrin **22** and bauerenol **23** are the three major metabolites of this class isolated in several *Diospyros* plants, with ursolic acid **21** accumulating in significant quantities and mostly co-existing with *α*-amyrin **22** (Mallavadhani et *al*., 1998).

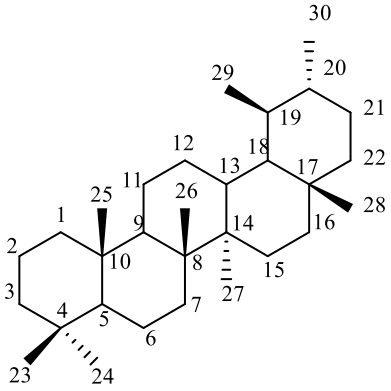

20

- **Oleanane**

Oleananes **24** have their pentacycles like ursanes **20**, with six verticles each. The only difference is that in contrast to ursanes, they have a second gem-dimethyl on the cycle E, at C-20. Oleanolic acid **25**, *β*-amyrin **26** and olean-12-ene-3-one **27** are the major metabolites of this class isolated from *Diospyros* species. Most of the triterpene glycosides isolated from *Diospyros* species have an oleanane skeleton, with oleanolic acid **25** as aglycone.

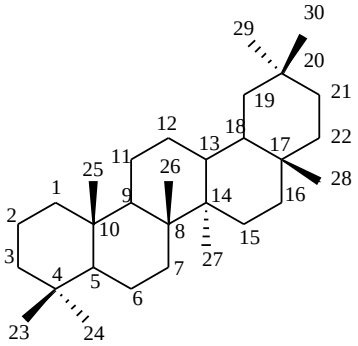

24

The **table 2** below is presenting the structures of some isolated triterpenes from the genus *Diospyros*.

Table 2 : Some triterpenes isolated from *Diospyros* species

Sources	Names and structures	References
Leaves of *D. mespiliformis*	Lupeol **17** : $R_1 = CH_3$; $R_2 = H$ Betulin **18** : $R_1 = CH_2OH$; $R_2 = H$ Betulinic acid **19 :** $R_1 = COOH$; $R_2 = H$ 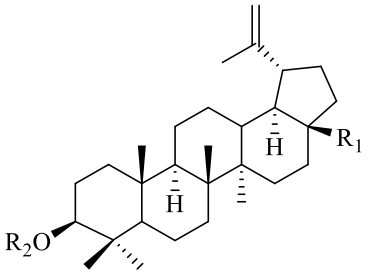	Mohamed et *al*., 2009
Roots of *D. melanoxylon*	Ursolic acid **21** ; R = COOH α-amyrin **22** ; R = H 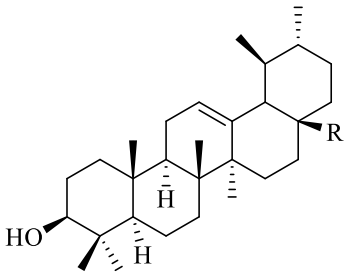	Mallavadhani et *al*.,1998
Leaves and fruits of *D. kaki*	Bauerenol **23** 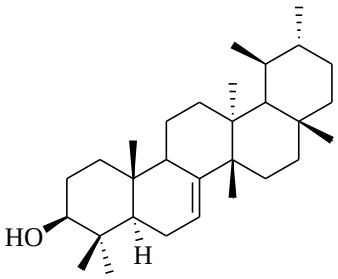	Mallavadhani et *al*.,1998

Stem of *D. glandulosa*	Oleanolic acid **25 :** R = COOH *β*-Amyrin **26 :** R = H 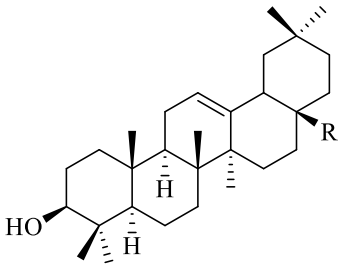	Thnakijcharoenpath et Theanphong., 2007
Leaves of *D. peregrina*	(3*β*)-17-Carboxy-28-norolean-12-en-3-yl-3-*O*-(6-deoxy-*α*-*L*-mannopyranosyl)-*β*-*D*-glucopyranosiduronic acid **28:** $R_1 = R_2 = H$ Putranoside C: **29** : R_1 = Glu; R_2 = H 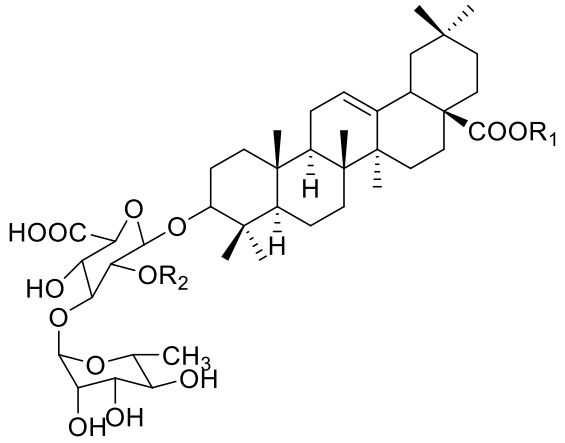	Mallavadhani et *al.*,1998
Leaves, stem and roots of *D. morrisiana*	Olean-12-en-3-one **27** 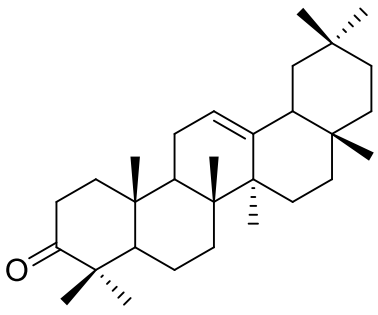	Mallavadhani et *al.*,1998

I.6.1.3. Biological and pharmacological properties of triterpenes

Triterpenes are characterized by remarkable structural diversity. This chemical diversity results in varied biological and pharmacological properties and therapeutic potential

in the most diverse fields: cytostatic, antiviral, anti-inflammatory, anti-oedematous, cytoprotective, immunomodulatory, analgesic, and antifungal (Zanatta et *al*., 2021).

Activity against fungi is well established in vitro, both against phytophatogenic species and various dermatophytes. It is probably a consequence of the reaction of triterpenes with membrane sterols of microorganisms. In the plant kingdom, they are secondary metabolites, whose ecological role has been proven, particularly in the communication and defence process (Bruneton, 1999).

Apart from their pharmacological potential, it appears that pentacyclic triterpenes, in the same way as other molecules (gibberellins, auxins, etc.), are involved in the control of plant growth and morphogenesis, as well as in wound healing (Boiteau et *al*., 1964).

I.6.2. Naphtoquinones

I.6.2.1. Generalities

They are naphthalene derivatives characterized by two carbonyl groups in position 1 and 4 for 1,4-naphthoquinones and position 1 and 2 for 1,2-naphthoquinones (Kumagai et *al*., 2012). Naphthoquinones are highly reactive organic compounds that can vary in colour from yellow to red. Being carbonyl compounds α,β-unsaturated, the conjugation between double bonds and carbonyls makes 1,4 derivatives the majority in nature, especially in many large plant families such as Plumbaginaceae, Ebenaceae, Boraginaceae, Iridaceae (Kumagai et *al*., 2012).

I.6.2.2. Naphtoquinones isolated from genus *Diospyros*

About 75% of phytochemical investigations carried out on plants of the genus *Diospyros* resulted in the isolation of monomers, dimers and even trimers of 1,4-naphthoquinones. Indeed, these plants are known to produce an incredible amount of these compounds, which could be considered as a chemical marker for a taxonomic study (Mallavadhani et *al*., 1998). Plumbagin **30** and 7-methyljuglone **31,** obtained by substitution of juglone **32,** are the most widespread monomers in *Diospyros* species. The majority of isolated naphthoquinones from this genus are dimers formed by coupling either two plumbagin **30** or two 7-methyljuglone **31** groups, or more rarely plumbagin **30** and 7-methyljuglone **31**. Plumbagin **30** is most abundant in leaves while 7-methyljuglone **31** is found in bark and wood (Mallavadhani et *al*., 1998).

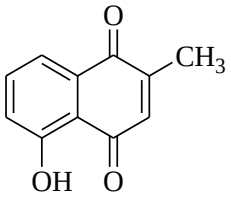

30

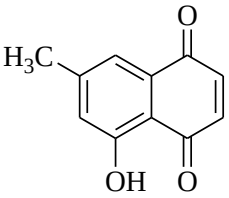

31

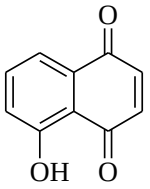

32

The table 3 below gives some naphtoquinones isolated from *Diospyros* species.

Table 3: Naphtoquinones isolated from some *Diospyros* species

Sources	Names and structures	References
Stem bark of *D. maritima*	3-bromoplumbagin **33** $R_1 = CH_3$ $R_2 = Br$ $R_3 = H$ 3-chloroplumbagin **34** $R_1 = CH_3$ $R_2 = Cl$ $R_3 = H$ Droserone **35** $R_1 = CH_3$, $R_2 = OH$, $R_3 = H$ 3-Methylplumbagin **36** $R_1 = CH_3$ $R_2 = CH_3$ $R_3 = H$ 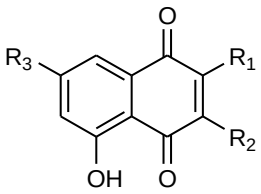	Higa et *al*., 2017
Leaves of *D. sylvatica*	Diospyrin **37** 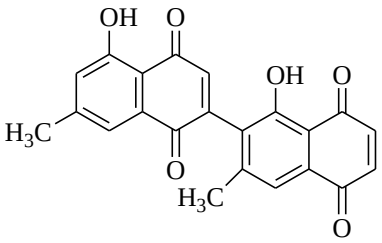	Ganapaty et *al*., 2004
	Isodiospyrin **38**	

	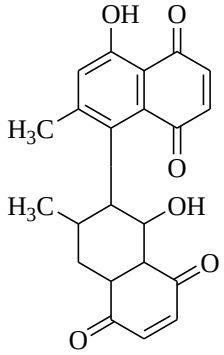	
Leaves and roots of *D. montana*	Cyclodiospyrin **39** 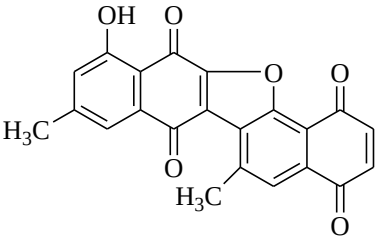	Mallavadhani et *al.*,1998
	8-hydroxydiospyrin **40** 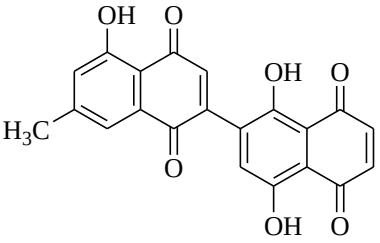	

I.6.2.3. Biological and pharmacological properties of naphtoquinones

Several naphthoquinones are antibacterial and fungicidal: their presence in tropical woods helps to understand their resistance to fungi, insects and, more generally, wood-eating organisms (Bruneton, 1999). They also serve as important links in electron transport chains, participate in multiple oxidative processes, and may act as defensive compounds in interspecies chemical warfare (Pinho et *al*., 2012). Thus, the biological and toxicological activities of naphthoquinones have been explored by the scientific community in an attempt to discover and develop new drugs. Diospyrin **37**, a bis-naphthoquinone and its derivatives, were reported to have inhibitory activity against protozoan parasites including Leishmania (Rauf et *al*., 2017). Atovaquone which was first developed for the treatment of pneumonia and toxoplasmosis is a naphthoquinone with important antimalarial activity. Plumbagin **30** was found to be active against the fungi *Candida albicans*, *Aspergillus niger*, and *Colletotrichum gloeosporioides*. Conocurvone, a natural compound with several naphthoquinones's moieties,

inhibits HIV integrase and HIV mediated cell fusion. *β*-alkannin, a monomer of juglone **32** exerts strong antioxidant activity against various types of ROS, having a high anti-lipid peroxidative ability. Lapachol and *β*-lapachone, two naphtoquinones revealed activity against a wide range of tumour cell lines, including breast, leukaemia and prostate, as well as several multridrug resistance cell lines (Pinho et *al*., 2012).

I.6.3. Naphthalene-based aromatics

Naphthalene-based aromatics are compounds derived from naphthalene and assumed to be the precursors of naphthoquinones. Due to their tendency to transform further, they were isolated from a limited number of *Diospyros* plants as mono, dimeric and glycoside naphtalenes. Mostly, these metabolites were isolated with aldehydic, carboxylic and phenolic functionalities (Mallavadhani et *al*., 1998). Diospyrol **43**, a dimeric naphthalene isolated from *Diospyros mollis* showed anthelmintic activity in hamsters infected with human hookworm, *Necator americanus*. It was also active against *Hymenolepis nana* and *Nematospiroides dubius* parasites in mice (Mallavadhani et *al*., 1998). Many other activities were observed for naphthalene derivatives, as antimicrobial, anti-inflammatory, and cytotoxic activities (Rokade et Sayyed, 2009; Huang et *al*., 2003). **Table 4** below gives some examples of structure belonging to this class and isolated from species belonging to *Diospyros* genus.

Table 4: naphthalene derivatives isolated from some *Diospyros* species

Sources	Names and structures	Ref.

Leaves, trunk and roots of *D. mollis*	3-methylnaphthalene-1,8-diol **41** 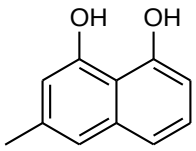 4-hydroxy-5,8-dimethoxy-2-naphthaldehyde **42** 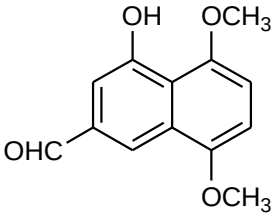 diospyrol **43** 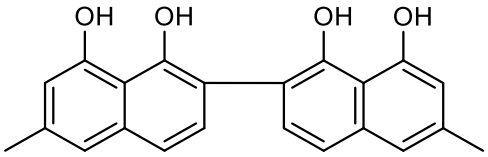	Jintasirikul et Thebtaranonth, 1996
Fruits of *D. cauliflora*	3,4-dihydro-4*β*,6-dihydroxy-5-methoxy-2*α*-methyl-1(2H)-naphthalenone **44** 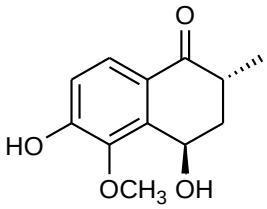	Auamcharoen et *al*., 2009
Stem bark of *D. paniculata*	R= H, 5-hydroxy-4,6-dimethoxy-2-naphthoic acid **45** R= -OCH_3, 4,5,6-trimethoxy-2-naphthoic acid **46** 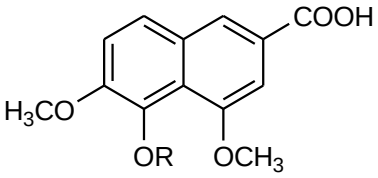	Mohamed et *al*., 2006

I.6.4. Isocoumarins

I.6.4.1. Generalities

Isocoumarin **47**, also known as 1H-2-benzopyran or 3,4-benzopyrone, is an isomer of coumarin in which the orientation of lactone is reversed. Thus isocoumarin is an unsaturated,

non conjugated oxygen heterocycle constituted by fusion of the benzene ring with the 3,4-position of the 2-pyrone ring **48** (Pal et Pal, 2018). It is neither a true aromatic nor a true aliphatic compound because it shows the properties of aliphatic and aromatic compounds. When the molecule is hydrogenated in positions 3 and 4 it is called dihydroisocoumarin **49**.

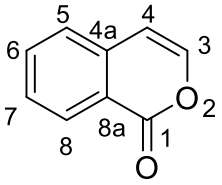

47

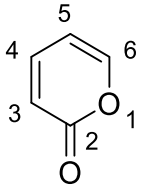

48

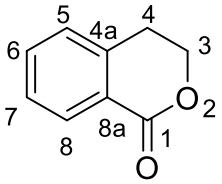

49

Many naturally occurring isocoumarins have been discovered and isolated from various natural sources. Thus, isocoumarins and 3,4-dihydroisocoumarins were found to be present in fungi, lichens, liverworts, bacte-ria, molds, and some higher plant families as piaceae, Leguminoseae, Ebenaceae, Compositae, Bignoniaceae, Saxifragaceae, Asteraceae, Caesalpiniaceae, Hydrangeaceae, and Myricaceae (Pal et Pal, 2018; Tangmouo et *al*., 2009).

I.6.4.2. Biosynthesis

In their biosynthesis, isocoumarins are derived either from shikimic acid or the acetate-malonate pathway, with a further cyclization leading to compounds with one or more phenolic rings. All the isocoumarin biogenetically derived from the acetate-malonate pathway are C-8 oxygenated and many of them have a C-3 alkyl substitution (Magid et *al*., 2007). Condensation of acetyl-SCoA units results in the formation of tetraketides and pentaketides (Pal et Pal, 2018). The latter cyclise to give the aromatic nucleus and then the lactone cycle. During this biosynthesis several types of reactions take place (enolisation, claisen condensation, hemiketal formation, methylation) and lead to a variety of isocoumarins (Noor et *al*., 2020). The following **scheme 2** present the acetate-malonate biosynthesis pathway.

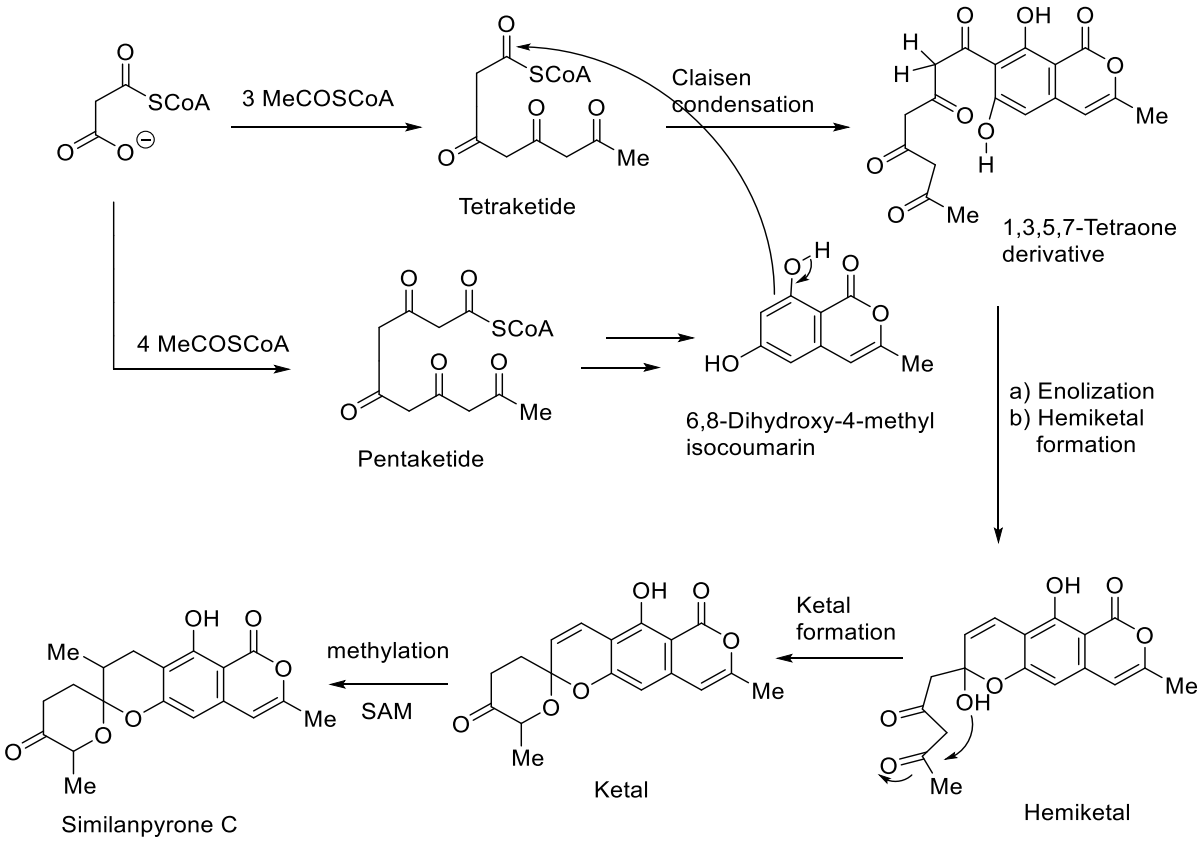

Scheme 2 : Biosynthesis of isocoumarins following the acetate-malonate pathways (Noor et *al.*, 2020; Pal et Pal, 2018)

The biosynthesis of one of the 3,4-dihydro isocoumarins, mullein, involved the condensation of four units of malonate with acetate, following a polymalonate pathway as shown by the **scheme 3** below.

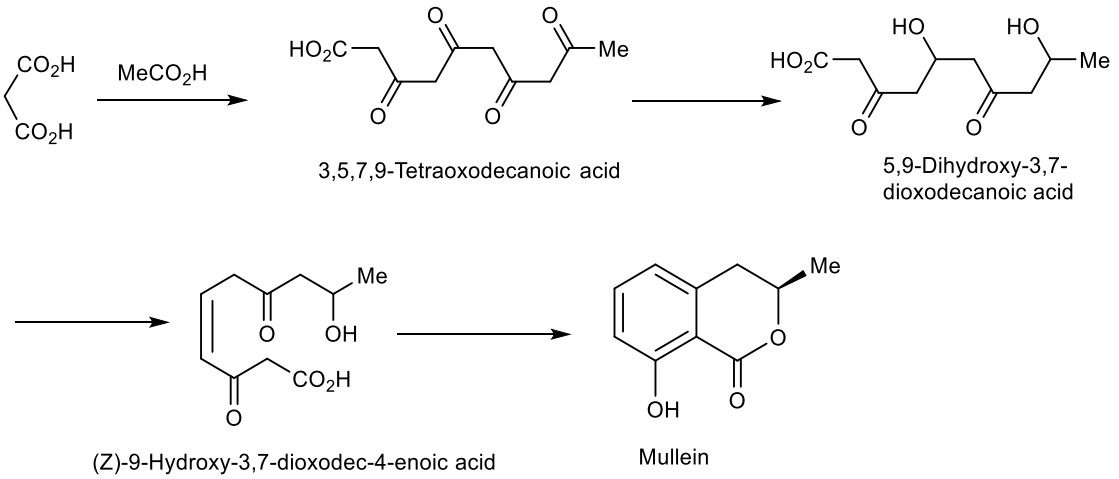

Scheme 3 : Biosynthesis of mullein (Pal et Pal, 2018; Magid et *al*., 2007)

Isocoumarin glycosides are relatively uncommon and few have been isolated as natural products (Saeed, 2005). Bergenin **51** biosynthesis involved C-glucosylation of gallic acid **50** followed by subsequent lactone formation (Pal et Pal, 2018).

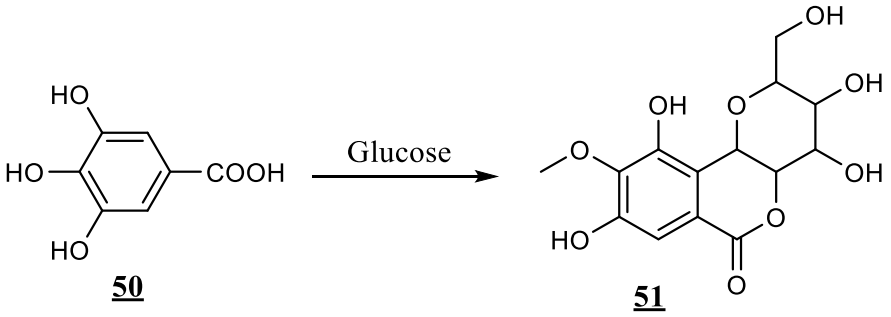

Scheme 4 : Bergenin biosynthesis (Pal et Pal, 2018)

I.6.4.3. Structural elucidation of isocoumarins

Structure determination of isocoumarins is carried out by means of several techniques, each of them providing crucial information in the building of the molecule. These techniques are infrared, ultraviolet, ^{1}H and ^{13}C NMR spectroscopy one- and two-dimensional, mass spectrometry.

- **^{1}H and ^{13}C NMR spectroscopy**

Most of naturally occurring isolates of this class of compounds are substituted at their C-3 position and then showed a singlet around δ_H 6.2-7.0 depending on the substituents in the benzene and pyrone ring (Abraham et *al.*, 1997). The ^{1}H NMR spectra of 3,4-dihydroisocoumarins are relatively more complex than those of isocoumarins because of the

vicinal coupling between the protons at C-3 and C-4 and/or germinal coupling between diastereotopic protons at C-4 (Pal et Pal, 2018). In their ^{13}C NMR spectra characteristic signal of a lactone group appears around δ_C 160-168.

- **Infra Red spectroscopy**

The characteristic absorption bands found on an IR spectrum of isocoumarin are: carbonyl of lactone at 1670-1755 cm^{-1}, the double bond in 3,4 position at 1615-1660 cm^{-1} for isocoumarin **47** and bands of aromatic ring at 1590-1625 and 1550-1590 cm^{-1}. Three bands are found in region 1500-1720 cm^{-1} with maxima of carbonyl group at 1670-1720 cm^{-1}, and aromatic ring at 1620 and 1580 cm^{-1} for dihydroisocoumarins **49** (Mallabaev et Sidyakin, 1972).

- **Ultra violet spectroscopy**

UV spectrum of isocoumarin showed characteristic maxima absorption bands in the range of 228-320 nm with a broad band characteristic at λmax 320 nm (Hay et Haynes, 1958).

I.6.4.4. Isocoumarins isolated from *Diospyros* species

The literature reported the isolation of isocoumarins, mainly derived from bergenin and norbergenin, in several species of the genus *Diospyros*. The **table 5** below shows some isocoumarins isolated from *Diospyros* species.

Table 5 : Isocoumarin isolated from genus *Diospyros*

Sources	Names and Structures	References
	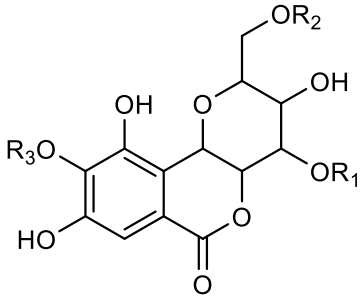 norbergenin **52** R_1= R_2= R_3=H 11-*O*-*p*-hydroxybenzoylnorbergenin **53** R_1= H, R_2= 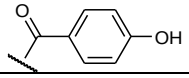 , R_3=H	

D. Sanza-minika *D. longiflora*	4-*O*-galloylnorbergenin **54** R_1= 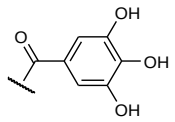 R_2= H, R_3=H 4-*O*-(3'-methylgalloyl)-norbergenin **55** R_1= 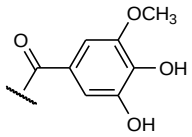 R_2= H, R_3=H 4-syringoylnorbergenin **56** R_1= 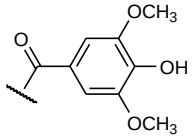 R_2= H, R_3=H Longiflorol **57** R_1=H, R_2= 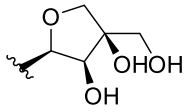 R_3=H	Tangmouo et *al*., 2009 Dongmo et *al*., 2018

I.6.4.5. Biological activities of isocoumarins

Several authors have evaluated the biological activities of some isocoumarins isolated from natural sources or synthesized. These include antioxidant, antibacterial, antifungal, cytotoxic, anti-inflammatory, antiplasmodial and antituberculous activities (Magid et *al*., 2007). Although it is not easy to generalize which parts/moieties/substituents of isocoumarin derivatives (and their 3,4-dihydro analogs) are responsible for their various pharmacological activities, it is clear that groups such as OH, OMe, OAc, COOH, and sugar attached to the core structure can directly interfere in the biological activities of the corresponding derivatives (Pal et Pal, 2018). A structure activity relationship (SAR) has been proposed to draw some conclusions on the pharmacological activities of isocoumarins. It appeared that the presence of OH group at C-8 position, a linear alkyl side chain at C-3 position, an aryl group at C-3 position or one unsaturation in the C-3 alkyl chain are beneficial for displaying promising pharmacological activities by isocoumarins (Pal et Pal, 2018). Overall, all these preceding examples and the related reports suggest that isocoumarin is an attractive template for the design, discovery, and development of new and potential drugs in various therapeutic areas.

I.6.4.6. Some routes of synthesis of isocoumarin and dihydroisocoumarin derivatives

Once the biological activities of isocoumarins were recognized, several pathways leading to their synthesis were proposed. One of the most well-known syntheses started from orcinol **58**, as shown in the following **scheme 5**.

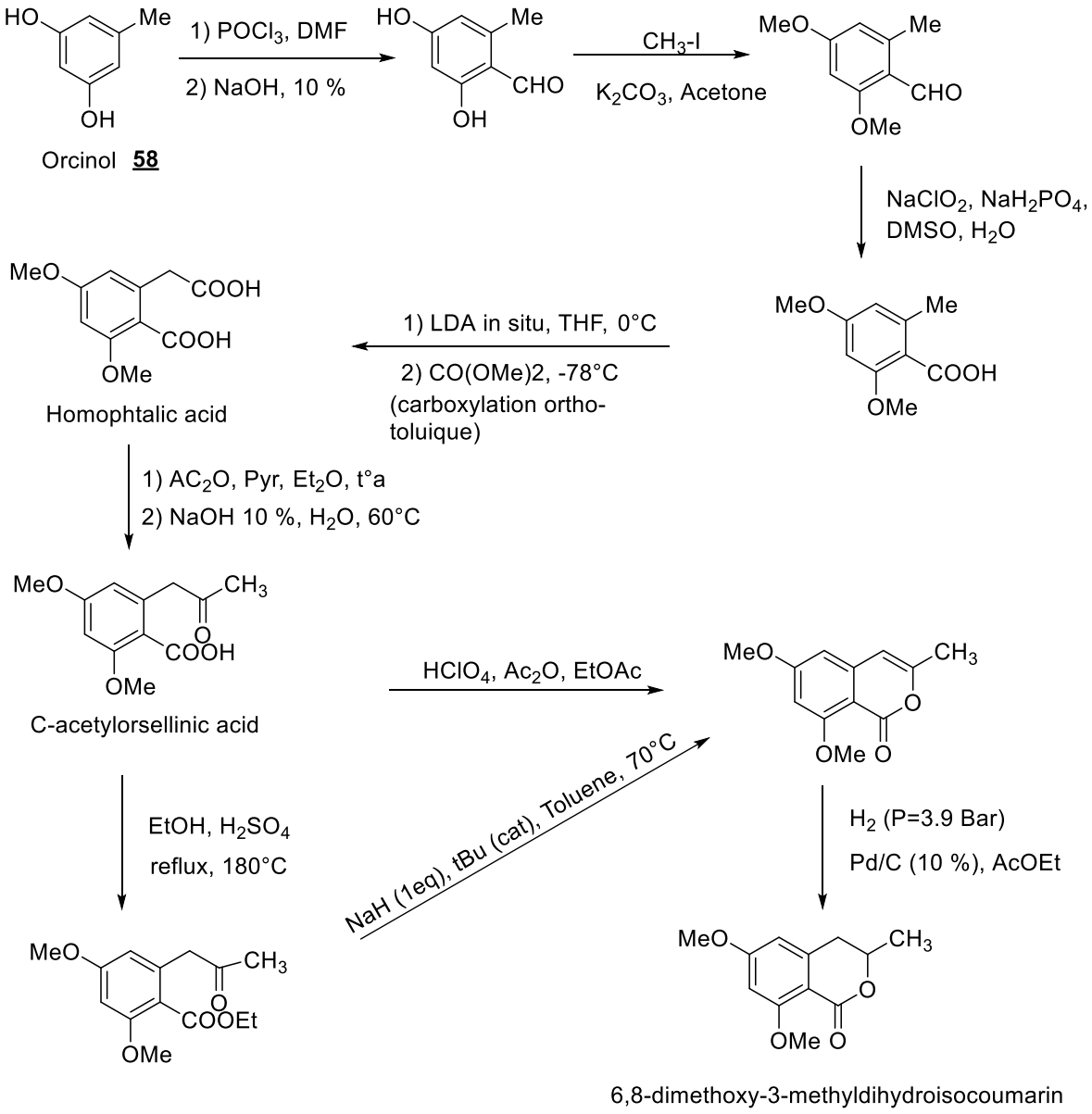

Scheme 5 : Total synthesis of isocoumarin and dihydroisocoumarin (Mustapha, 2005)

Bergenin **51** has gained much attention from the beginning of 21st century, as its pharmacological properties were gradually explored. A short five-step synthesis of 8,10-di-*O*-methylbergenin was reported by Herzner et *al*. (Herzner et *al*., 2002).

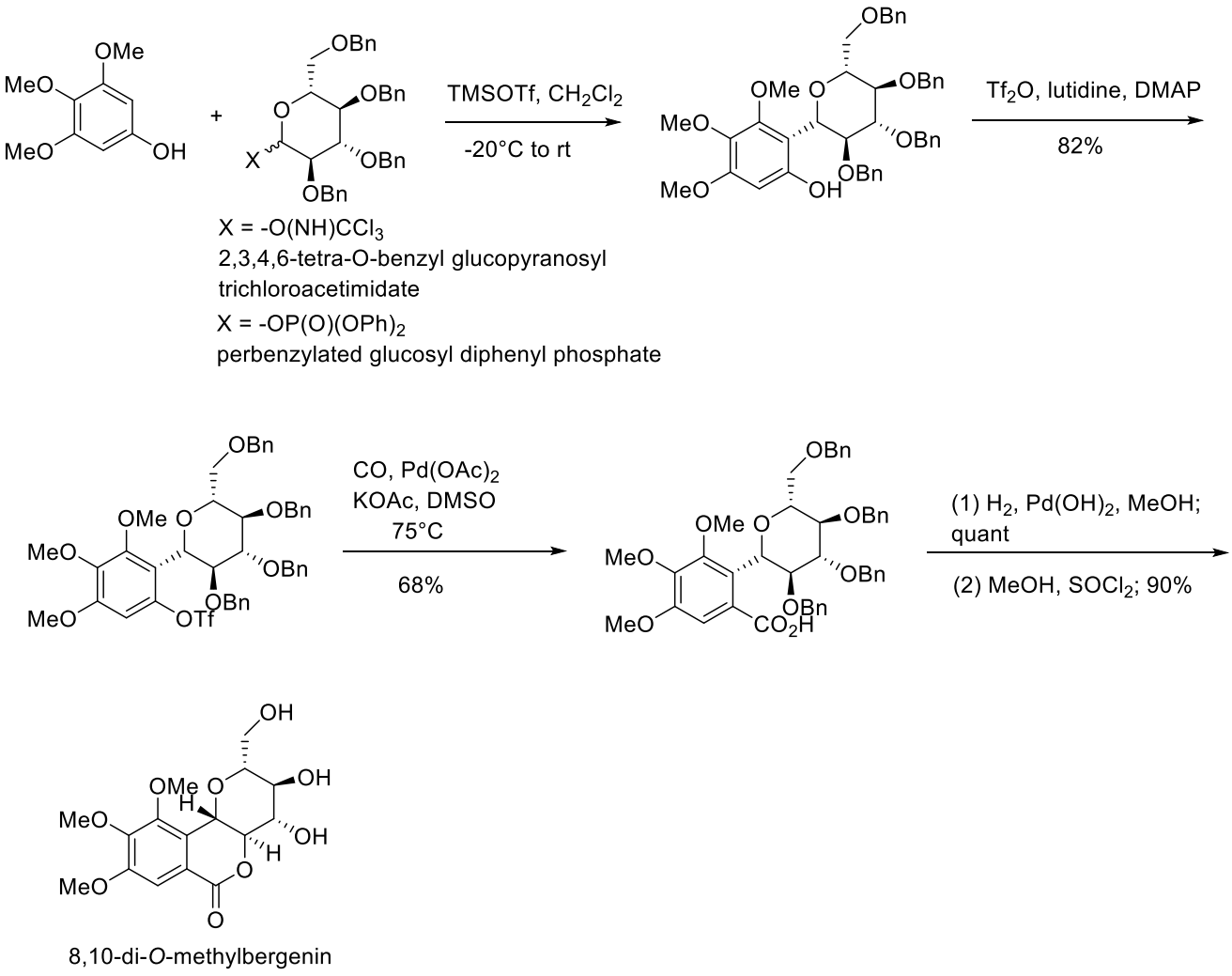

Scheme 6 : Synthesis of bergenin derivative

From all the above, it appears that plants of the genus *Diospyros* are widely used in traditional medicine because of their therapeutic virtues. The secondary metabolites they contain are mostly triterpen and phenolic compounds with great structural diversity, varied and interesting biological activities. All this shows that there is still interest in exploring other plants of the genus *Diospyros*, hence our work on the species *D. gilletii* and *D. fragrans*.

CHAPTER II:

RESULTS AND DISCUSSION

II.1. STUDIES ON CHEMICAL CONSTITUENTS OF *DIOSPYROS GILLETII* AND *DIOSPYROS FRAGRANS*

II.1.1. Plants material

The leaves, twigs and stem bark of *D. gilletii* De Wild were collected in March 2018 at Mbalmayo, Centre region-Cameroon, while its roots were collected at the same place in November 2018. The same parts of *D. fragrans* Gürke were collected in December 2018 at Abang, Centre region-Cameroon. M. Nana victor, a botanist at the Cameroon National Herbarium did the identification of both species, and voucher specimens are deposited under the numbers N^{o} 15418 HNC and N^{o} 60166 HNC for *D. gilletii* and *D. fragrans* respectively.

II.1.2. Extraction and isolation of compounds

The different parts of these two plants were cut, dried and grounded separately and the powders obtained were extracted one after the other by maceration with 10 L of MeOH at room temperature for 72 hours. The methanolic filtrates were further evaporated to dryness under reduced pressure to give methanolic residues. The amount of powders and methanolic residues obtained from each part are given in the **table 6** below.

Table 6: Powders and crude extracts amount obtained from the different parts of *D. gilletii* and *D. fragrans*.

Species	Parts	Powders amount (Kg)	Methanolic residue amount (g)
D. gilletii	Leaves	0.95	122.1
	Stem bark	0.8	158.0
	Twigs	1.5	99.1
D. fragrans	Leaves	3.2	101.7
	Roots	2.8	78.9

The leaves, stem bark and twigs extracts of *Diospyros gilletii* as well as the leaves and roots extracts of *Diospyros fragrans* were processed using standard chromatographic methods.

Thus, from *Diospyros gilletii* were isolated thirteen compounds from the leaves labelled DGF_1 to DGF_{11} (**Scheme 7**), eight compounds from the stem bark labelled $DGETH_1$ to $DGET_5$ (**Scheme 8**) and twelve compounds from the twigs labelled $DGTFI_1$ to $DGTFIV_4$ (**Scheme 9**).

From *Diospyros fragrans* were isolated seventeen compounds from the leaves labelled DFFFI3 to DFFFII17D (**Scheme 10**) and twelve compounds from the roots labelled DFR1 to DFR6 (**Scheme 11).**

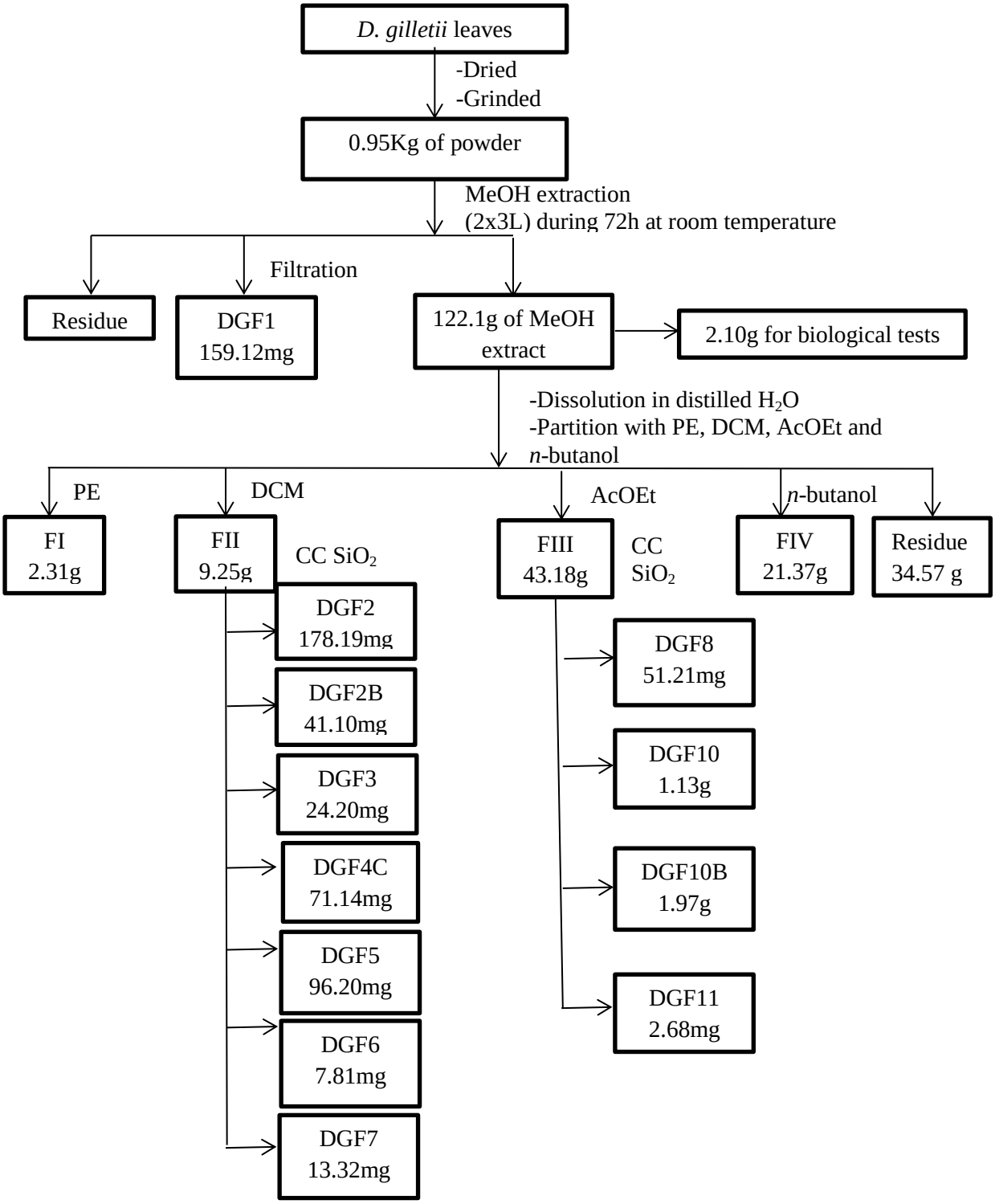

Scheme 7 : Extraction and isolation procedure of compounds from the leaves of *D. gilletii*

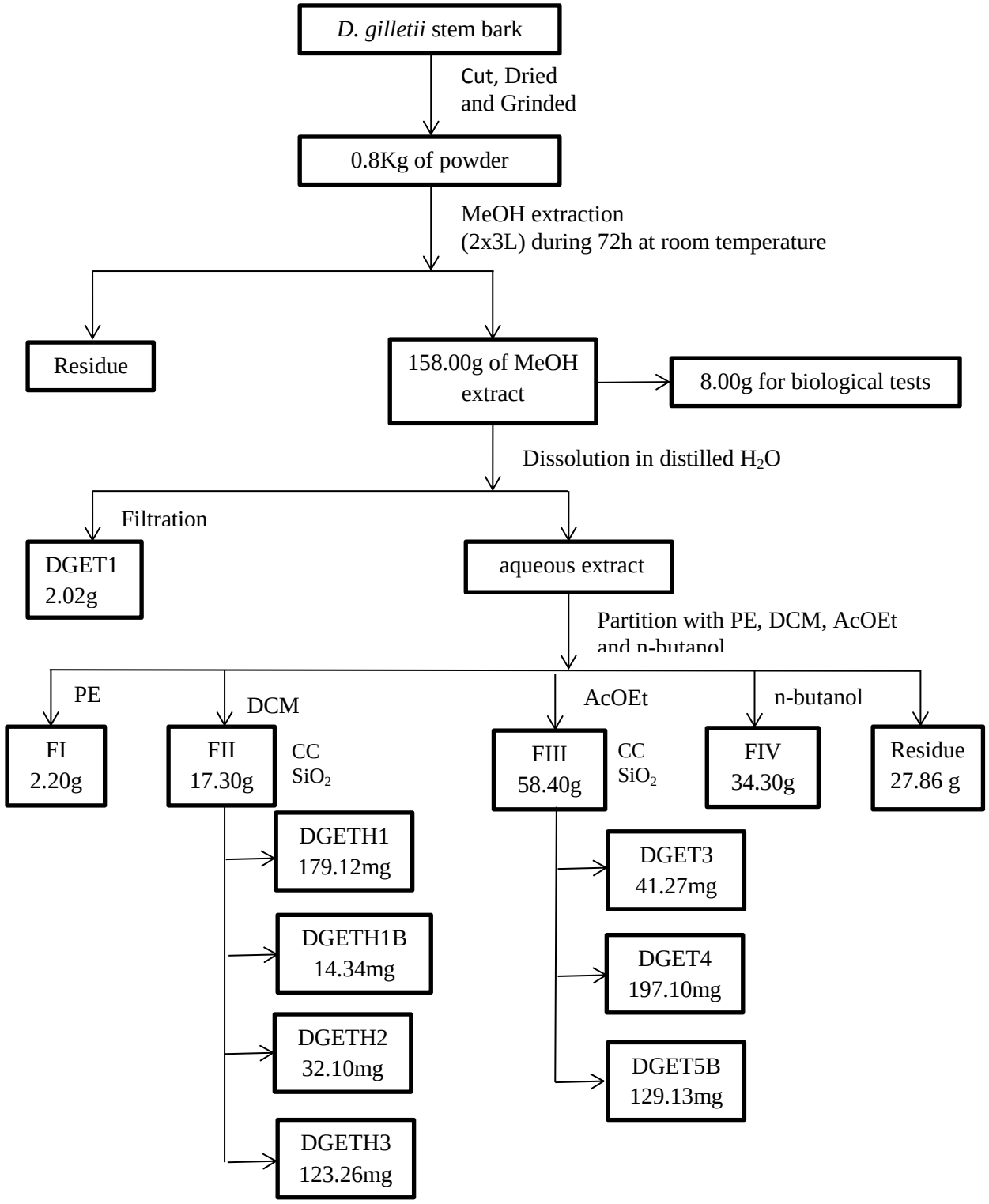

Scheme 8 : Extraction and isolation procedure of compounds from the stem bark of *D. gilletii*

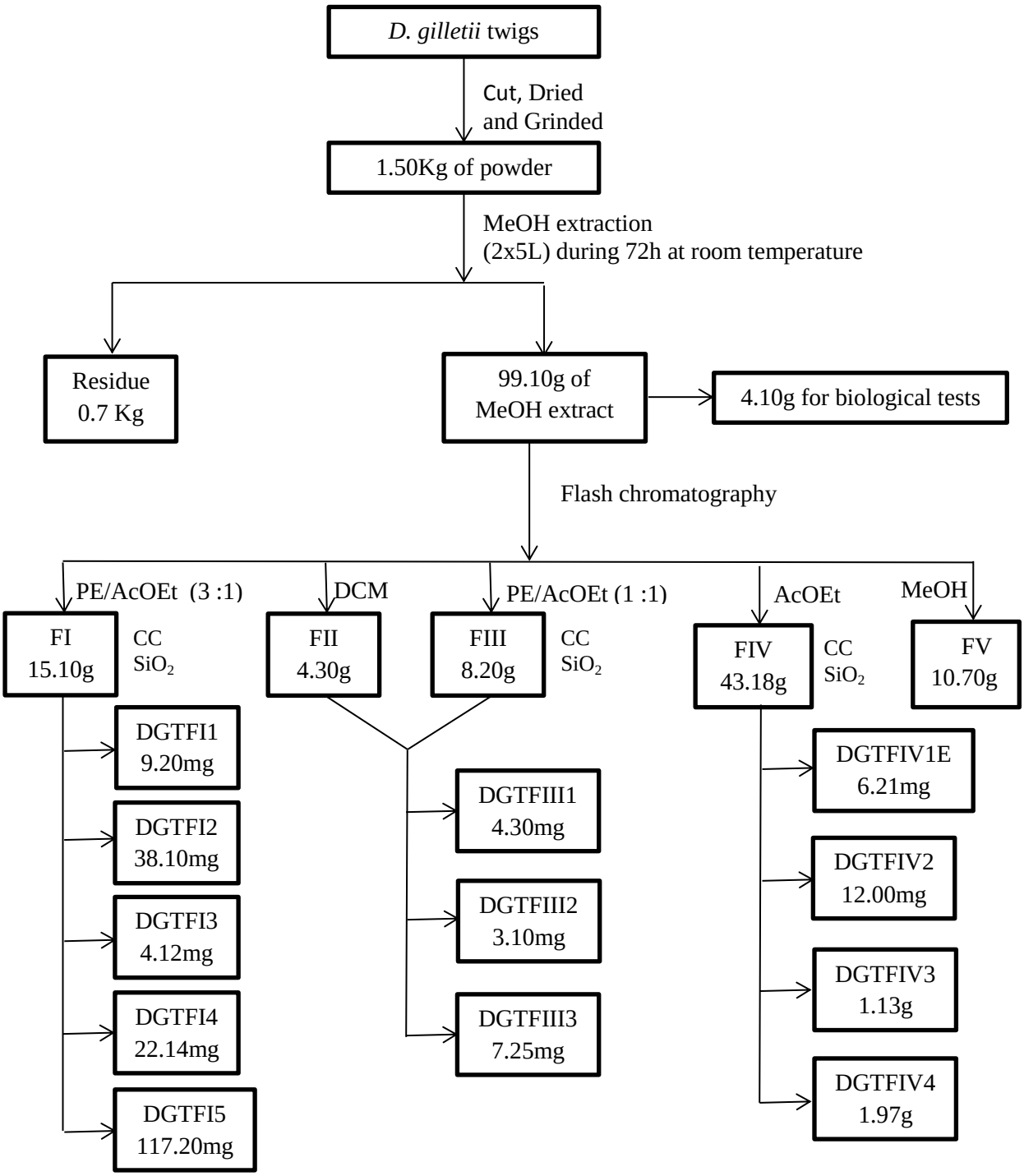

Scheme 9 : Extraction and isolation procedure of compounds from the twigs of *D. gilletii*

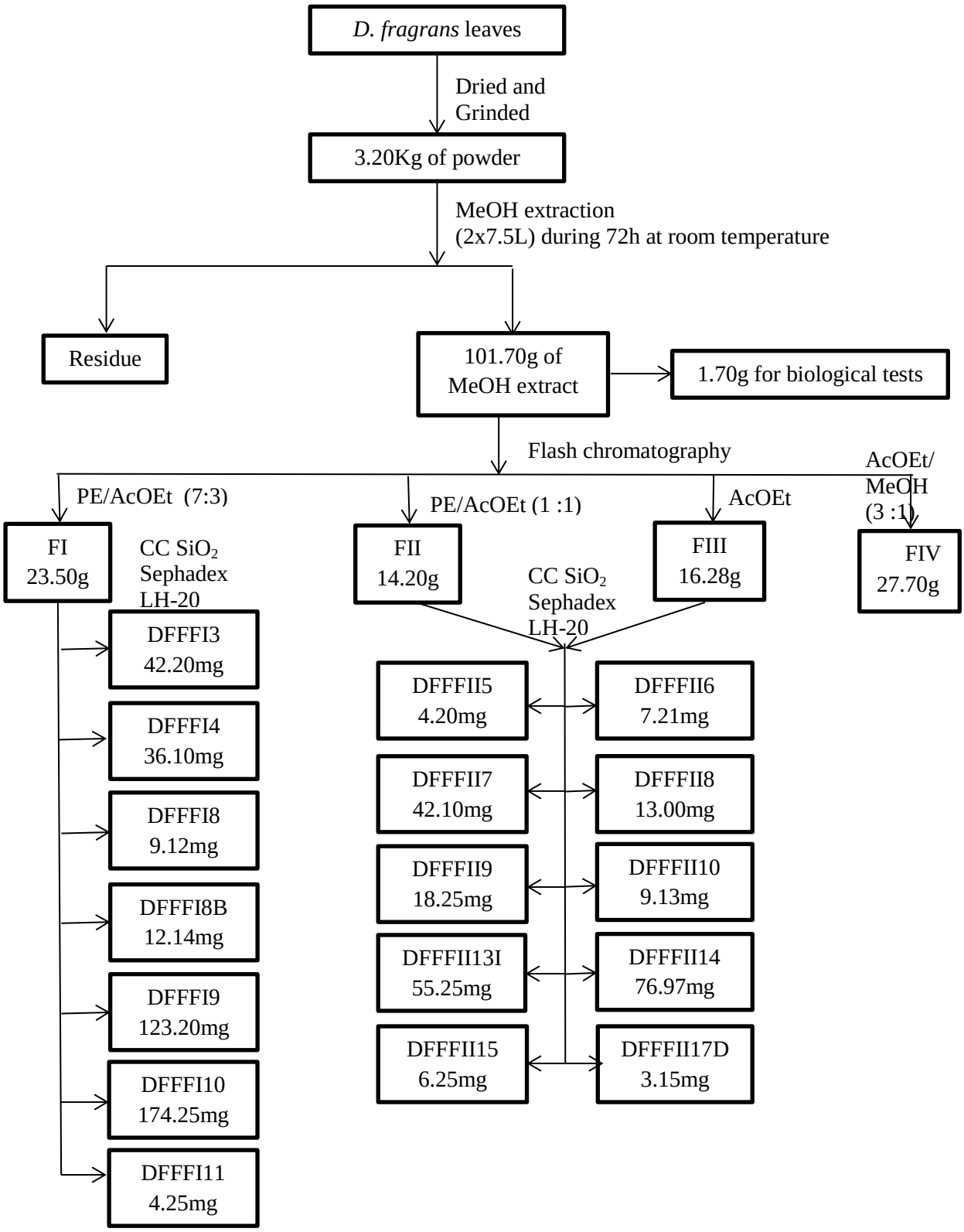

Scheme 10 : Extraction and isolation procedure of compounds from the leaves of *D. fragrans*

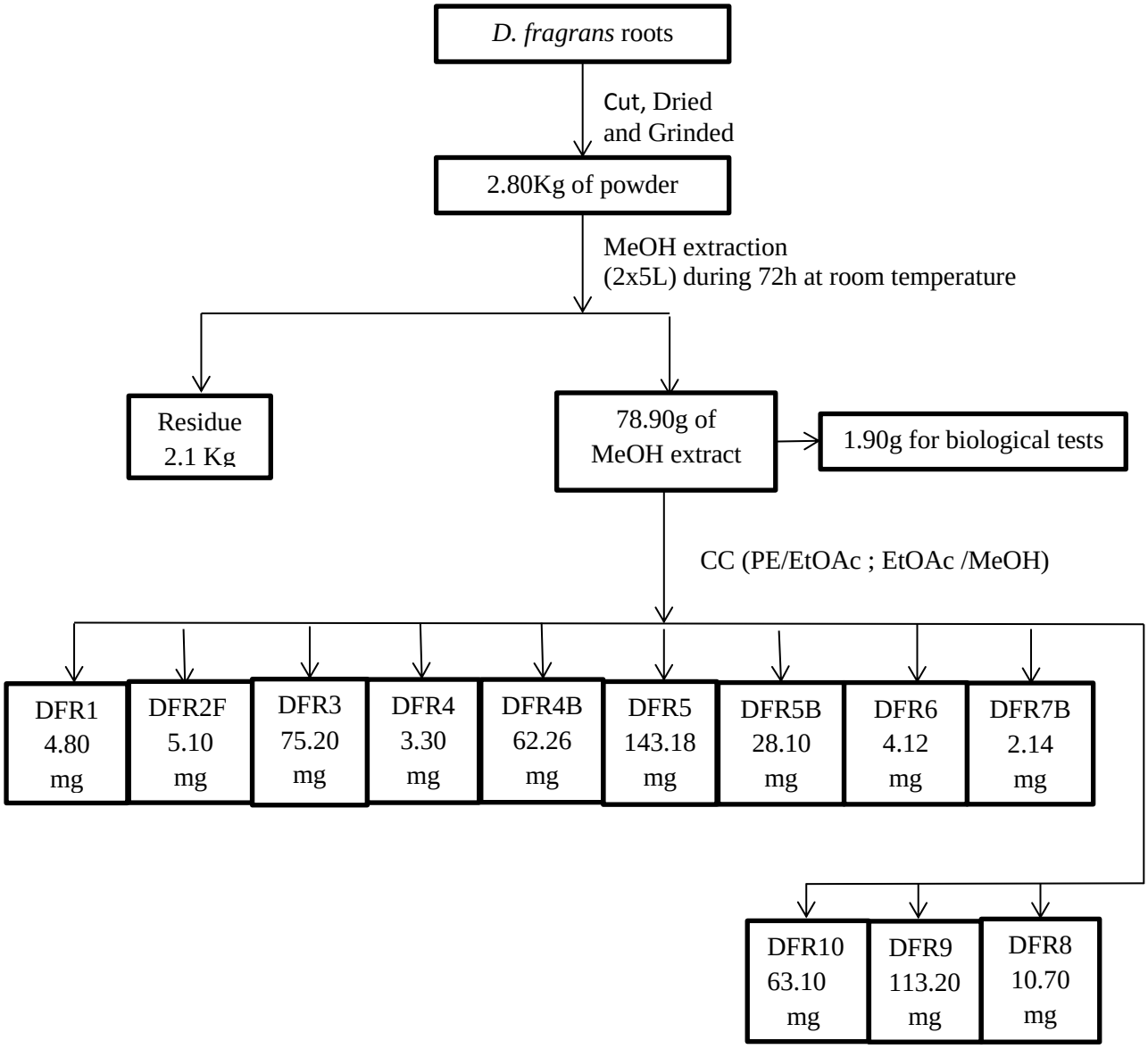

Scheme 11 : Extraction and isolation procedure of compounds from the roots of *D. fragrans*

fragrans. Since among those compounds some were identical on the basis of comparative TLC, the total number of distinct secondary metabolites isolated was reduced to 34. The **table 7** below gives us a summary of the similar compounds obtained from the different parts of these plants.

Table 7: balance of the compounds isolated from the different parts of the two plants.

D. gilletii			*D. fragrans*	
Leaves	**Twigs**	**Stem bark**	**Leaves**	**Roots**
/	/	/	/	DFR1
/	/	/	/	DFR2F
/	/	/	/	DFR4
/	/	/	DFFFII17D	/
DGF1	/	/	/	/
DGF2 = DGTFI2	DGTFI2 = DGETH1	DGETH1 = DFFFI3	DFFFI3 = DFR3	DFR3 = DGF2
DGF2B= DGTFI4	DGTFI4 = DGETH1B	DGETH1B = DFFFI4	DFFFI4 = DFR4B	DFR4B = DGF2B
DGF3 = DGETH2	/	DGETH2 =DGF3	/	/
DGF4C = DGTFI5	DGTFI5 = DGETH3	DGETH3 = DFFFI9	DFFFI9 = DFR5	DFR5 = DGF4C
DGF5 = DFFFI10	/	/	DFFFI10 = DFR5B	DFR5B = DGF5
DGF6 = DFFFII15	/	/	DFFFII5 = DGF6	/
DGF7 = DGTFIII1	DGTFIII1 = DFFFII6	/	DFFFII6 = DGF7	/
/	DGTFIII2	/	/	/
DGF8	/	/	/	/
DGF9 = DGTFIII3	DGTFIII3 = DGET3	DGET3 = DFFFII8	DFFFII8 = DFR9	DFR9 = DGF9
DGF10 = DGTFIV2	DGTFIV2 = DGET4	DGET4 = DGF10	/	/
DGF10B = DGTFIV3	DGTFIV3 = DGET1	DGET1 = DGF10B	/	/
DGF11 = DGTFIV4	DGTFIV4 = DGET5B	DGET5B = DGFI1	/	/
/	DGTFIV1E	/	/	
/	/	/	DFFFI11	/
/	/	/	DFFFI8	/
/	/	/	DFFFI8B	/
/	/	/	DFFFII15	/
/	/	/	DFFFII13I = DFR8	DFR8 = DFFFII13I
/	/	/	DFFFII7	/
/	/	/	DFFFII9	/
/	/	/	DFFFII10	/
/	/	/	DFFFII14 = DFR10	DFR10 = DFFFII14
/	DGTFI3	/	/	/
/	DGTFI1	/	/	/
/	/	/	/	DFR6
/	/	/	/	DFR7B

From these compounds, 28 were entirely characterized as belonging to different classes of natural substances:

- Twelve pentacyclic triterpenes distributed in three lupanes (DGF2, DGF3, DFR5), six ursanes (DGF5, DGF7, DFFFI8, DFFFI8B, DFFFII13I, DGTFIII2) and three oleananes (DGF6, DFFFI11, DFFFII15).
- Four sterols (DGTFI4, DGTFIII3)
- Five isocoumarins (DGET1, DGET4, DGET5B, DGF8, DGTFIV1E)
- One polyterpene (DFR4)
- One carotenoid (DFFFII17D)
- Three polyols (DGF1, DFFFII9, DFFFII14)
- One naphthalene derivative: DFR7B
- One monoglyceride: DFR6

Structural determination of these compounds was achieved by analysis of their spectral data, and for the known compounds, by comparison of their spectroscopic and physical data with those described in the literature.

II.1.3. Structural elucidation of isolated compounds

II.1.3.1. Isocoumarins

II.1.3.1.1. Elucidation of DGET5B

Compound DGET5B was isolated as a white amorphous powder in the solvent system EtOAc/MeOH (19:1). Its purple coloration with ferric chloride ($FeCl_3$) reagent indicated the presence of phenolic hydroxyl group in its structure. The ESIMS of this compound (**figure 15**) showed in negative mode the pseudo-molecular ion peak $[M-H]^-$ at *m/z* 312.9, which was in accordance with the molecular formula $C_{13}H_{14}O_9$ implying 7 degrees of unsaturation.

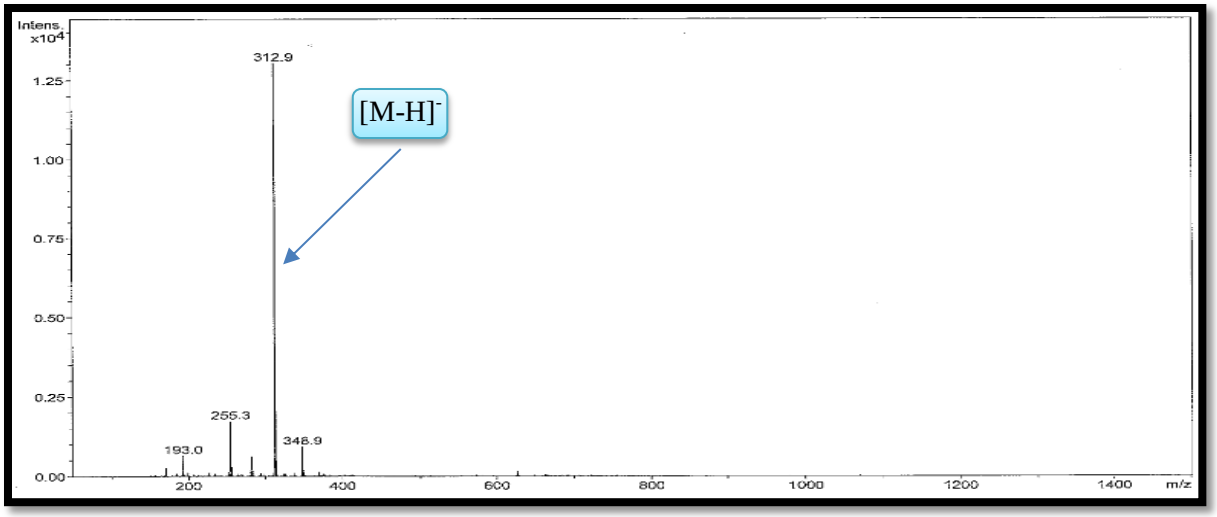

Figure 15: ESI mass spectrum of compound DGET5B

On its ^{1}H- NMR spectrum (**Figure 18**) coupled to its HMQC spectrum (**Figure 22**) we observed signals of Five oxymethines at δ_H 4.94/ δ_C 72.1, δ_H 3.93 / δ_C 79.6, δ_H 3.63 / δ_C 73.6, δ_H 3.56 / δ_C 81.5, δ_H 3.18 / δ_C 71.0 and one oxymethylene at δ_H 3.84 and 3.56 / δ_C 61.0. The ^{1}H-^{1}H COSY (**Figure 16**) correlations observed between these protons indicated the presence of a glucopyranose ring in the structure of this compound. In addition to these signals, we could also observe signals of one aryl proton at δ_H 6.95 / δ_C 109.2 and six hydroxyl protons at δ_H 9.52, 9.35, 8.27, 5.61, 5.42 and 4.90.

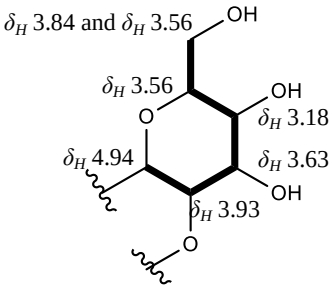

Figure 16 : ^{1}H-^{1}H COSY correlations of compound DGET5B

Its ^{13}C-NMR spectrum (**Figure 19**) coupled to its DEPT 135 spectrum (**Figure 20**) showed thirteen signals associated with: Six aromatic carbons including one methine at δ_C 109.2, two quaternary carbons at δ_C 112.4 and 115.8 and three oxygenated quaternary carbons at δ_C 145.8, 142.4 and 139.5 corresponding to a benzene ring, one carbonyl of lactone at δ_C 163.8 and six signals of the glucopyranose ring at δ_C 72.1, δ_C 73.6, δ_C 71.0, δ_C 79.6, δ_C 81.5 and δ_C 61.0.

The HMBC correlations (**Figure 17**) observed between the aryl proton at δ_H 6.95/ δ_C 109.2 and the aromatic carbons at δ_C 112.4 and 145.8 on one hand and between this same proton and the carbonyl of lactone at δ_C 163.8 on the other hand indicated that the benzene ring was connected to the lactone ring to give a isocoumarin moiety.

It remained to establish the link between this isocoumarin moiety and the glucopyranose ring. This was made possible by the correlations observed on the HMBC spectrum between the oxymethine proton at δ_H 4.94/ δ_C 72.1 and the aromatic carbons at δ_C 142.4, 115.8, 112.4 and also between proton at δ_H 3.93 / δ_C 79.6 and carbons at δ_C 163.8 and δ_C 115.8, indicating the fusion of these two moieties through carbons at δ_C 72.1 and δ_C 79.6.

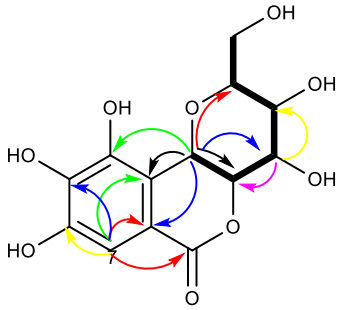

Figure 17: **HMBC correlations of compound DGET5B**

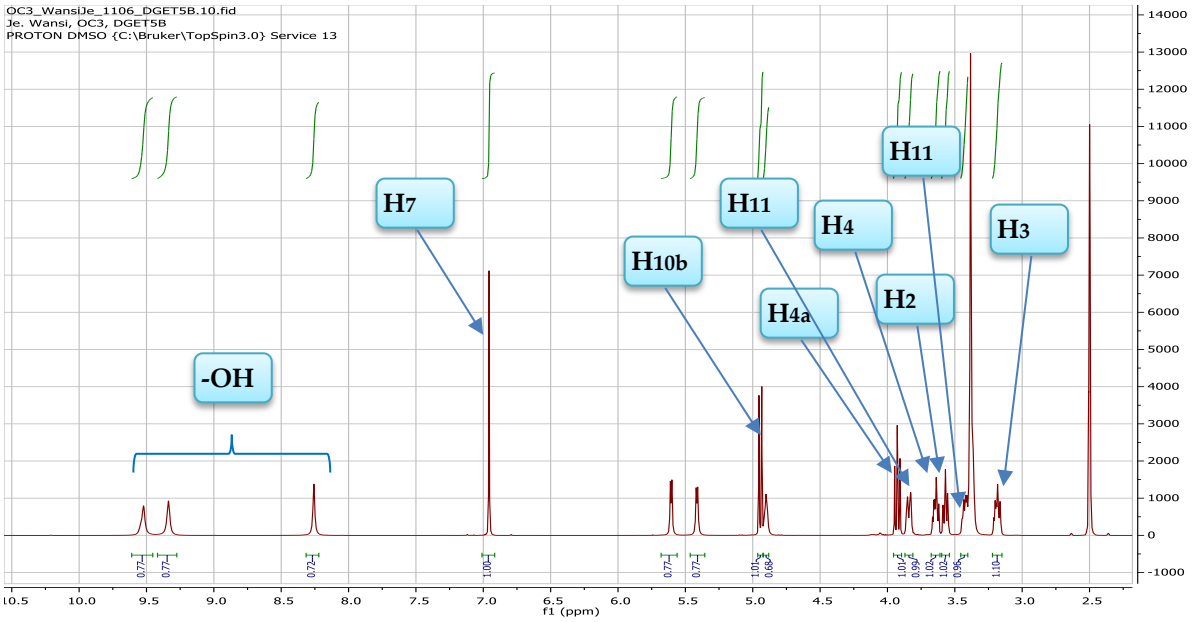

Figure 18: ^{1}H- NMR (500MHz) spectrum of compound DGET5B in DMSO-d_6

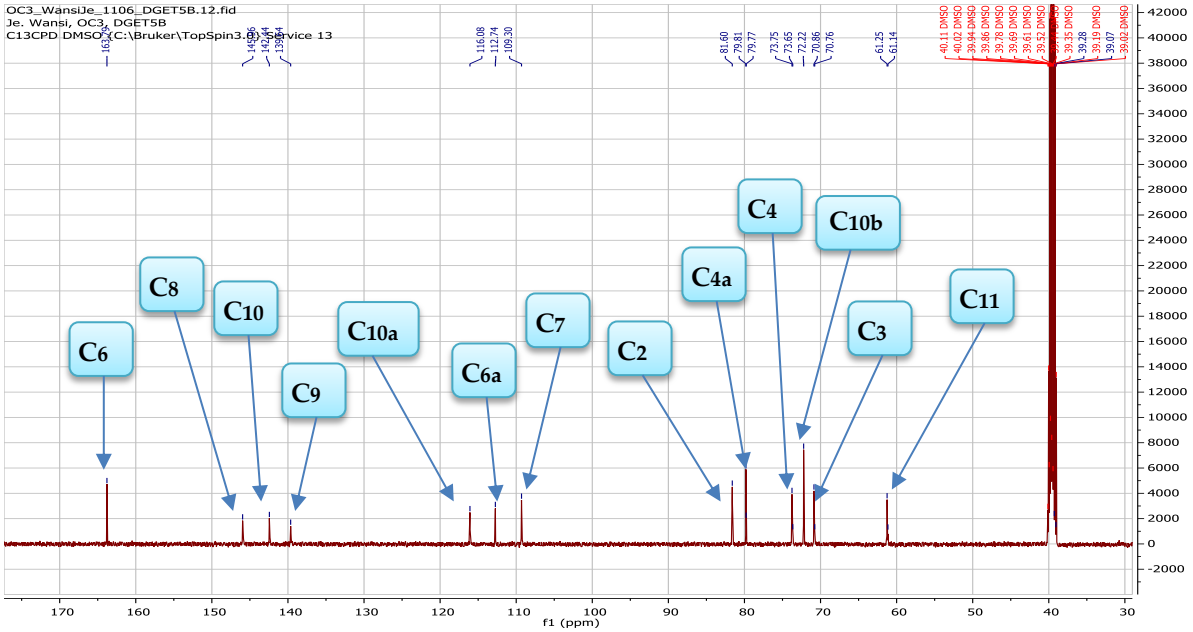

Figure 19 : ^{13}C NMR (125 MHz) spectrum of compound DGET5B in DMSO-d_6

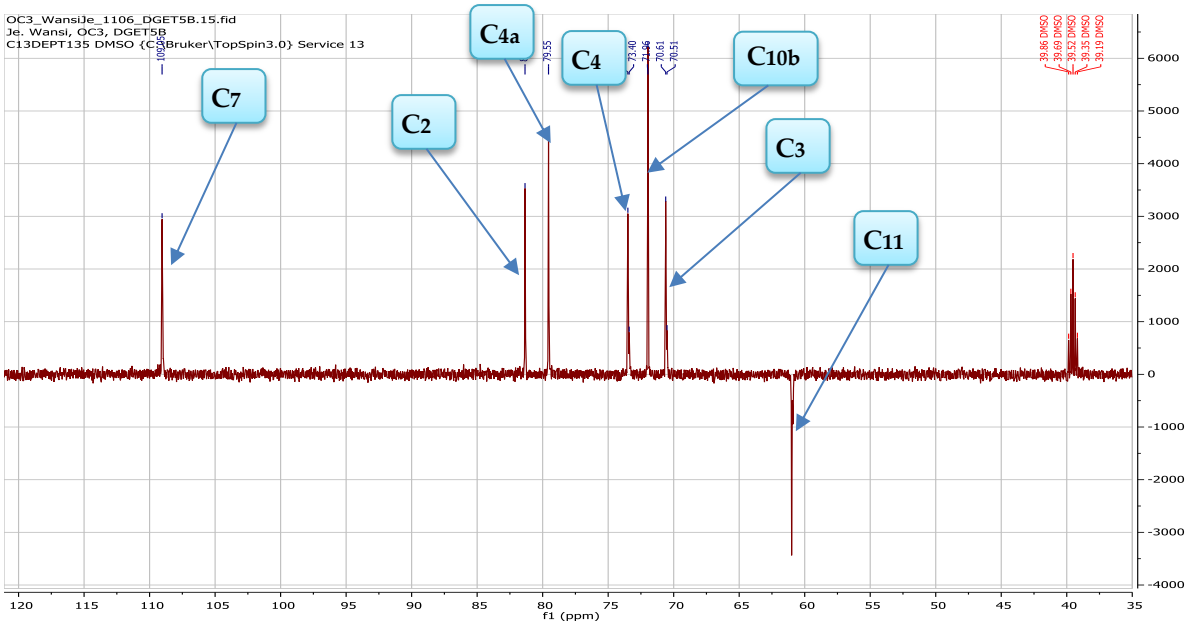

Figure 20: DEPT 135 NMR (125 MHz) spectrum of compound DGET5B in DMSO-d_6

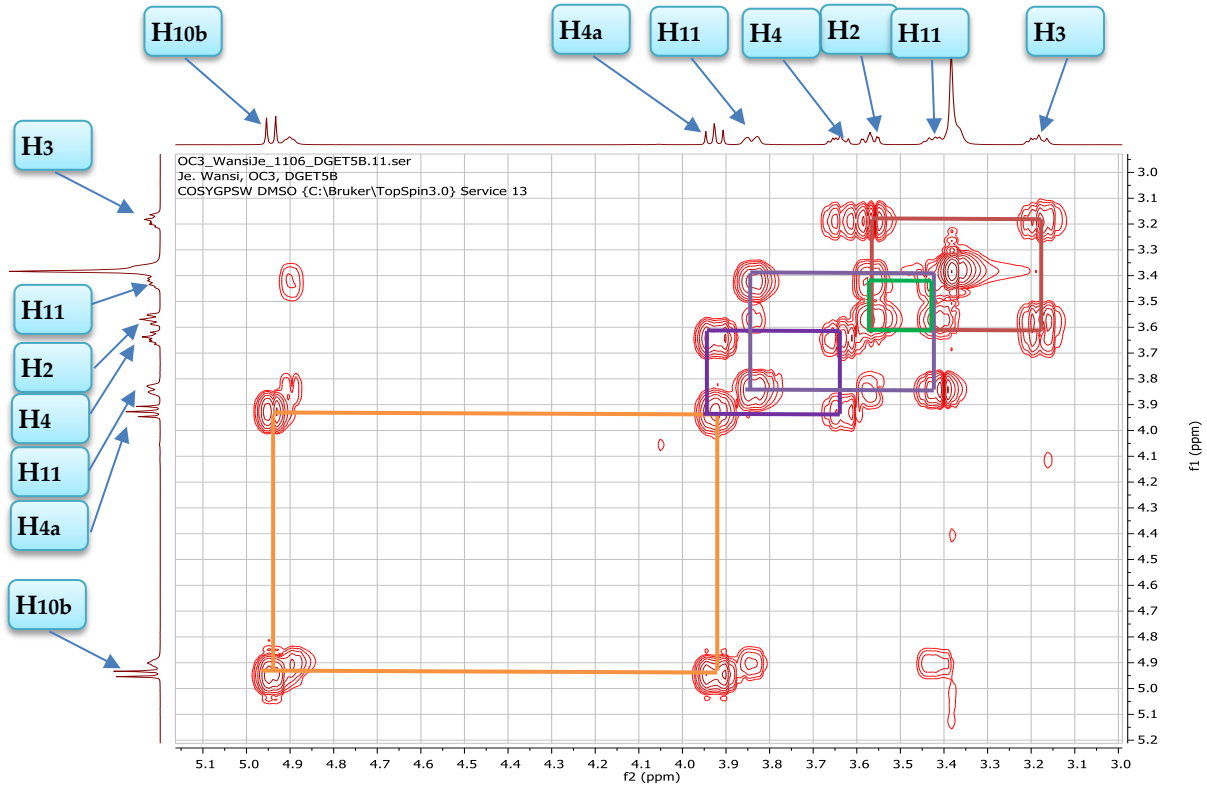

Figure 21: COSY spectrum of compound DGET5B

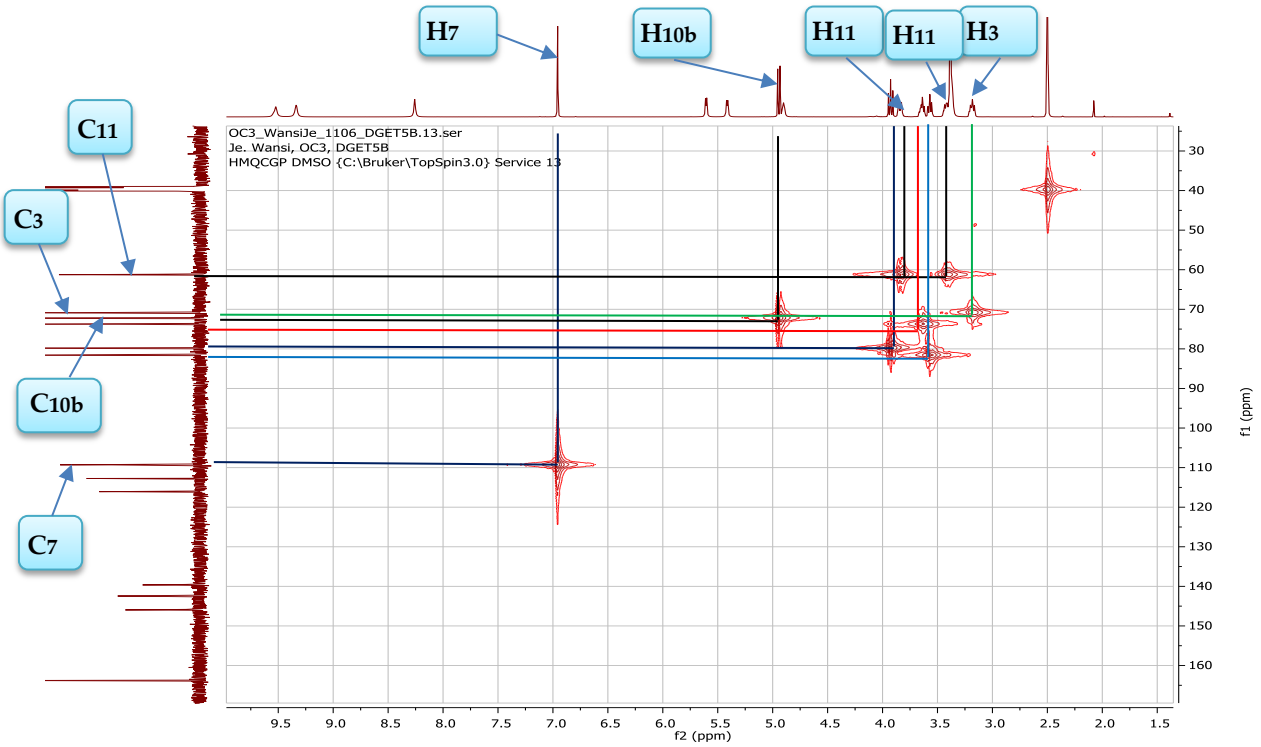

Figure 22: HMQC spectrum of compound DGET5B

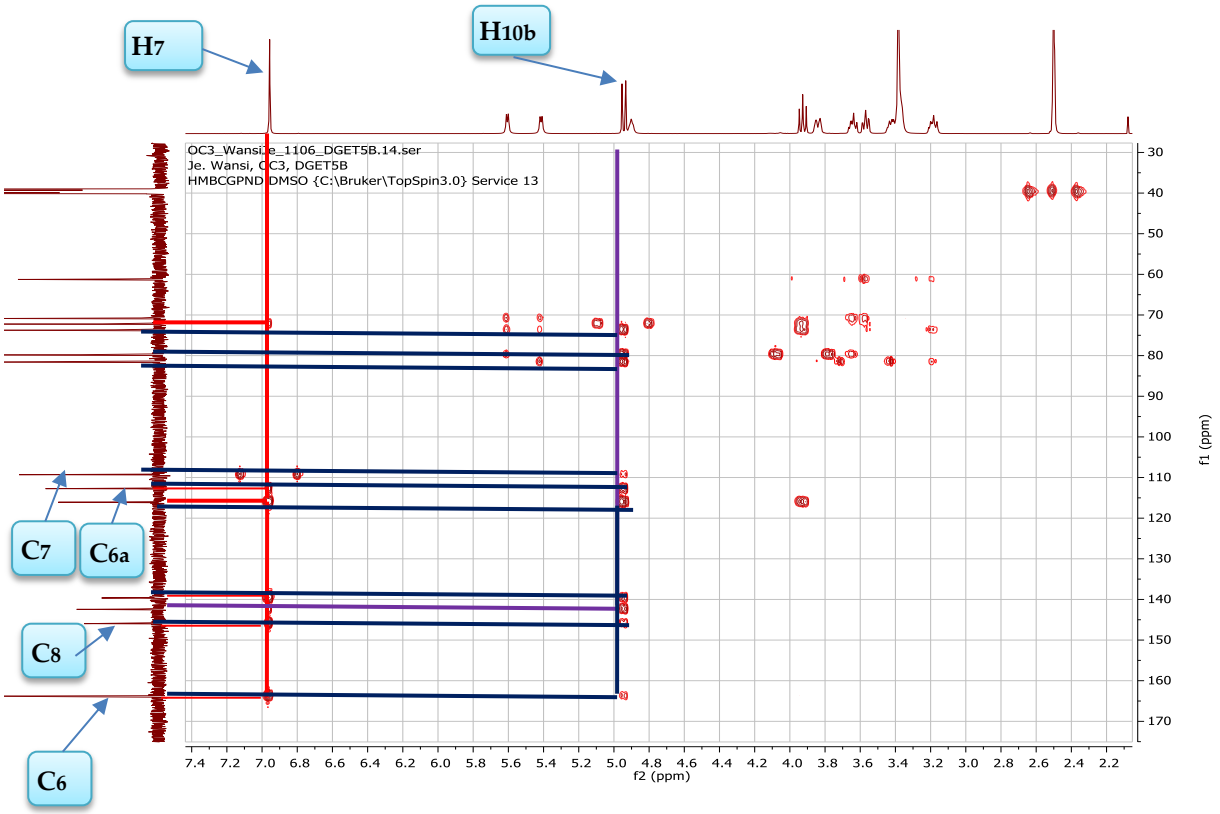

Figure 23 : HMBC spectrum of compound DGET5B

Based on the above evidence and the literature data, the structure of compound DGET5B was determined to be norbergenin **52**, a known compound isolated for the first time from *Woodforlia fruticosa* by Khalidhar et *al* in 1981.

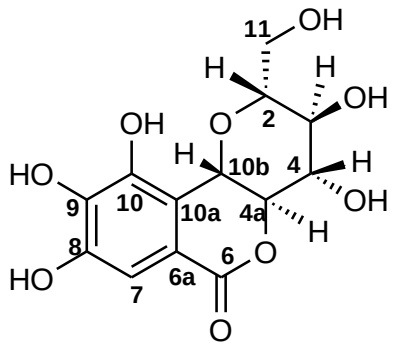

52

Table 8 : ^{1}H (500 MHz) and ^{13}C (125 MHz) NMR data of compound DGET5B and norbergenin in DMSO-*d_6*

Position	DGET5B		Norbergenin literature data[a]	
	δ_H mult (*J* in Hz)	δ_C, mult.	δ_H mult (*J* in Hz)	δ_C, mult.
2	3.56 m	81.5 CH	-	81.5 CH
3	3.18 m	71.0 CH	-	70.9 CH
4	3.63 m	73.6 CH	-	73.7 CH
4a	3.93 t (9.7)	79.6 CH	-	79.8 CH
6	-	163.8 C	-	163.7 C
6a	-	112.4 C	-	112.7 C
7	6.95 s	109.2 CH	7.13 s	109.3 CH
8	-	145.8 C	-	145.9 C
9	-	139.5 C	-	139.6 C
10	-	142.4 C	-	142.4 C
10a	-	115.8 C	-	116.1 C
10b	4.94 d (10.8)	72.1 CH	4.96 d (10.3)	72.2 CH
11	3.84 m; 3.56 m	61.0 CH_2	-	61.2 CH_2
OH	9.52 m	-	-	-
OH	9.35 m	-	-	-
OH	8.27 m	-	-	-
OH	5.61 m	-	-	-
OH	5.42 m	-	-	-
OH	4.90 m	-	-	-

[a] (Taneyama et *al*., 1983)

II.1.3.1.2. Elucidation of DGET4

Compound DGET4 was obtained as a white powder in the solvent system PE/EtOAc (1:3). It gave a purple coloration with ferric chloride reagent on TLC indicative of phenolic

hydroxyl groups. Its molecular formula, $C_{20}H_{18}O_{11}$, implying twelve double bond equivalents, was determined from its HR-TOF-ESIMS spectrum (**figure 24**) which showed in positive mode the pseudo-molecular ion pic $[M+Na]^+$ at *m/z* 457.0738 (calculated for $C_{20}H_{18}O_{11}Na$: *m/z* 457.0741).

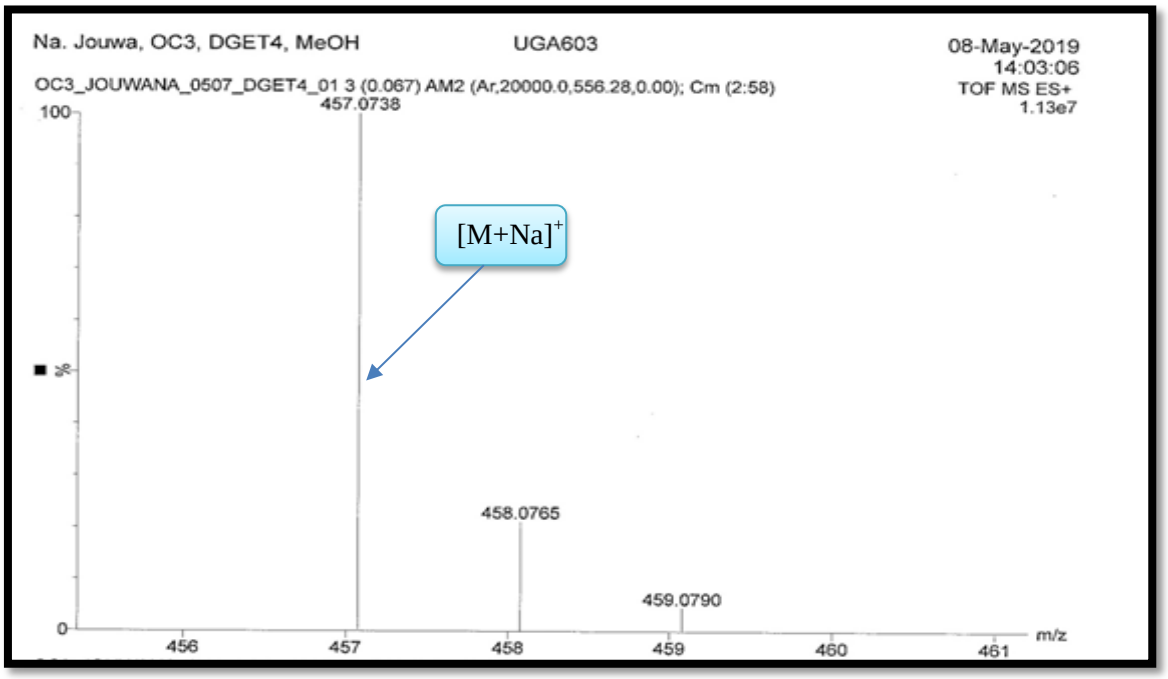

Figure 24: HR-TOF-ESIMS of compound DGET4

Its UV spectrum (**figure 26**) exhibited absorption bands at λmax 218 and 262 nm while its IR spectrum (**figure 25**) indicated vibration bands characteristic of hydroxyl group (-OH) at 3392 cm^{-1}; carbonyl esters (C=O) at 1714, 1699 cm^{-1} and aromatic at 1608, 1470 cm^{-1}

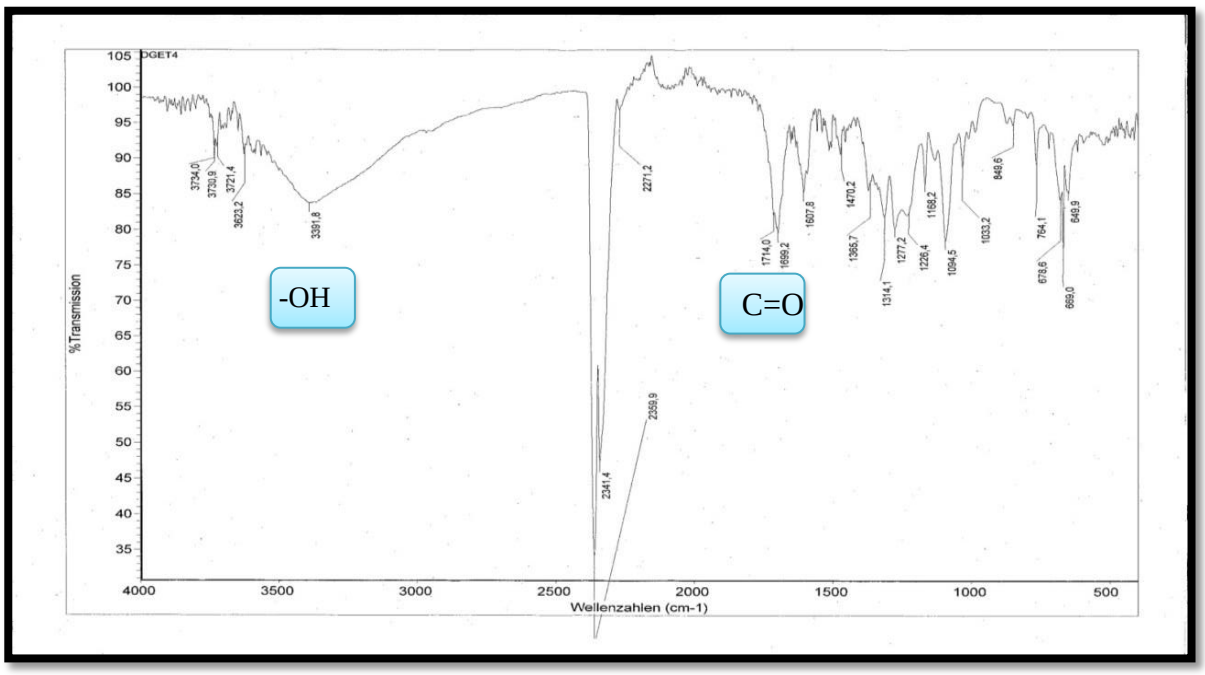

Figure 25: IR Spectrum of compound DGET4

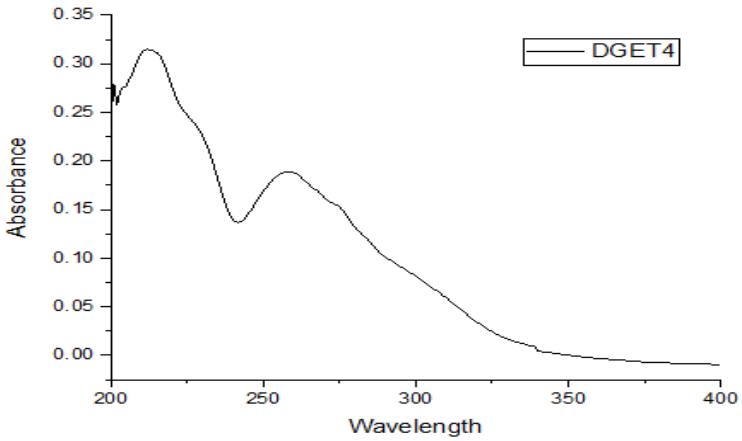

Figure 26: UV spectrum of compound DGET4

The ^{1}H, ^{13}C, HMQC and DEPT 135 NMR spectra of compound DGET4 (**figures 27**, **29, 31** and **30** respectively) displayed a very close resemblance to those of norbergenin **52** previously described. In fact, all the signals observed in the spectra of norbergenin **52**, except the signals of the hydroxyl protons were also found in the spectra of compound DGET4. These signals were constituted of one aromatic proton singlet at δ_H 7.08 (1H, s) / δ_C 111.1, five oxymethines at δ_H 5.60 (1H, dd, J = 8.4, 9.8 Hz) / δ_C 76.2, δ_H 5.14 (1H, d, J = 10.4 Hz) / δ_C 74.4, δ_H 4.42 (1H, t, J = 10.4 Hz) / δ_C 79.1, δ_H 3.82 (1H, m) / δ_C 83.1 and δ_H 3.80 (1H, m) / δ_C 70.2, two diastereotopic oxymethylenes at δ_H 4.04 (1H, dd, J = 11.6; 1.6 Hz) / δ_C 62.5 and δ_H 3.75 (1H, m) / δ_C 62.5, one carbonyl ester at δ_C 166.0, and aromatic carbons at δ_C 114.1,

δ_C 117.0, δ_C 147.4, δ_C 141.5 and δ_C 143.7 attributed to norbergenin moiety. This was supported, on one hand, by the COSY spectrum (**figure 28**) in which correlations were observed between aliphatic oxymethine H-4a (δ_H 4.42) and protons H-10b (δ_H 5.14) and H-4 (δ_H 5.60); oxymethine H-3 (δ_H 3.80) and protons H-4 (δ_H 5.60) and H-2 (δ_H 3.82) which also correlated with the diastereotopic oxymethylene protons H-11 (δ_H 4.04 / δ_H 3.75). On the other hand the norbergenin moiety was also supported by HMBC correlations (**figure 34**) observed between the oxymethine proton H-10b (δ_H 5.14) and carbons C-2 (δ_C 83.1), C-10a (δ_C 117.0), C-6a (δ_C 114.1); proton H-4a (δ_H 4.42) and carbons C-6 (δ_C 166.0) and C-10a (δ_C 117.0); aromatic methine H-7 (δ_C 7.08) and carbons C-6 (δ_C 166.0), C-6a (δ_C 114.1), C-10a (δ_C 117.0), C-8 (δ_C 147.4), C-9 (δ_C 141.5). The relative configuration of the oxymethine asymmetric carbons was deduced from the NOESY spectrum (**figure 33**) which showed correlations between protons H-10b, H-4 and H-2, and between protons H-4a, H-3 and H-11.

After removing the signals of the norbergenin moiety, those remaining were constituted of two doublets of two protons each at δ_H 7.97 (2H, d, J = 8.8 Hz) / δ_C 133.2 and δ_H 6.84 (2H, d, J = 8.8 Hz) / δ_C 116.1, one carbonyl ester at δ_C 167.5 and one oxygenated aromatic carbon at δ_C 163.7 corresponding to a *para*-hydroxybenzoyl group.

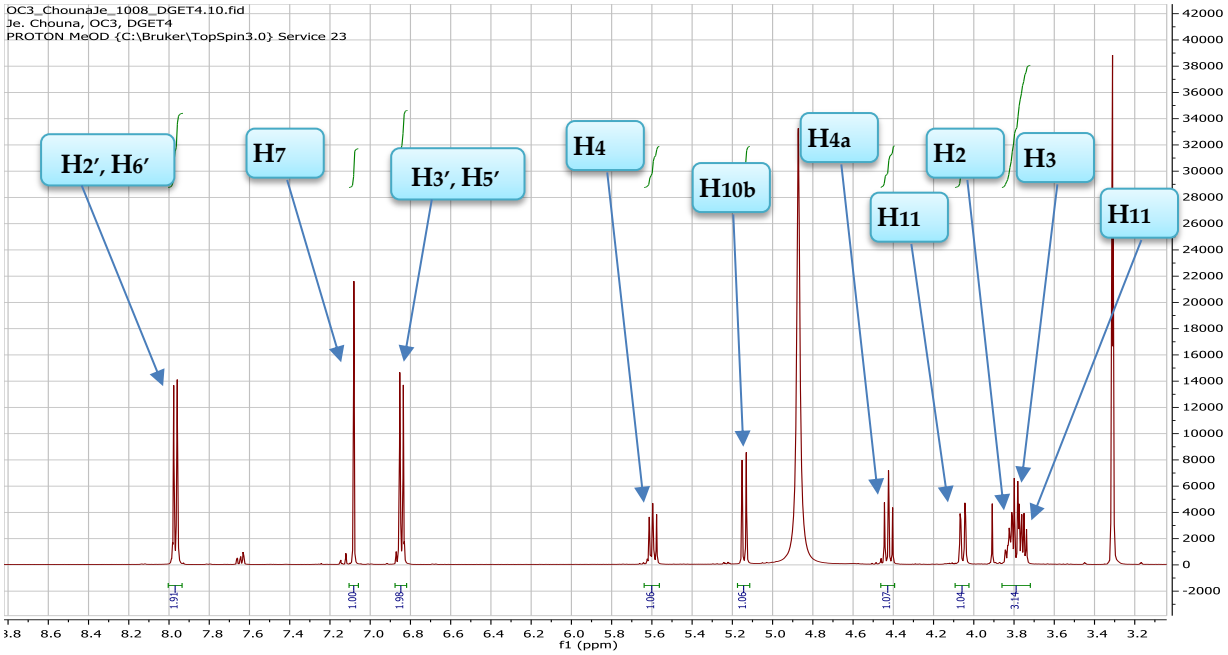

Figure 27 : ^{1}H NMR spectrum (500 MHz) of compound DGET4 in Methanol-d_4

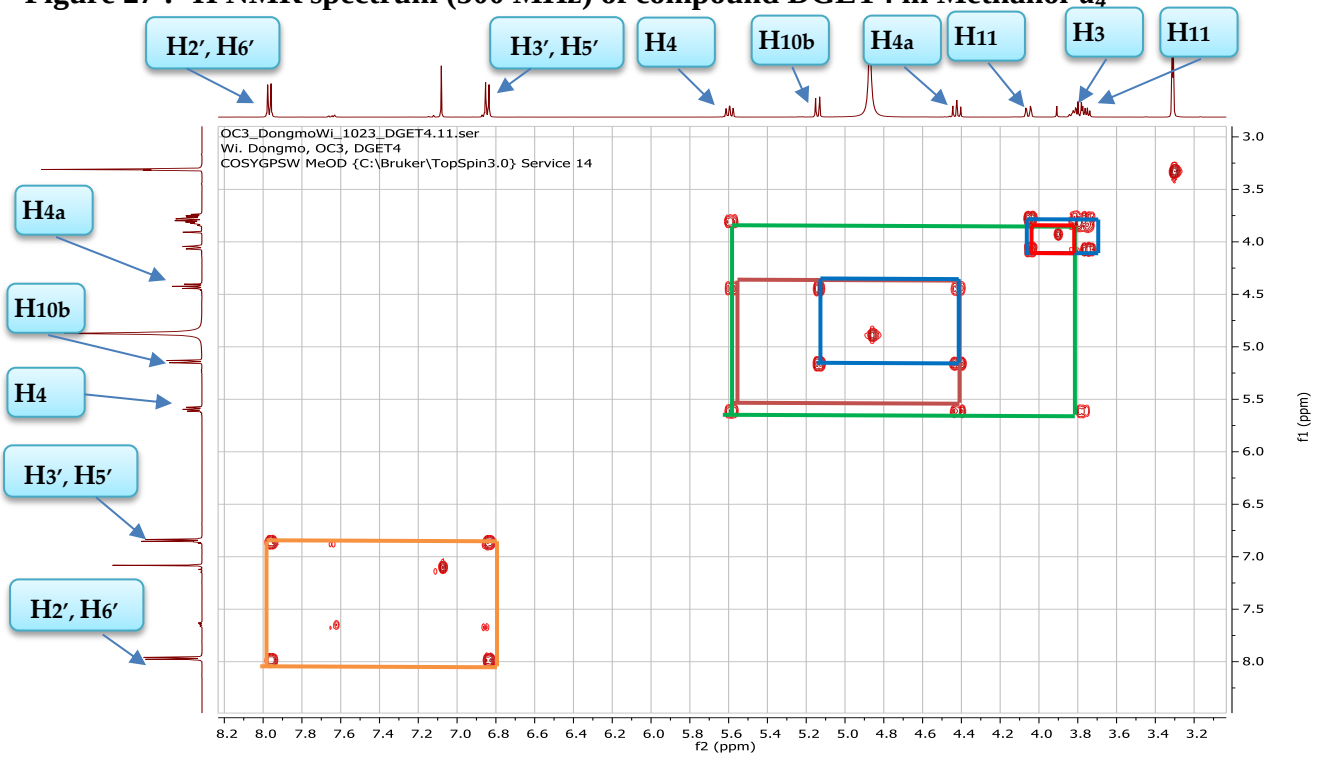

Figure 28 : COSY spectrum of compound DGET4

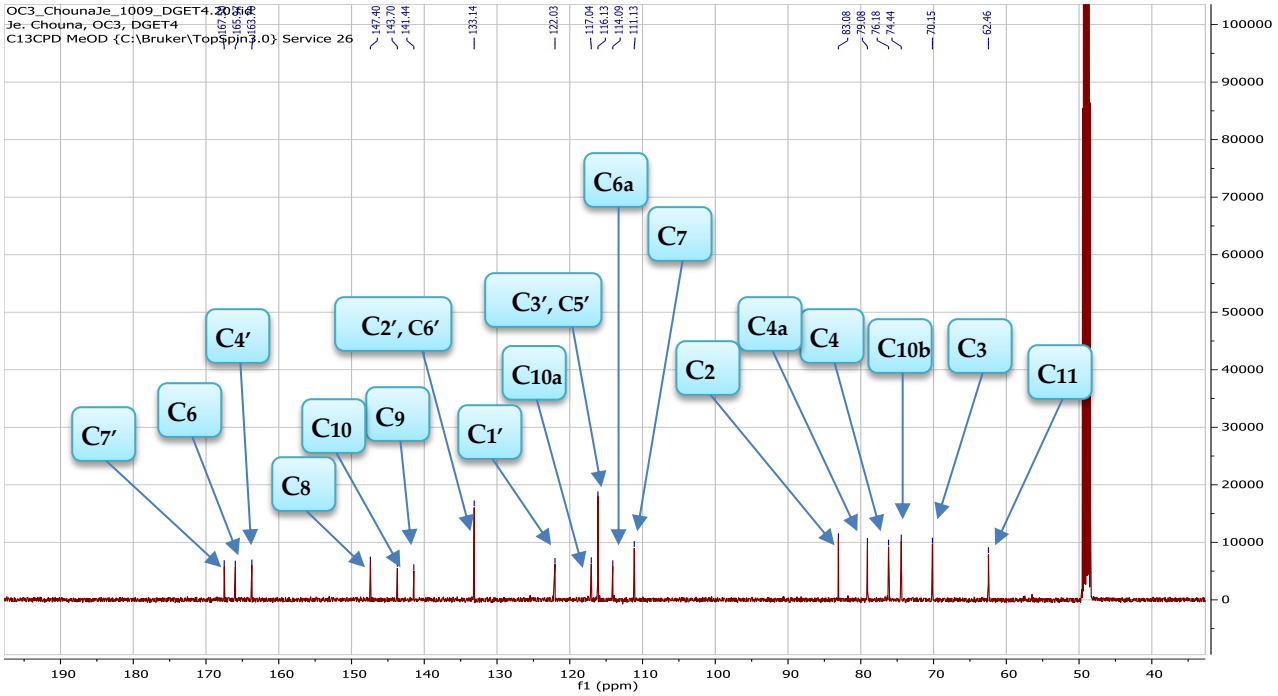

Figure 29: ^{13}C NMR spectrum (125 MHz) of compound DGET4 in Methanol-d_4

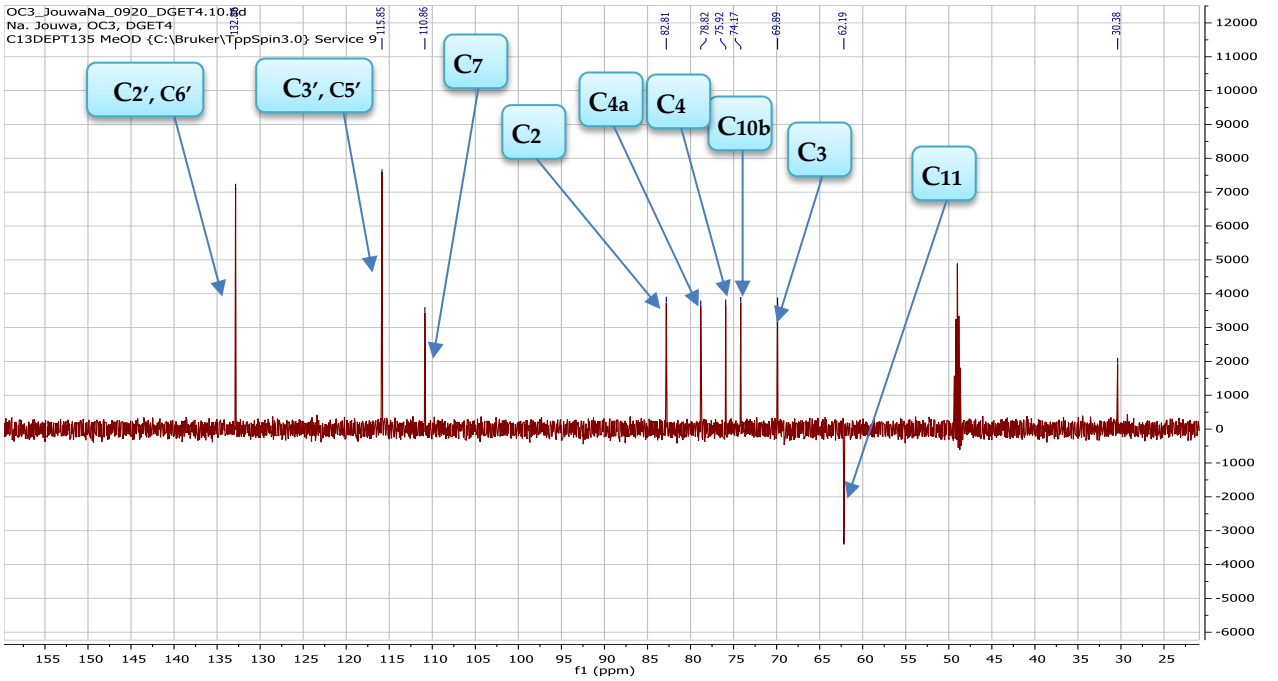

Figure 30: DEPT 135 NMR spectrum (125 MHz) of compound DGET4 in Methanol-d_4

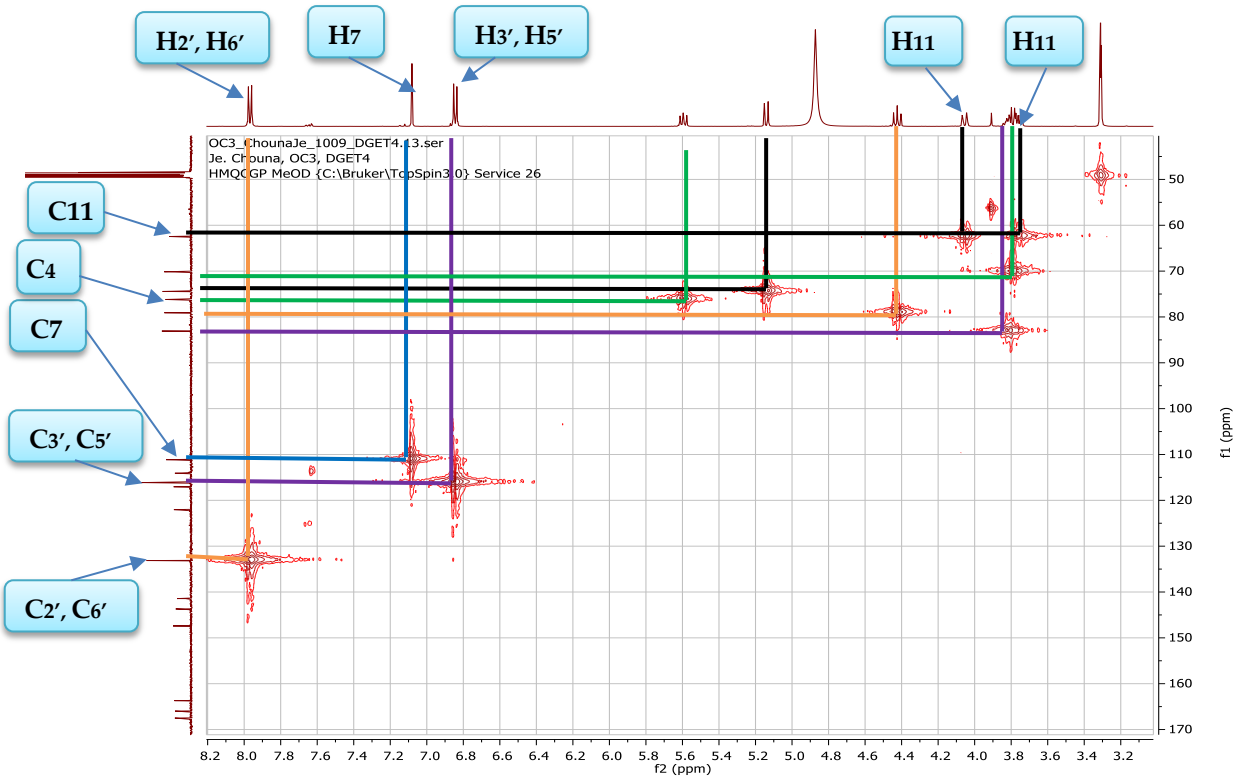

Figure 31: HMQC spectrum of compound DGET4

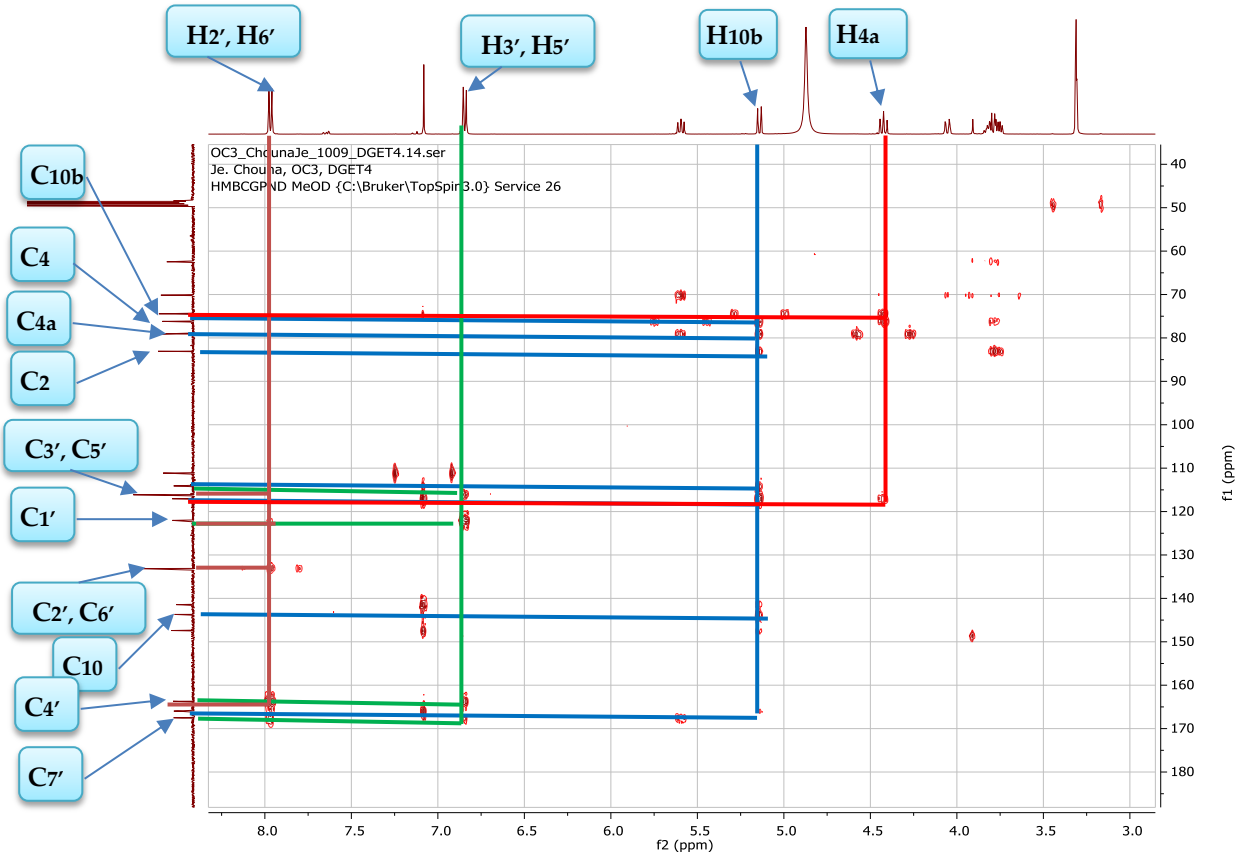

Figure 32: HMBC spectrum of compound DGET4

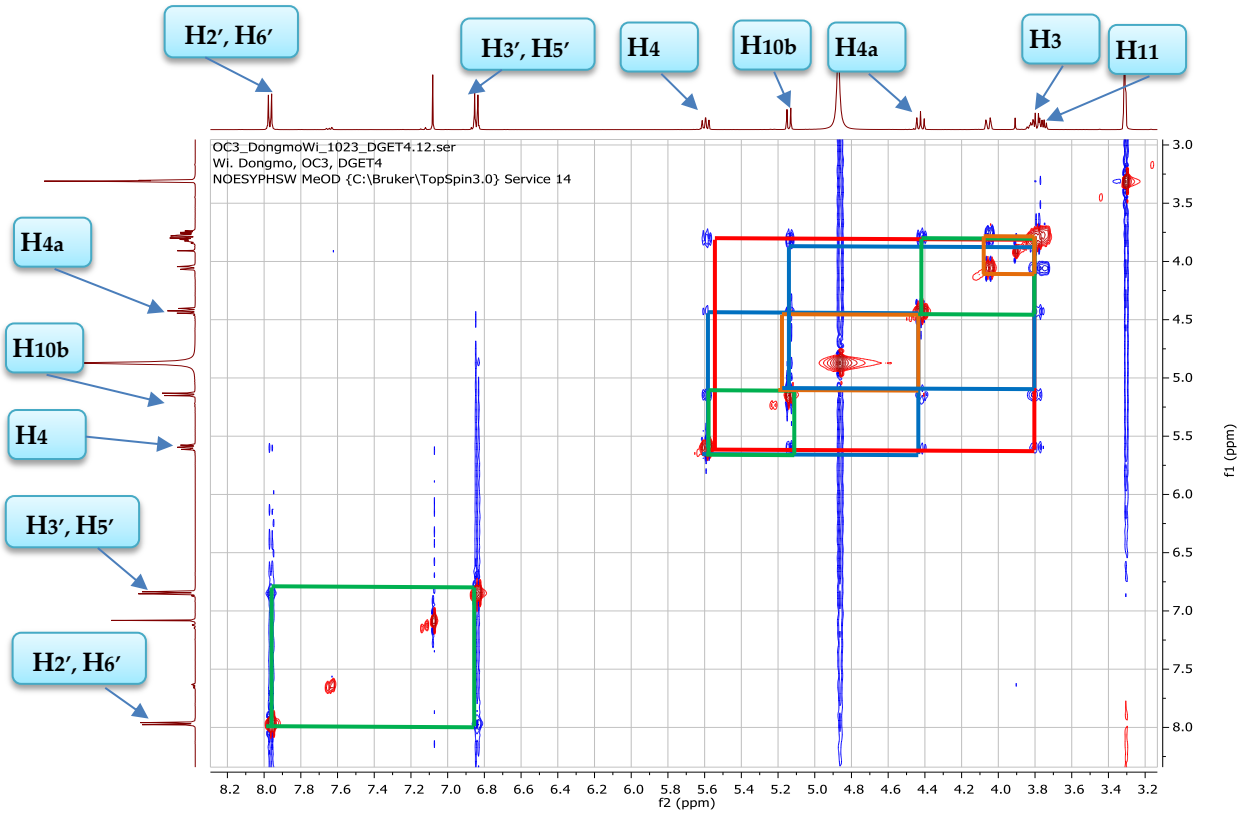

Figure 33: NOESY spectrum of compound DGET4

It remained to establish the position of the *para*-hydroxybenzoyl group on the norbergenin skeleton. The significant downfield shift of the signal at δ_H 5.60 (1H, dd, J = 8.4, 9.8 Hz, H-4) suggested that in compound DGET4 the oxygen of C-4 was esterified. This position was confirmed by the correlation observed in the HMBC spectrum between H-4 (δ_H 5.60) and C-7' (δ_C 167.5), showing that the *para*-hydroxybenzoyl group was fixed at C-4.

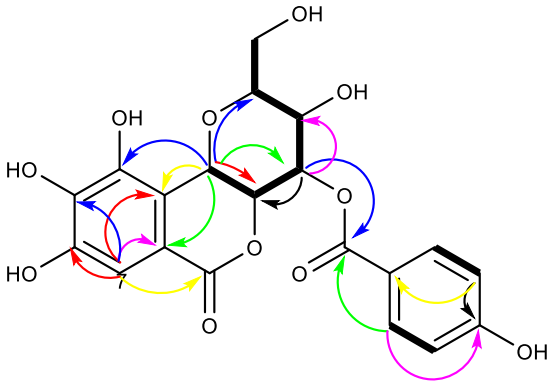

Figure 34: HMBC and COSY correlations of compound DGET4

From the above evidence, compound DGET4 was characterized as 4-*O*-*p*-hydroxybenzoylnorbergenin, a new natural product.

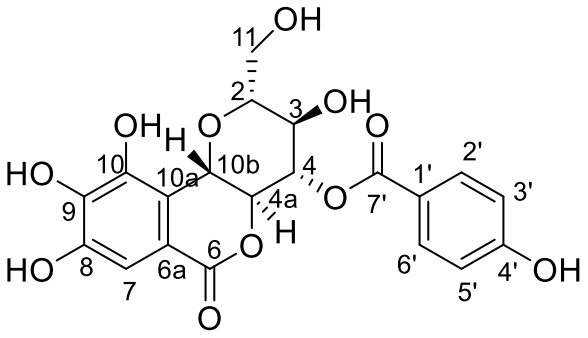

59

Moreover, this structure was confirmed by the X-ray of compound DGET4

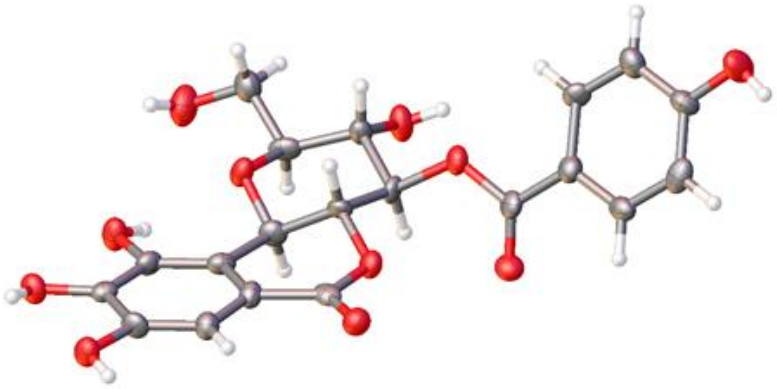

Figure 35: ORTEP-like view of compound DGET4

Table 9: ^{1}H (500 MHz) and ^{13}C (125 MHz) NMR data of compound DGET4 in Methanol-d_4

Position	DGET4	
	δ_H, mult (*J* in Hz)	δ_C, mult
2	3.82, m	83.1, CH
3	3.80, m	70.2, CH
4	5.60, dd (8.4, 9.8)	76.2, CH
4a	4.42, t (10.4)	79.1, CH
6	-	166.0, C
6a	-	114.1, C
7	7.08, s	111.1, CH
8	-	147.4, C
9	-	141.5, C
10	-	143.7, C
10a	-	117.0, C
10b	5.14, d (10.4)	74.4, CH
11	4.04, dd (11.6, 1.6)	62.5, CH_2
	3.75, m	
1'	-	122.0, C
2'/6'	7.97, d (8.8)	133.2, CH
3'/5'	6.84, d (8.8)	116.1, CH
4'	-	163.7, C
7'	-	167.5, C

II.1.3.1.3. Elucidation of DGTFIV1E

Compound DGTFIV1E was obtained as a white powder in the solvent system PE/EtOAc (1:3). It gave a purple coloration with ferric chloride reagent on TLC indicative of phenolic hydroxyl groups. Its ESIMS (**figure 36**) showed in positive mode a pseudo molecular ion peak $[M+Na]^+$ at *m/z* 457.1 compatible with the molecular formula $C_{20}H_{18}O_{11}$ and implying twelve degrees of unsaturation.

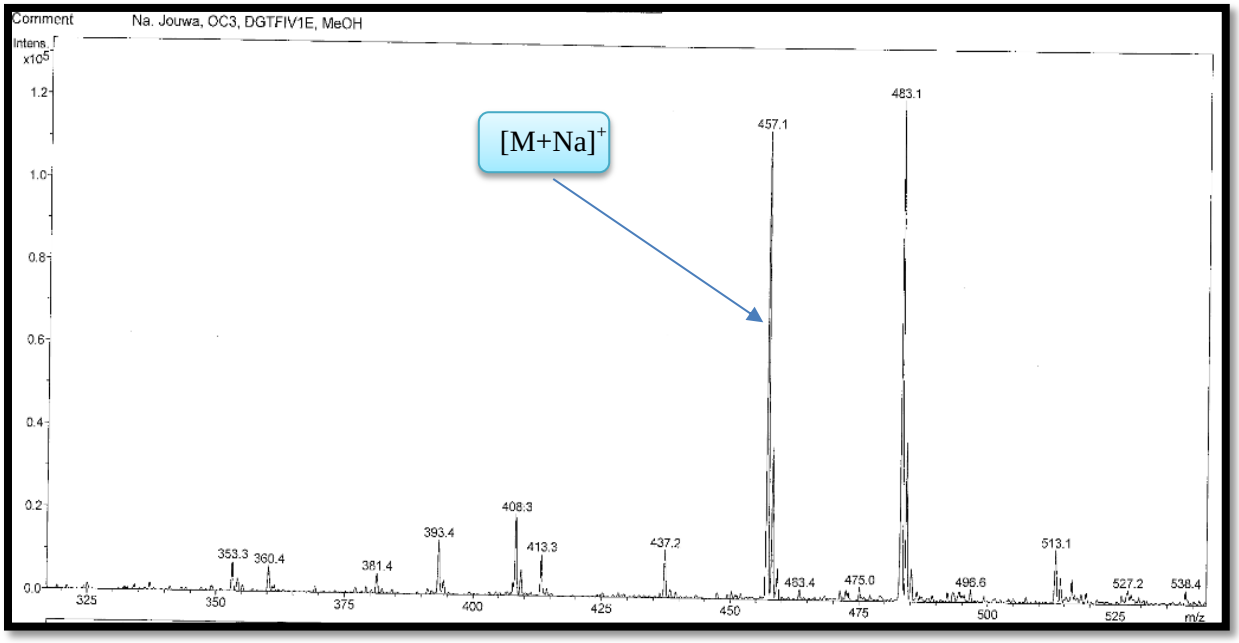

Figure 36: ESI mass spectrum of compound DGTFIV1E

Its ESIMS, UV, IR , ^{1}H and ^{13}C-NMR spectral data were identical to those of 4-*O*-*p*-hydroxybenzoylnorbergenin **59**, indicating that compound DGTFIV1E also possess norbergenin and *para*-hydroxybenzoyl group moieties, what makes these two compounds isomers. The presence of those two units in compound DGTFIV1E was further confirmed by the ^{1}H (**figure 37**) and ^{13}C NMR (**figure 38**) spectral data coupled to HMQC spectrum (**figure 39**) on which peaks characteristic of norbergenin were observed at δ_H 3.97 (H-2)/ δ_C 80.7, δ_H 3.53 (H-3)/ δ_C 72.0, δ_H 3.85 (H-4)/ δ_C 75.5, δ_H 4.07 (H-4a)/ δ_C 81.3, δ_H 7.09 (H-7)/ δ_C 110.9, δ_H 5.03 (H-10b)/ δ_C 74.6, δ_H 4.37, 4.89 (H-11)/ δ_C 64.8, δ_C 113.4, δ_C 117.0, δ_C 142.4, δ_C 143.6, δ_C 147.5, and δ_C 166.5. Those attributable to *para*-hydroxybenzoyl moiety appeared at δ_H 7.93 (2H, d, H-2', H-6')/ δ_C 133.0, δ_H 6.84 (2H, d, H-3', H-5')/ δ_C 116.4, δ_C 164.0 and δ_C 168.0.

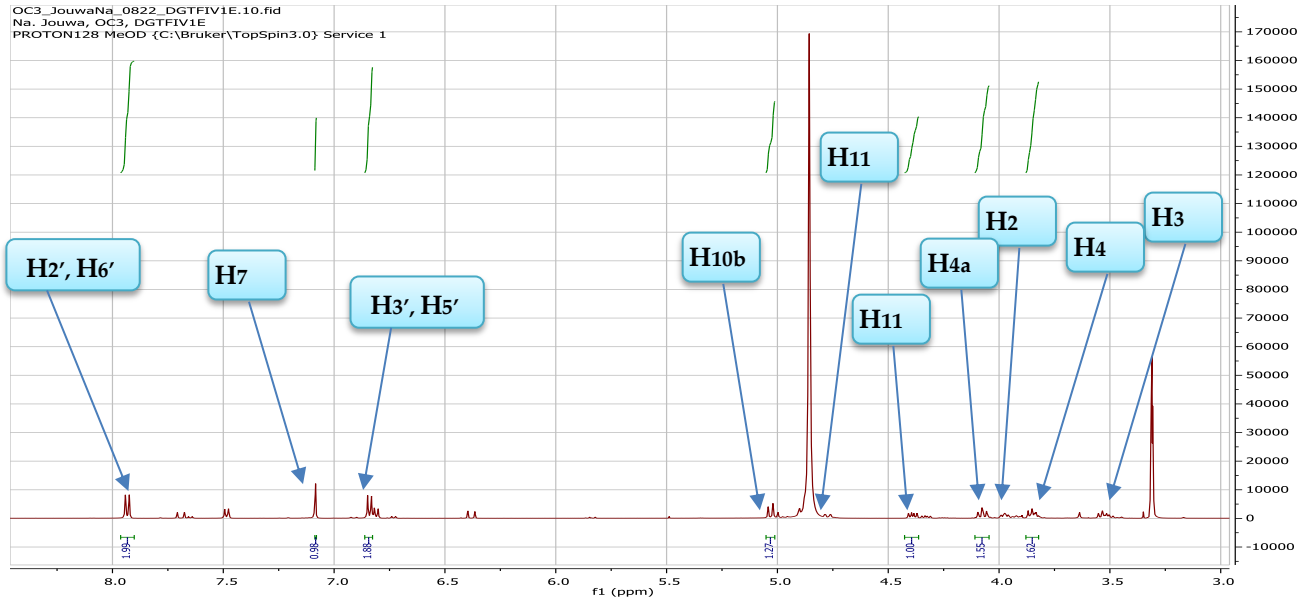

Figure 37: ^{1}H NMR spectrum (500 MHz) of compound DGTFIV1E in Methanol-d_4

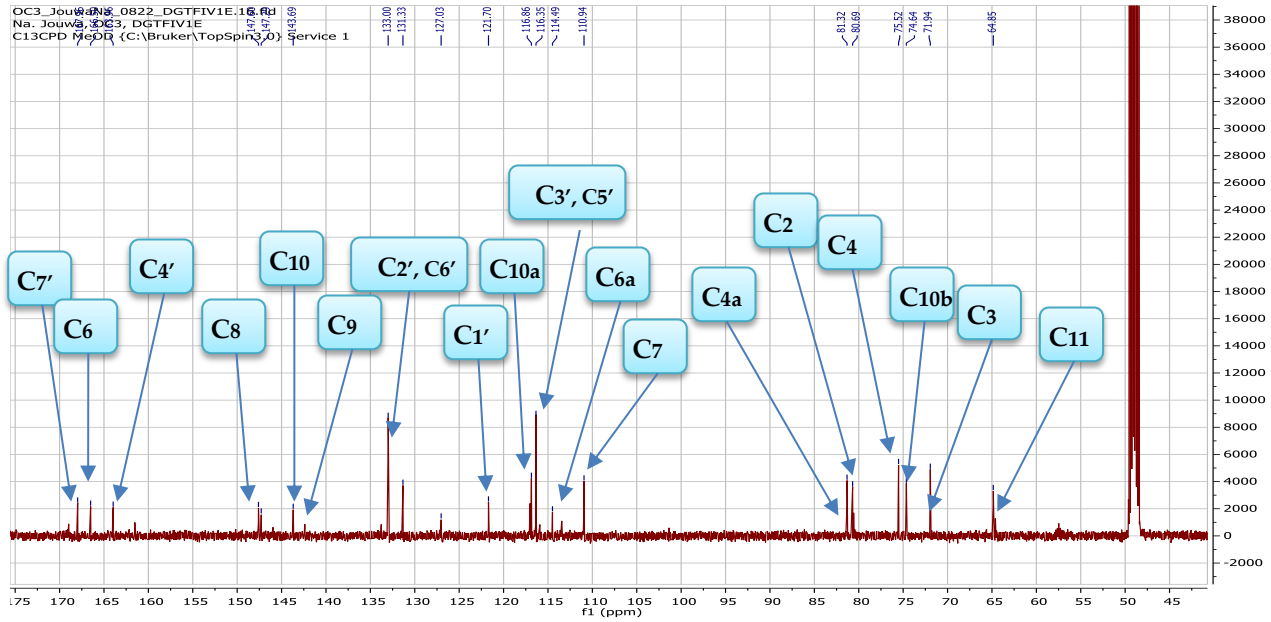

Figure 38: ^{13}C NMR spectrum (125 MHz) of compound DGTFIV1E in Methanol-d_4

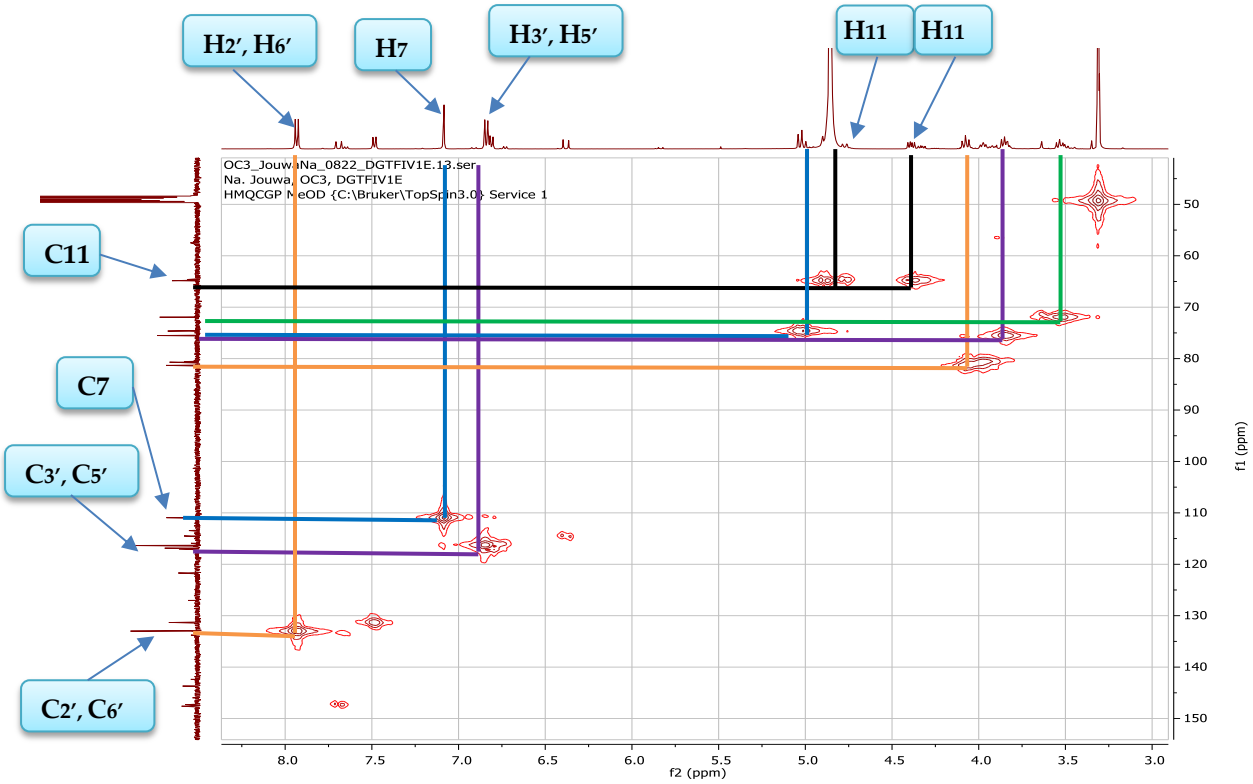

Figure 39: HMQC spectrum of compound DGTFIV1E

The difference between 4-*O*-*p*-hydroxybenzoylnorbergenin **59** and compound DGTFIV1E was the position of *para*-hydroxybenzoyl moiety on the norbergenin skeleton. While in compound 4-*O*-*p*-hydroxybenzoylnorbergenin **59** this *para*-hydroxybenzoyl moiety was located in carbon C-4 of the norbergenin skeleton, in compound DGTFIV1E, the site of esterification was located in carbon C-11. In fact, the significant downfield shift of the signals at δ_H 4.37, 4.89 (H-11)/ δ_C 64.8 as well as the correlation observed in the HMBC spectrum between methylene protons H-11 and carbonyl carbon C-7' (δ_C 168.0) permitted to confirm this position.

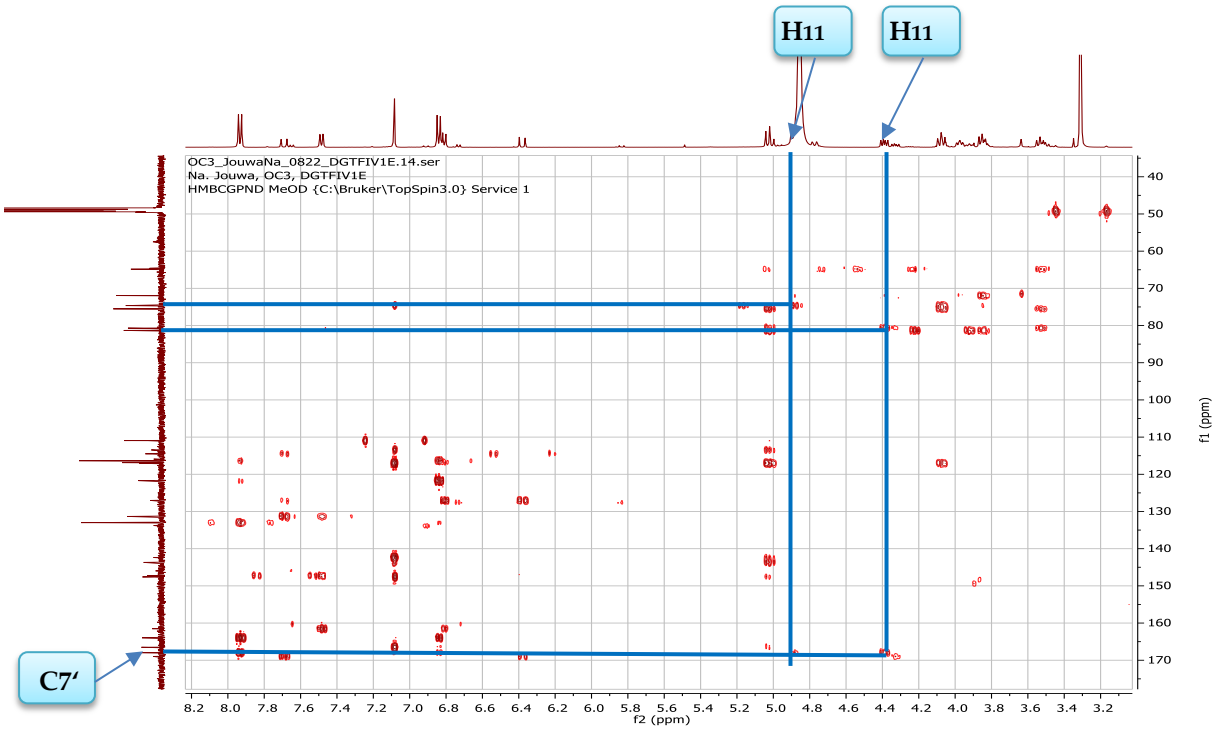

Figure 40: HMBC spectrum of compound DGTFIV1E

Therefore, compound DGTFIV1E was identified as 11-*O*-*p*-hydroxybenzoylnorbergin, a known compound isolated for the first time from *Diospyros sanza-minika* by Tangmouo et *al* in 2009.

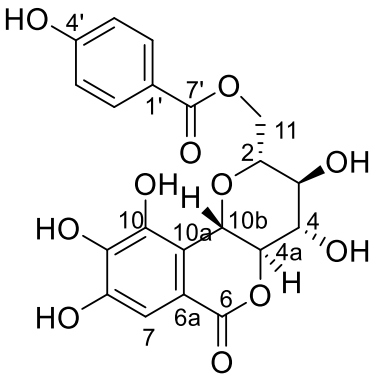

53

Table 10: ^{1}H (500MHz) and ^{13}C (125MHz) NMR assignments of compound DGTFIV1E and 11-*O*-*p*-hydroxybenzoylnorbergenin in Methanol-d_4

Position	DGTFIV1E		11-*O*-*p*-hydroxybenzoylnorbergenin literature data[a]	
	δ_H, mult (*J* in Hz)	δ_C, mult	δ_H, mult (*J* in Hz)	δ_C, mult
2	3.97, m	80.7, CH	4.11, m	81.2, CH
3	3.53, m	72.0, CH	3.68, t (9.9)	72.1, CH
4	3.85, m	75.5, CH	3.94, t (9.0)	75.8, CH
4a	4.07, m	81.3, CH	4.13, m	80.6, CH
6	-	166.5, C	-	164.5, C
6a	-	113.4, C	-	115.4, C
7	7.09, s	110.9, CH	7.12, s	111.1, CH
8	-	147.5, C	-	147.2, C
9	-	142.4, C	-	140.3, C
10	-	143.6, C	-	143.6, C
10a	-	117.0, C	-	117.1, C
10b	5.03, d (10.4)	74.6, CH	5.14, d (10.5)	74.6, CH
11	4.89, m	64.8, CH_2	4.97, dd (2.2 ,12.2)	64.9, CH_2
	4.39, dd (7.0, 12.2)		4.45, dd (6.9 ,12.2)	
1'	-	122.0, C	-	122.6, C
2'/6'	7.93, d (8.8)	133.0, CH	7.97, d (8.8)	133.1, CH
3'/5'	6.84, d (8.8)	116.4, CH	6.96, d (8.8)	116.6, CH
4'	-	164.0, C	-	163.3, C
7'	-	168.0, C	-	167.1, C

[a] (Tangmouo et *al*., 2009)

II.1.3.1.4. Elucidation of DGF8

Compound DGF8 was isolated as a white amorphous powder in the solvent system PE/EtOAc (1:3). It gave a blue dark coloration with ferric chloride reagent indicative of the presence of phenolic hydroxyl groups. Its molecular formula, $C_{22}H_{20}O_{10}$ was assigned from its HR-TOF-ESIMS (**figure 41**) which exhibited in positive mode, the sodium adduct ion peak $[M+Na]^+$ at m/z 467.0949 (calculated for $C_{22}H_{20}O_{10}Na$: m/z 467.09487).

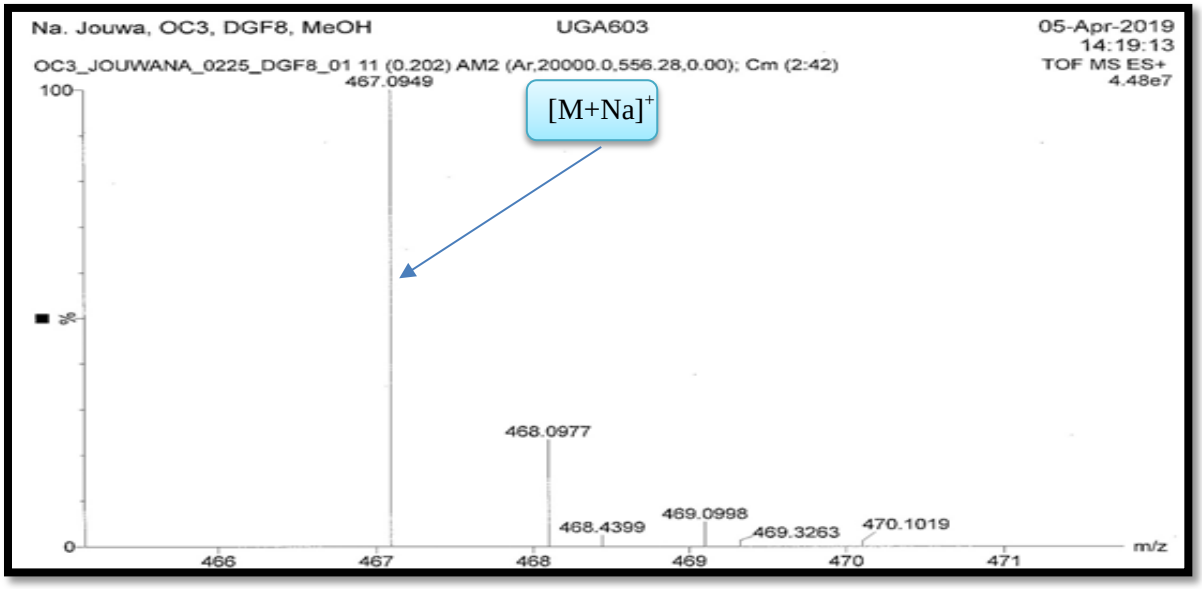

Figure 41: HR-TOF-ESIMS of compound DGF8

The UV spectrum (**figure 42**) of this compound showed maxima absorption bands at λ_{max} 217 and 279 nm while in its IR spectrum (**figure 43**), the vibration bands due to hydroxyl group (3354 cm^{-1}) and carbonyl function (1698 and 1635 cm^{-1}) were observed.

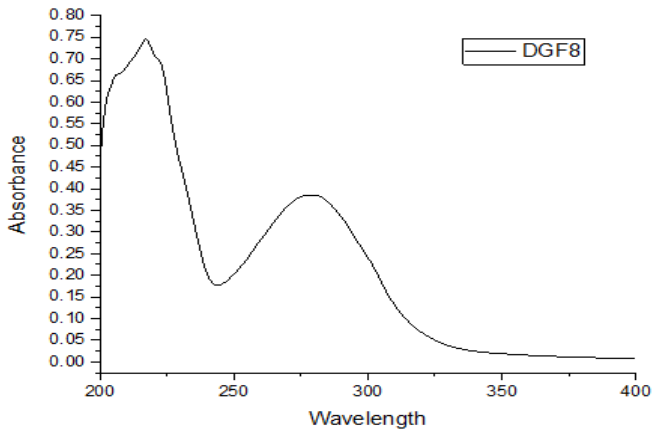

Figure 42: UV spectrum of compound DGF8

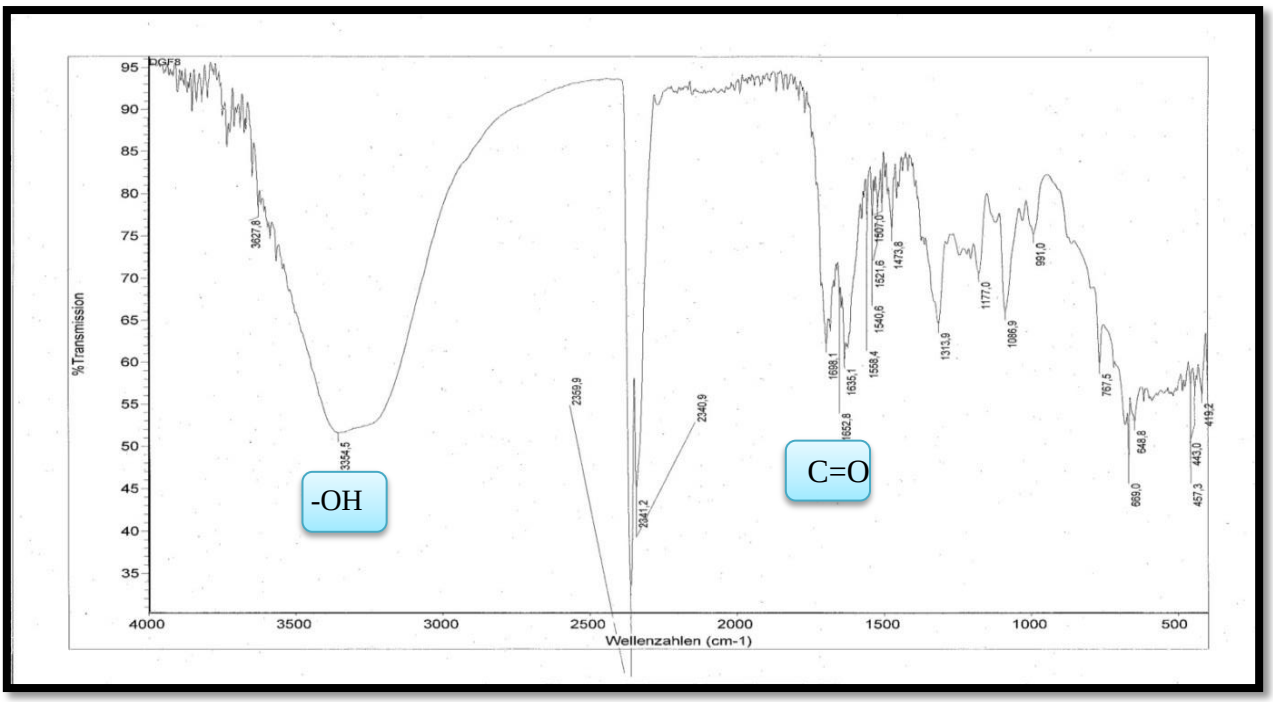

Figure 43: IR spectrum of compound DGF8

The comparison of ^{1}H, ^{13}C, HMQC and DEPT NMR spectra of compound DGF8 (**figures 44, 46, 48** and **47** respectively) showed close similarities to those of compound 4-*O*-*p*-hydroxybenzoylnorbergenin **59**. These data indicated the presence of a norbergenin skeleton through the aromatic singlet at δ_H 7.09 (1H, s, H-7) / δ_C 111.1, the five norbergenin types oxymethines at δ_H 5.01 (1H, d, *J*= 10.5 Hz, H-10b) / δ_C 74.5, δ_H 4.08 (1H, t, *J*= 9.4, 10.5 Hz, H-4a) / δ_C 81.3, δ_H 3.93 (1H, ddd, *J*= 2.2, 7.0, 9.9 Hz, H-2) / δ_C 80.5, δ_H 3.84 (1H, brt, *J*= 9.0 Hz, H-4) / δ_C 75.5, δ_H 3.52 (1H, t, *J*= 8.7, 9.9 Hz, H-3) / δ_C 71.9, the oxymethylene at δ_H 4.80 (1H, dd, *J*= 2.2, 12.2 Hz, H-11), δ_H 4.36 (1H, dd, *J*= 7.0, 12.2 Hz, H-11) / δ_C 64.8, the carbonyl ester at δ_C 166.3 (C-6) and the aromatic carbons at δ_C 147.4 (C-8), δ_C 143.5(C-10), δ_C 141.2 (C-9), δ_C 117.0 (C-10a) and δ_C 114.2 (C-6a). The differences between the two compounds were the nature of the substituent and its position on the norbergenin skeleton. The signals of this substituent were constituted of two olefinic methines which appeared as an AB spin system with a *trans* coupling at δ_H 6.59 (1H, d, *J*= 16 Hz, H-8') / δ_C 118.2 (C-8') and δ_H 7.76 (1H, d, *J*= 16 Hz, H-7') / δ_C 147.0 (C-7'), five aromatic protons at δ_H 7.63 (2H, m, H-2', H-6') / δ_C 129.4 (C-2'/C-6') and δ_H 7.41 (2H, m, H-3', H-5',) / δ_C 130.0 (C-3'/ C-5'), δ_H 7.41 (1H, m, H-4') / δ_C 131.7 (C-4'), δ_C 135.6 (C-1') and signal of one carbonyl ester at δ_C 168.4 (C-9') corresponding to a cinnamoyl group.

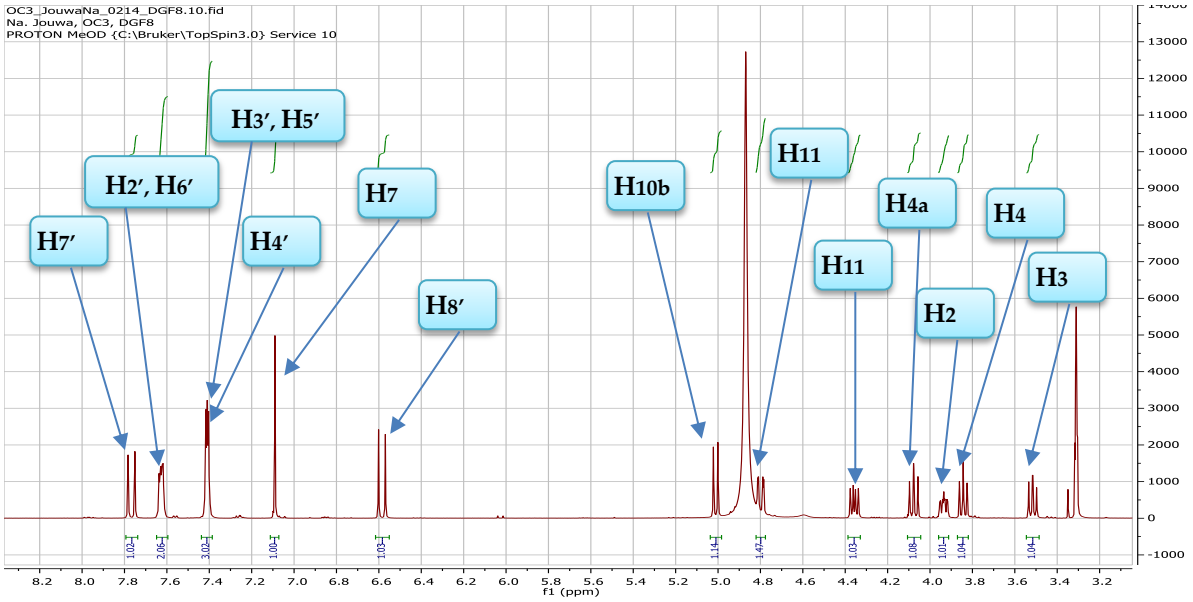

Figure 44: ^{1}H NMR spectrum (500 MHz) of compound DGF8 in Methanol-d_4

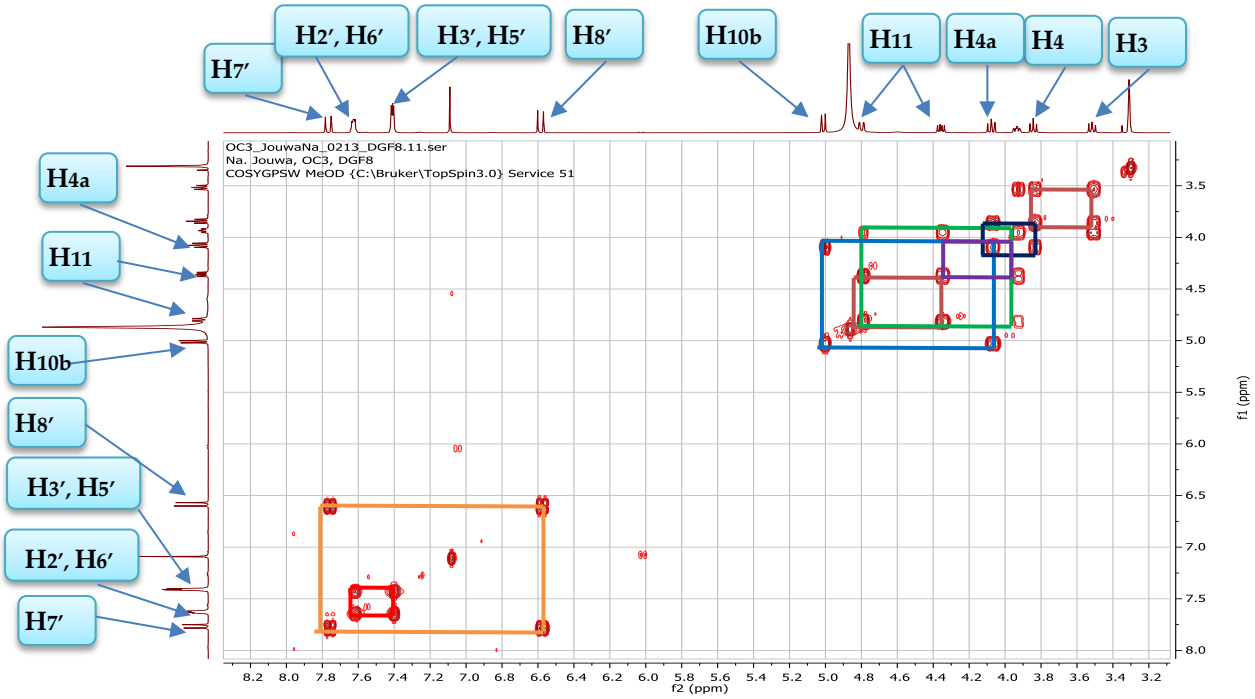

Figure 45: COSY spectrum of compound DGF8

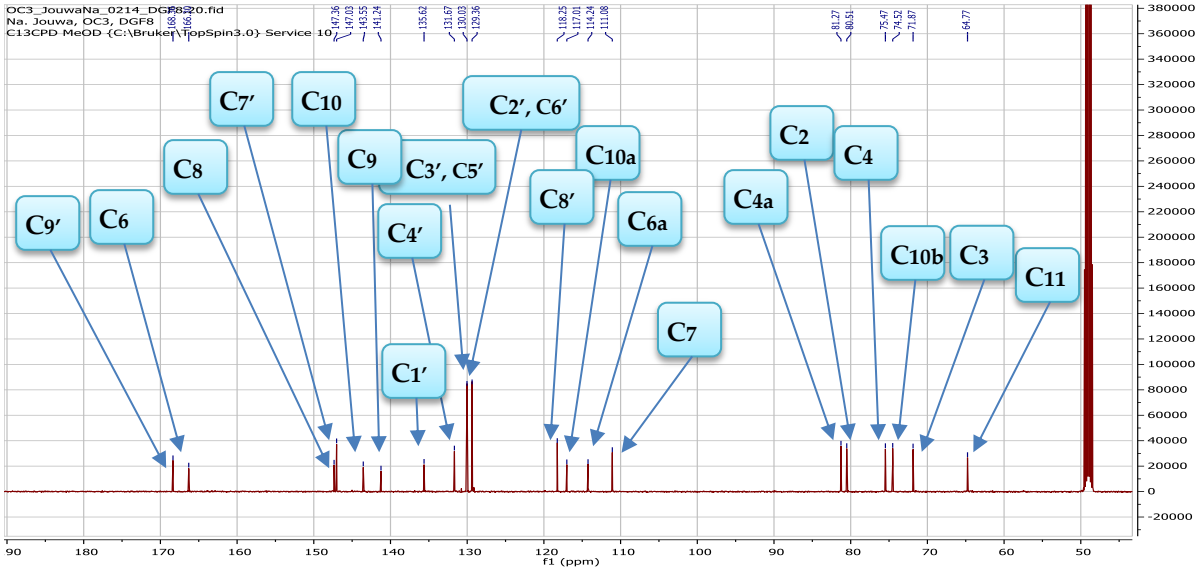

Figure 46: ^{13}C NMR spectrum (125 MHz) of compound DGF8 in Methanol-d_4

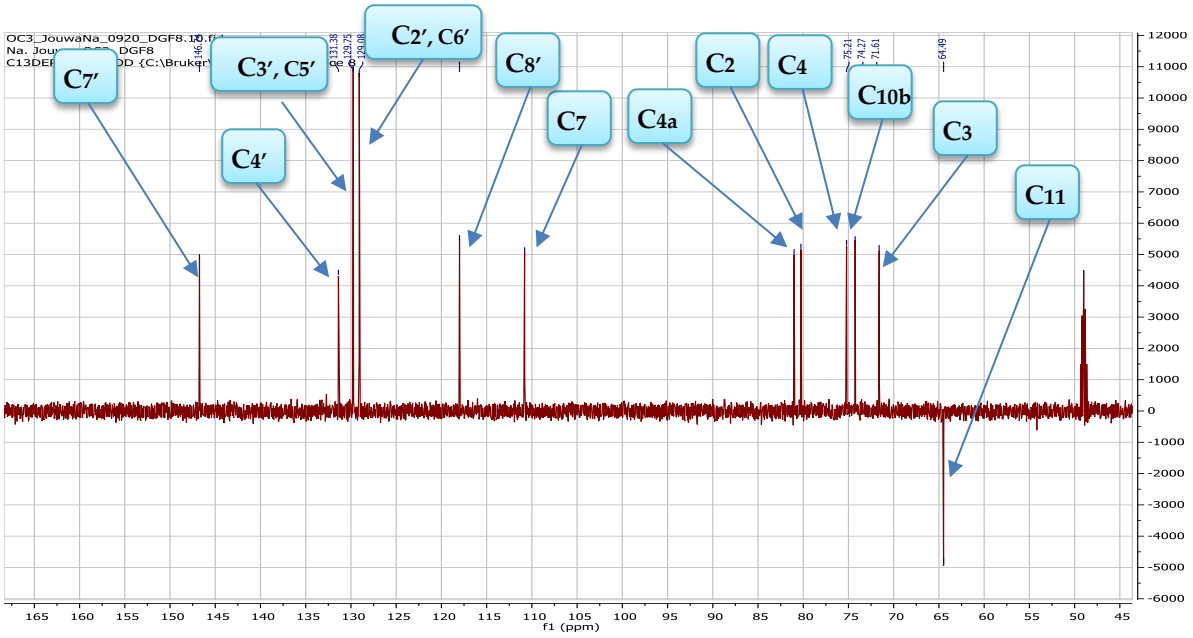

Figure 47: DEPT 135 NMR spectrum (125 MHz) of compound DGF8 in Methanol-d_4

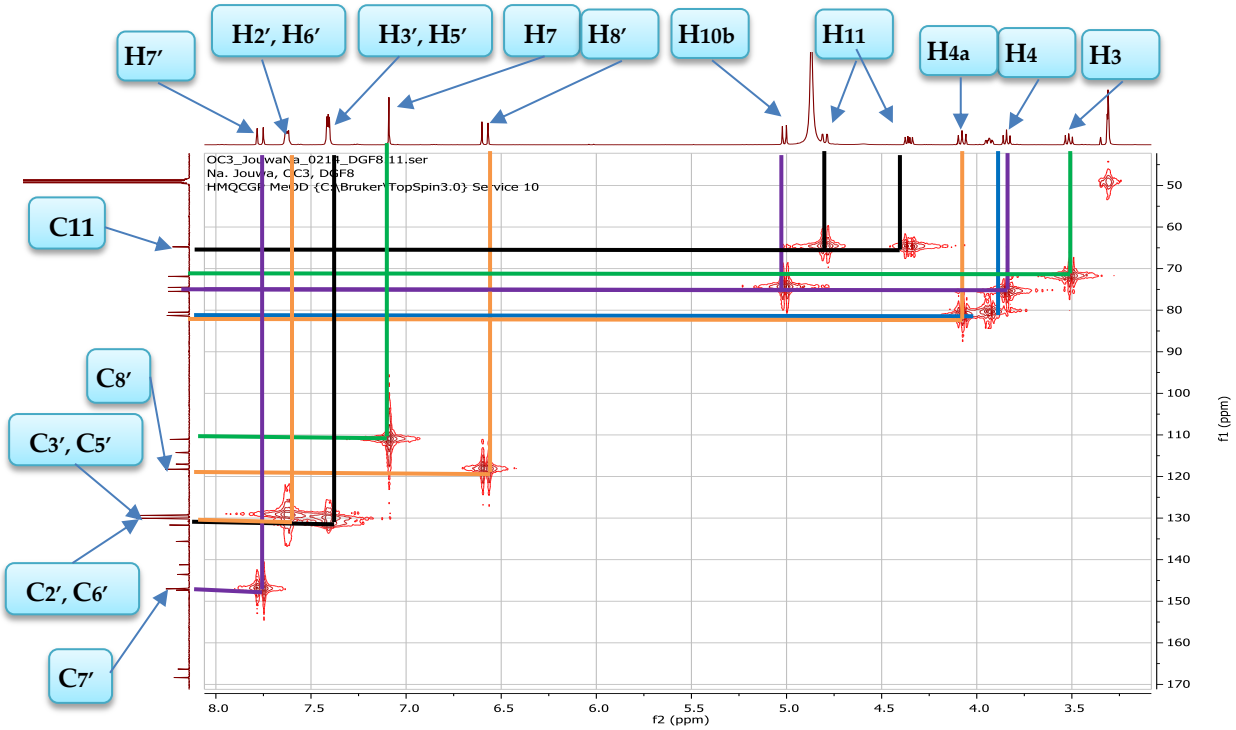

Figure 48: HMQC spectrum of compound DGF8

The position of this subtituent on the norbergenin backbone was established to be at carbon C-11 by evidence of deshielding of the diastereotopic oxymethylene protons (H-11) of norbergenin appearing at δ_H 4.80 and δ_H 4.36 in compound DGF8 compared to their values in compound DGET4. This was confirmed by the HMBC correlations (**figure 49**) observed between diastereotopic protons H-11 and carbonyl of the cinnamoyl group C-9' at δ_C 168.4.

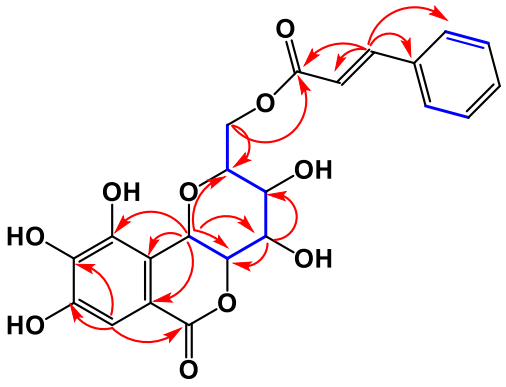

Figure 49: COSY (blue) and HMBC (red) correlations of compound DGF8

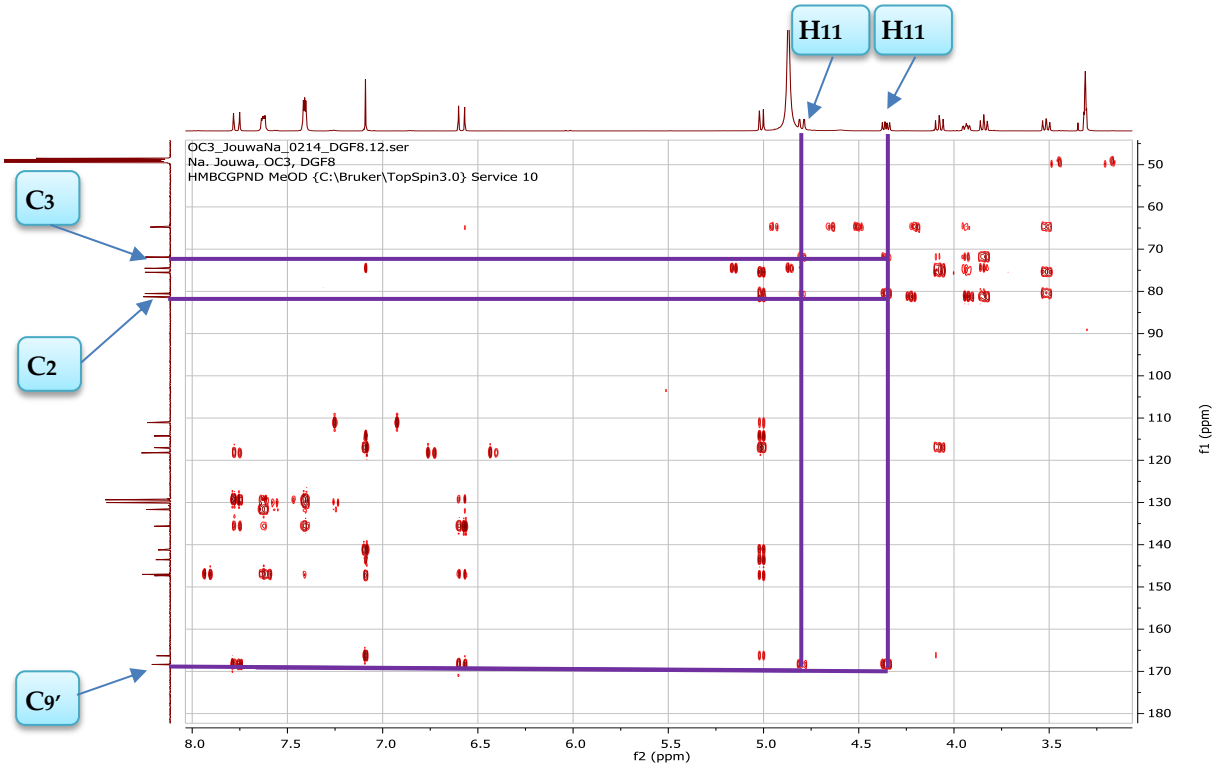

Figure 50: HMBC spectrum of compound DGF8

The relative stereochemistry of the oxymethine protons in compound DGF8 was established to be trans diaxial from the value of the coupling constant (8-10) and the NOESY experiment (**Figure 51).**

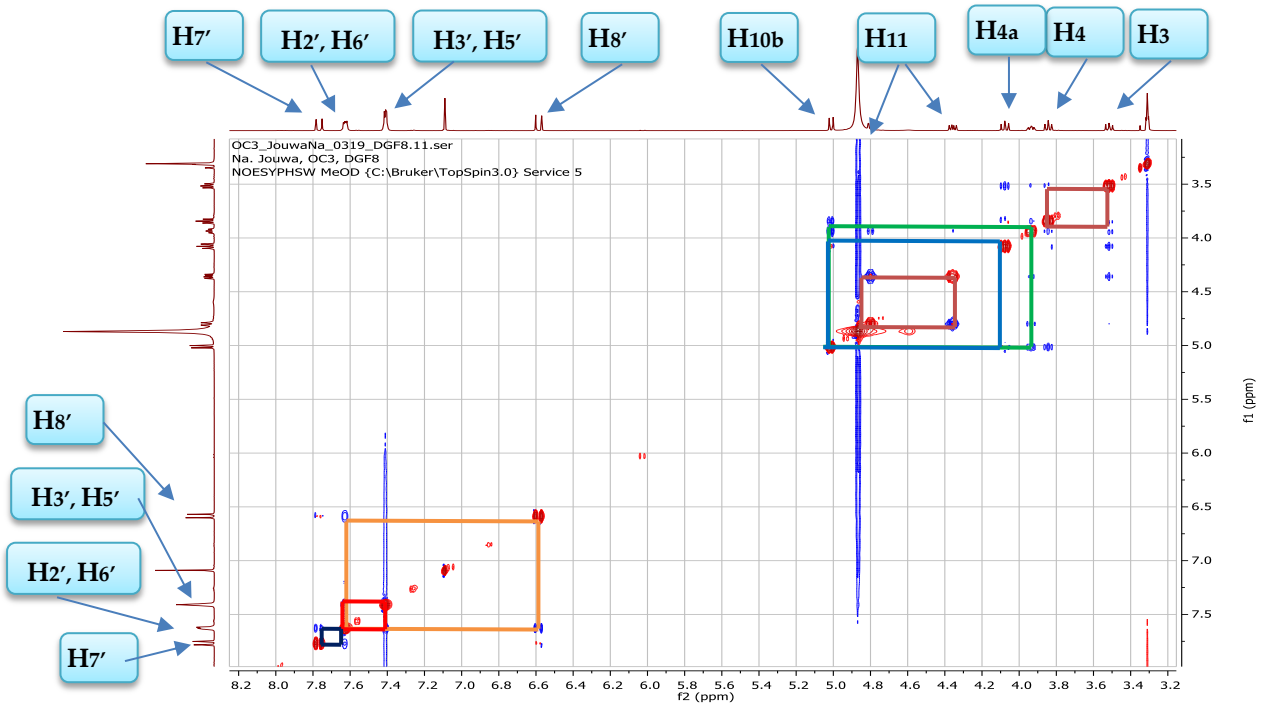

Figure 51: NOESY spectrum of compound DGF8

From the above spectroscopic data, compound DGF8 was identified as 11-*O-(E)*-cinnamoylnorbergenin described from natural source for the first time.

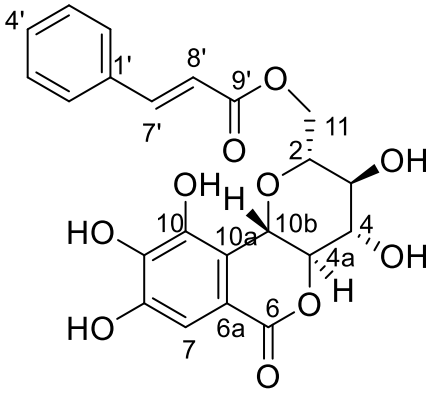

60

Table 11: ^{1}H (500MHz) and ^{13}C (125MHz) NMR assignments of compound DGF8 (11-*O-(E)*-cinnamoylnorbergenin) in Methanol-d_4

Position	DGF8	
	δ_H, mult (*J* in Hz)	δ_C, mult
2	3.93, ddd (2.2, 7.0, 9.9)	80.5, CH
3	3.52, t (8.7, 9.9)	71.9, CH
4	3.84, brt (9.0)	75.5, CH
4a	4.08, t (9.4, 10.5)	81.3, CH
6	-	166.3, C
6a	-	114.2, C
7	7.09, s	111.1, CH
8	-	147.4, C
9	-	141.2, C
10	-	143.5, C
10a	-	117.0, C
10b	5.01, d (10.5)	74.5, CH
11	4.80, dd (2.2 ,12.2)	64.8, CH_2
	4.36, dd (7.0 ,12.2)	
1’	-	135.6, C
2’/6’	7.63, m	129.4, CH
3’/5’	7.41, m	130.0, CH
4’	7.41, m	131.7, CH
7’	7.76, d (16.0)	147.0, CH
8’	6.59, d (16.0)	118.2, CH
9’	-	168.4, C

II.1.3.1.5. Elucidation of compound DGET1

Compound DGET1 was isolated as white amorphous powder in the solvent system. It gave a blue coloration with ferric chloride reagent on TLC indicative of phenolic hydroxyl groups. Its HR-ESIMS (**Figure 52**) showed in positive mode a pseudo molecular ion peak $[M+Na]^+$ at *m/z* 489.0696 due to the molecular formula $C_{20}H_{18}O_{13}$ and implying twelve double bond equivalent.

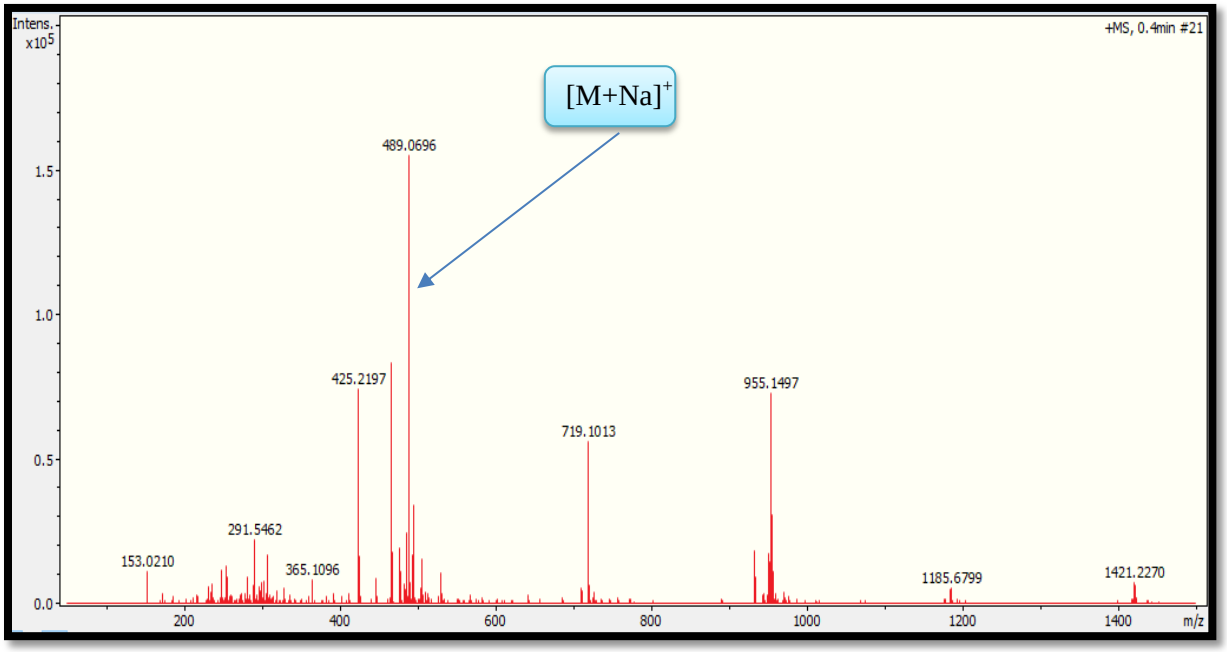

Figure 52: HRESI spectrum of compound DGET1

The comparison of ^{1}H- and ^{13}C- NMR spectral data of this compound (**Figures 53** and **54** respectively) with those of 11-*O-(E)*-cinnamoylnorbergenin **60** revealed close similarities. In fact, all the signals attributed to the norbergenin moity found in the spectra of 11-*O-(E)*-cinnamoylnorbergenin **60** were also present in the spectra of compound DGET1. These included a signal of one singlet proton at δ_H 7.08 / δ_C 111.1, signals of five oxymethines at δ_H 3.78 (1H, m, H-3)/ δ_C 70.0, δ_H 3.80 (1H, m, H-2)/ δ_C 83.0 , δ_H 4.38 (1H, t, *J* = 10.1 Hz, H-4a) / δ_C 79.0 , δ_H 5.12 (1H, d, *J* = 10.4 Hz, H-10b) / δ_C 74.4 , δ_H 5.56 (1H, t, *J* = 9.9 Hz, H-4)/ δ_C 76.2, signals of one oxymethylene at δ_H 3.77 (1H, m, H-11) and 4.05 (1H, dd, *J* = 11.9, 1.8 Hz, H-11) / δ_C 62.4, signal of one carbonyl of lactone at δ_C 166.0 and signals of aromatic carbons at δ_C 114.0, δ_C 117.0, δ_C 147.7, δ_C 141.5, δ_C 143.6. The main difference between the spectra of these two compounds was the presence in the spectra of compound DGET1 of additional signals including a singlet of two protons at δ_H 7.14 / δ_C 110.4, a carbonyl of

lactone at δ_C 167.7, oxygenated aromatic carbons at δ_C 146.4 and δ_C 139.9 and aromatic quaternary carbon at δ_C 121.2 corresponding to a galloyl moiety.

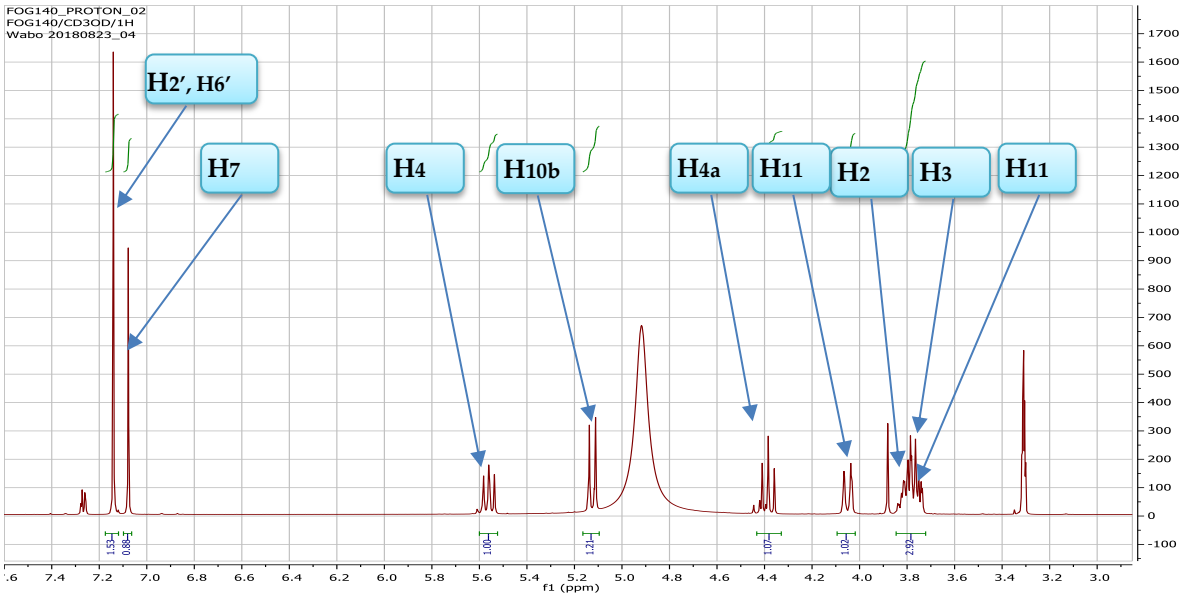

Figure 53: ^{1}H NMR spectrum (500 MHz) of compound DGET1 in Methanol-d_4

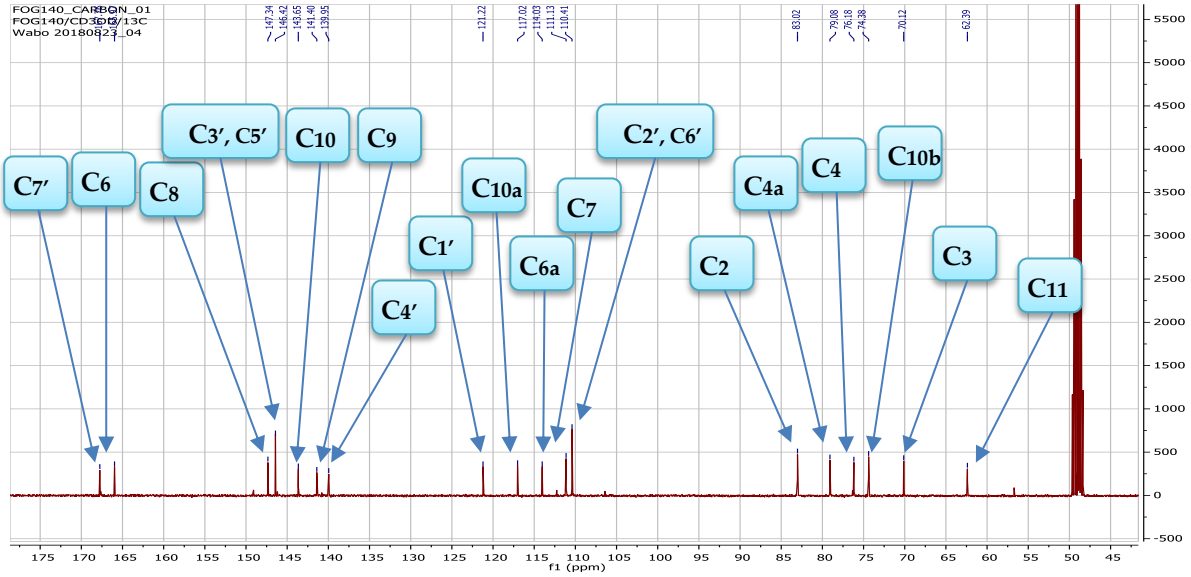

Figure 54: ^{13}C NMR spectrum (125 MHz) of compound DGET1 in Methanol-d_4

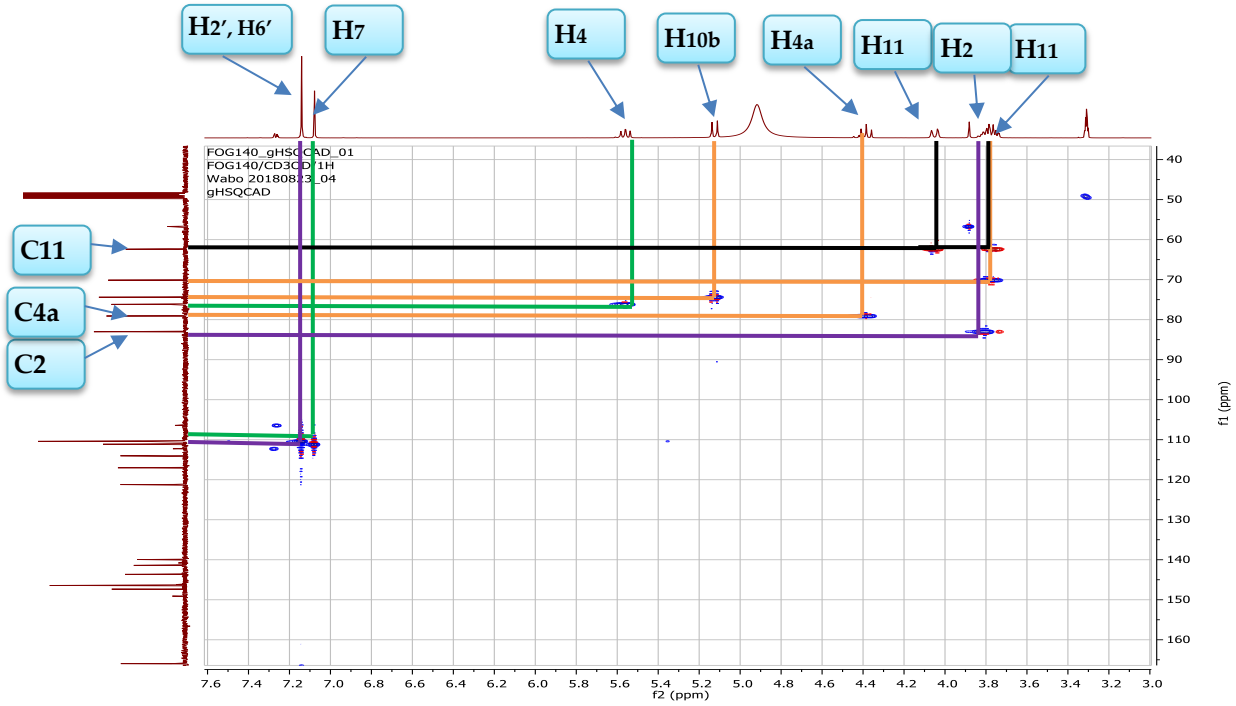

Figure 55: HSQC spectrum of compound DGET1.

It remained to establish the position of this galloyl substituent on the norbergenin squeleton. This position was established based on one hand on the significant downfield shift of the signal at δ_H 5.56 (1H, t, J = 9.9 Hz, H-4) which suggested that the oxygen of C-4 was esterified and on the other hand by the correlation observed in the HMBC spectrum (**Figure 56**) between H-4 (δ_H 5.56) and C-7' (δ_C 167.7), showing that the galloyl group was fixed at C-4.

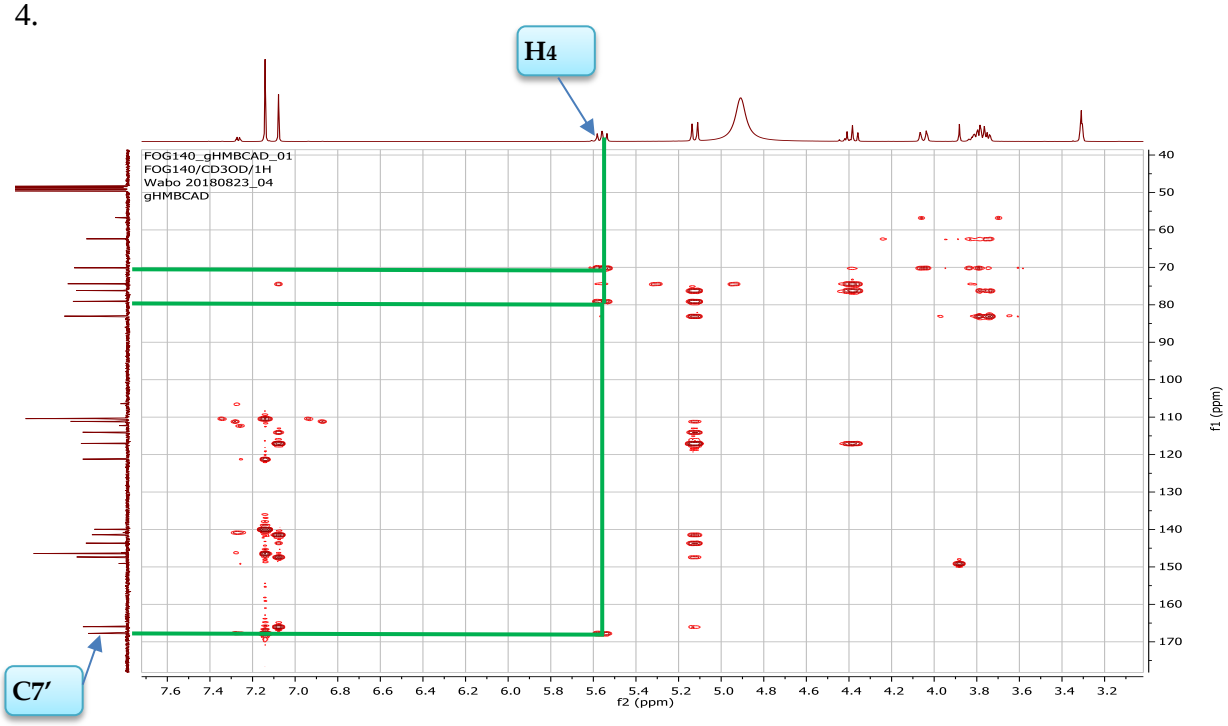

Figure 56: **HMBC spectrum of compound DGET1.**

Based on the above evidence, compound DGET1 was identified as 4-*O*-galloylnorbergenin, a known compound isolated for the first time from *Mallotus japonicus* by Saijo et *al* in 1990.

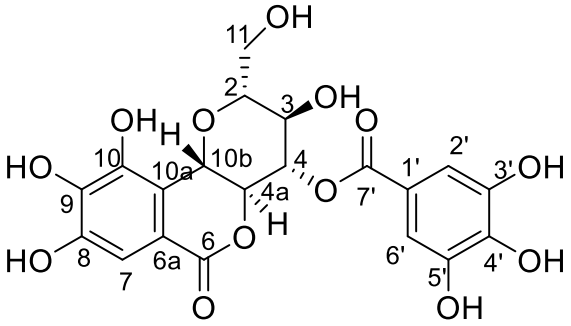

54

Table 12: ^{1}H (500MHz) and ^{13}C (125MHz) NMR assignments of compound DGET1 and 4-*O*-galloylnorbergenin in Methanol-*d*$_4$

Position	DGET1		4-*O*-galloylnorbergenin literature data[a]	
	δ_H, mult (*J* in Hz)	δ_C, mult	δ_H, mult (*J* in Hz)	δ_C, mult
2	3.80, m	83.0, CH	3.83, m	81.9, CH
3	3.78, m	70.0, CH	3.81, m	69.0, CH
4	5.56, t (9.9)	76.2, CH	5.57, t (9.8)	75.1, CH
4a	4.38, t (10.1)	79.0, CH	4.39, t (10.5)	78.0, CH
6	-	166.0, C	-	164.8, C
6a	-	114.0, C	-	115.9, C
7	7.08, s	111.1, CH	7.10, s	110.0, CH
8	-	147.7, C	-	146.2, C
9	-	141.5, C	-	140.2, C
10	-	143.6, C	-	142.5, C
10a	-	117.0, C	-	113.0, C
10b	5.12, d (10.4)	74.4, CH	5.14, d (10.5)	73.3, CH
11	3.77, m	62.4, CH_2	3.80, m	61.3, CH_2
	4.05, dd (1.8, 11.9)		4.06, dd (1.6 ,12.0)	
1'	-	121.2, C	-	120.1, C
2'/6'	7.14, s	110.4, CH	7.14, s	109.3, CH
3'/5'	-	146.4, C	-	145.3, CH
4'	-	139.9, C	-	138.8, C
7'	-	167.7, C	-	166.6, C

[a] (Tangmouo et *al*., 2009)

II.1.3.2. Naphthalene derivative: Elucidation of DFR7B

Compound DFR7B was obtained as a brown oil in the solvent system PE/EtOAc (1:1). It gave a purple coloration with ferric chloride reagent on TLC indicative of phenolic hydroxyl groups. Its molecular formula, $C_{11}H_{12}O_3$ was assigned from its HR-ESIMS (**figure 57**) which exhibited in positive mode, the proton adduct ion peak $[M+H]^+$ at *m/z* 193.0860 (calcd for $C_{11}H_{12}O_3H$: *m/z* 193.0859).

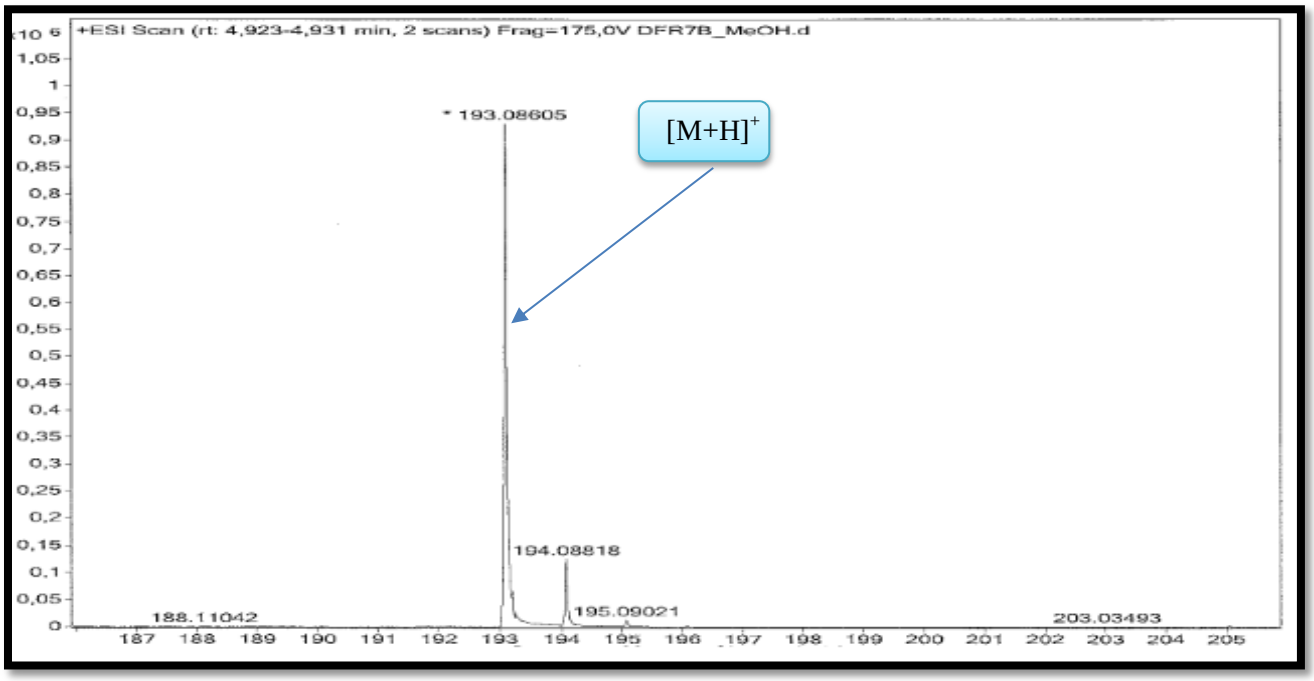

Figure 57: HR-ESI mass spectrum of compound DFR7B

In its UV spectrum, two maxima absorptions were observed at λ_{max} 231 and 279 nm, while its IR spectrum showed vibration bands characteristic of hydroxyl group (-OH) at 3270 cm^{-1}, conjugated carbonyl of ketone (C=O) at 1646 cm^{-1} and aromatic double bond C=C at 1577, 1465 cm^{-1}.

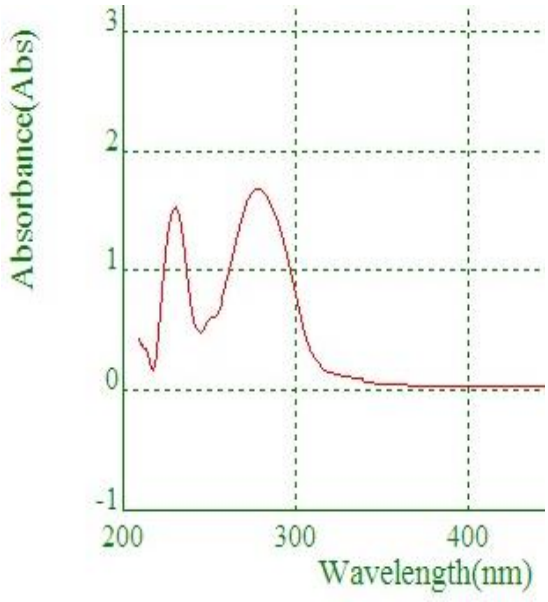

Figure 58: UV spectrum of compound DFR7B

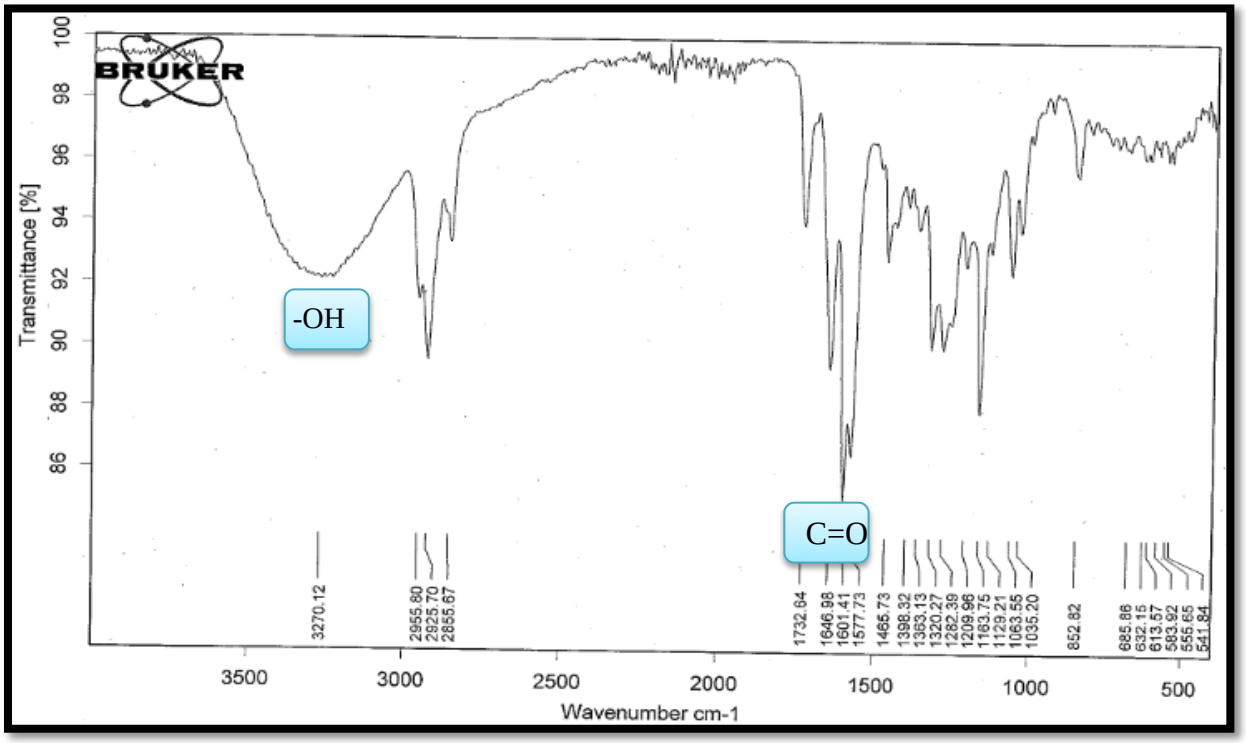

Figure 59: IR spectrum of compound DFR7B

On its ^{1}H and HMQC NMR spectrum (**Figures 62** and **66** respectively), signals of four diastereotopic protons corresponding to two methylene groups as well as a signal of one hydroxymethine proton were observed at δ_H 2.58 (dd, J = 16.5; 8.5 Hz) / δ_C 49.8; δ_H 2.83 (ddd, J = 16.5; 4.0; 1.4 Hz) / δ_C 49.8; δ_H 2.90 (dd, J = 15.9; 7.9 Hz) / δ_C 40.5; δ_H 3.15 (dd, J =

15.9; 4.0 Hz) / δ_C 40.5; and δ_H 4.22 (m) / δ_C 67.0. The ^{1}H-^{1}H COSY correlations (**figure 60**) observed between these protons permitted to build the first part of the molecule.

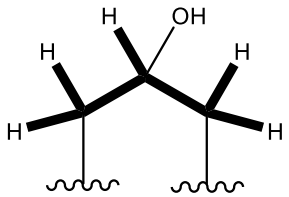

Figure 60: COSY correlations of compound DFR7B

In addition to the signals observed, These spectra also exhibited signals of two aromatic protons at δ_H 6.54 (d, J = 2.5 Hz) / δ_C 118.8 and δ_H 6.56 (d, J = 2.5 Hz) / δ_C 114.8 and a signal of one deshielded methyl at δ_H 2.54 (s) / δ_C 23.8 corresponding to a benzene substituted ring and the value of the coupling constant (2.5 Hz) among the two aromatic methines indicated that they were at position meta of each other. This position was confirmed by the HMBC correlations (**Figure 61**) observed between the proton at δ_H 6.54 and the carbon at δ_C 114.8 and between the proton at δ_H 6.56 and the carbon at δ_C 118.8. The presence of the benzene ring was further confirmed by the ^{13}C NMR spectrum of this compound which displayed eleven signals corresponding to the eleven carbon atoms presents in the molecule among which downfield signals of a carbonyl of ketone at δ_C 199.5, sp^2 carbons bearing oxygen atom at δ_C 163.0, aromatic quaternary carbons at δ_C 145.6, 146.9 and 124.3 and aromatic methines at δ_C 118.8 and 114.8. The HMBC correlations observed between the aromatic protons at δ_H 6.54 and 6.56 and the aromatic oxygenated carbon at δ_C 163.0 and between the methyl protons at δ_H 2.54 and the aromatic quaternary carbons at δ_C 145.6 and 124.3 permitted to build the second part of the molecule.

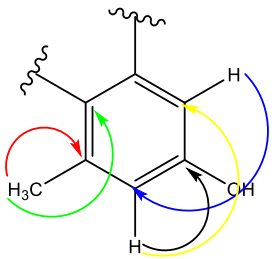

Figure 61: HMBC correlations of compound DFR7B

It remained to establish the link between the two parts of the molecule and the carbonyl of ketone. This was made possible by the HMBC correlations observed on one hand between the methylene protons at δ_H 2.58 and δ_H 2.83 and the carbonyl of ketone at δ_C 199.5

and on the other hand between the methylene protons at δ_H 2.90 and 3.15 and the aromatic quaternary carbons at δ_C 124.3 and 146.9, indicating that it was a naphtalenone squeletton.

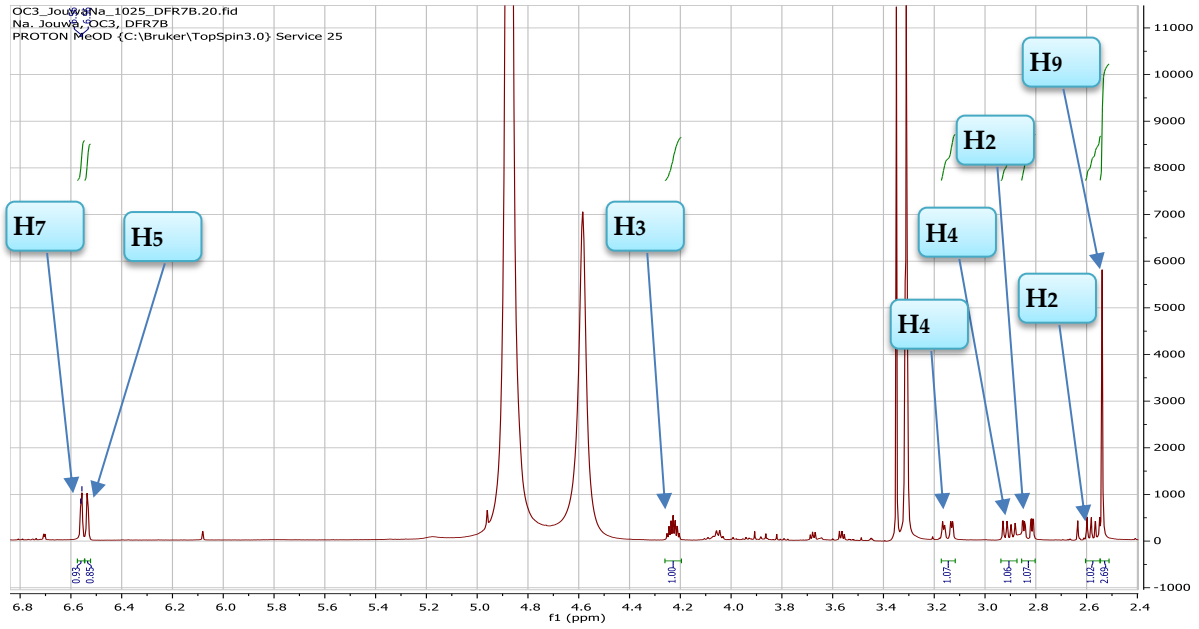

Figure 62: ^{1}H NMR spectrum (600 MHz) of compound DFR7B in Methanol-d_4

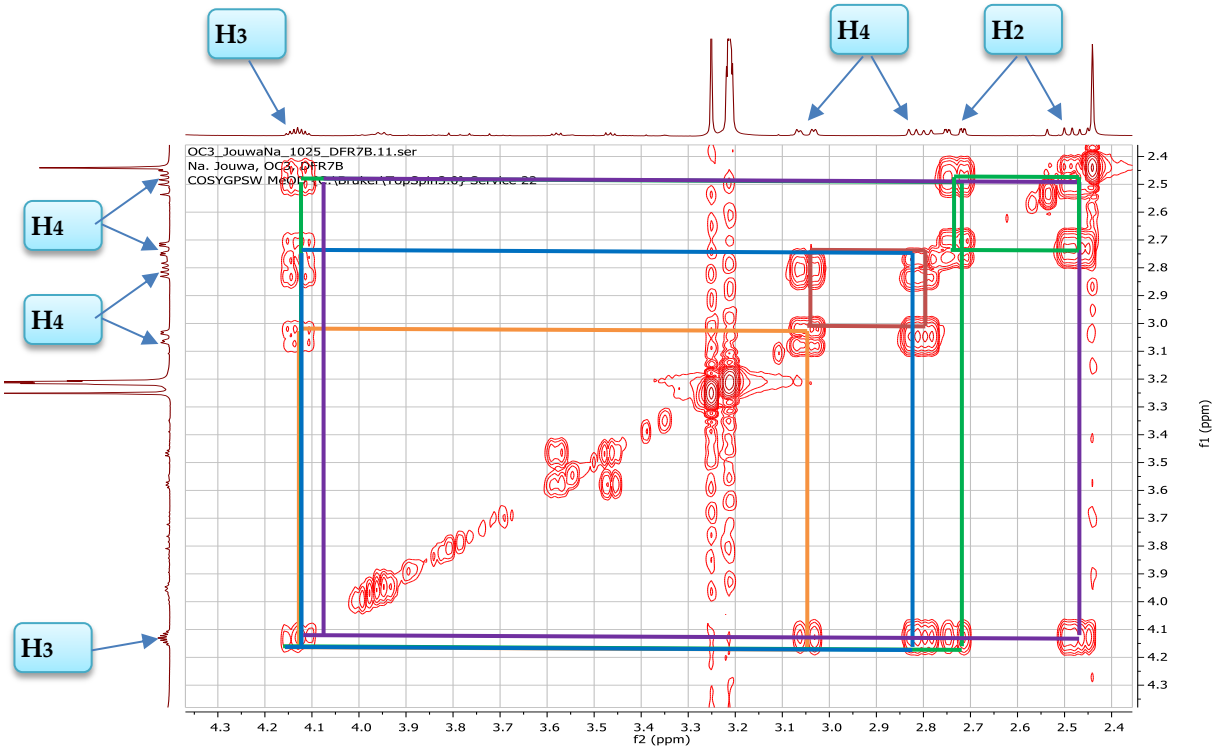

Figure 63: COSY spectrum of compound DFR7B.

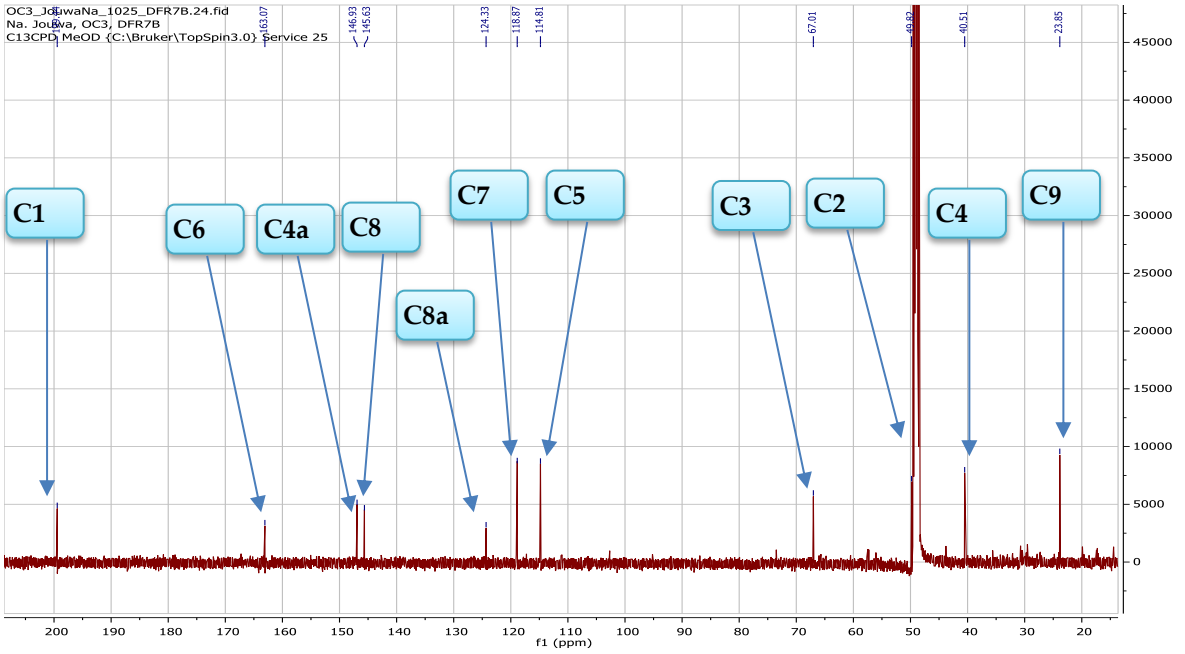

Figure 64: ^{13}C NMR spectrum (150 MHz) of compound DFR7B in Methanol-d_4

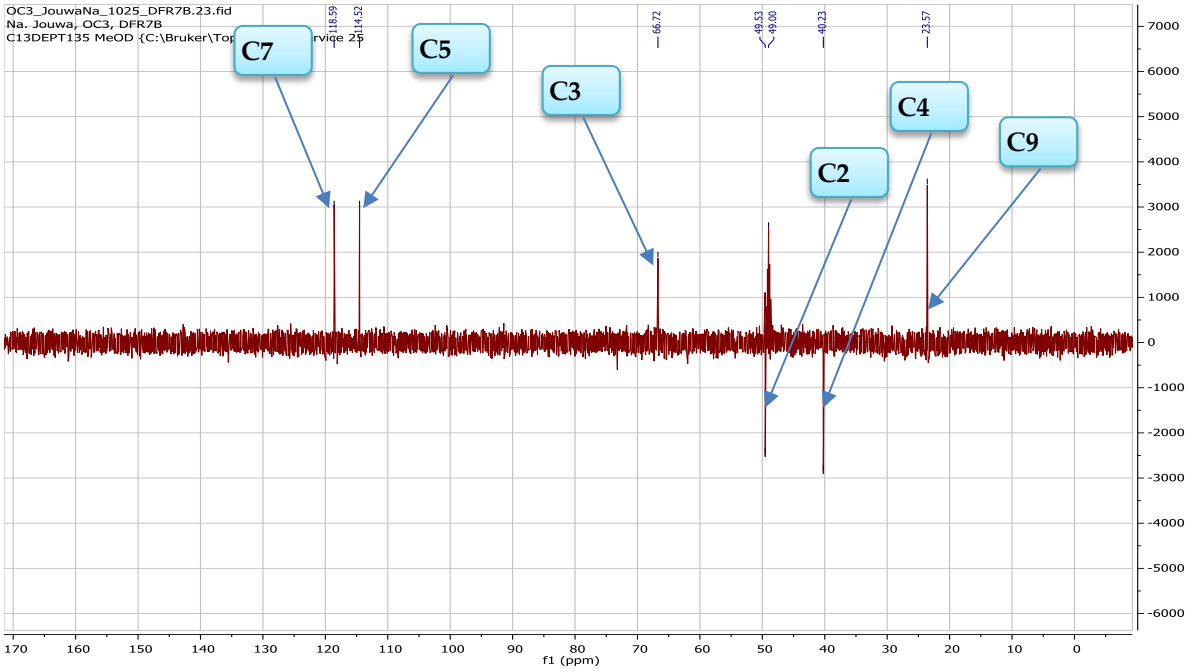

Figure 65: DEPT 135 NMR spectrum (150 MHz) of compound DFR7B in Methanol-d_4

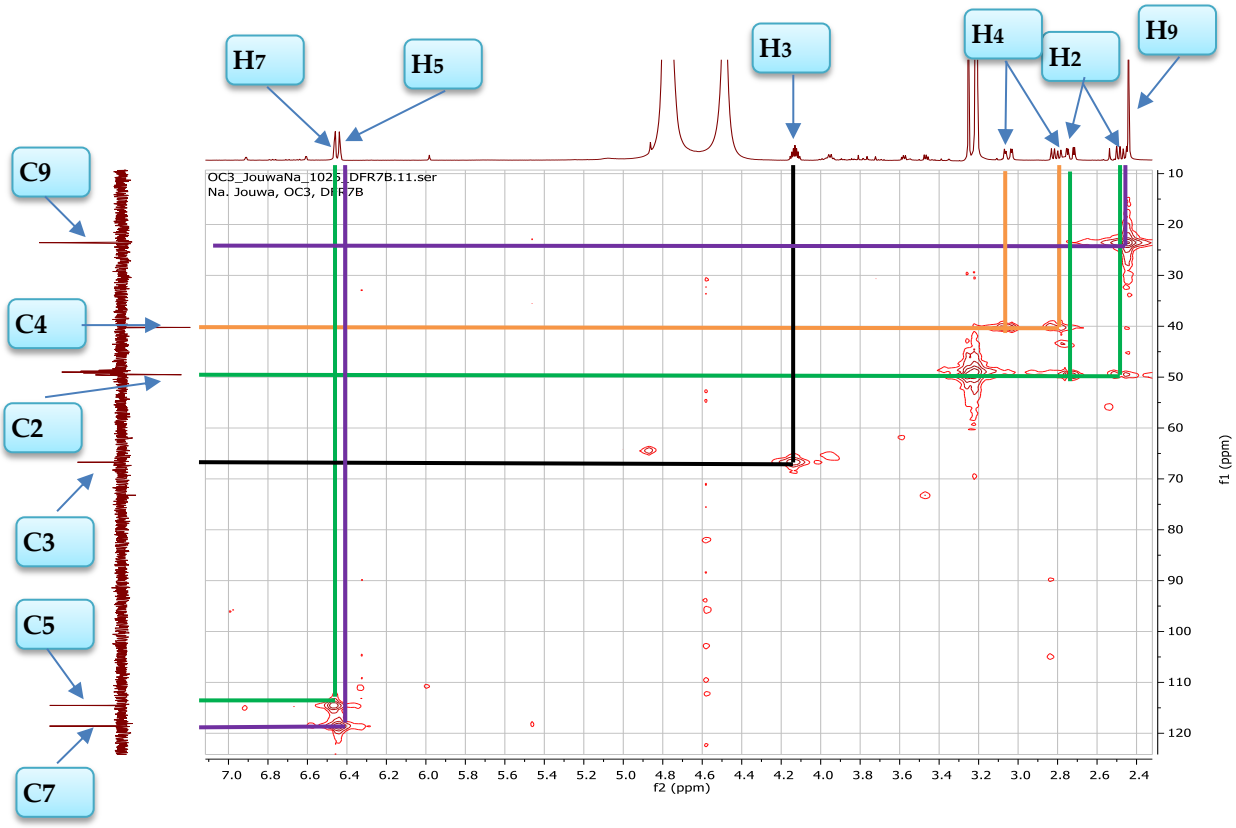

Figure 66: HMQC spectrum of compound DFR7B

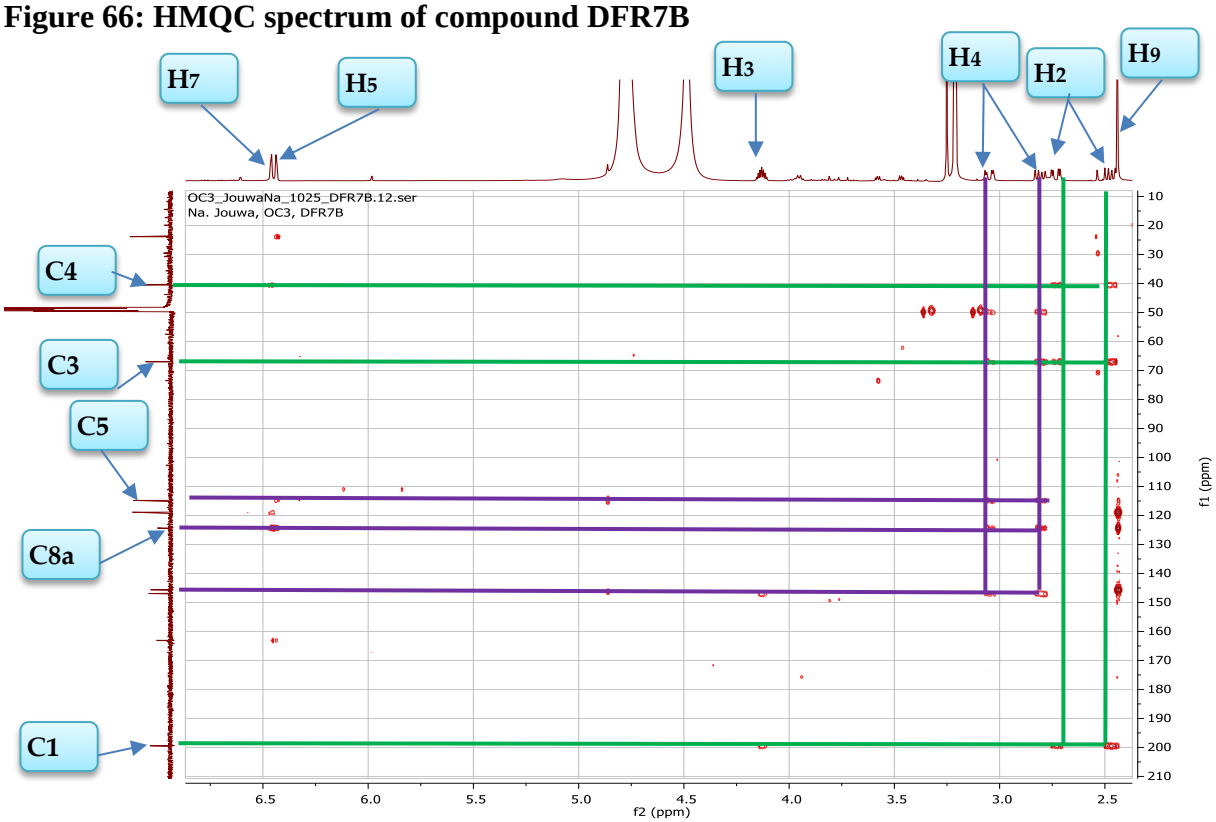

Figure 67: HMBC spectrum of compound DFR7B.

On the basis of the above evidence, compound DFR7B was elucidated as the new derivative 3,6-dihydroxy-8-methyl-3,4-dihydronaphthalen-1(2H)-one, also named fragranone and to which the following structure was assigned:

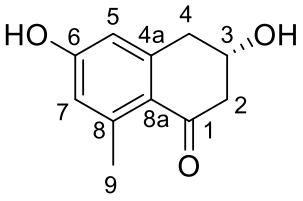

61

The stereochemistry of this compound was established from the observed axial-axial coupling constant of both methylene protons H-2 and H-4 with the hydroxymethine proton H-3.

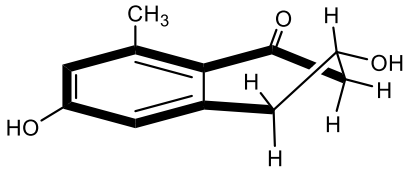

Table 13: ^{1}H (600MHz) and ^{13}C (150MHz) NMR assignments of compound DFR7B (fragranone) in Methanol-*d*$_4$

Position	DFR7B	
	δ_H, mult (*J* in Hz)	δ_C, mult
1	-	199.5, C
2	2.58, dd (16.5, 8.5)	49.8, CH_2
	2.83, ddd (16.5, 4.0, 1.4)	
3	4.22, m	67.0, CH
4	2.90, dd (15.9, 7.9)	40.5, CH_2
	3.15, dd (15.9, 4.0)	
4a	-	146.9, C
5	6.56, d (2.5)	114.8, CH
6	-	163.0, C
7	6.54, d (2.5)	118.8, CH
8	-	145.6, C
8a	-	124.3, C
9	2.54, s	23.8, CH_3

II.1.3.3. Pentacyclic triterpenes

II.1.3.3.1. Ursans

II.1.3.3.1.1. Elucidation of DGF5

Compound DGF5 was isolated as white amorphous powder in the solvent system PE/EtOAc (3:1). It gave a brick red colour with the Liebermann Burchard reagent characteristic of pentacyclic triterpene. Its ESIMS (**figure 68**) showed in positive mode a pseudo molecular ion peak $[M+Na]^+$ at *m/z* 479.4 in agreement with the molecular formula $C_{30}H_{48}O_3$ corresponding to seven double bond equivalent.

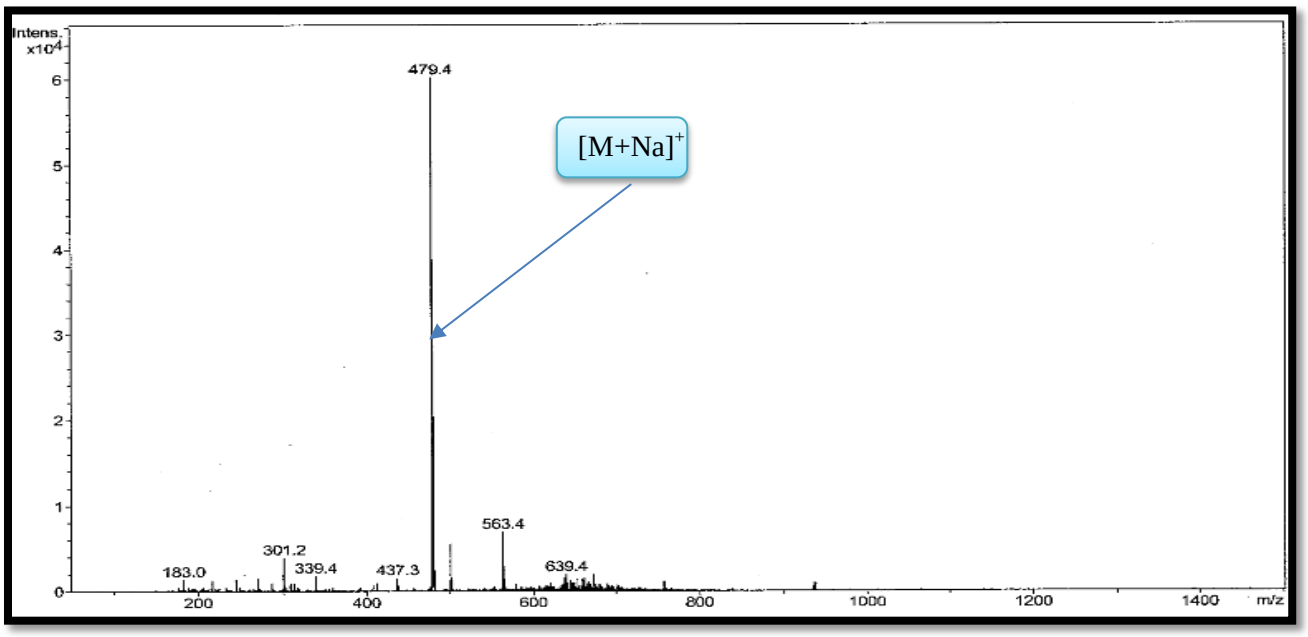

Figure 68: ESI mass spectrum of compound DGF5

Its ^1H and ^{13}C NMR spectrum (**Figures 69** and **70**) showed signals of two *sec*-methyls at δ_H 0.89 (d, J = 7.0 Hz) / δ_C 17.7 and δ_H 0.97 (d, J = 7.0 Hz) / δ_C 21.6, five signals of *ter*-methyls at δ_H 0.78/ δ_C 16.4, δ_H 0.85/ δ_C 17.8, δ_H 0.96/ δ_C 16.0, δ_H 0.98/ δ_C 28.7 and δ_H 1.12/ δ_C 24.1, one signal of an olefinic proton at δ_H 5.23 (t, J = 3.7 Hz) / δ_C 126.8, one signal of an allylic proton at δ_H 2.20 (d, J = 11.4Hz)/ δ_C 54.4, and one signal of an oxymethine at δ_H 3.15 (dd, J = 10.4, 5.5 Hz) / δ_C 79.7. These signals in addition to those observed in the ^{13}C NMR spectrum of this compound at δ_C 126.8 and 139.5 are characteristic of a pentacyclic triterpene belonging to the urs-12-ene series. A signal of one carboxylic group at δ_C 181.4 was also observed.

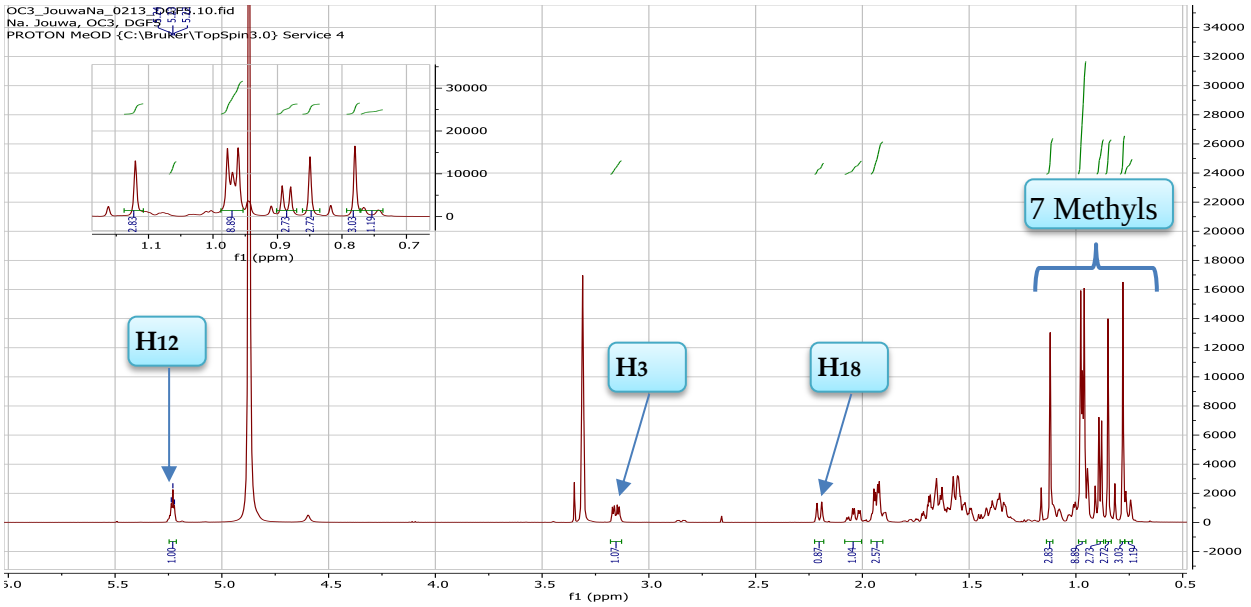

Figure 69: ^{1}H NMR spectrum (500 MHz) of compound DGF5 in Methanol-d_4 + $CDCl_3$

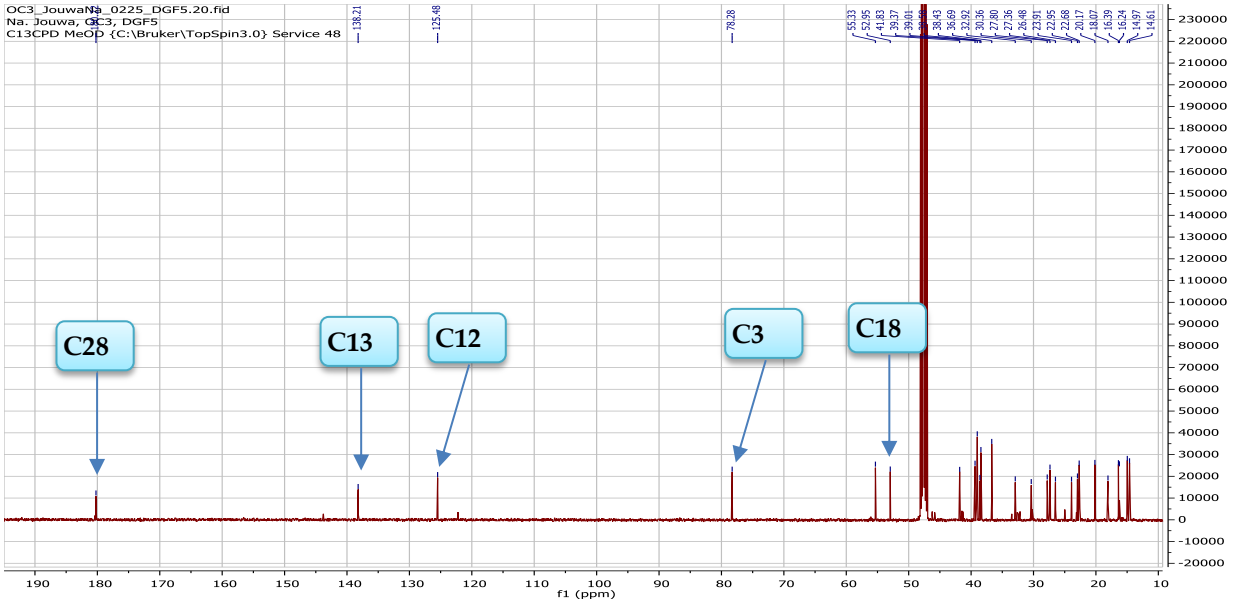

Figure 70: ^{13}C NMR spectrum (125MHz) of compound DGF5 in Methanol-d_4 + $CDCl_3$

Therefore, compound DGF5 was identified as ursolic acid, a known compound previously isolated from *Scyphiphora hydrophyllacea* by Sameera et *al* in 2018.

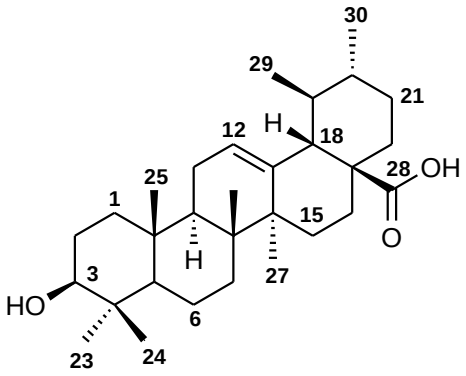

22

Table 14: ^{1}H (500MHz) and ^{13}C (125MHz) NMR assignments of compound DGF5 in Methanol-d_4 + $CDCl_3$ and ursolic acid in $CDCl_3$

	DGF5		Ursolic acid literature data[a]	
Position	δ_H mult (*J* in Hz)	δ_C, mult.	δ_H mult (J in Hz)	δ_C
1		38.5 CH_2		38.6
2		27.4 CH_2		28.2
3	3.15 dd (5.5, 10.4)	79.7 CH	3.22 dd (4.9, 10.8)	78.7
4	-	38.9 C		38.5
5	1.27 m	55.3 CH	1.34 m	55.2
6		18.7 CH_2		18.3
7		32.8 CH_2		32.9
8		40.1 C		39.5
9		47.4 CH		47.3
10		37.2 C		37.0
11		23.6 CH_2		23.7
12	5.23 t (3.7)	126.8 CH	5.27 dd (3.5, 3.6)	125.9
13		139.5 C		137.9
14		42.1 C		42.0
15		26.1 CH_2		28.1
16		23.5 CH_2		25.0
17		46.7 C		48.1
18	2.20 d (11.4)	54.4 CH	2.20 m	53.8
19		39.4 CH		38.5
20		39.3 CH		38.5
21		30.7 CH_2		30.3
22		36.7 CH_2		37.4
23	0.98 s	28.7 CH_3	1.02 s	28.9
24	0.78 s	16.4 CH_3	0.84 s	15.6
25	0.96 s	16.0 CH_3	0.74 s	15.4

26	0.85 s	17.8 CH_3	0.95 s		17.1
27	1.12 s	24.1 CH_3	0.97 s		23.5
28		181.4 C			179.6
29	0.89 d (7.0)	17.7 CH_3		0.77 d (6.3)	17.0
30	0.97 d (7.0)	21.6 CH_3	0.81d (6.4)		21.4

[a] (Sameera et *al*., 2018)

II.1.3.3.1.2. Elucidation of DGF7

Compound DGF7 was isolated as white amorphous powder in the solvent system PE-EtOAc (7:3). It responded positively to the Liebermann-Burchard test with a red coloration characteristic of triterpenes. The ESIMS of this compound (**figure 71**) showed in positive mode a pseudo molecular ion peak $[M+Na]^+$ at *m/z* 495.3 compatible with the molecular formula $C_{30}H_{48}O_4$ and implying thirteen degrees of unsaturation.

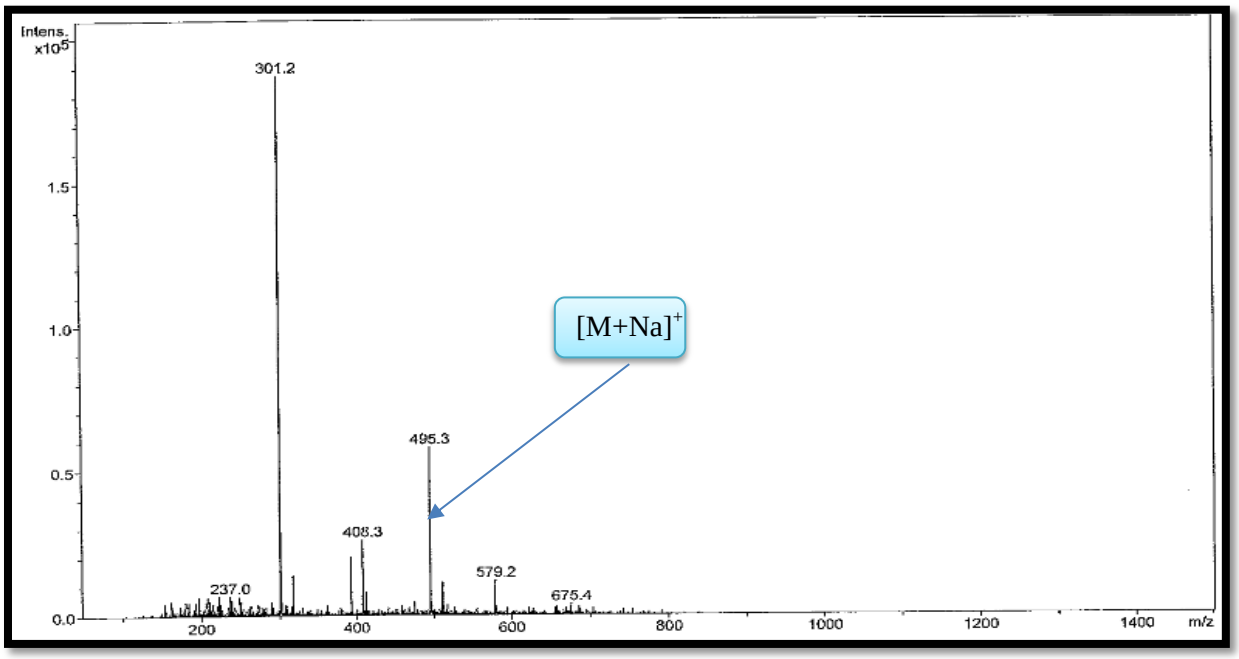

Figure 71: ESI mass spectrum of compound DGF7

The ^1H and ^{13}C NMR spectra of this compound (**Figures 72** and **74**) were close similar to those of ursolic acid **22** and displayed characteristic signals of a pentacyclic triterpene type urs-12-ene at δ_H 0.84 (d, J = 7.0 Hz) / δ_C 17.5, δ_H 0.93 (d, J = 7.0 Hz) / δ_C 21.5, δ_H 0.78/ δ_C 17.5, δ_H 0.81/ δ_C 17.6, δ_H 0.98/ δ_C 17.2, δ_H 0.99/ δ_C 29.2 and δ_H 1.08/ δ_C 24.1 corresponding respectively to two secondary and five angular methyls. Signals of the oxymethine H-3, the allylic H-18 and the olefinic H-12 protons were also observed at δ_H 2.91 (d, J = 9.7 Hz) / δ_C 84.2, δ_H 2.18 (d, J = 12.0 Hz)/ δ_C 53.9 and δ_H 5.22 (t, J = 3.7 Hz) / δ_C 126.2 respectively. As

in ursolic acid **22**, a signal of one carboxylic acid was also observed at δ_C 181.4. The main difference between these two compounds was the appearance of another oxymethine as multiplet at δ_H 3.62 / δ_C 69.3 and the correlation observed in COSY spectrum (**Figure 73**) between this proton and proton H-3 allowed us to fix this oxymethine at position 2. Furthermore the coupling constant of 9.7 Hz observed between proton H-2 and H-3 showed that these protons were trans of each other.

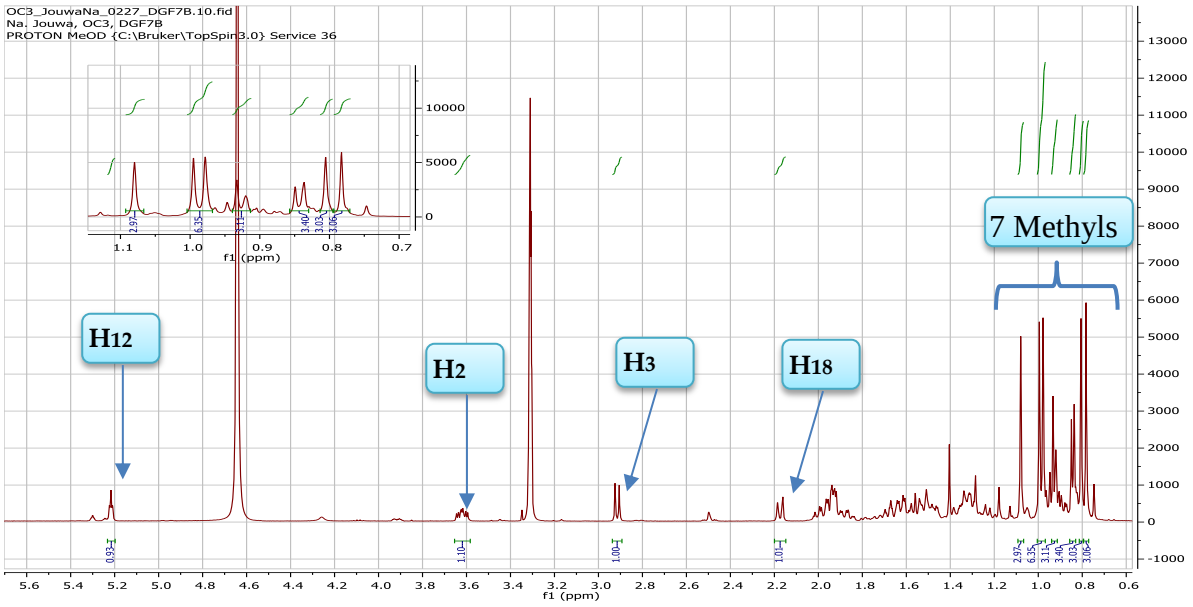

Figure 72: ^{1}H NMR spectrum (500 MHz) of compound DGF7 in Methanol-d_4 + $CDCl_3$

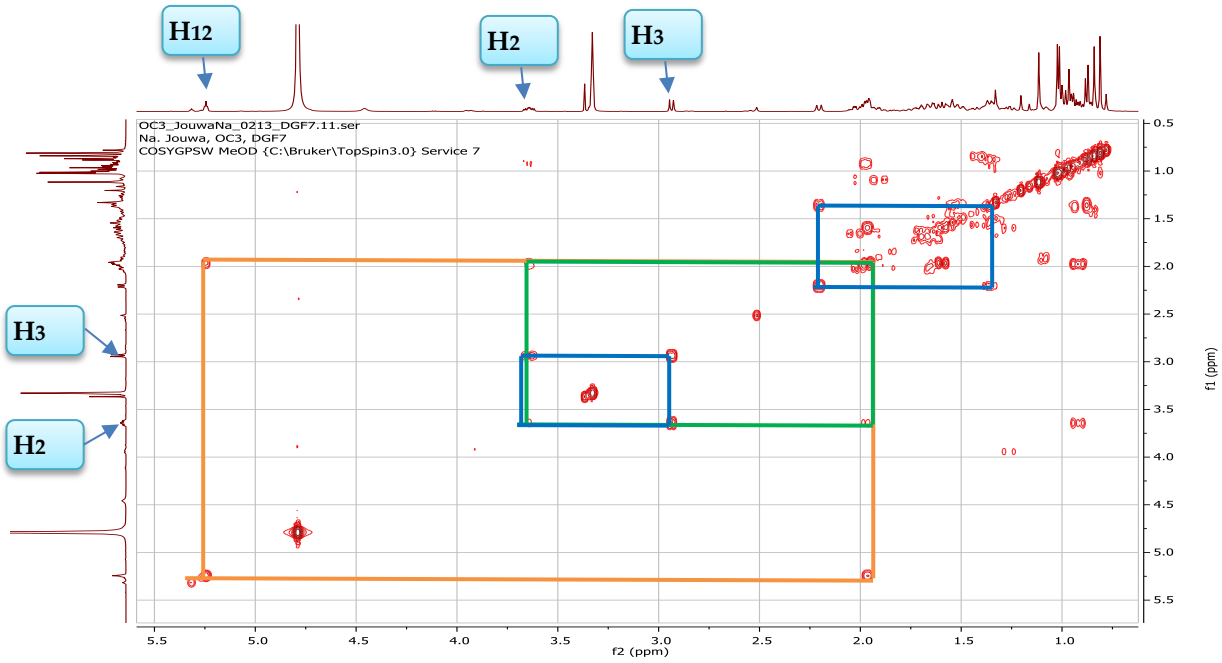

Figure 73: COSY spectrum of compound DGF7

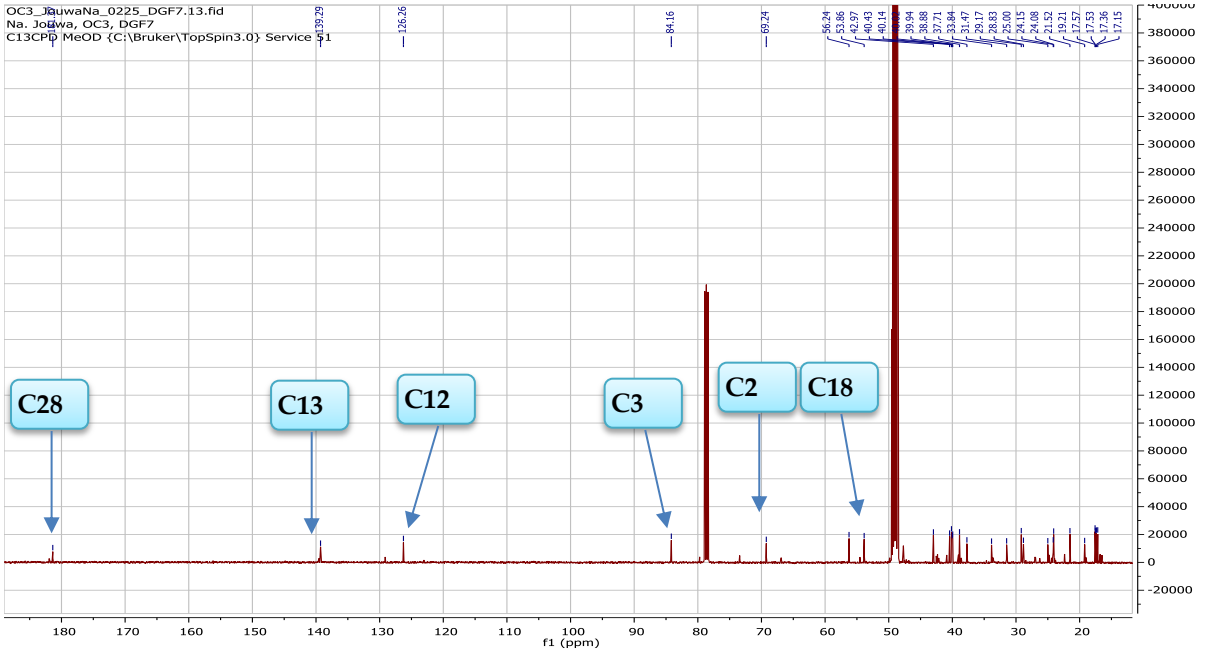

Figure 74: ^{13}C NMR spectrum (125MHz) of compound DGF7 in Methanol-d_4 + $CDCl_3$

The above spectroscopic data coupled to reported literature identified compound DGF7 as corosolic acid, previously isolated from *Eriobotrta japonica* by Wei et Guangyuan in 2007.

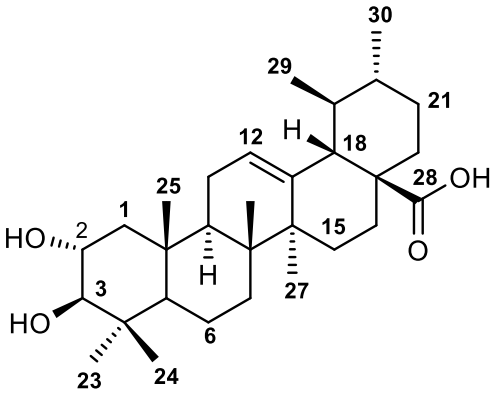

62

Table 15: ^{1}H (500MHz) and ^{13}C (125MHz) NMR assignments of compound DGF7 in Methanol-d_4 + $CDCl_3$ and corosolic acid in C_5D_5N

Position	DGF7		Corosolic acid literature data[a]	
	δ_H mult (*J* in Hz)	δ_C, mult.	δ_H mult (*J* in Hz)	δ_C
1		43.0 CH_2		48.1
2	3.62 m	69.3 CH	4.08 td (4.5, 11.0)	68.7
3	2.91 d (9.7)	84.2 CH	3.38 d (9.5)	83.9
4		38.7 C		40.1
5		55.3 CH		55.8
6		19.1 CH_2		18.9
7		32.6 CH_2		33.7
8		40.1 C		40.2
9		47.6 CH		47.8
10		37.7 C		37.3
11		23.8 CH_2		24.1
12	5.22 t (3.7)	126.2 CH	5.46 t-like (3.5)	128.2
13		139.5 C		140.1
14		40.4 C		42.4
15		29.1 CH_2		29.5
16		25.0 CH_2		26.3
17		48.0 C		48.3
18	2.18 d (12.0)	53.9 CH	2.61 d (11.0)	54.4
19		39.9 CH		41.3
20		40.0 CH		42.2
21		30.6 CH_2		27.1
22		38.8 CH_2		38.5
23	0.98 s	28.8 CH_3	1.25 s	29.6
24	0.78 s	21.4 CH_3	1.20 s	22.2
25	0.96 s	17.5 CH_3	1.06 s	16.8
26	0.85 s	17.3 CH_3	0.94 s	17.5
27	1.12 s	24.1 CH_3	1.03 s	24.6
28		181.4 C		180.7
29	0.89 d (7.0)	17.5 CH_3	1.01 d (6.5)	27.3
30	0.97 d (7.0)	17.1 CH_3	0.97 d (6.5)	16.6

[a] (Wei et Guangyuan, 2007)

II.1.3.3.1.3. Elucidation of DFFFI8B

Compound DFFFI8B was obtained as a white powder in the solvent system PE/EtOAc (17:3). It gave a positive red coloration to the Liebermann-Burchard test indicative its

triterpenic nature. Its ESIMS shows in positive mode a pseudomolecular ion pic $[M+Na]^+$ at *m/z* 465.3 corresponding to the molecular formula $C_{30}H_{50}O_2$ with seven double bond equivalent.

The ^1H and ^{13}C NMR spectra of compound DFFFI8B (**Figure 75** and **76** respectively) and ursolic acid **22** showed close similarities including the olefinic proton at δ_H 5.15 (t, J = 3.7 Hz) / δ_C 126.3, the oxymethine proton H-3 of triterpene at δ_H 3.16 (dd, J = 11.7, 4.6 Hz) / δ_C 79.7, the seven methyls at δ_H 0.84 (d, J = 6.3 Hz) / δ_C 17.7, δ_H 0.94 (d, J = 6.4 Hz) / δ_C 21.5, δ_H 0.79/ δ_C 16.1, δ_H 1.04/ δ_C 17.1, δ_H 0.99/ δ_C 16.1, δ_H 0.99/ δ_C 28.4 and δ_H 1.13/ δ_C 23.7. These similarities indicated that compound DFFFI8B, as ursolic acid **22** was a pentacyclic triterpene of the urs-12-ene series. The main difference between those two compounds was the disappearance of the signal of carbonyl of carboxylic acid observed in the ^{13}C NMR spectra of ursolic acid **22** at δ_C 181.4 and the appearance in the ^1H and ^{13}C NMR spectra of compound DFFFI8B of two signals of diastereotopic protons of an oxymethylene at δ_H 3.03 (d, J = 11.0Hz) / δ_C 70.2 and δ_H 3.56 (d, J = 11.0Hz) / δ_C 70.2.

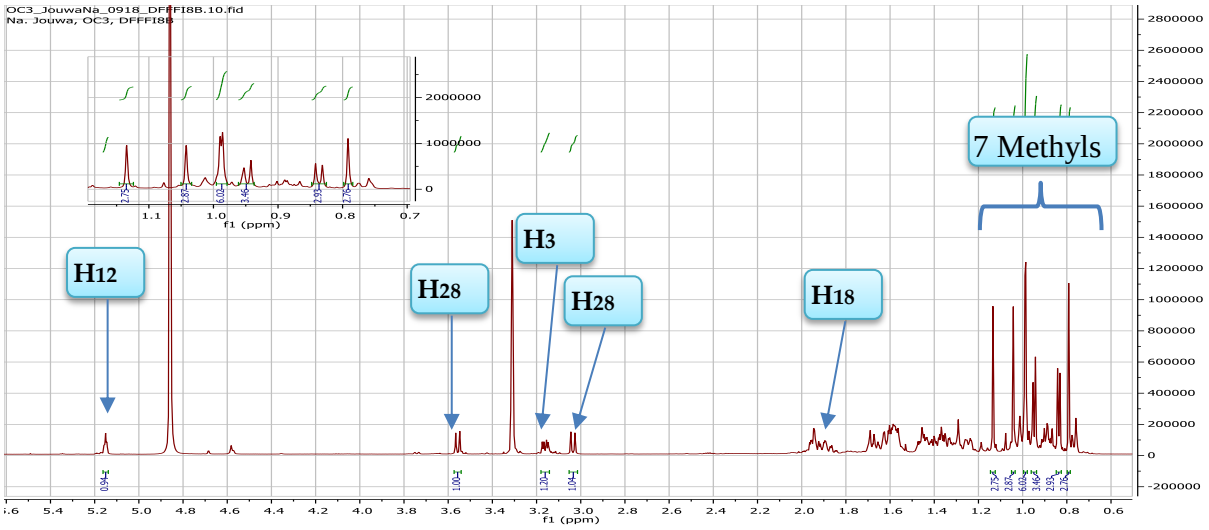

Figure 75: ^1H NMR spectrum (500 MHz) of compound DFFFI8B in Methanol-d_4

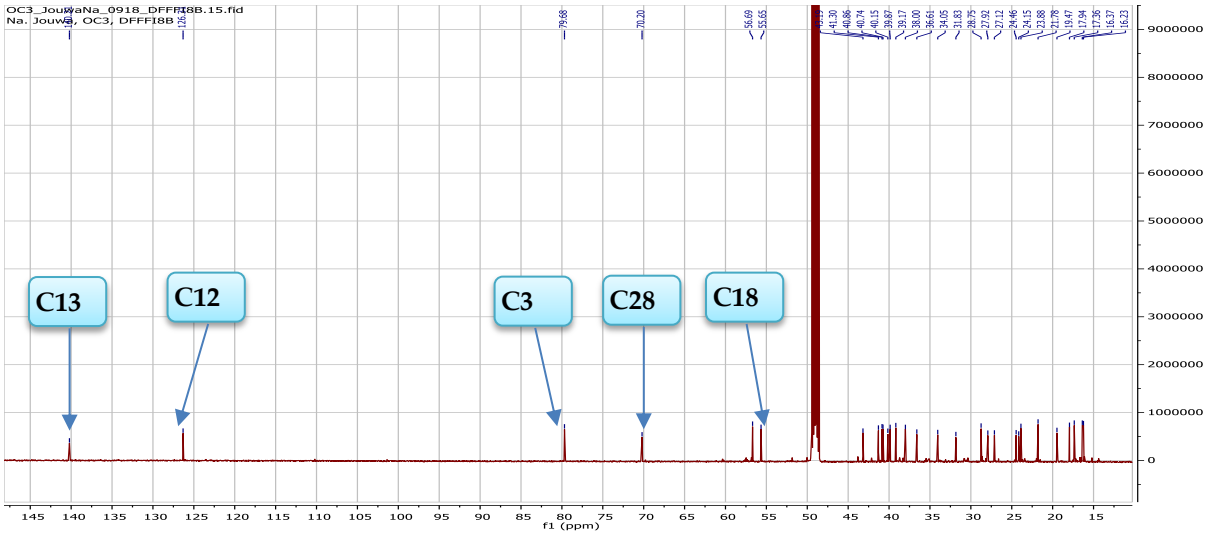

Figure 76: ^{13}C NMR spectrum (125MHz) of compound DFFFI8B in Methanol-d_4

These informations combined with the literature data allowed us to identify compound DFFFI8B as uvaol, a known compound previously isolated from *Ochrosia elliptica* by Riham et *al*. in 2017.

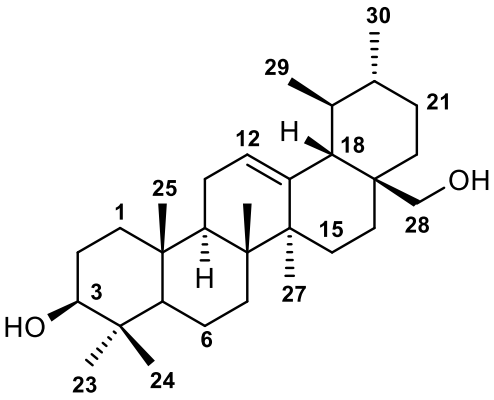

63

Table 16: ^{1}H (500MHz) and ^{13}C (125MHz) NMR spectral data of compound DFFFI8B in Methanol-d_4 and Uvaol in $CDCl_3$

Position	DFFFI8B		Uvaol literature data[a]	
	δ_H mult (*J* in Hz)	δ_C, mult.	δ_H mult (*J* in Hz)	δ_C
1		39.5 CH_2		39.3
2		27.4 CH_2		27.3
3	3.44 t (8.0)	79.7 CH	3.23 m	79.0
4	-	38.9 C		38.8
5	0.77 m	56.4 CH		55.2
6		18.7 CH_2		18.3
7		32.8 CH_2		32.8
8		40.1 C		40.0
9		47.7 CH		47.6
10		37.2 C		36.9
11		23.6 CH_2		23.4
12	5.15 t (3.7)	126.3 CH	5.16 t (3.6)	125.0
13		140.2 C		138.7
14		42.2 C		42.0
15		26.1 CH_2		26.0
16		23.5 CH_2		23.4
17		36.9 C		36.9
18	1.37 m	55.6 CH		54.0
19		39.4 CH		39.4
20		39.3 CH		39.4
21		30.7 CH_2		30.6
22		36.7 CH_2		36.4
23	0.99 s	28.4 CH_3	1.02 s	28.1
24	0.99 s	16.1 CH_3	0.84 s	15.7
25	0.79 s	16.1 CH_3	0.74 s	15.6
26	1.04 s	17.1 CH_3	0.95 s	16.8
27	1.13 s	23.7 CH_3	0.97 s	23.3
28	3.56 d (11.0); 3.03 d (11.0)	70.2 CH_2	3.54 d (11.2); 3.20 d (11.2)	70.0
29	0.84 d (6.3)	17.7 CH_3	0.77 d (3.4)	17.3
30	0.94 d (6.4)	21.5 CH_3	0.81d (3.3)	21.3

[a] (Riham et *al*., 2017)

II.1.3.3.1.4. Elucidation of DFFFI8

Compound DFFFI8 was isolated as a white powder in the solvent system PE/EtOAc (17:3). Its positive reaction to the Liebermann-Burchard test with a red colour observed is indicative of its triterpenic nature. The ESIMS (**Figure 77**) of this compound showed in positive mode a pseudo molecular ion peak $[M+Na]^+$ at *m/z* 479.3 compatible with the molecular formula $C_{30}H_{48}O_3$ and implying seven degrees of unsaturation.

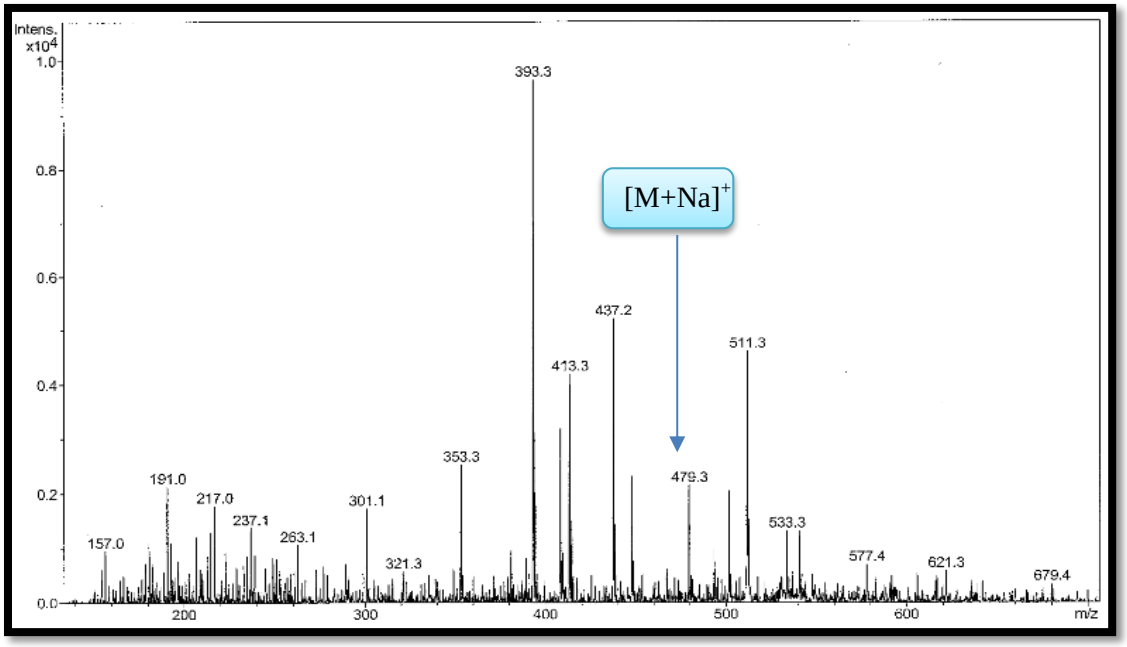

Figure 77: ESI mass spectrum of compound DFFFI8

The ^{1}H NMR spectrum (**figure 78**) of compound DFFFI8, combined with its ^{13}C NMR spectrum (**Figure 79**) showed, in upfield region, seven methyls among which five angulars at δ_H 0.83/ δ_C 15.2, δ_H 0.93/ δ_C 27.8, δ_H 0.75/ δ_C 13.4, δ_H 1.10/ δ_C 23.6, δ_H 0.92/ δ_C 23.6 and two secondary at δ_H 0.80 (d, J = 6.5 Hz) / δ_C 21.9 and δ_H 0.89 (d, J = 6.4 Hz) / δ_C 23.2. These spectrums also displayed signals of one olefinic methine proton at δ_H 5.46 (brs,) / δ_C 118.3, one oxymethine proton attributable to H-3 of triterpene at δ_H 3.17 / δ_C 79.5, one allylic proton attributable to H-18 at δ_H 2.51 (brs) / δ_C 52.5 and one olefinic tertiary carbon at δ_C 145.2 characteristics of pentacyclic triterpenes of the *D:C*-friedours-7-ene series. In addition to these signals observed, the ^{13}C NMR spectrum of compound DFFFI8 also displayed a signal of a carbonyl of carboxylic acid at δ_C 183.3.

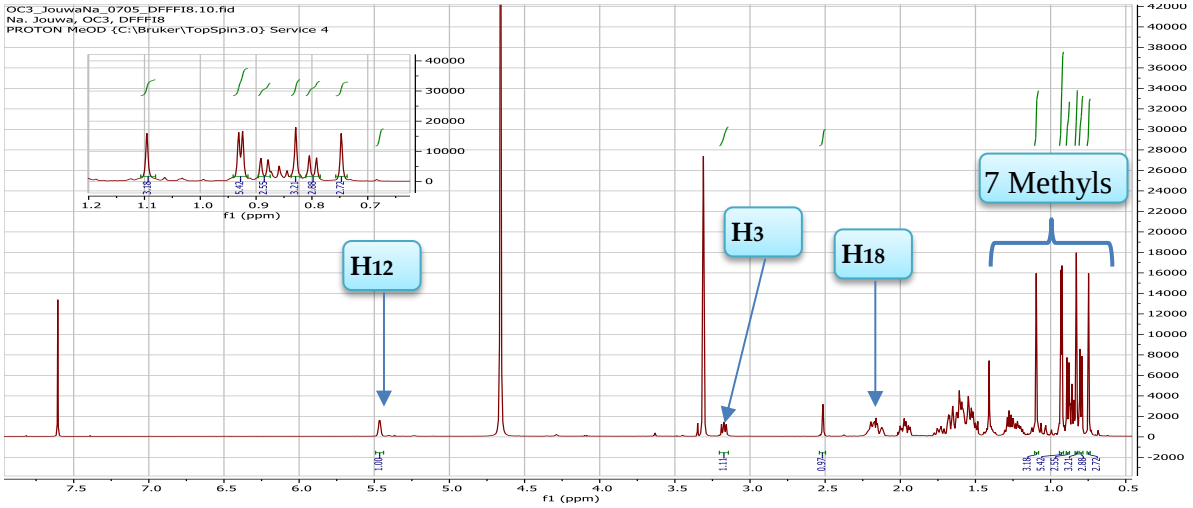

Figure 78: ^{1}H NMR spectrum (500 MHz) of compound DFFFI8 in Methanol-d_4 + $CDCl_3$

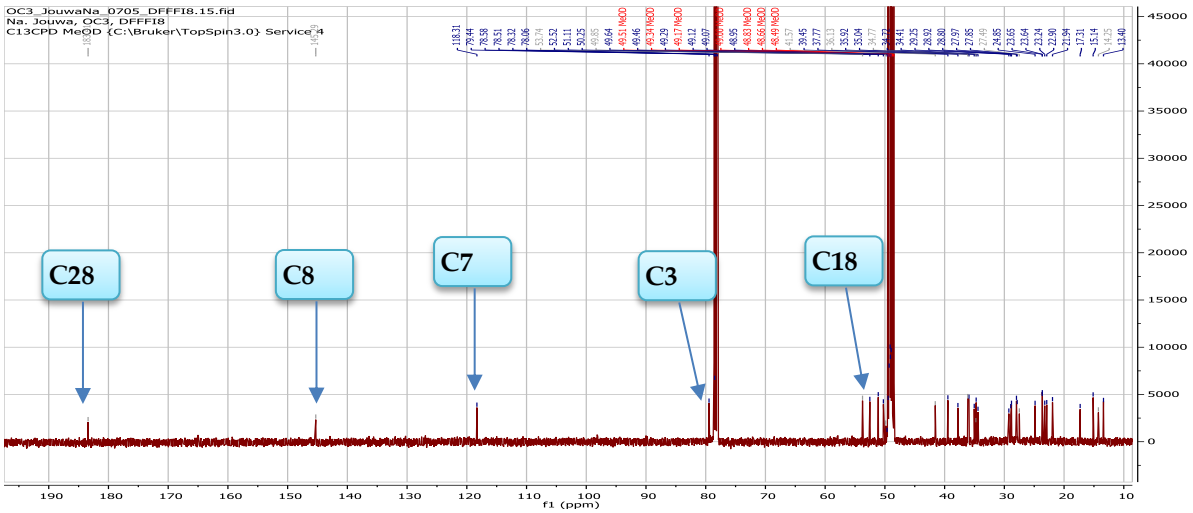

Figure 79: ^{13}C NMR spectrum (125 MHz) of compound DFFFI8 in Methanol-d_4 + $CDCl_3$

On the basis of the above spectroscopic data, compound DFFFI8 was identified as myrtifolic acid, a known compound first isolated from *Mesua myrtifolia* (Gunasekera et Sultanbawa, 1977).

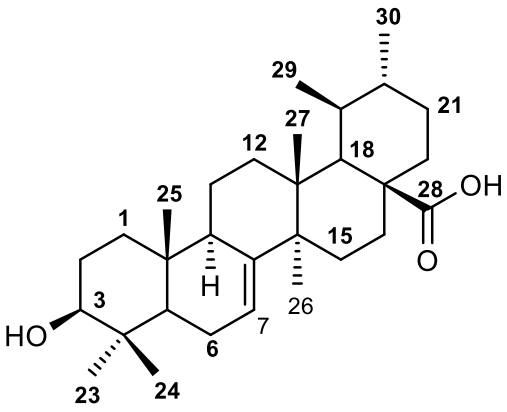

Table 17: ^{1}H (500MHz) and ^{13}C (125MHz) NMR spectral data of compound DFFFI8 in Methanol-d_4 + $CDCl_3$ and Myrtifolic acid in $CDCl_3$

Position	DFFFI8		Myrtifolic acid literature data[a]	
	δ_H mult (*J* in Hz)	δ_C, mult.	δ_H mult (*J* in Hz)	δ_C
1		38.5 CH_2		38.9
2		27.4 CH_2		28.2
3	3.17 m	79.5 CH	3.24 dd (3.9, 9.3)	78.7
4	-	38.9 C		38.5
5	1.27 m	55.3 CH	1.34 m	55.2
6		18.7 CH_2		18.3
7	5.46 brs	118.3 CH	5.42 m	118.6
8		145.2 C		145.4
9		47.4 CH		47.3
10		37.2 C		37.0
11		23.6 CH_2		23.7
12		32.8 CH_2		33.5
13		40.1 C		41.2
14		42.1 C		42.0
15		26.1 CH_2		28.1
16		23.5 CH_2		25.0
17		36.9 C		38.1
18	2.51 brs	52.5 CH	2.49 m	53.8
19		39.4 CH		38.5
20		39.3 CH		38.5
21		30.7 CH_2		30.3
22		36.7 CH_2		37.4
23	0.93 s	27.8 CH_3	1.04 s	28.9
24	0.75 s	13.4 CH_3	0.76 s	14.6
25	0.83 s	15.2 CH_3	0.98 s	15.4
26	1.10 s	23.6 CH_3	0.87 s	22.1
27	0.92 s	23.6 CH_3	1.08 s	23.5
28		183.3 C		182.5
29	0.89 d (6.4)	23.2 CH_3	0.87 brs	22.8
30	0.80 d (6.5)	21.9 CH_3	1.08 brs	21.4

[a] (Mahato et Kundu, 1994; Meksuriyen et *al*., 1986)

II.1.3.3.1.5. Elucidation of DGTFIII2

Compound DGTFIII2 was isolated as a white amorpheous powder in the solvent system PE/EtOAc (7:3). Its positive reaction to the Liebermann-Burchard test with a red

coloration observed was indicative of its triterpenic nature. The pseudo molecular ion peak $[M-H]^-$ *at m/z* 487.2 observed in negative mode on ESIMS spectrum (**Figure 80**) of this compound was in agreement with the molecular formula $C_{30}H_{48}O_5$ corresponding to seven double bond equivalent.

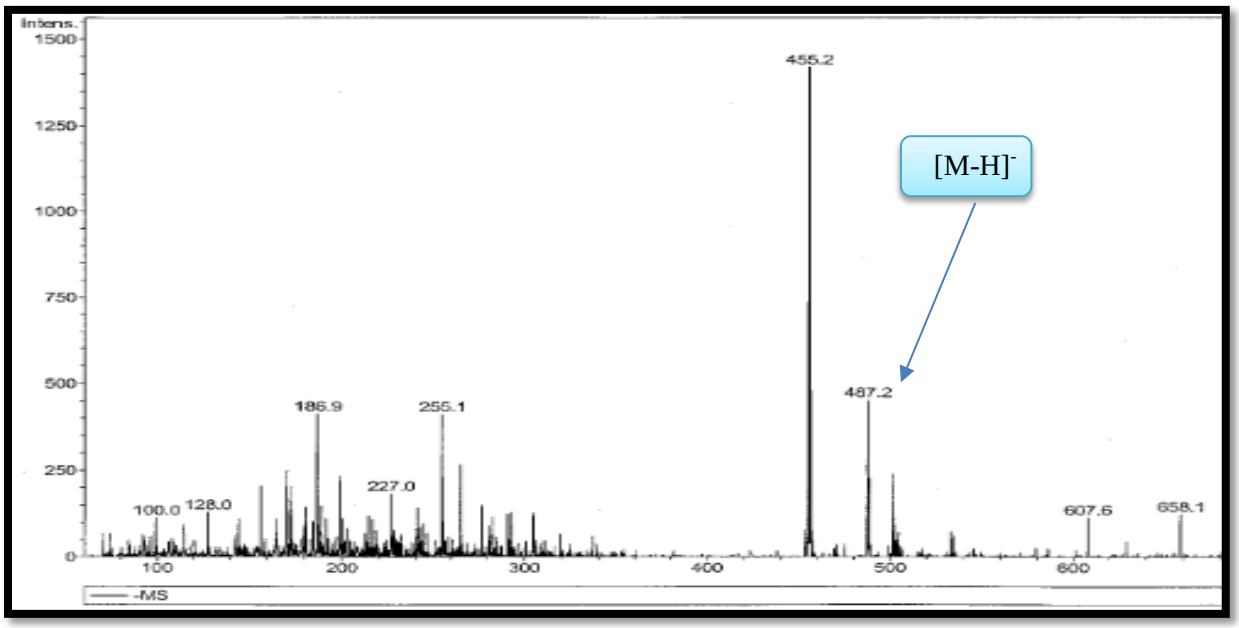

Figure 80: ESI mass spectrum of compound DGTFIII2

The ^1H and ^{13}C NMR spectral data of this compound (**Figures 81** and **82** respectively) displayed signals of six methyl groups among which five angular at δ_H 0.71 / δ_C 12.9, 0.98 / δ_C 16.0, δ_H 0.80 / δ_C 17.3, δ_H 1.34 / δ_C 24.8, δ_H 1.19 / δ_C 27.0 and one secondary at δ_H 0.92 (d, J = 6.7 Hz) / δ_C 16.3. These NMR spectra also showed one signal of an olefinic proton at δ_H 5.29 (t, J = 3.7 Hz) / δ_C 129.4, one signal of an oxymethine proton at δ_H 3.61 (dd, J = 11.7, 4.6 Hz) / δ_C 74.0, one signal of an allylic proton at δ_H 2.50 (s) / δ_C 55.0, and two signals of olefinic carbons at δ_C 129.4 and δ_C 140.0 characteristic of a pentacyclic triterpene belonging to the urs-12-ene series. In addition, signals of two diastereotopic protons of an oxymethylene at δ_H 3.30 (in the solvent) / δ_C 67.5 and δ_H 3.53 (d, J = 10.9Hz) / δ_C 67.5 together with a signal of one quaternary sp3 carbon bearing an oxygene atom at δ_C 73.6 and a signal of a carbonyl of carboxylic acid at δ_C 182.7 were also observed. It remained to establish the position of these groups on the urs-12-ene skeleton. The HMBC correlations (**Figure 83**) observed between the proton H-18 at δ_H 2.50 and the carbonyl carbon at δ_C 182.7 on one hand, and between this same proton and the quaternary carbon at δ_C 73.6 on the other hand allowed us to locate these groups at position C-28 for the carboxylic acid and position C-19 for the tertiary oxygenated carbon. The HMBC correlation observed between the proton H-3 at δ_H 3.61 and the

oxymethylene carbon at δ_C 67.5 on one hand, and between protons H-24 and that same oxymethylene carbon on the other hand showed that methyl C-23 was oxydated in alcohol.

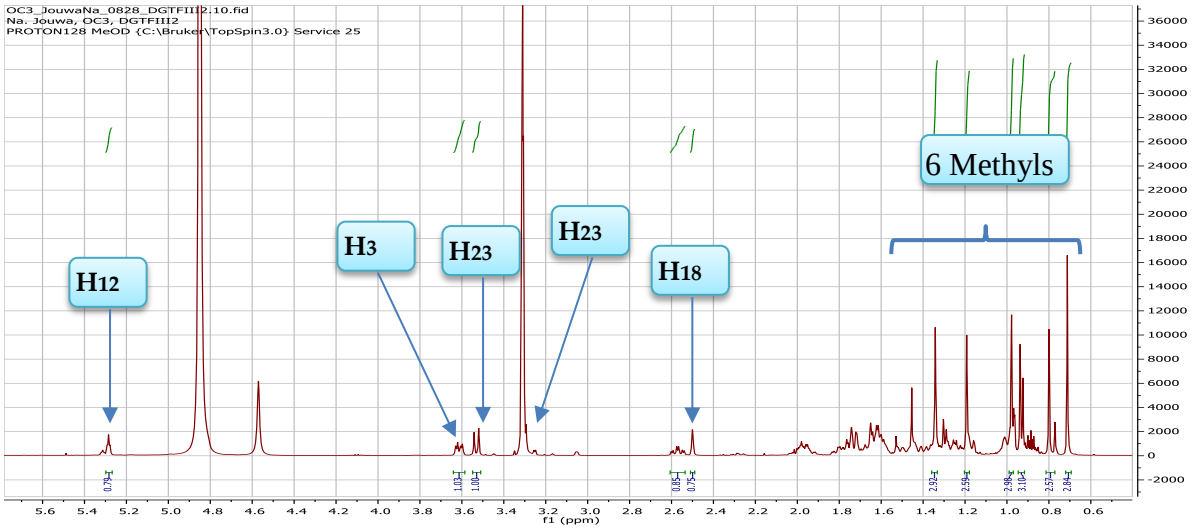

Figure 81: ^{1}H NMR spectrum (500 MHz) of compound DGTFIII2 in Methanol-d_4

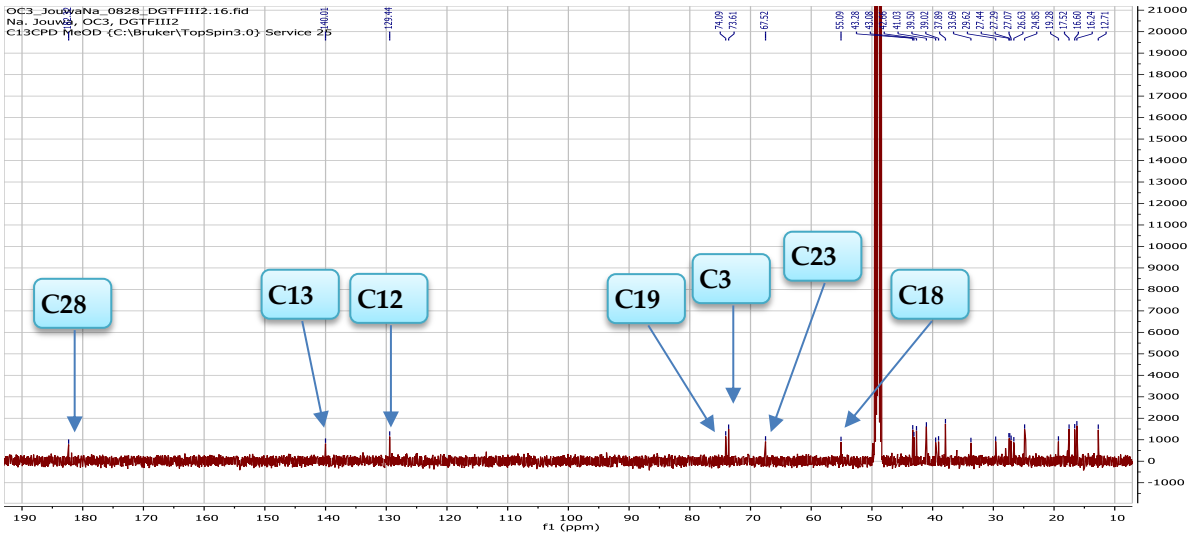

Figure 82: ^{13}C NMR spectrum (125 MHz) of compound DGTFIII2 in Methanol-d_4

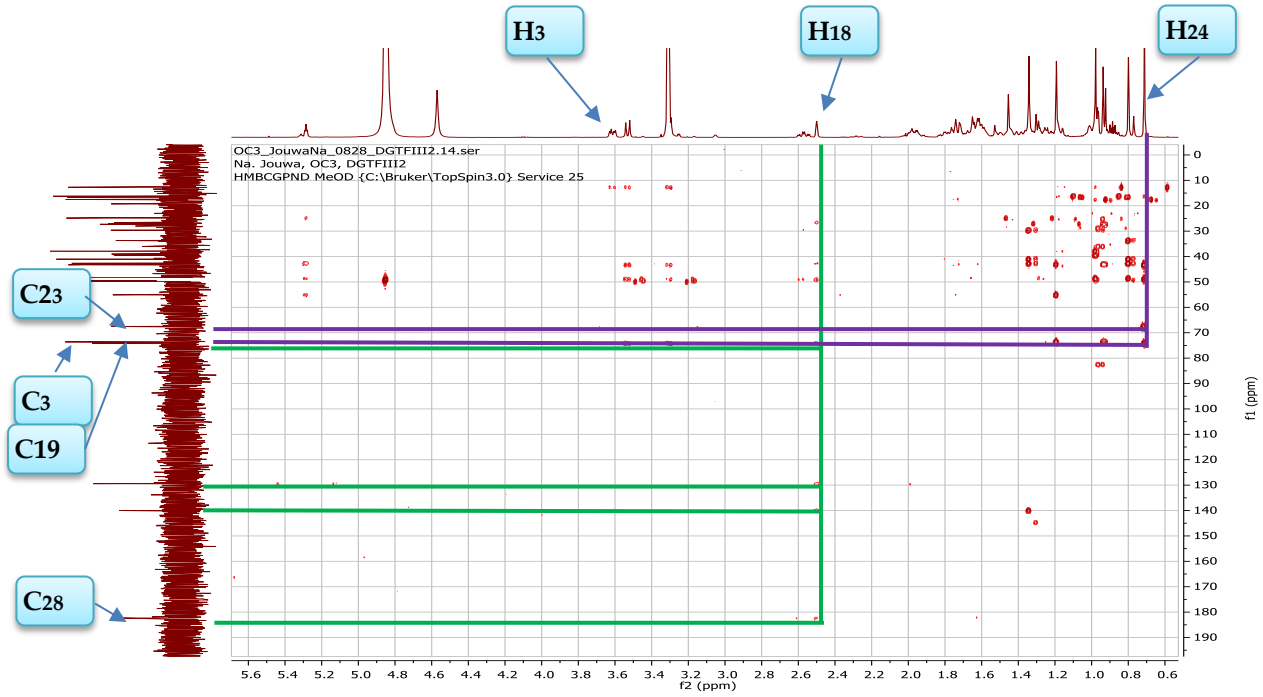

Figure 83: HMBC spectrum of compound DGTFIII2

The above spectroscopic data coupled to reported literature data identified compound DGTFIII2 as rotundic acid, a known compound first isolated from *Ilex rotunda* (Oyama et *al*., 1968).

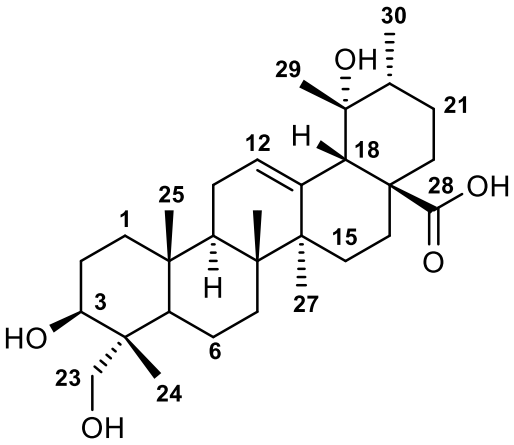

65

Table 18: ^{1}H (500MHz) and ^{13}C (125MHz) NMR spectral data of compound DGTFIII2 in Methanol-d_4 and rotundic acid in C_5D_5N

Position	DGTFIII2		rotundic acid literature data[a]	
	δ_H mult (*J* in Hz)	δ_C, mult.	δ_H mult (*J* in Hz)	δ_C
1		38.5 CH_2		39.2
2		27.4 CH_2		28.2
3	3.61 dd (4.6, 11.7)	74.0 CH	4.24 dd (4.5, 10.0)	73.5
4	-	38.9 C		38.5
5	1.15 m	52.3 CH		51.7
6		18.7 CH_2		19.1
7		33.6 CH_2		33.6
8		41.0 C		39.5
9		48.7 CH		48.2
10		37.2 C		37.6
11		23.6 CH_2		24.5
12	5.29 t (3.7)	129.4 CH	5.64 brs	128.4
13		140.0 C		140.5
14		42.9 C		40.8
15		29.6 CH_2		29.8
16		42.8 CH_2		42.5
17		49.7 C		43.4
18	2.50 s	55.0 CH	3.08 s	55.0
19		73.6 C		73.0
20		43.5 CH		42.8
21		27.3 CH_2		27.4
22		36.7 CH_2		39.0
23	3.53 d (10.9) 3.30 brs	67.5 CH_2	3.75 d (10.0) 4.21 d (10.0)	67.7
24	0.71 s	12.9 CH_3	1.08 s	13.7
25	0.80 s	17.3 CH_3	1.01 s	16.5
26	0.98 s	16.0 CH_3	1.16 s	17.7
27	1.34 s	24.8 CH_3	1.71 s	25.1
28		182.7 C		181.3
29	1.19 s	27.0 CH_3	1.46 s	27.5
30	0.92 d (7.0)	16.3 CH_3	1.13 d (6.5)	17.3

[a] (Lee et *al*., 2005)

II.1.3.3.1.6. Elucidation of DFFFII13I

Compound DFFFII13I was isolated as a white amorphous powder in the solvent system PE/EtOAc (1:1). The red coloration observed after reaction between this compound and the Lieberman-burchard reagent testify of its triterpenic nature. The ESIMS (**Figure 84**) of this compound showed in positive mode a pseudo molecular ion peak $[M+Na]^+$ at *m/z* 541.4 compatible with the molecular formula $C_{30}H_{46}O_7$ and implying eight degrees of unsaturation.

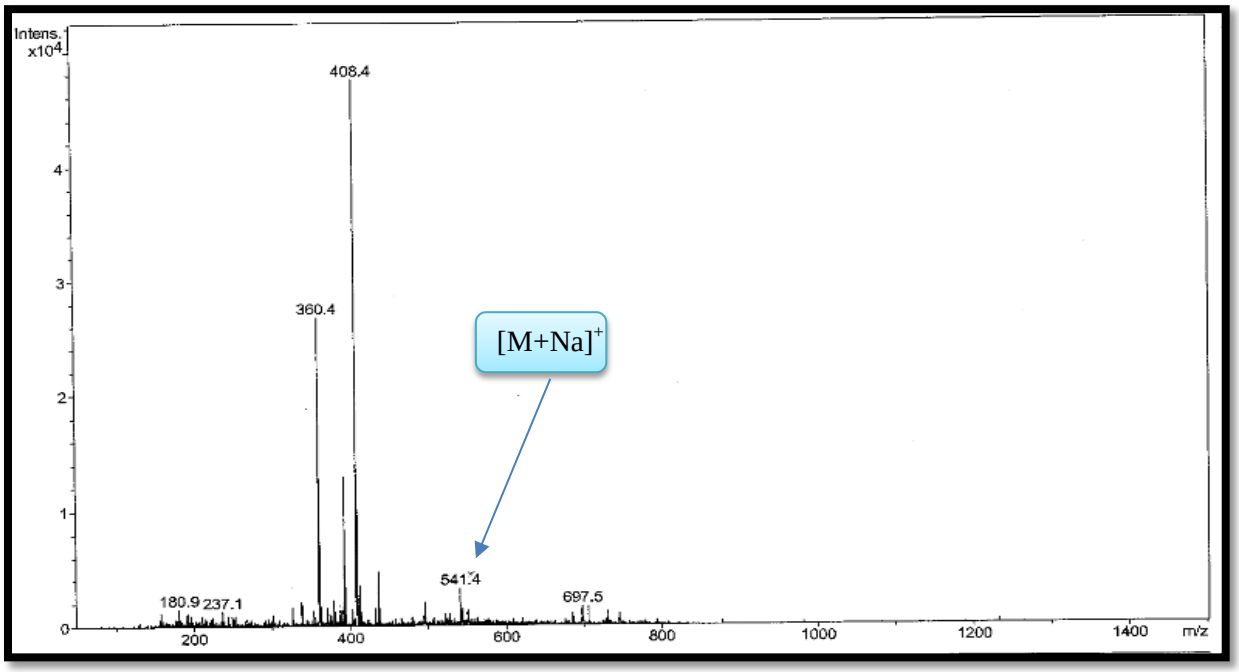

Figure 84: ESI mass spectrum of compound DFFFII13I

The ^1H and ^{13}C NMR data (**Figures 85** and **86** respectively) of compound DFFFII13I and corosolic acid **62** previously described showed some similarities, including six methyls at δ_H 1.29/ δ_C 24.8, 0.85/ δ_C 15.0, δ_H 0.70/ δ_C 17.0, δ_H 1.29/ δ_C 24.4, δ_H 1.08/ δ_C 26.9 and δ_H 0.84 (d, J = 6.7 Hz) / δ_C 16.8, two oxymethines at δ_H 3.93 (m) / δ_C 67.3 and δ_H 2.75 (d, J = 9.5 Hz) / δ_C 83.0, two olefinic sp^2 carbons at δ_C 127.2 and δ_C 139.0 and one carbonyl of carboxylic acid at δ_C 179.5. These similarities indicated that compound DFFFII13I, as corosolic acid **62** was a pentacyclic triterpene of the urs-12-ene series with a hydroxyl group at C-2 and a carboxylic function at C-28 positions. The main difference between the two compounds was the appearance in the NMR spectra of compound DFFFII13I of a signal of one quaternary sp^3 carbon bearing a hydroxyl group at δ_C 72.2 and a signal of one another carbonyl of carboxylic acid at δ_C 178.3. The HMBC correlations observed between proton H-3 at δ_H 2.75 and the carbonyl carbon at δ_C 178.3 allowed the fixation of this carboxylic function at position C-24.

To locate the position of the quaternary oxygenated carbon at C-19, we also used the HMBC spectrum (**Figure 87**) which showed correlations between proton H-18 at δ_H 2.38 and carbon C-19 at δ_C 72.2

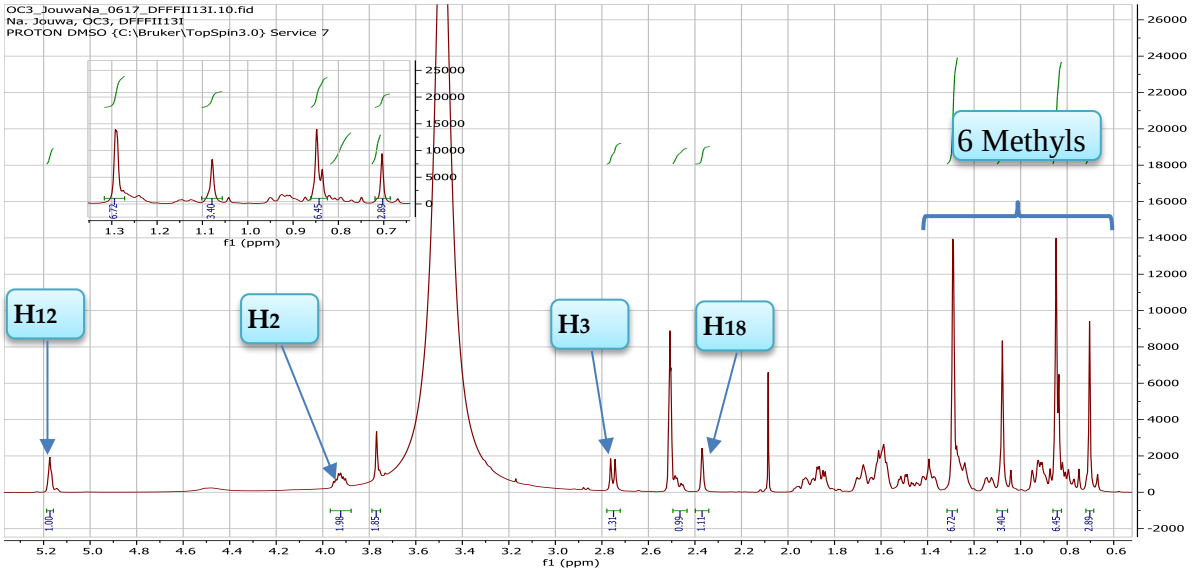

Figure 85: ^{1}H NMR spectrum (500 MHz) of compound DFFFII13I in DMSO-d_6

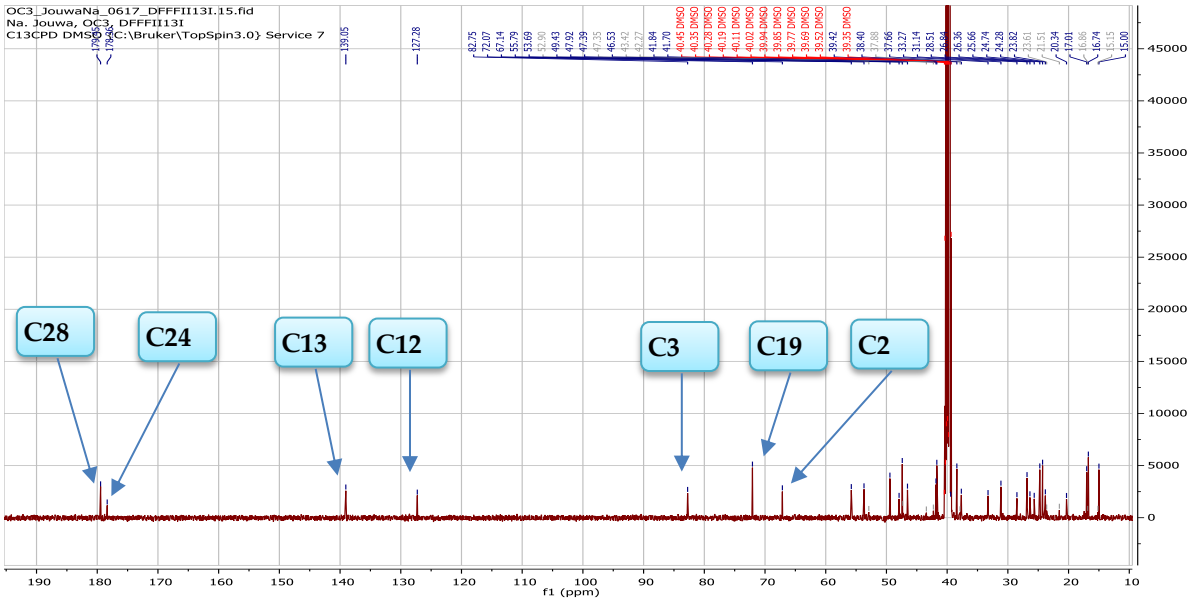

Figure 86: ^{13}C NMR Spectrum (125 MHz) of compound DFFFII13I in DMSO-d_6

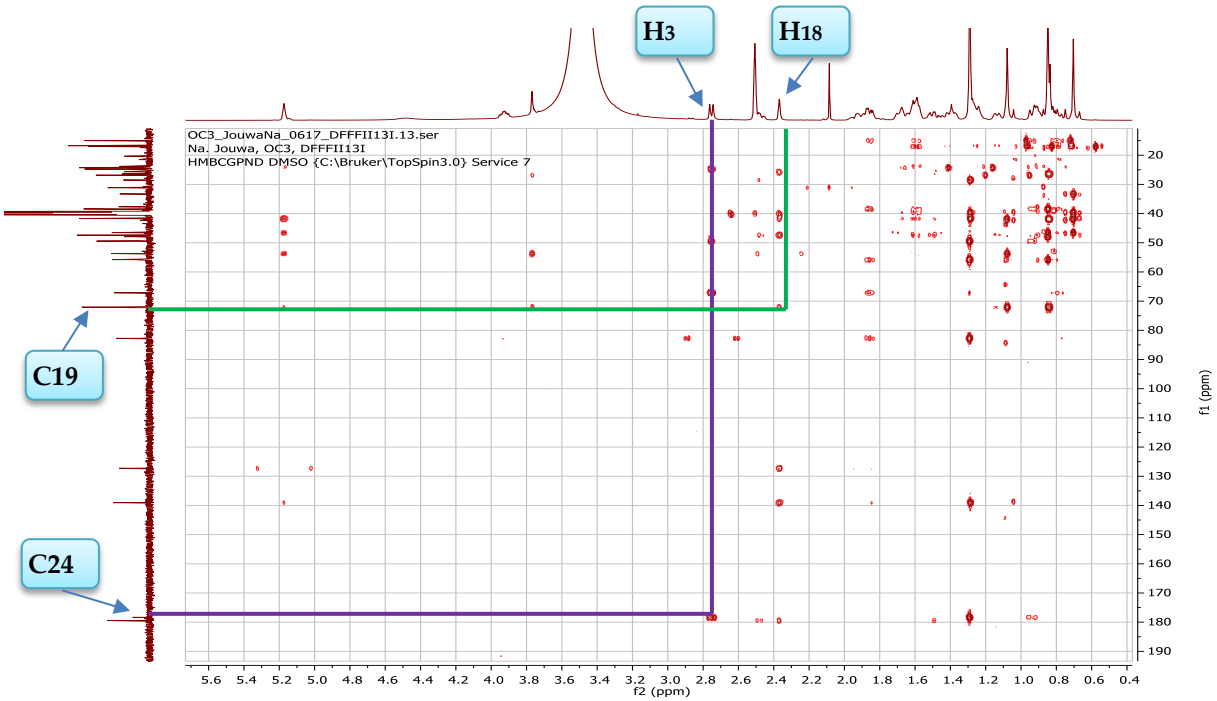

Figure 87: HMBC spectrum of compound DFFFII13I

Therefore compound DFFFII13I was identified as vismiaefolic acid, a known compound first isolated from *Vochysia vismiaefolia* (Araújo et Souza, 1990).

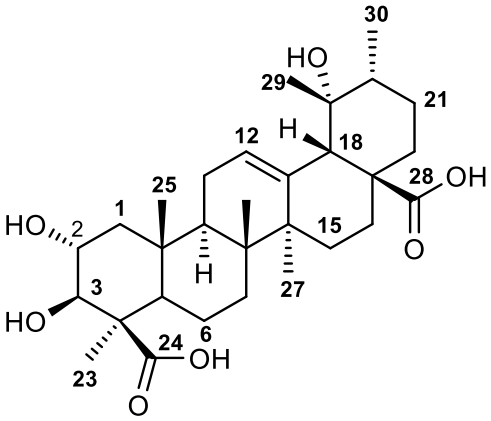

66

Table 19: ^{1}H (500MHz) and ^{13}C (125MHz) NMR spectral data of compound DFFFII13I in DMSO-d_6 and vismiaefolic acid in $CDCl_3$

Position	DFFFII13I		vismiaefolic acid literature data[a]	
	δ_H mult (*J* in Hz)	δ_C, mult.	δ_H mult (*J* in Hz)	δ_C
1		47.9 CH_2		47.9
2	3.93 m	67.3 CH	4.69 m	68.2
3	2.75 d (9.7)	83.0 CH	3.34 d (9.0)	83.7
4		49.3 C		49.7
5	0.94 m	55.9 CH	1.18 m	56.5
6		19.1 CH_2		20.6
7		32.6 CH_2		33.4
8		40.1 C		39.9
9		46.7 CH	1.87 m	46.8
10		38.3 C		38.6
11		24.2 CH_2		23.9
12	5.18 t (3.7)	127.3 CH	5.51 brs	127.6
13		139.0 C		139.5
14		40.4 C		41.9
15		29.1 CH_2		28.9
16		25.0 CH_2		26.0
17		47.6 C		47.9
18	2.38 s	53.7 CH	2.96 s	54.3
19		72.2 C		72.3
20		41.7 CH		42.0
21		26.6 CH_2		26.5
22		38.8 CH_2		38.1
23	1.29 s	24.8 CH_3	1.68 s	24.7
24		178.3 C		180.3
25	0.85 s	15.0 CH_3	1.11 s	14.9
26	0.70 s	17.0 CH_3	1.05 s	16.8
27	1.29 s	24.4 CH_3	1.65 s	24.2
28		179.5 C		180.5
29	1.08 s	26.9 CH_3	1.39 d (6.5)	26.7
30	0.84 d (6.7)	16.8 CH_3	1.06 d (6.0)	16.4

[a](Zhang et *al*., 1999)

II.1.3.3.2. Lupans

II.1.3.3.2.1. Elucidation of DGF2

Compound DGF2 was obtained as a white amorphous powder in the solvent system PE/EtOAc (19:1). It responded positively to the Liebermann Burchard test for pentacyclic triterpen. Its ESIMS (**Figure 88**) in positive mode displayed the sodium adduct fragment ion $[M+Na]^+$ at *m/z* 449.4 which is compatible with the molecular formula $C_{30}H_{50}O$ with six double bond equivalent.

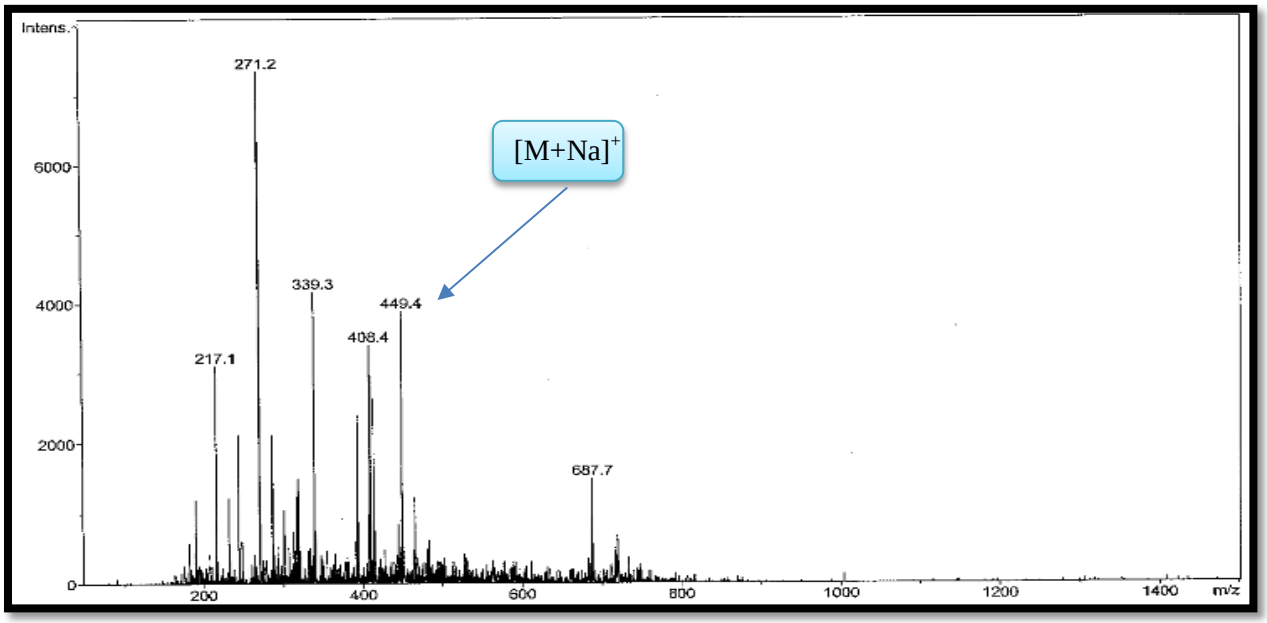

Figure 88: ESI mass spectrum of compound DGF2

Its ^1H and ^{13}C NMR spectrum (**figures 89** and **90** respectively) showed seven tertiary methyls singlet among which six appeared between δ_H 0.76-1.03 and one more deshielded at δ_H 1.68 corresponding to a vinylic methyl, one oxymethine attributable to H-3 proton of triterpene at δ_H 3.18 (dd, J = 11.4, 4.9 Hz) / δ_C 79.0, two olefinic methylene protons singlet at δ_H 4.69 and δ_H 4.57/ δ_C 109.3 and one olefinic tertiary carbon at δ_C 151.2.

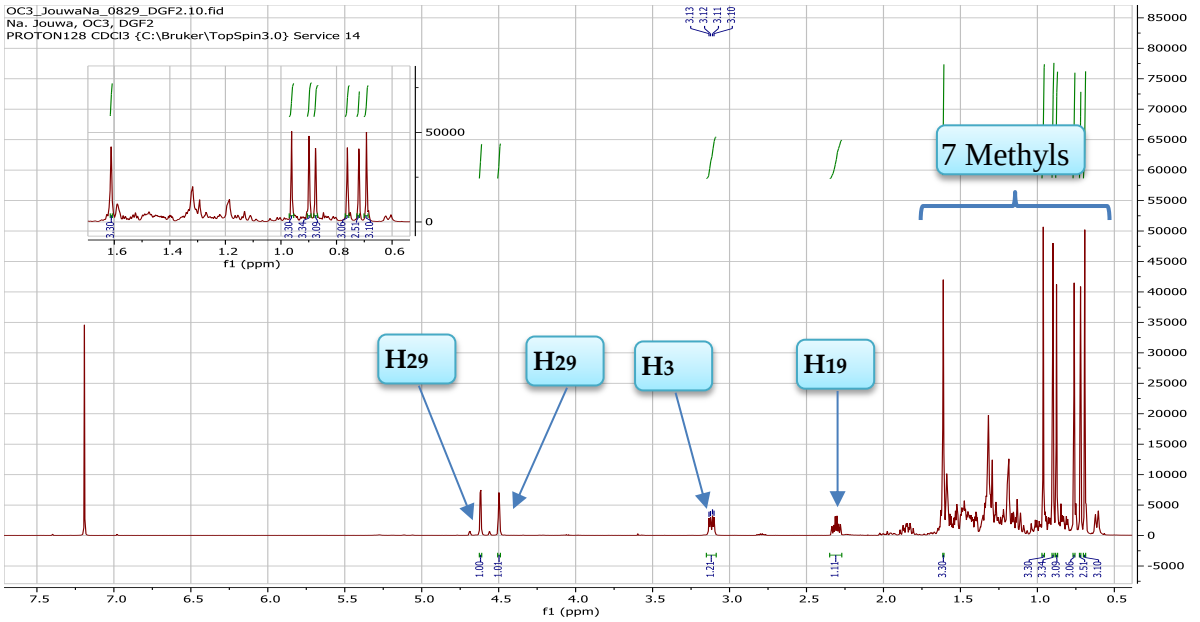

Figure 89: ^{1}H NMR spectrum (500 MHz) of compound DGF2 in $CDCl_3$

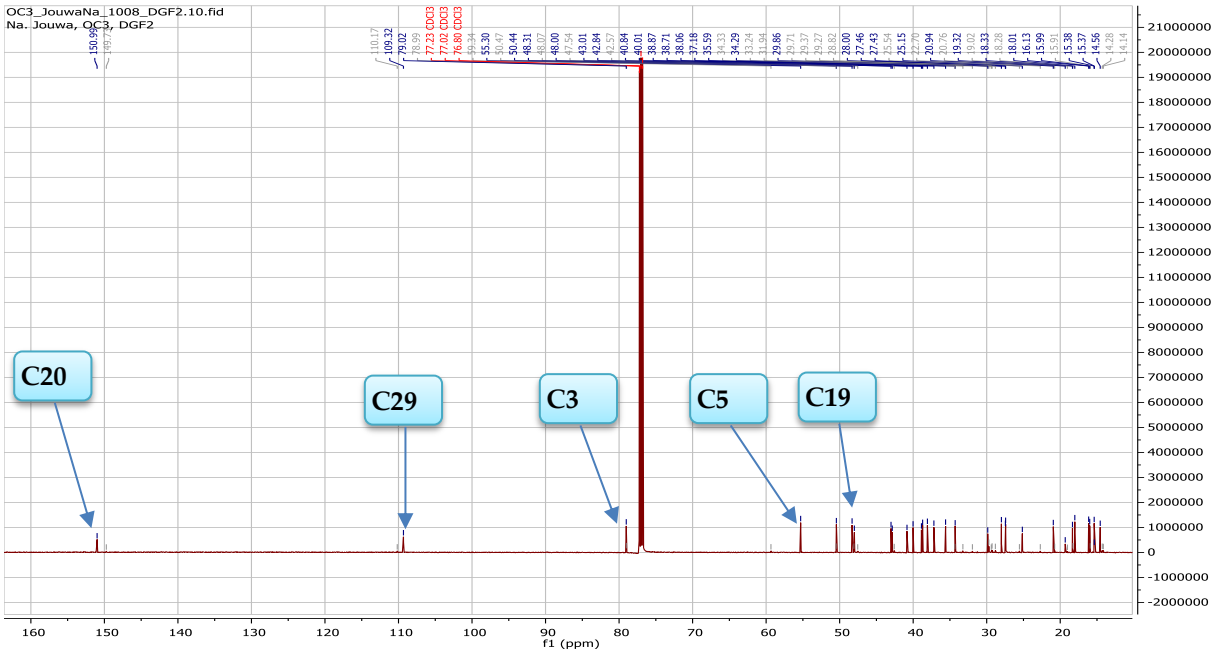

Figure 90: ^{13}C NMR spectrum (125 MHz) of compound DGF2 in $CDCl_3$

These spectroscopic data were in concordance with the literature data of lupeol, a pentacyclic triterpene from the lup-20(29)-ene series first isolated from *Lupinus luteus* (Mahato et Kundu, 1994; Thnakijcharoenpath et Theanphong., 2007).

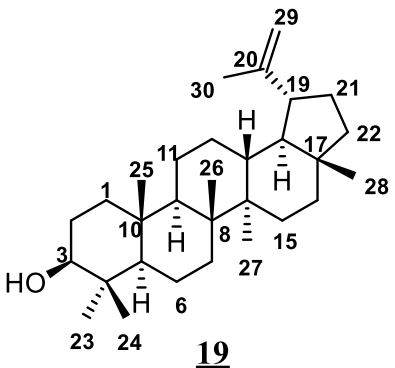

19

Table 20: ^{1}H (500MHz) and ^{13}C (125MHz) NMR spectral data of compound DGF2 and lupeol in $CDCl_3$

Position	DGF2		Lupeol literature data[a]	
	δ_H mult (*J* in Hz)	δ_C, mult.	δ_H mult (*J* in Hz)	δ_C, mult.
1		38.8 CH_2		38.7
2		27.4 CH_2		27.4
3	3.18 dd (11.4, 4.9)	79.0 CH	3.17 dd (10.2, 5.1)	79.0
4	-	38.8 C	-	38.9
5	0.68 d (8.8)	55.3 CH	0.66 d (8.7)	55.3
6		18.3 CH_2		18.3
7		34.3 CH_2		34.3
8	-	40.8 C		40.7
9		50.4 CH		50.0
10		37.1 C		37.2
11		20.9 CH_2		20.8
12		25.1 CH_2		25.1
13		38.0 CH		38.1
14		42.8 C		42.8
15		27.4 CH_2		27.2
16		35.6 CH_2		34.9
17		43.0 C		42.8
18		48.3 CH		48.3
19	2.38 m	48.0 CH	2.36 m	48.0
20	-	151.2	-	151.0
21		29.8 CH_2		30.0
22		40.0 CH_2		40.0
23	0.94 s	28.1 CH_3	0.94 s	28.0
24	0.76 s	15.4 CH_3	0.74 s	15.9
25	0.83 s	16.1 CH_3	0.81 s	15.8
26	1.03 s	16.0 CH_3	1.01 s	16.4

27	0.97 s	14.5 CH_3	0.92 s	14.5
28	0.79 s	18.0 CH_3		18.0
29	4.69 brs	109.3 CH_2	4.67 brs	109.3
	4.57 brs		4.55 brs	
30	1.68 s	19.2 CH_3	1.66 s	19.1

[a] (Thnakijcharoenpath et Theanphong., 2007)

II.1.3.3.2.2. Elucidation of DGF3

Compound DGF3 was isolated as a white amorphous powder in the solvent system PE/EtOAc (17:3). It reacted positively to the Liebermann-Burchard test with a red coloration observed characteristic of pentacyclic triterpenes. Its HR-ESIMS (**Figure 91**) showed in positive mode the pseudo-molecular ion peak $[M+H]^+$ at *m/z* 443.3881 corresponding to the molecular formula $C_{30}H_{50}O_2$ and implying six degree of unsaturations.

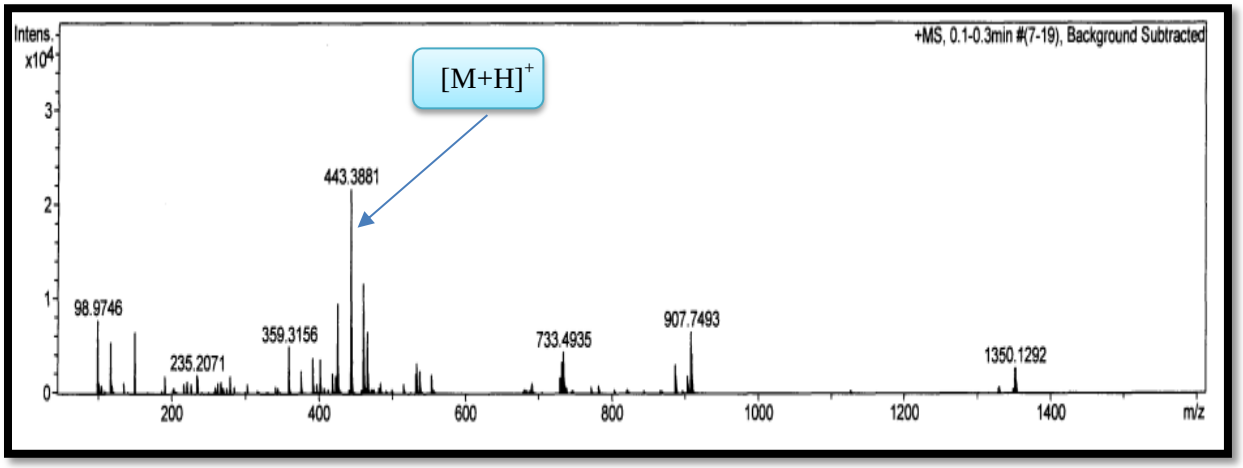

Figure 91: HR-ESI mass spectrum of compound DGF3

The ^1H and ^{13}C NMR spectra of compound DGF3 (**Figures 92** and **93** respectively) showed close similarities to those of lupeol **19** including five tertiary methyls between δ_H 0.76-1.02 and a vinylic one at δ_H 1.68, two olefinic protons at δ_H 4.58, 4.68/ δ_C 109.8, one vinylic methine at δ_H 2.38/ δ_C 50.5 one oxymethine at δ_H 3.18 (dd, J = 11.4, 4.8 Hz) / δ_C 79.1 and one olefinic quaternary carbon at δ_C 150.6, indicating that compound DGF3, as lupeol **19**, was also a pentacyclic triterpene of the lup-20(29)-ene series. The main difference between these two compounds was the disappearance in the NMR spectra of compound DGF3 of the tertiary methyl C-28 and the appearance of one oxymethylene at δ_H 3.33 (d, J = 10.8 Hz), 3.80 (d, J = 10.8 Hz) / δ_C 60.7, showing that carbon C-28 was oxydated in alcohol.

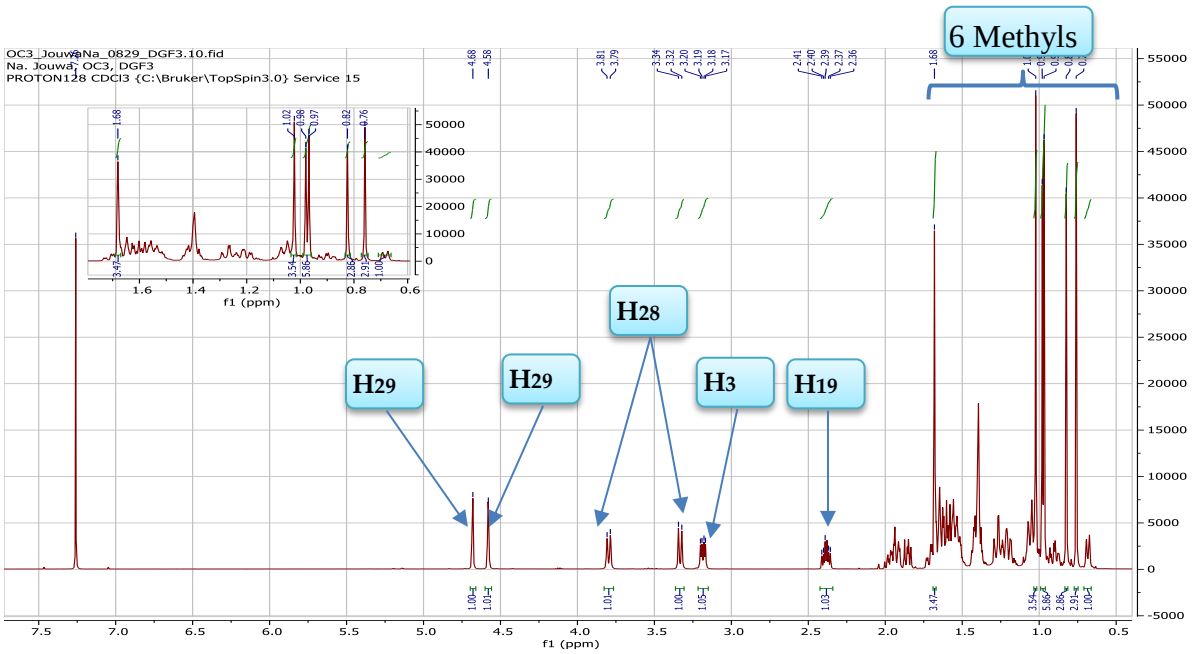

Figure 92: ^{1}H NMR (500 MHz) spectrum of compound DGF3 in $CDCl_3$

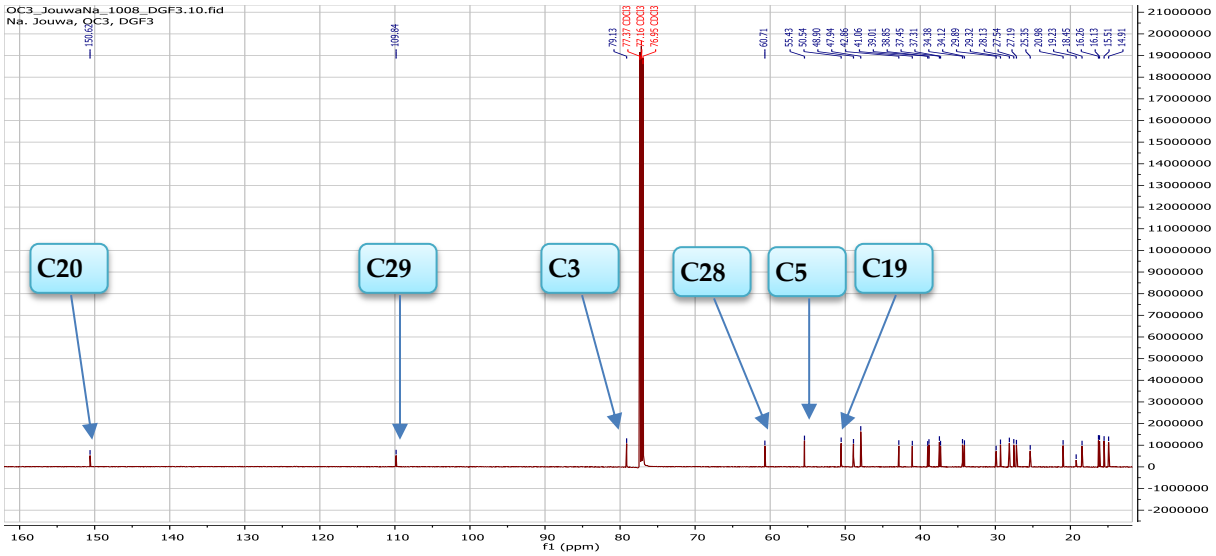

Figure 93: ^{13}C NMR (125 MHz) spectrum of compound DGF3 in $CDCl_3$

All those NMR data were in accordance with the literature data of betulin, a known compound previously isolated from *Phaulopsis imbricate* by Kengne et *al*. in 2016.

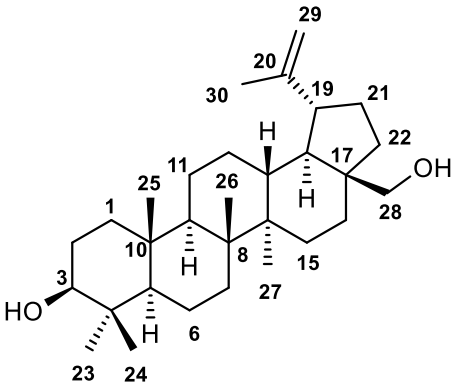

20

Table 21: ^{1}H (500MHz) and ^{13}C (125MHz) NMR spectral data of compound DGF3 and betulin in $CDCl_3$

	DGF3		betulin literature data[a]	
Position	δ_H mult (*J* in Hz)	δ_C, mult.	δ_H mult (*J* in Hz)	δ_C, mult.
1		38.8 CH_2		38.7
2		27.4 CH_2		27.4
3	3.18 dd (11.4, 4.8)	79.1 CH	3.18, dd (15.0, 5.0)	79.0
4	-	38.8 C	-	38.9
5	0.68 d (8.9)	55.4 CH	0.67 m	55.3
6		18.3 CH_2		18.3
7		34.3 CH_2		34.3
8	-	40.8 C		40.8
9		50.4 CH		50.4
10		37.1 C		37.2
11		20.9 CH_2		21.2
12		25.1 CH_2		25.1
13		38.0 CH		38.2
14		42.8 C		43.1
15		27.4 CH_2		27.7
16		35.6 CH_2		35.9
17		43.0 C		42.7
18		48.3 CH		48.3
19	2.38 m	50.5 CH	2.38 m	48.0
20	-	150.6	-	151.0
21		29.8 CH_2		30.0
22		40.0 CH_2		40.0
23	0.97 s	28.1 CH_3	0.93 s	27.4
24	0.76 s	15.4 CH_3	0.76 s	15.9
25	0.82 s	16.1 CH_3	0.82 s	16.3

26	1.02 s	16.0 CH_3	0.98 s	16.1
27	0.98 s	14.5 CH_3	0.90 s	15.4
28	3.33 d (10.8)	60.7 CH_3	3.33 d (10.0)	60.6
	3.80 d (10.8)		3.80 d (10.0)	
29	4.68 brs	109.8 CH_2	4.66 brs	109.7
	4.56 brs		4.58 brs	
30	1.68 s	19.3 CH_3	1.68 s	19.1

[a] (Kengne et *al.*, 2016)

II.1.3.3.2.3. Elucidation of DFR5

Compound DFR5 was obtained as a white amorphous powder in the solvent system PE/EtOAc (4:1). It gave a red coloration to the Liebermann-Burchard test indicative its triterpenic nature. The ESIMS (**Figure 94**) of this compound showed in positive mode the pseudo molecular ion peak $[M+Na]^+$ at *m/z* 479.3 which correspond to the molecular formula $C_{30}H_{48}O_3$ implying seven double bond equivalent.

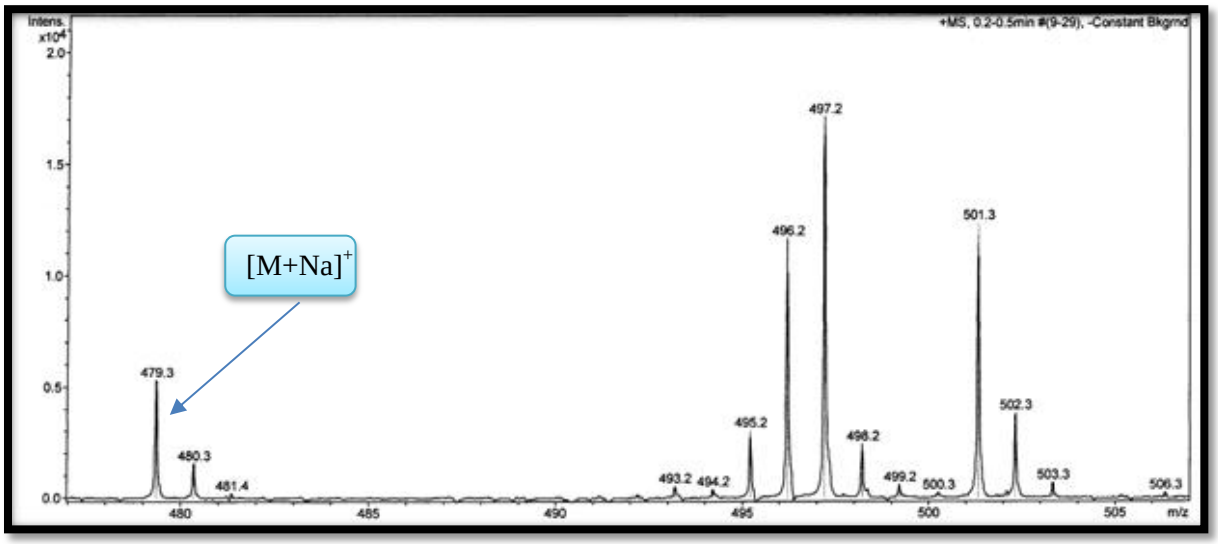

Figure 94: ESI mass spectrum of compound DFR5

Its ^1H and ^{13}C NMR spectra (**Figures 95** and **96**) were quite similar to those of lupeol **19** indicating that compound DFR5 as lupeol **19** was also a pentacyclic triterpene of the lup-20(29)-ene series. The main difference between the two compounds was the loss in compound DFR5 of the signal of one of the tertiary methyl, which was replaced by the signal of a carboxylic function appearing at δ_C 179.5 in the ^{13}C NMR spectrum. It was deduced from the comparison of these data with those published in literature that it is the position C-28 of the lup-20(29)-ene skeleton which was oxydated in carboxylic acid.

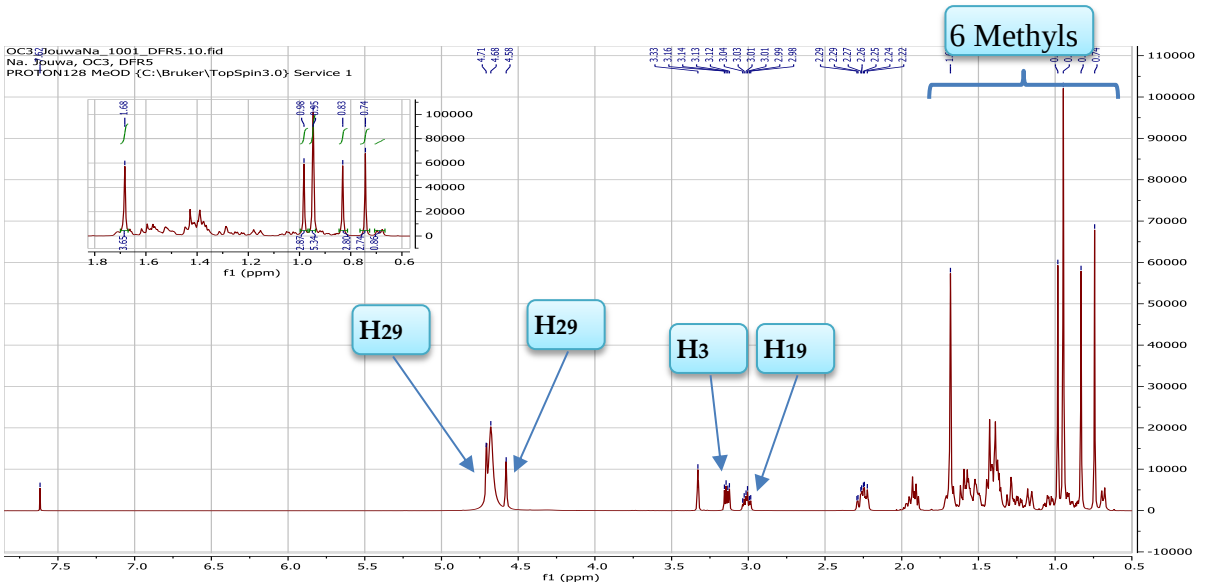

Figure 95: ^{1}H NMR (500 MHz) spectrum of compound DFR5 in Methanol-d_4 + $CDCl_3$

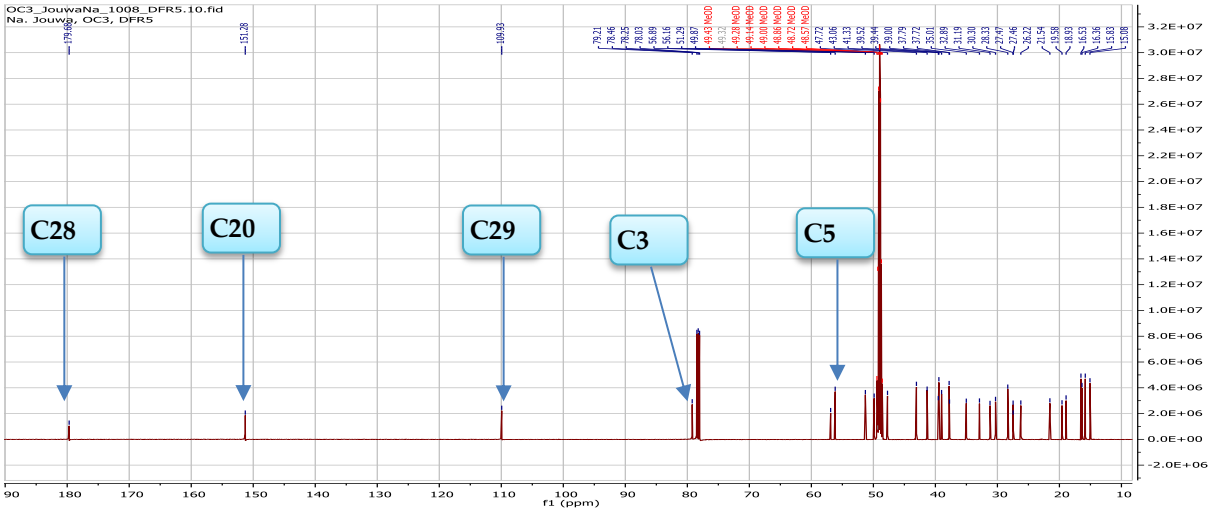

Figure 96: ^{13}C NMR (125 MHz) spectrum of compound DFR5 in Methanol-d_4 + $CDCl_3$

All those NMR data were in accordance with the literature data of betulinic acid, a known compound previously isolated from *Platanus acerifolia* (Cichewicz et Kouzi, 2004).

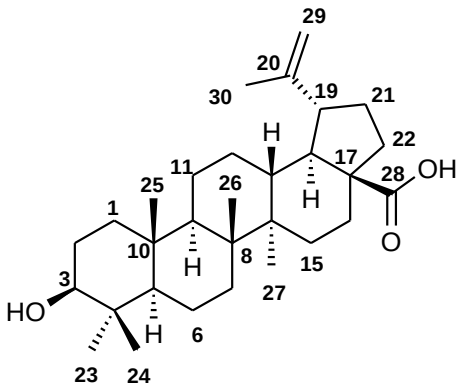

21

Table 22: ^{1}H (500MHz) and ^{13}C (125MHz) NMR assignments of compound DFR5 in Methanol-d_4 + $CDCl_3$ and betulinic acid in C_5D_5N.

Position	DFR5		Betulinic acid literature data[a]	
	δ_H mult (*J* in Hz)	δ_C, mult.	δ_H mult (*J* in Hz)	δ_C
1		38.8 CH_2		39.3
2		27.4 CH_2		28.3
3	3.12 dd (10.9, 5.4)	79.1 CH	3.45 t (7.2)	78.1
4	-	38.8 C		39.5
5	0.67 m	55.4 CH	0.82 m	56.0
6		18.3 CH_2		18.8
7		34.3 CH_2		34.9
8		40.8 C		41.1
9		50.4 CH		51.0
10		37.1 C		37.6
11		20.9 CH_2		21.2
12		25.1 CH_2		26.2
13		38.0 CH		38.7
14		42.8 C		42.9
15		27.4 CH_2		30.3
16		35.6 CH_2		32.9
17		56.5 C		56.6
18		48.3 CH		49.8
19	3.02 m	47.3 CH	3.52 m	47.8
20		151.6		151.3
21		29.8 CH_2		31.2
22		37.1 CH_2		37.6
23	0.99 s	28.1 CH_3	1.22 s	28.7
24	0.83 s	15.4 CH_3	1.00 s	16.3
25	0.74 s	16.1 CH_3	0.83 s	16.4
26	0.95 s	16.0 CH_3	1.06 s	16.4
27	0.95 s	14.5 CH_3	1.07 s	14.9
28	-	179.5 C	-	178.8
29	4.71 brs	109.8 CH_2	4.95 s	109.9
	4.58 brs		4.77 s	
30	1.68 s	19.3 CH_3	1.79 s	19.5

[a] (Cichewicz et Kouzi, 2004)

II.1.3.3.3. Oleananes

II.1.3.3.3.1. Elucidation of DGF6

Compound DGF6 was obtained as a white amorphous powder in the solvent system PE/EtOAc (3:1). It gave a brick red colour with the Liebermann Burchard reagent characteristic of pentacyclic triterpene. The ESIMS of this compound showed in positive mode the pseudo-molecular ion peak $[M+Na]^+$ at *m/z* 479.4 in agreement with the molecular formula $C_{30}H_{48}O_3$ corresponding to seven double bond equivalent.

Its ^1H and ^{13}C NMR spectrum (**Figures 97** and **98**) showed seven signals of *ter*-methyls at δ_H 0.88 / δ_C 17.9, δ_H 0.99 / δ_C 30.1, δ_H 0.91 / δ_C 17.5, δ_H 0.78 / δ_C 19.1, δ_H 0.94/ δ_C 25.5, δ_H 0.84 / δ_C 35.2 and δ_H 1.13/ δ_C 29.7, one signal of an olefinic proton at δ_H 5.51 (brs) / δ_C 124.3, one signal of an allylic proton at δ_H 3.31 (m) / δ_C 43.6, and one signal of an oxymethine at δ_H 3.47 (t, J = 8.0 Hz) / δ_C 79.7. These signals in addition to those observed in the ^{13}C NMR spectrum of this compound at δ_C 124.3 and 146.2 are characteristic of a pentacyclic triterpene belonging to the olean-12-ene series. A signal of one carboxylic group at δ_C 181.6 was also observed.

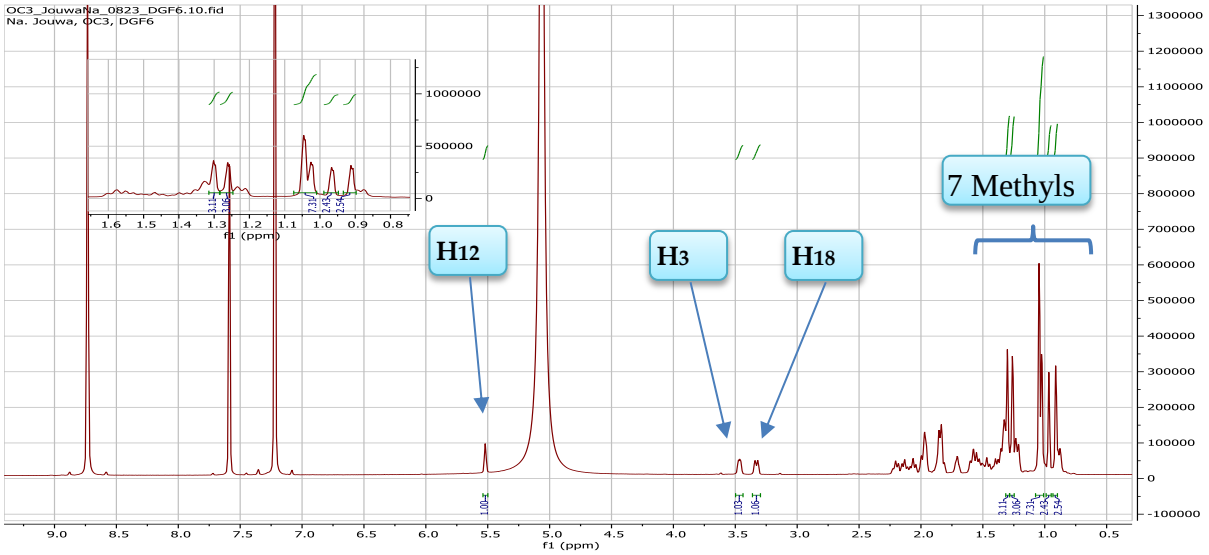

Figure 97: ^1H NMR spectrum (500MHz) of compound DGF6 in C_5D_5N

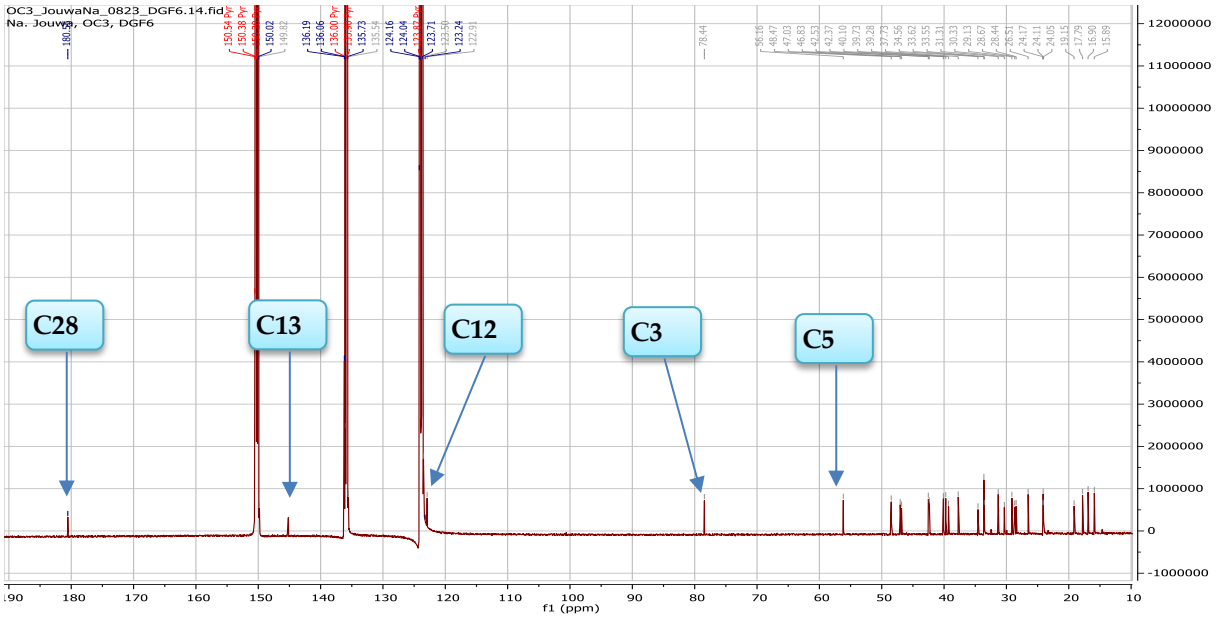

Figure 98: ^{13}C NMR (125MHz) spectrum of compound DGF6 in C_5D_5N

From the above evidence, compound DGF6 was identified as oleanolic acid, a known compound previously isolated from *Lantana camara* by Verma et *al*. in 2013.

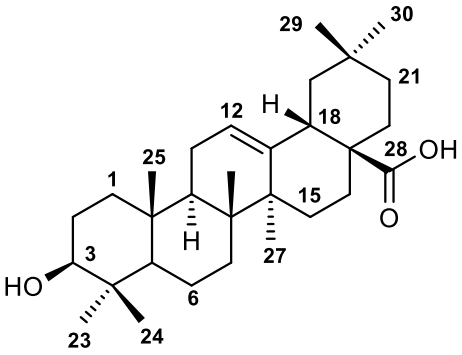

25

Table 23: ^{1}H (500MHz) and ^{13}C (125MHz) NMR assignments of compound DGF6 and oleanolic acid in C_5D_5N.

Position	DGF6		Oleanolic acid literature data[a]	
	δ_H mult (*J* in Hz)	δ_C, mult.	δ_H mult (*J* in Hz)	δ_C
1		39.5 CH_2		40.7
2		27.4 CH_2		29.6
3	3.47 t (8.0)	79.7 CH	3.37 t (8.2)	80.0
4	-	38.9 C		39.0
5		57.5 CH		57.6
6		20.1 CH_2		20.4
7		32.8 CH_2		32.6
8		40.9 C		41.0
9		49.7 CH		49.9
10		39.2 C		39.0
11		25.2 CH_2		25.5
12	5.51 brs	124.3 CH	5.43 brs	124.2
13		146.2 C		146.4
14		41.2 C		41.4
15		27.6 CH_2		27.8
16		25.4 CH_2		25.4
17		48.3 C		48.3
18	3.31 m	43.6 CH	3.20 dd (3.6, 10.0)	43.7
19		48.1 CH_2		48.3
20		31.7 C		31.6
21		34.8 CH_2		34.9
22		32.5 CH_2		32.5
23	0.99 s	30.1 CH_3	1.10 s	30.4
24	0.88 s	17.9 CH_3	0.87 s	18.1
25	0.91 s	17.5 CH_3	0.94 s	17.8
26	0.78 s	19.1 CH_3	0.81 s	19.1
27	1.13 s	29.7 CH_3	1.15 s	30.0
28	-	181.6 C	-	181.7
29	0.84 s	35.2 CH_3	0.84 s	35.0
30	0.94 s	25.5 CH_3	0.93 s	25.4

[a] (Verma et *al*., 2013)

II.1.3.3.3.2. Elucidation of DFFFII15

Compound DFFFII15 was isolated as a white powder in the solvent system PE/EtOAc (2:3). It gave a brick red colour with the Liebermann Burchard reagent characteristic of pentacyclic triterpene. Its ESIMS (**figure 99**) showed in positive mode a pseudo molecular ion peak $[M+Na]^+$ at *m/z* 495.3 in agreement with the molecular formula $C_{30}H_{48}O_4$ corresponding to seven double bond equivalent.

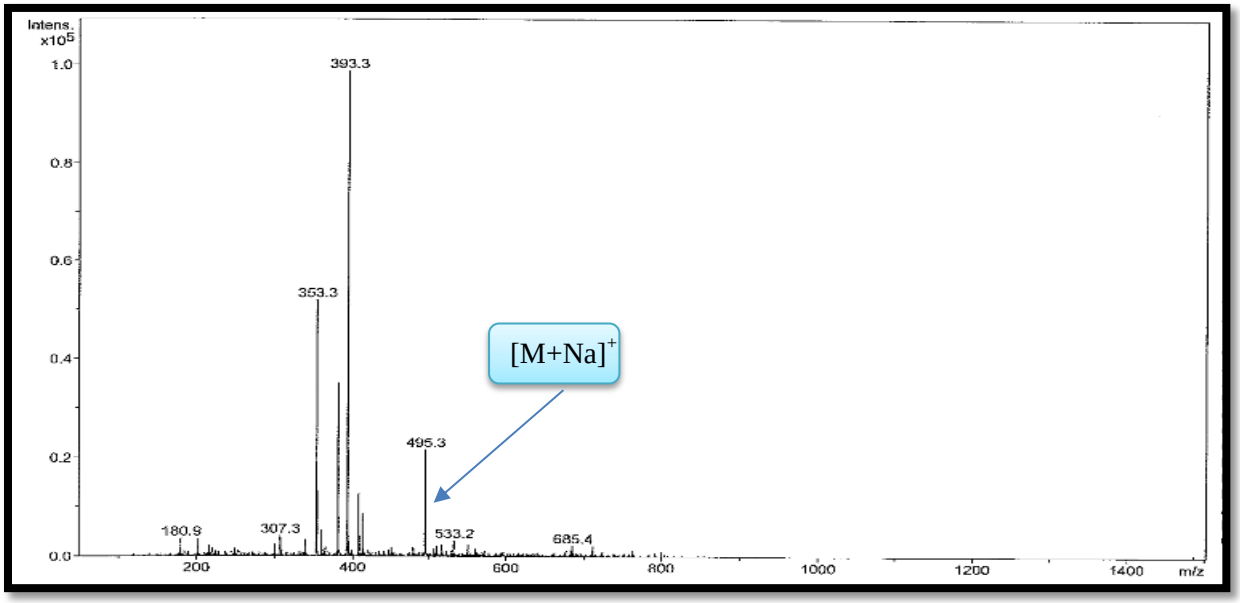

Figure 99: ESI mass spectrum of compound DFFFII15

The ^1H and ^{13}C NMR spectra of this compound (**Figures 100** and **101** respectively) were similar to those of oleanolic acid **25** and displayed characteristic signals of a pentacyclic triterpene type olean-12-ene at δ_H 0.77 / δ_C 16.7, δ_H 0.78 / δ_C 11.5, δ_H 0.87 / δ_C 32.7, δ_H 0.90 / δ_C 23.1, δ_H 0.93 / δ_C 15.4, δ_H 1.12 / δ_C 25.6 corresponding to six angular methyls, at δ_H 2.80 (dd, J = 13.9, 4.5 Hz) / δ_C 41.2 corresponding to allylic H-18 proton, at δ_H 3.59 (m) / δ_C 75.7 corresponding to oxymethine proton H-3, and at δ_H 5.23 (t, J = 3.7 Hz) / δ_C 122.4 and 143.7 corresponding to olefinic proton and carbons. In addition, a signal of a carbonyl of carboxylic acid was also observed at δ_C 180.8. The main difference between those two compounds was the disappearance in the NMR spectra of compound DFFFII15 of signal of angular methyl C-23 and the appearance of two signals of diastereotopic protons at δ_H 3.35 (m) / δ_C 69.3 and δ_H 3.59 (m) / δ_C 69.3, showing that carbon C-23 was oxydated in alcohol.

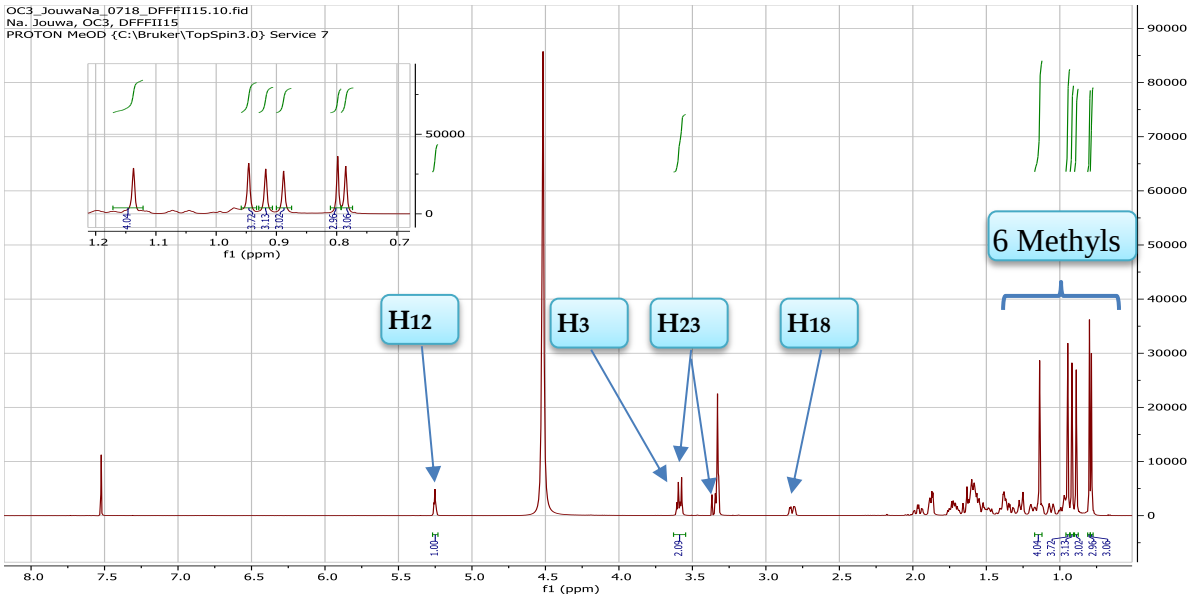

Figure 100: ^{1}H NMR spectrum (500 MHz) of compound DFFFII15 in Methanol-*d_4* + $CDCl_3$

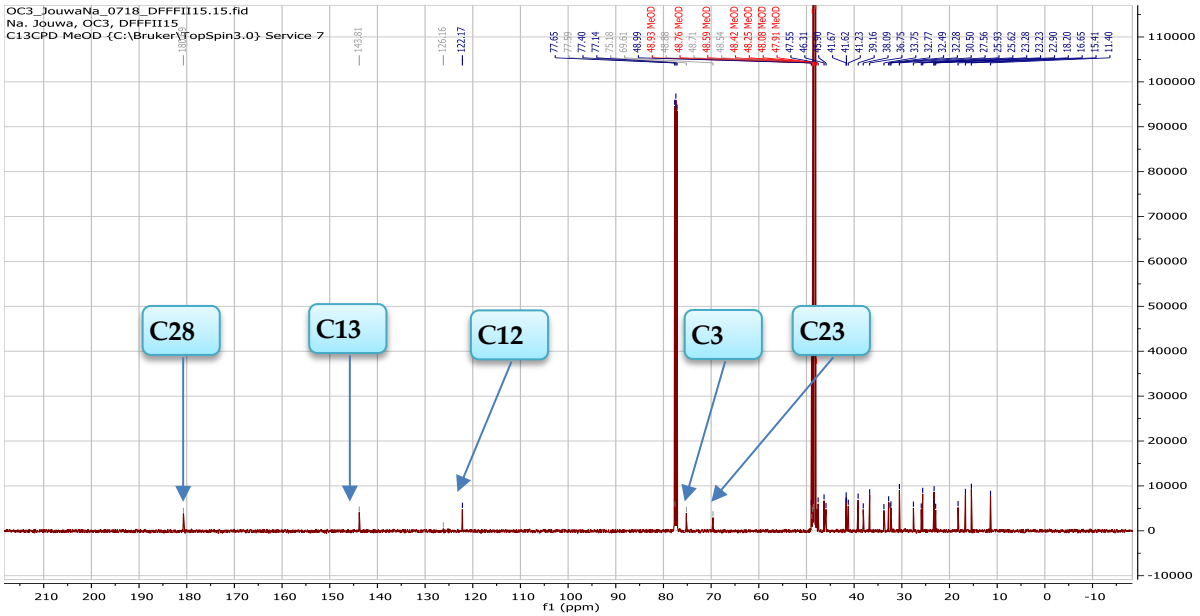

Figure 101: ^{13}C NMR spectrum (125 MHz) of compound DFFFII15 in Methanol-*d_4* + $CDCl_3$

All those NMR data were in accordance with the literature data of hederagenin, a known compound previously isolated from *Nigella sativa* by Joshi et *al*. in 1999.

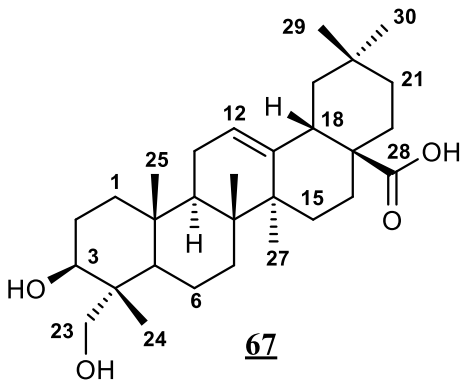

67

Table 24: ^{1}H (500MHz) and ^{13}C (125MHz) NMR spectral data of compound DFFFII15 in Methanol-d_4 + $CDCl_3$ and hederagenin in C_5D_5N

Position	DFFFII15		hederagenin literature data[a]	
	δ_H mult (*J* in Hz)	δ_C, mult.	δ_H mult (*J* in Hz)	δ_C
1		38.4 CH_2		38.9
2		27.4 CH_2		27.6
3	3.59 m	75.7 CH	4.23	73.5
4	-	40.9 C		43.0
5		46.9 CH	1.53	48.7
6		20.1 CH_2		18.7
7		32.8 CH_2		33.1
8		40.6 C		39.9
9		48.7 CH		48.3
10		38.2 C		37.4
11		24.8 CH_2		24.0
12	5.23 t (3.7)	122.4 CH	5.51	122.7
13		143.7 C		145.0
14		41.9 C		42.3
15		27.9 CH_2		28.5
16		23.4 CH_2		23.8
17		47.5 C		46.9
18	2.80 dd (13.9, 4.5)	41.2 CH	3.31	42.1
19		48.1 CH_2		46.6
20		31.7 C		31.1
21		33.7 CH_2		34.3
22		32.5 CH_2		33.4
23	3.35 d (12.1) 3.58 m	69.3 CH_2	4.18 3.73	67.8
24	0.88 s	11.5 CH_3	1.05 s	13.3
25	0.91 s	15.4 CH_3	0.97 s	16.1

26	0.78 s	16.6 CH_3	1.04 s	17.7
27	1.12 s	25.6 CH_3	1.26 s	26.3
28	-	180.8 C	-	180.2
29	0.84 s	33.3 CH_3	0.95 s	33.4
30	0.94 s	23.4 CH_3	1.02 s	23.8

[a] (Joshi et *al*., 1999)

II.1.3.3.3.3. Elucidation of DFFFI11

Compound DFFFI11 was obtained as a white powder in the solvent system PE/EtOAc (19:1). Its positive reaction to the Liebermann-Burchard test with a red coloration observed was indicative of its triterpenic nature. The ESIMS (**Figure 102**) in positive mode of this compound displayed the sodium adduct fragment ion $[M+Na]^+$ at *m/z* 491.4 which is compatible with the molecular formula $C_{32}H_{52}O_2$ corresponding to seven double bond equivalent.

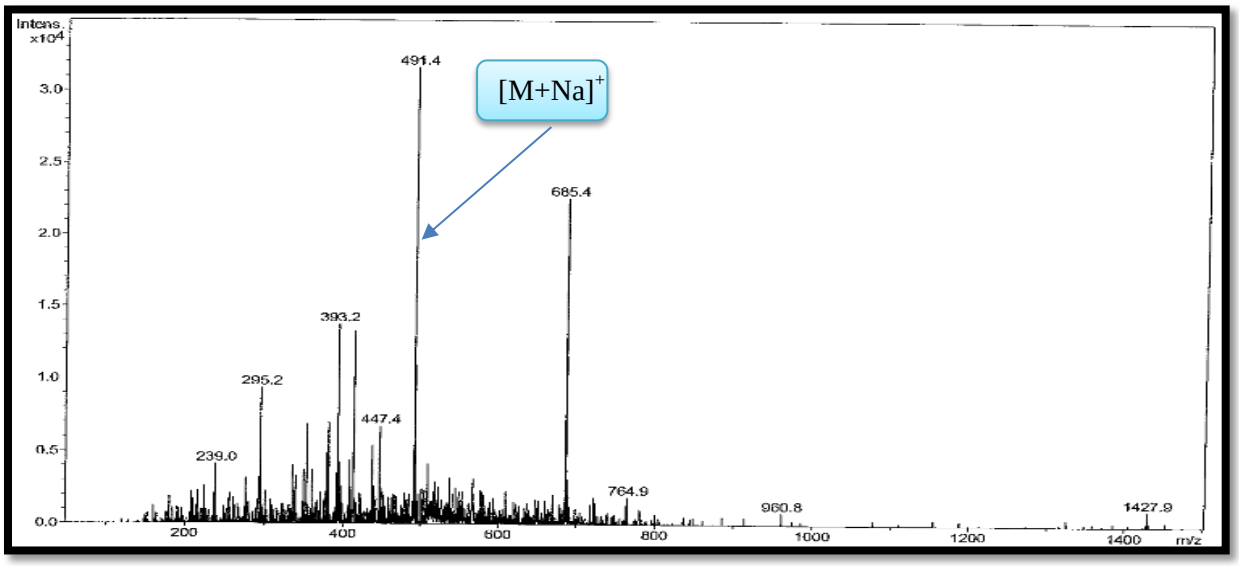

Figure 102: ESI mass spectrum of compound DFFFI11

The ^1H and ^{13}C NMR spectra (**Figures 103** and **104** respectively) of this compound displayed characteristic signals of triterpenes belonging to olean-12-ene serie including signals of eight angular methyls at δ_H 0.80 / δ_C 16.8, δ_H 0.80 / δ_C 28.1, δ_H 0.89 / δ_C 15.6, δ_H 0.89 / δ_C 16.8, δ_H 1.05 / δ_C 26.1, δ_H 0.75 / δ_C 28.6, 0.80 / δ_C 23.7 and δ_H 0.80 / δ_C 33.4, signal of an oxymethine proton at δ_H 4.43 (m) / δ_C 81.1 and signal of olefinic proton and carbons at δ_H 5.11 (t, J = 3.7 Hz) / δ_C 122.1 and δ_C 145.5. In addition, these spectra also displayed signals of an acetate group including one deshielded methyl at δ_H 1.97 / δ_C 21.3 and one carbonyl of ester at δ_C 171.8. The location of this acetate groupement was found to be at C-3

position regarding the deshielding of the oxymethine proton H-3 and carbon C-3 appearing at δ_H 4.43 and δ_C 81.1 respectively.

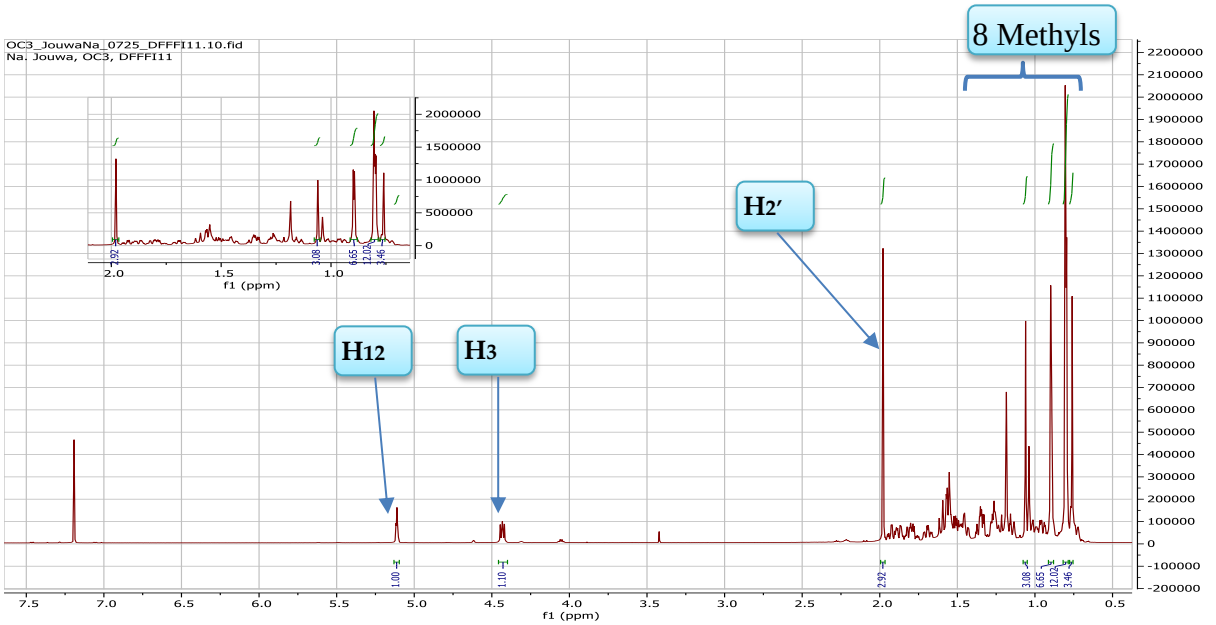

Figure 103: ^{1}H NMR spectrum (500MHz) of compound DFFFI11 in $CDCl_3$

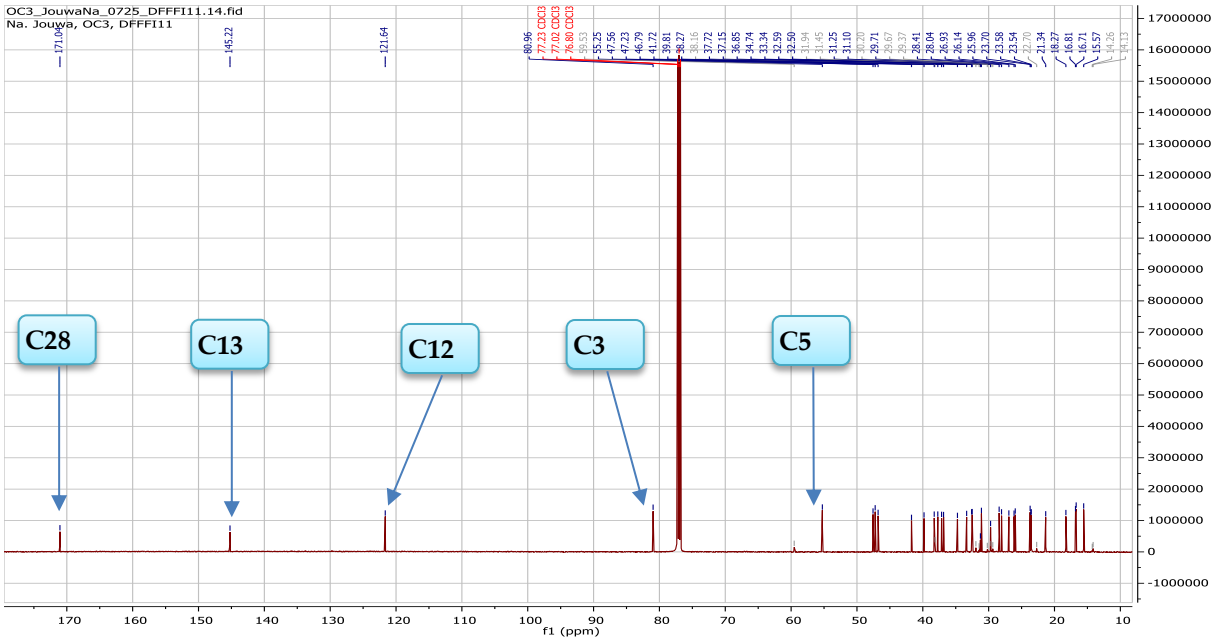

Figure 104: ^{13}C NMR spectrum (125MHz) of compound DFFFI11 in $CDCl_3$

Therefore, the above spectroscopic data coupled to those reported in the literature identified compound DFFFI11 as *β*-amyrin acetate, a known compound previously isolated from *Wrightia tomentosa* by Maurya et *al*. in 2012.

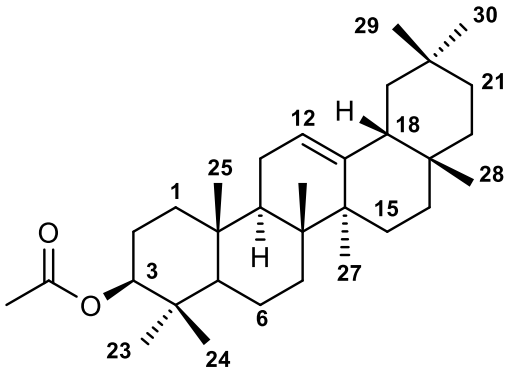

68

Table 25: ^{1}H (500MHz) and ^{13}C (125MHz) NMR spectral data of compound DFFFI11 and *β*-amyrin acetate in $CDCl_3$

Position	DFFFI11		*β*-amyrin acetate literature data[a]	
	δ_H mult (*J* in Hz)	δ_C, mult.	δ_H mult (*J* in Hz)	δ_C
1		39.0 CH_2		38.8
2		27.4 CH_2		26.8
3	4.43 m	81.1 CH	4.48 dd (4.4, 11.5)	81.2
4	-	38.9 C		38.9
5		55.5 CH	0.71	55.3
6		19.1 CH_2	1.53	18.6
7		32.8 CH_2		32.9
8		40.9 C		40.2
9		47.7 CH		47.4
10		37.2 C		37.1
11		23.2 CH_2	1.84	23.8
12	5.11 t (3.7)	122.1 CH	5. 16 t (3.5)	121.9
13		145.5 C		145.4
14		41.8 C		41.9
15		26.6 CH_2		26.3
16		27.1 CH_2		27.1
17		32.6 C		32.7
18	1.90 m	47.7 CH	1.89	47.8
19		47.2 CH_2		46.7
20		31.4 C		31.0
21		37.3 CH_2		37.3
22		35.0 CH_2		34.9
23	0.80 s	16.8 CH_3	0.77 s	15.7
24	0.80 s	28.1 CH_3	0.98 s	28.8

25	0.89 s	15.6 CH_3	0.92 s	14.8
26	0.89 s	16.8 CH_3	0.94 s	17.0
27	1.05 s	26.1 CH_3	1.11 s	26.7
28	0.75	28.6 CH_3	0.81 s	28.6
29	0.80 s	33.4 CH_3	0.85 s	33.8
30	0.80 s	23.7 CH_3	0.85 s	23.9
1'	-	171.8	-	171.5
2'	1.97	21.3	2.02	21.5

[a] (Okoye et *al*., 2014)

II.1.3.4. Polyols

II.1.3.4.1. Elucidation of DGF1

Compound DGF1 was isolated as beige crystals during the maceration of the leaves of *D. gilletii*. It gave a red coloration with molish test characteristic of sugars. Its ESIMS showed in negative mode the pseudo molecular ion peak $[M-H]^-$ at *m/z* 163.4 which is in agreement with the molecular formula $C_6H_{12}O_5$ implying one degree of unsaturation. On its ^1H and ^{13}C NMR spectra (**Figures 105** and **106** respectively) were observed signals of five oxymethines at δ_H 3.29 (td, J = 8.9, 3.8 Hz)/ δ_C 75.3, δ_H 3.40 (m) / δ_C 71.7, δ_H 3.47 (m) / δ_C 69.2, δ_H 3.59 (q, J = 3.5 Hz) / δ_C 73.1, δ_H 3.67 (t, J = 3.4 Hz) / δ_C 68.7, a signal of one methylene group at δ_H 1.61 (m) / δ_C 35.0 and signals of five hydroxyl groups at δ_H 4.38 (d, J = 5.9 Hz), δ_H 4.55 (d, J = 4.3 Hz), δ_H 4.58 (d, J =4.8 Hz), δ_H 4.65 (d, J =3.6 Hz) and δ_H 4.88 (d, J =3.4 Hz).

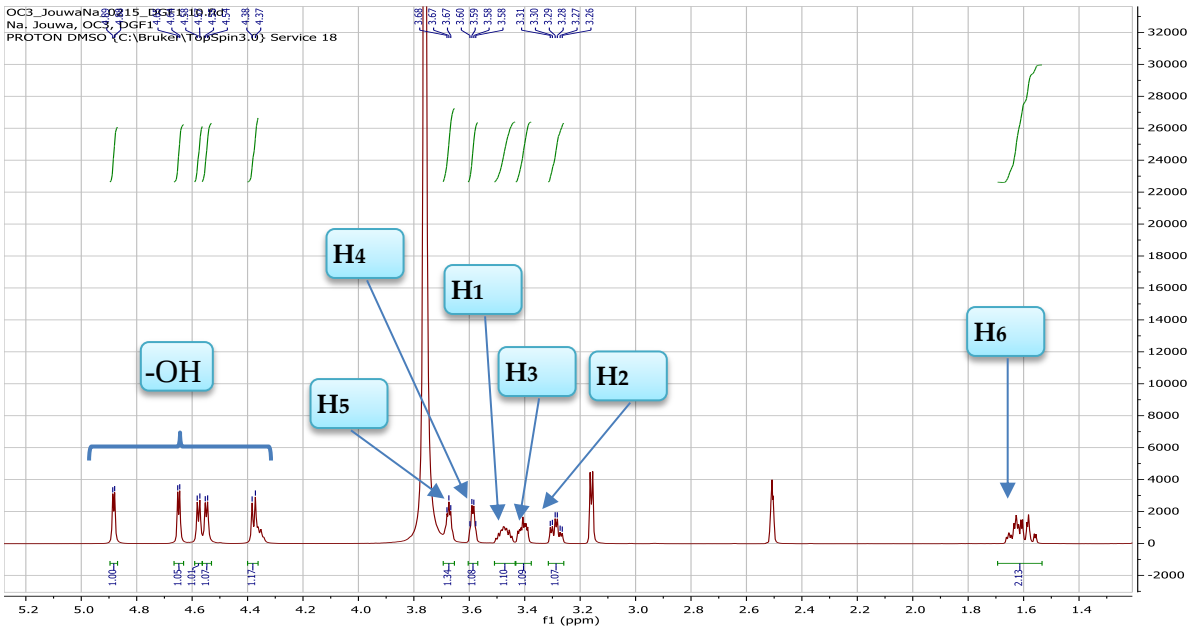

Figure 105: ^1H NMR spectrum (500 MHz) of compound DGF1 in DMSO-d_6

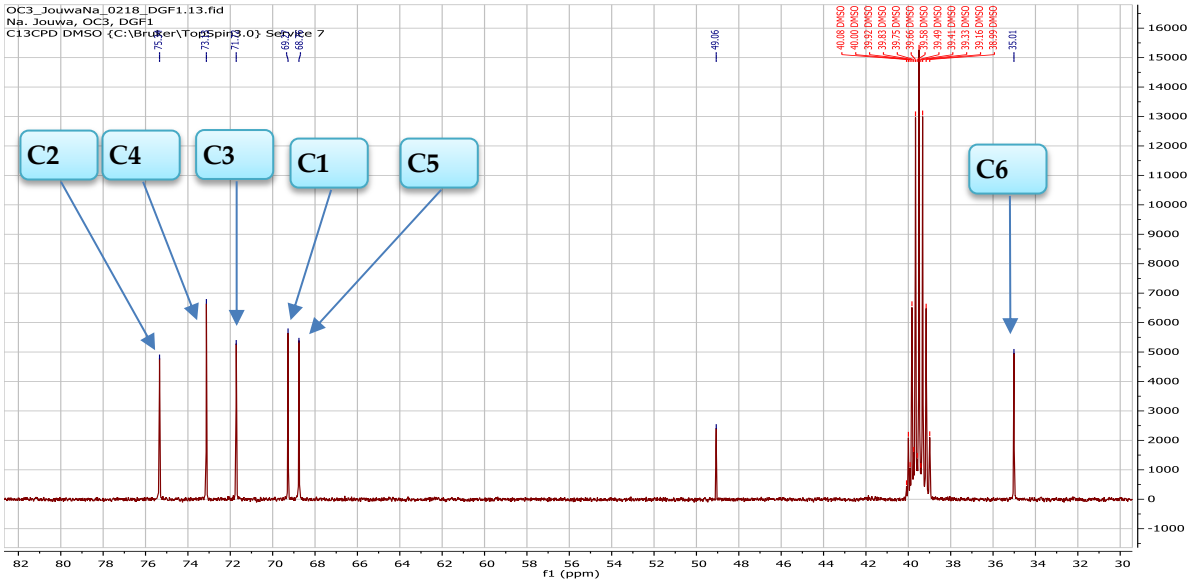

Figure 106: ^{13}C NMR spectrum (125 MHz) of compound DGF1 in DMSO-d_6

The Comparison of these spectroscopic data with those existing in the literature established compound DGF1 as *D*-Quercitol, a known compound previously isolated from *Mimusops elengi* by Venkateswara et *al*. in 2014.

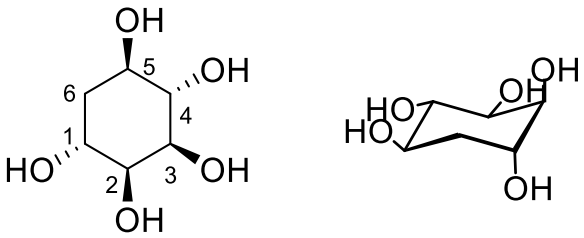

69

Moreover, the X ray diffraction of this compound permitted to establish its relative configuration.

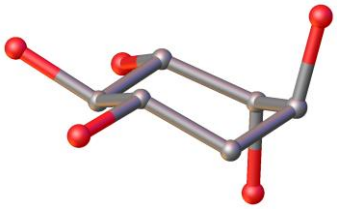

Figure 107: ORTEP-like view of compound DGF1

Table 26: ^{1}H (500MHz) and ^{13}C (125MHz) NMR assignments of compound DGF1 in DMSO-d_6 and Quercitol in D_2O.

Position	DGF1		Quercitol literature data[a]	
	δ_H, mult (J in Hz)	δ_C, mult	δ_H, mult (J in Hz)	δ_C, mult
1	3.47, m	69.2, CH	3.82, m	68.8, CH
2	3.29, td (3.8, 8.9)	75.3, CH	3.55, m	73.7, CH
3	3.40, m	71.7, CH	3.57, br s	71.4, CH
4	3.59, q (3.5)	73.1, CH	3.52, br s	70.8, CH
5	3.67 t (3.4)	68.7, CH	4.05, m	66.8, CH
6	1.61, m	35.0, CH_2	1.78, dd (3.2, 10.0)	33.2, CH_2
OH	4.58, d (4.8)	-	-	-
OH	4.55, d (4.3)	-	-	-
OH	4.38, d (5.9)	-	-	-
OH	4.65, d (3.6)	-	-	-
OH	4.88, d (3.4)	-	-	-

[a] (Shih et *al*., 2005)

II.1.3.4.2. Elucidation of DFFFII14

Compound DFFFII14 was isolated as white crystals in the solvent system EtOAc 100%. It responded positively to the Molish test for sugar. The pseudo molecular ion peak $[M+Na]^+$ at *m/z* 217.2 in ESIMS spectrum in positive mode was in agreement with the molecular formula $C_7H_{14}O_6$ corresponding to one double bond equivalent. Its ^1H and ^{13}C NMR spectral data (**Figures 108** and **109** respectively) displayed signals of five oxymethines at δ_H 3.18 (dd, *J* = 9.2, 7.8 Hz) / δ_C 75.1, δ_H 3.29 (m) / δ_C 71.6, δ_H 3.30 (m) / δ_C 78.1, δ_H 3.37 (m) / δ_C 78.0, δ_H 4.19 (d, *J* = 7.8 Hz) / δ_C 105.5, signals of one oxymethylene group at δ_H 3.69 (dd, *J* = 4.4, 9.5 Hz), δ_H 3.89 (m) / δ_C 62.9 and a signal of one methoxy group at δ_H 3.55 (s) / δ_C 57.4.

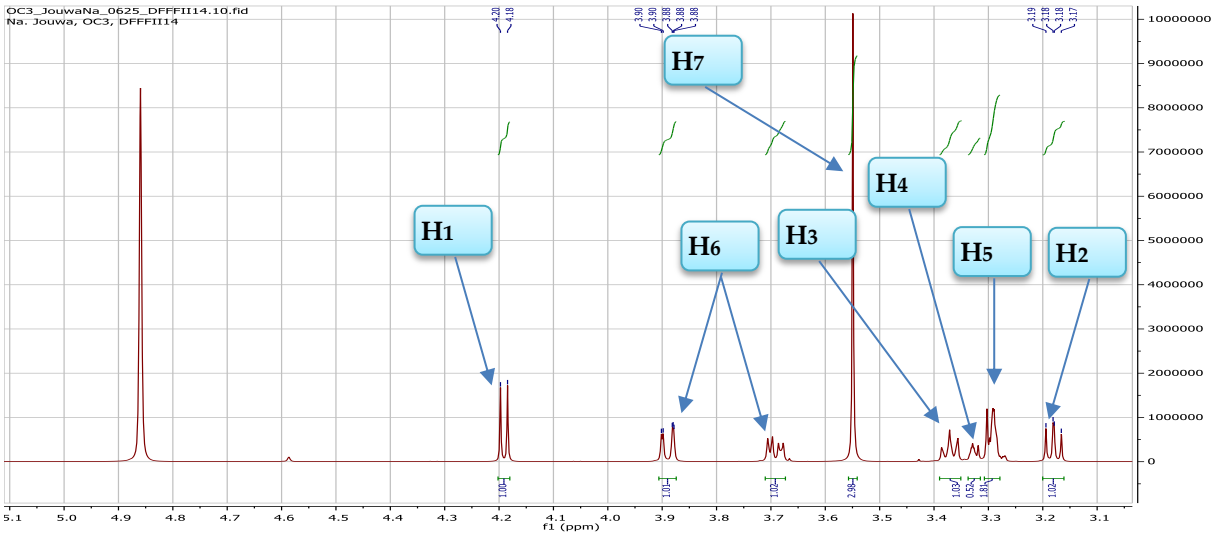

Figure 108: ^1H NMR spectrum (500 MHz) of compound DFFFII14 in Methanol-d_4

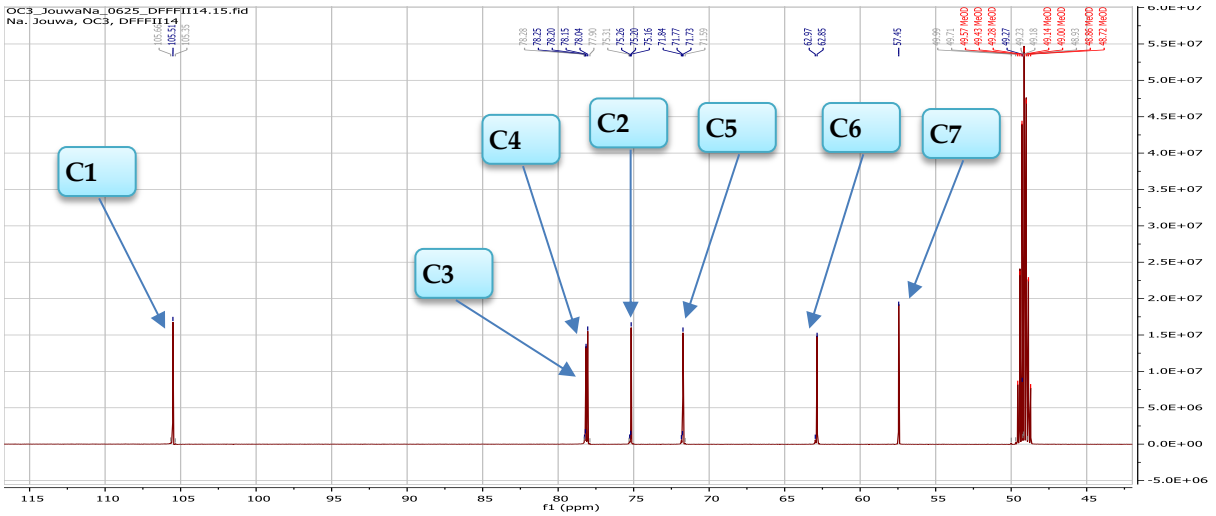

Figure 109: ^{13}C NMR spectrum (125 MHz) of compound DFFFII14 in Methanol-d_4

The above spectroscopic data compared to those of the literature established compound DFFFII14 to be methyl-*β*-*D*-glucopyranoside, which ^{13}C NMR spectroscopic data are reported here for the first time.

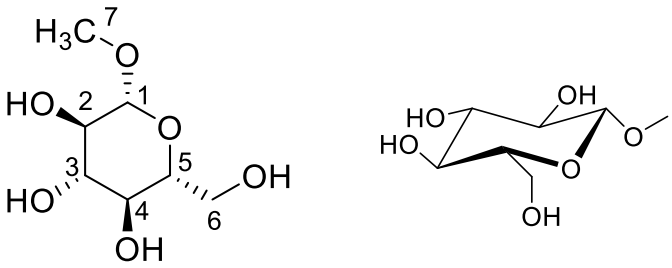

70

The stereochemistry was established using X-ray diffraction of this compound.

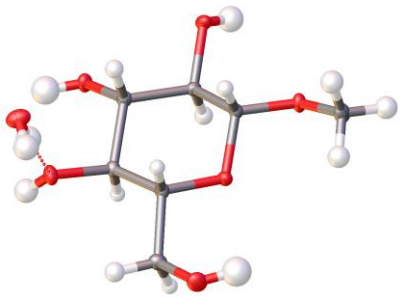

Figure 110: ORTEP-like view of compound DFFFII14.

Table 27: ^{1}H (500MHz) and ^{13}C (125MHz) NMR assignments of compound DFFFII14 in Methanol-*d_4*.

Position	**DFFFII14**		**methyl-*β*-*D*-glucopyranoside literature data[a]**
	δ_H, mult (*J* in Hz)	δ_C, mult	δ_H, mult (*J* in Hz)
1	4.19, d (7.8)	105.5, CH	3.82, m
2	3.18, dd (7.8, 9.2)	75.1, CH	3.55, m
3	3.37, m	78.0, CH	3.57, br s
4	3.30, m	78.1, CH	3.52, br s
5	3.29, m	71.6, CH	4.05, m
6	3.69, dd (4.4, 9.5)	62.9, CH_2	3.78, dd (3.2, 10.0)
	3.89, m		
7	3.55, s	57.4, CH_3	-

II.1.3.4.3. Elucidation of DFFFII9

Compound DFFFII9 was isolated as a beige powder in the solvent system PE/EtOAc (1:3). It gave a positive reaction to the molish test characteristic of sugar. On its ^{1}H and ^{13}C NMR spectra (**Figures 111** and **112** respectively), signals of six oxymethines at δ_H 2.68 (1H, t, J = 9.2 Hz) / δ_C 86.0, δ_H 3.13 (2H, m) / δ_C 72.3, δ_H 3.43 (2H, dd, J = 9.5, 4.9 Hz) / δ_C 72.6, δ_H 3.69 (1H, m) / δ_C 72.9, a signal of one methoxy group at δ_H 3.45 (s) / δ_C 62.2 and three doublets corresponding to hydroxyl groups at δ_H 4.63 (2H, d, J = 4.8 Hz,), δ_H 4.51 (1H, d, J = 3.5 Hz) and δ_H 4.43 (2H, d, J = 5.6 Hz) were observed.

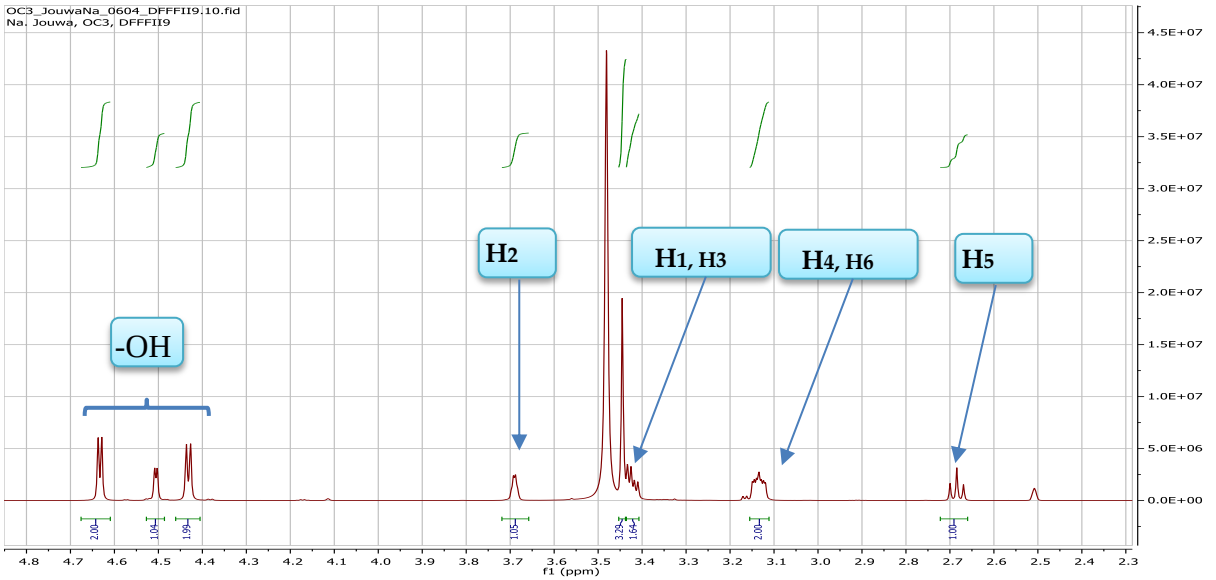

Figure 111: ^{1}H NMR spectrum (500 MHz) of compound DFFFII9 in DMSO-d_6

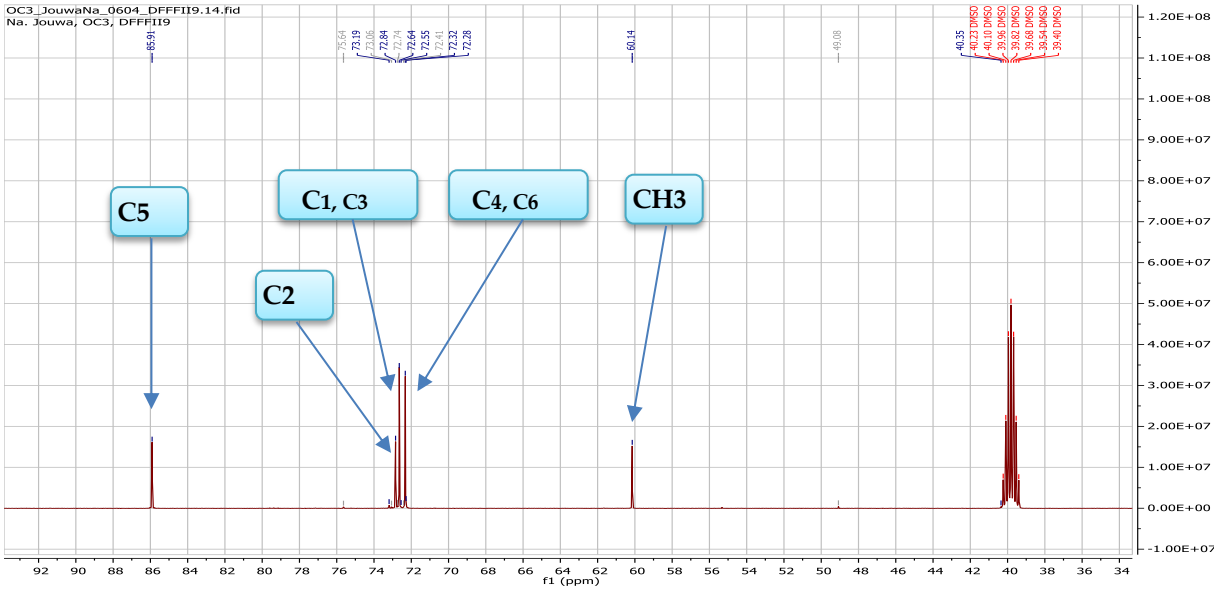

Figure 112: ^{13}C NMR spectrum (125 MHz) of compound DFFFII9 in DMSO-d_6

A comparison between these spectral data with those in the literature permitted unambiguously to attribute to compound DFFFII9 the structure of 5-*O*-methyl-myo-inositol, isolated from *Podocarpus sellowii* by Mukherjee et De Medeiros in 1988.

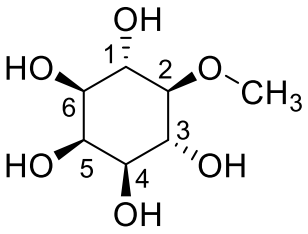

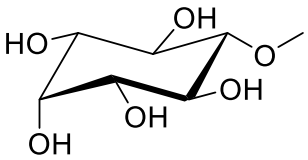

71

Table 28: ^{1}H (500MHz) and ^{13}C (125MHz) NMR assignments of compound DFFFII9 and 5-*O*-methyl-myo-inositol in DMSO-d_6.

Position	**DFFFII9**		**5-*O*-methyl-myo-inositol literature data[a]**	
	δ_H, mult (*J* in Hz)	δ_C, mult	δ_H, mult (*J* in Hz)	δ_C, mult
1/3	3.43, dd (4.9, 9.5)	72.6, CH	3.82, m	68.8, CH
2	3.69, m	72.9, CH	3.55, m	73.7, CH
4/6	3.13, m	72.3, CH	3.57, br s	71.4, CH
5	2.68, t (9.2)	86.0, CH	3.52, br s	70.8, CH
CH_3	3.45, s	62.2, CH_3	4.05, m	66.8, CH
OH	4.63, d (4.8)	-	-	-
OH	4.43, d (5.6)	-	-	-
OH	4.51, d (3.5)	-	-	-

[a](Mukherjee and De Medeiros, 1988)

II.1.3.5. Polyterpene: elucidation of DFR4

Compound DFR4 was obtained as an incolor oil in the solvent system PE/EtOAc (19:1). Its ESI mass spectrum showed in positive mode the pseudo molecular ion peak $[M+Na]^+$ at *m/z* 429.2 compatible with the molecular formula $C_{29}H_{50}O_2$ and implying five degrees of unsaturations. The ^1H and ^{13}C NMR spectra of this compound displayed signals of aromatic quaternary carbons at δ_C 121.0, δ_C 122.6, δ_C 118.4, δ_C 117.1 and two other bearing oxygen atoms at δ_C 144.5, δ_C 145.5. These spectra also displayed signals of five methyl groups at δ_H 0.88 (m) / δ_C 22.6, δ_H 0.85 (m) / δ_C 22.7, δ_H 0.83 (m) / δ_C 19.6, δ_H 0.84/ δ_C 19.7, δ_H 1.16 (s) / δ_C 23.8 attached to an aliphatic chain and three other at δ_H 2.04/ δ_C 11.3, δ_H 2.04/ δ_C 11.8 and δ_H 2.10/ δ_C 12.2 fixed to the benzene ring characteristics of tocopherols.

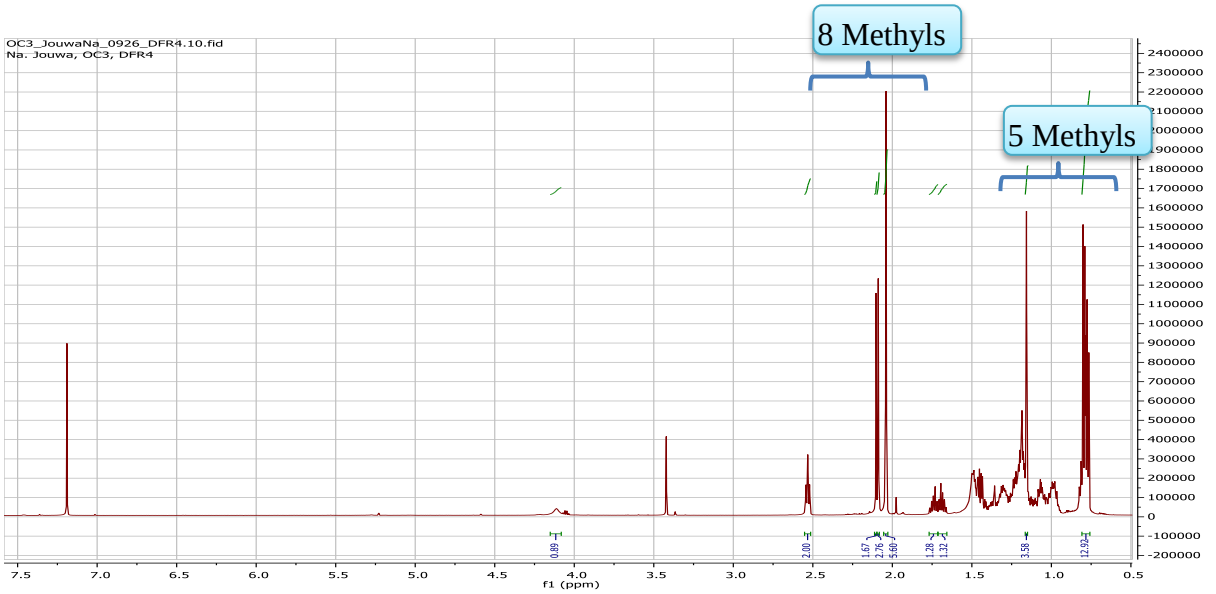

Figure 113: ^1H NMR spectrum (500 MHz) of compound DFR4 in $CDCl_3$

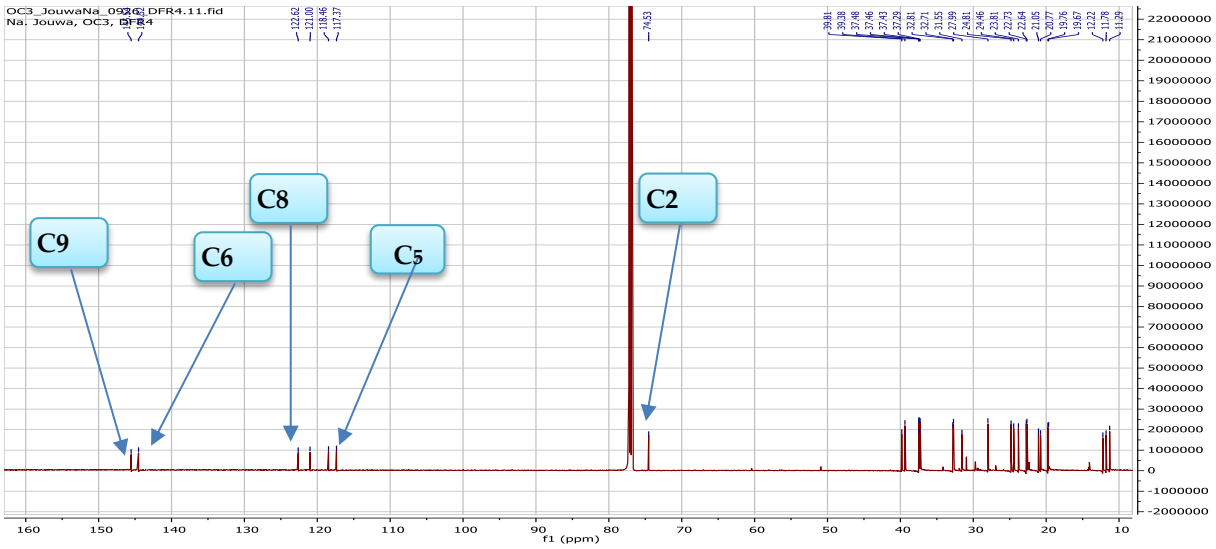

Figure 114: ^{13}C NMR spectrum (125 MHz) of compound DFR4 in $CDCl_3$

The above spectroscopic data coupled to those reported in the literature identified compound DFR4 as *α*-tocopherol, a known compound previously isolated from *Euryale ferox* by Han et *al*. in 2012.

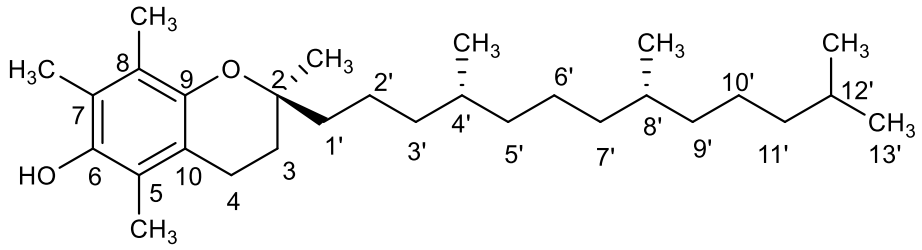

72

Table 29: ^{1}H (500MHz) and ^{13}C (125MHz) NMR assignments of compound DFR4 and *α*-tocopherol in $CDCl_3$

Position	DFR4		*α*-tocopherol literature data[a]	
	δ_H mult (*J* in Hz)	δ_C, mult.	δ_H mult (*J* in Hz)	δ_C
2		74.7 C		74.5
3		31.5 CH_2		31.5
4	2.53	20.7 CH_2	2.60	20.8
5		118.4 C		118.5
6		144.5 C		144.9
7		121.6 C		121.0
8		122.6 C		122.5
9		145.5 C		145.6
10		117.1 C		117.3
1'		39.3 CH_2		39.8
2'		20.7 CH_2	1.13	21.0
3'		37.4 CH_2		37.4
4'		32.7 CH		32.9
5'		37.4 CH_2		37.4
6'		24.1 CH_2		24.5
7'		37.3 CH_2		37.2
8'		32.8 CH		32.7
9'		37.4 CH		37.4
10'		24.8 CH_2		24.5
11'		39.4 CH_2		39.6
12'		27.8 CH		28.0
13'	0.85 m	22.7 CH_3	0.85	22.6
C2-CH_3	1.16 s	23.8 CH_3	1.17	23.8
C5-CH_3	2.04 s	11.3 CH_3	2.054	11.3
C7-CH_3	2.10 s	12.2 CH_3	2.11	12.2
C8-CH_3	2.04 s	11.8 CH_3	2.04	11.9
C4'-CH_3	0.84 m	19.7 CH_3	0.86	19.7
C8'-CH_3	0.83 m	19.6 CH_3	0.83	19.5
C12'-CH_3	0.88 m	22.9 CH_3	0.87	22.6

[a] (Baker et Myers, 1991)

II.1.3.6. Carotenoid: elucidation of DFFFII17D

Compound DFFFII17D was obtained as a red powder in the solvent system PE/EtOAc (4:1). Its ESI mass spectrum showed in positive mode the pseudo molecular ion peak $[M+H]^+$ at *m/z* 569.4 compatible with the molecular formula $C_{40}H_{56}O_2$ and implying thirteen degrees of unsaturations. Analysis of its ^1H and ^{13}C NMR data identified DFFFII17D as lutein, a known compound previously isolated from *Oxyanthus speciosus* by Aro et *al*. in 2019.

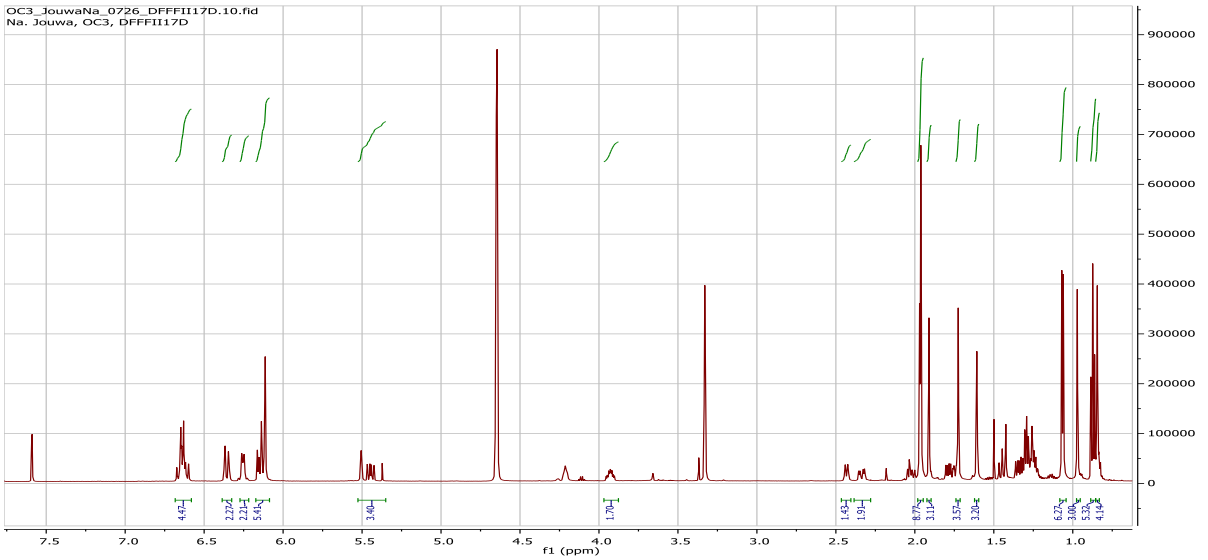

Figure 115: ^1H NMR spectrum of compound DFFFII17D (500MHz) in Methanol-d_4 + $CDCl_3$

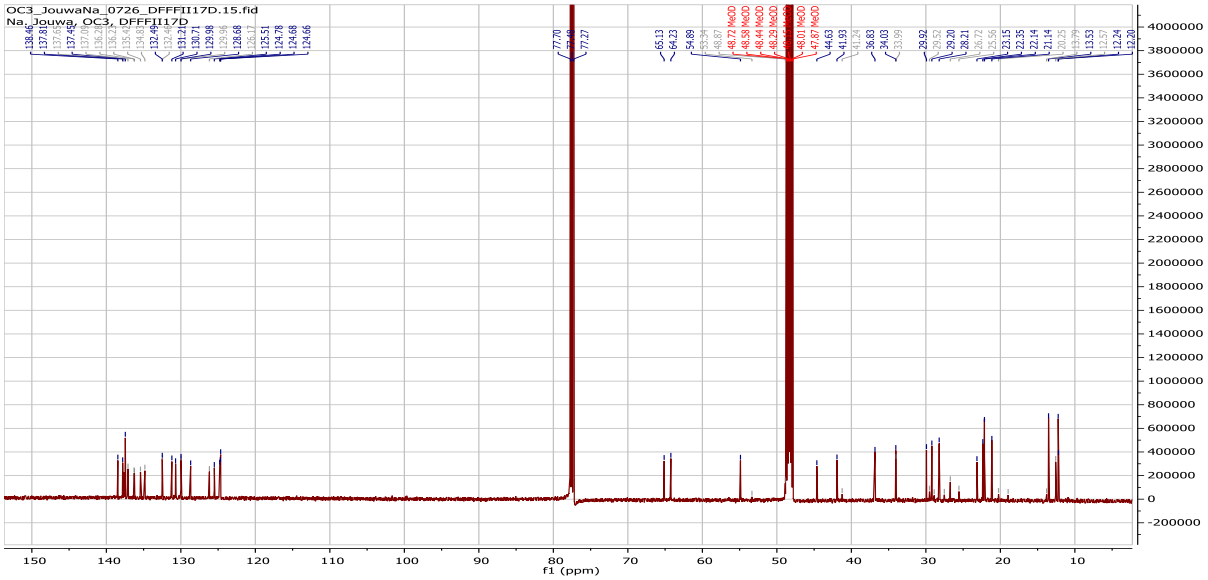

Figure 116: ^{13}C NMR spectrum (125 MHz) of compound DFFFII17D in Methanol-d_4 + $CDCl_3$

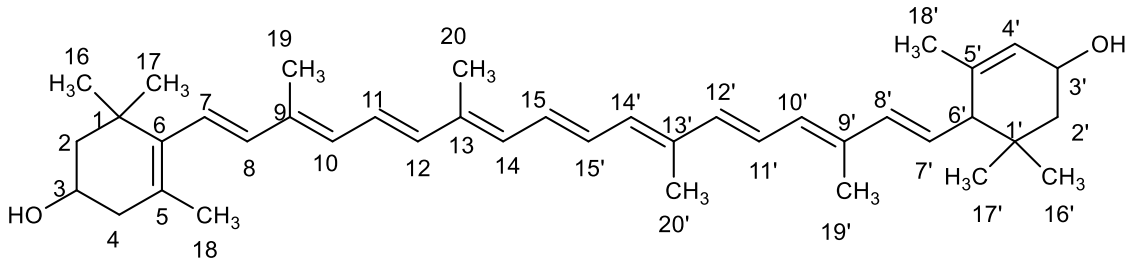

73

Table 30: ^{1}H (500MHz) and ^{13}C (125MHz) NMR assignments of compound DFFFII17D in Methanol-*d_4* + $CDCl_3$ and lutein in Acetone-*d_6*

Position	DFFFII17D			lutein literature data[a]	
	δ_H mult (*J* in Hz)	δ_C, mult.		δ_H mult (*J* in Hz)	δ_C
1/1'		37.3/34.7	C		37.1/34.1
2/2'		48.8/43.9	CH_2	1.50/1.37 m	48.4/44.7
3/3'		65.6/65.5	CH	4.03/4.26 m	65.1/65.9
4/4'		42.7/125.0	CH_2	2.05/2.42 m	42.5/125.6
5/5'		126.3/138.1	C		126.2/137.8
6/6'		136.9/54.7	C		137.6/55.0
7/7'	6.14/5.50 m	126.2.128.1	CH	6.12/5.46	125.6/128.6
8/8'	6.69/6.70 m	138.1/137.3	CH	6.67/6.67	138.5/137.8
9/9'		135.9/135.4	C		135.6/135.0
10/10'		131.3/130.5	CH		131.3/130.8
11/11'	6.73/6.73 m	125.6	CH	6.73/6.74 dd	124.9
12/12'	6.32/6.33 m	137.1	CH	6.30/6.30 d	137.6
13/13'		136.8	C		136.5
14/14'	6.22/6.23 m	132.0	CH	6.25/6.25	132.6
15/15'	6.64/6.64 m	130.6	CH_2	6.63/6.63 m	130.0
16/16'	1.06/1.04	29.6	CH_3	1.08/1.01	28.7
17/17'	1.07/0.88	30.8	CH_3	1.08/0.86	30.2
18/18'	1.78/1.62	22.4/22.7	CH_3	1.74/1.63	21.7/21.6
19/19'	1.97/1.90	13.7/13.4	CH_3	1.97/1.92	12.8/12.7
20/20'	1.96/1.31	13.6/13.5	CH_3	1.97/1.26	12.8/12.7

[a] (Moss, 1976; Kull et Pfander, 1997)

II.1.3.7. Monoglyceride: elucidation of compound DFR6

Compound DFR6 was obtained as a brown oil in the solvent system PE/EtOAc (3:2). The molecular formula $C_{31}H_{62}O_5$ of this compound was established by its HR-ESI mass

spectrum which showed the pseudo molecular ion peak $[M+Na]^+$ at *m/z* 537.4487 and corresponding to one unsaturation.

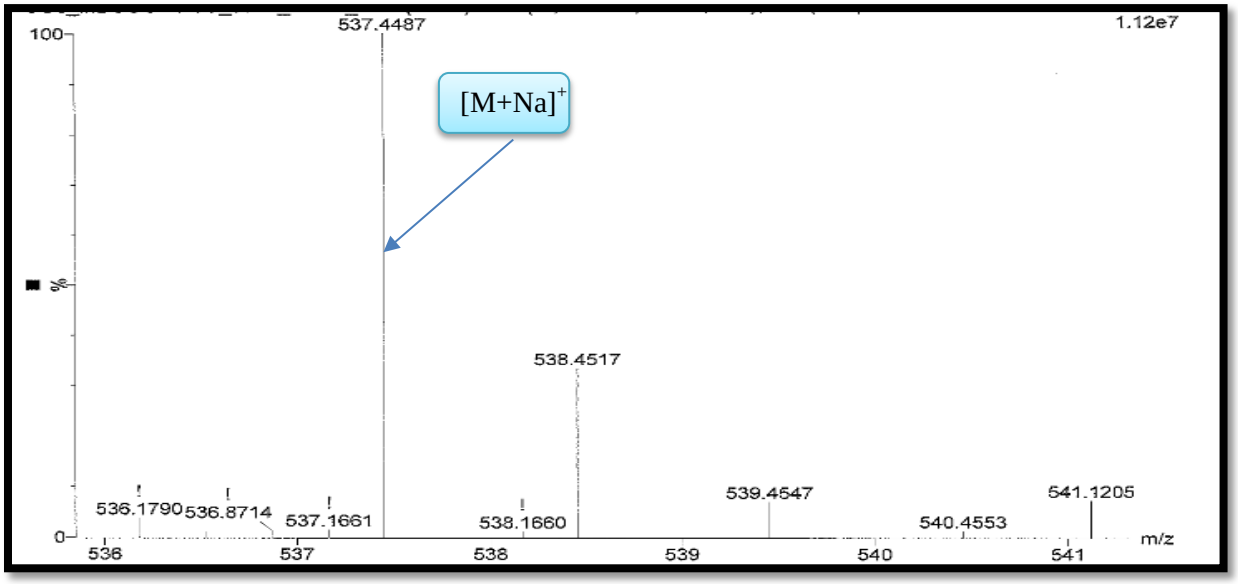

Figure 117: HR-ESI mass spectrum of compound DFR6

Its ^1H and ^{13}C NMR spectra exhibited signals of alkoxy protons and carbons at δ_H 4.71 (ddd, *J* = 11.1, 4.6, 2.4 Hz)/ δ_C 66.6, δ_H 4.64 (ddd, *J* = 11.1, 6.4, 2.4 Hz)/ δ_C 66.6, δ_H 4.44 (m)/ δ_C 70.8, δ_H 4.12 (dd, *J* = 5.5, 2.4 Hz), signals of four alkyl deshielded methylenes at δ_H 2.34 (m)/ δ_C 34.2, δ_H 1.74(m)/ δ_C 33.5, δ_H 1.62(m)/ δ_C 26.3 and δ_H 1.49(m)/ δ_C 25.0 signal of one carbonyl of ester at δ_C 173.3 and signals of the alkyl chain. The ^1H COSY correlations observed between proton at δ_H 4.44 and the other four alkoxy protons were indicative of the presence of a glycerol moiety (Chang et *al*., 2008). Additional signal was observed at δ_H 3.87 (td, *J* = 6.6, 2.3 Hz) / δ_C 61.9 corresponding to one oxymethylene and the absence of terminal methyl in the spectra of this compound suggested that this oxymethylene was terminal.

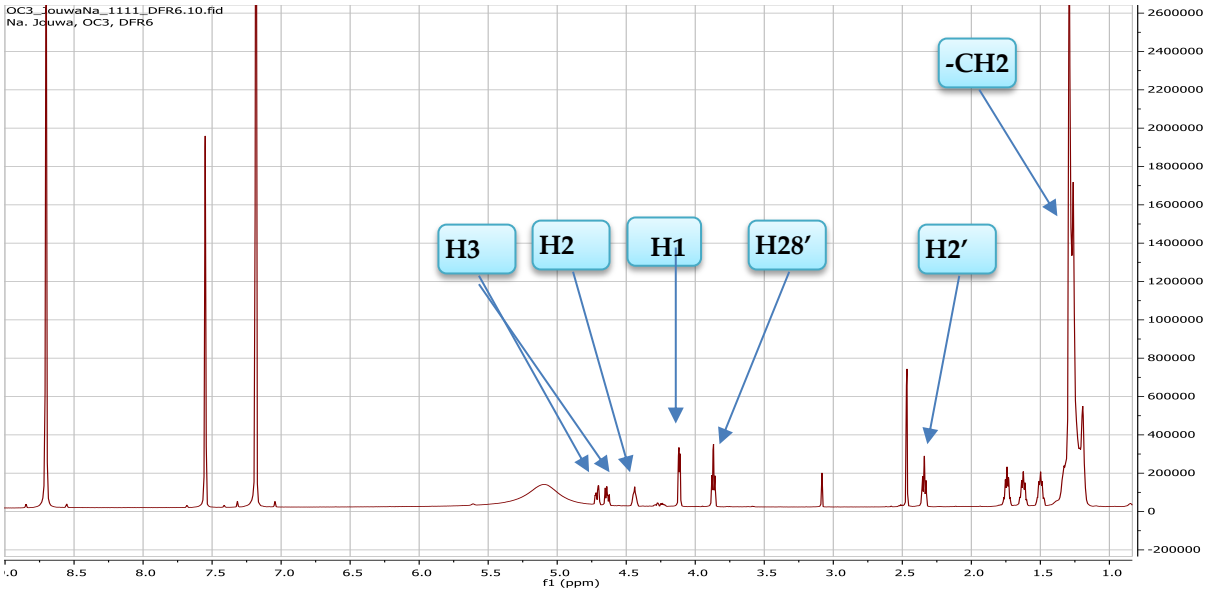

Figure 118: ^{1}H NMR spectrum (500 MHz) of compound DFR6 in C_5D_5N

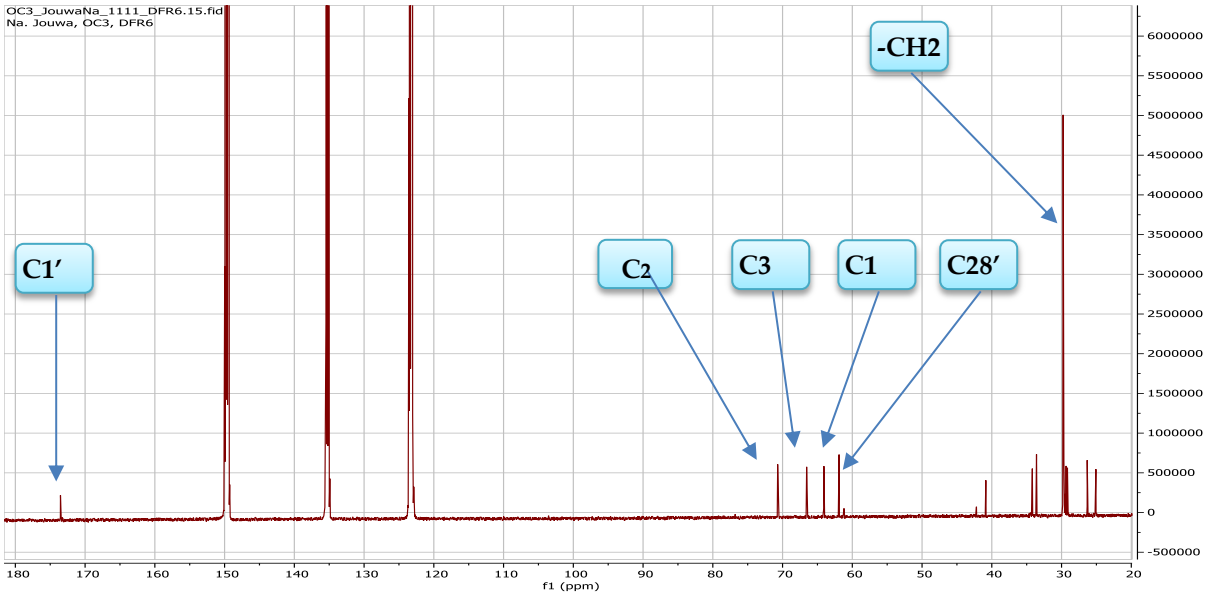

Figure 119: ^{13}C NMR spectrum (125 MHz) of compound DFR6 in C_5D_5N

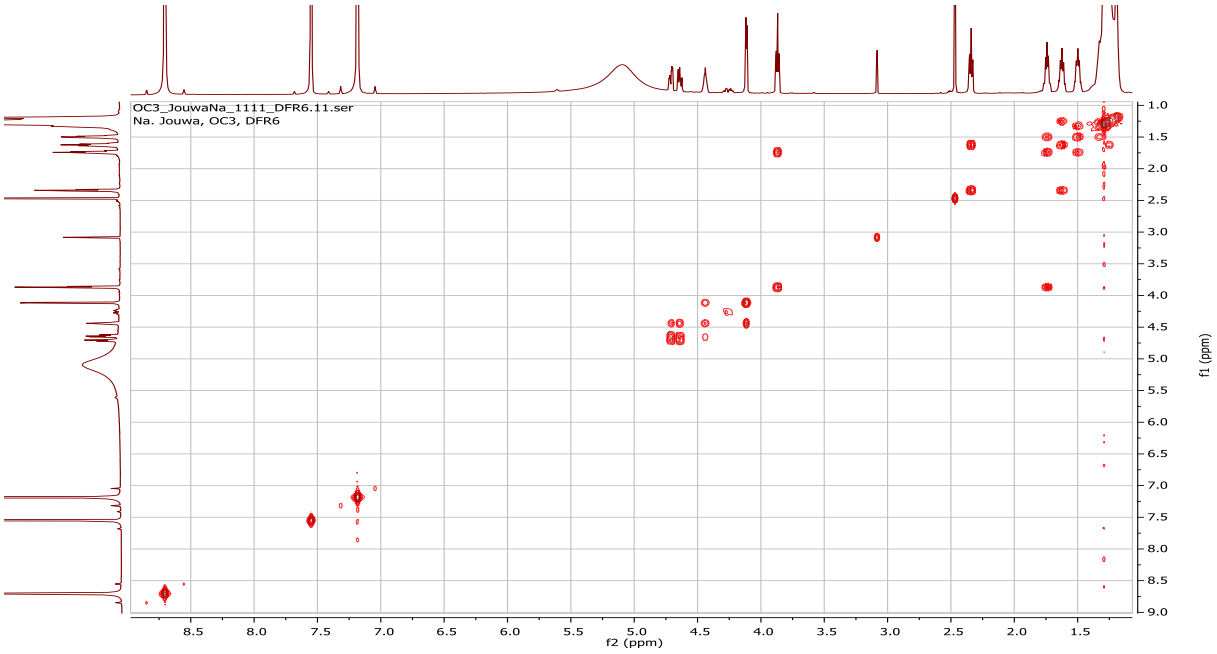

Figure 120 : COSY spectrum of compound DFR6

Based on the above spectroscopic data, compound DFR6 was identified as 1-*O*-(28-hydroxyoctacosanoyl) glycerol, a known compound isolated for the first time from *cinnamomum camphora* by Mukherjee et *al.* in 1994.

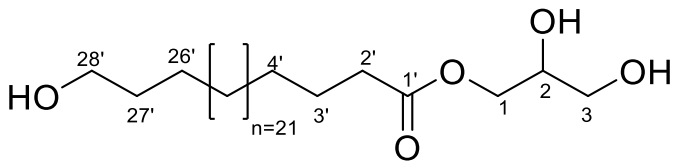

74

Table 31: ^{1}H (500MHz) and ^{13}C (125MHz) NMR assignments of compound DFR6 in C_5D_5N and 1-(28-hydroxyoctacosanoyl)glycerol in C_5D_5N

Position	DFR6		1-(28-hydroxyoctacosanoyl)glycerol literature data[a]	
	δ_H mult (*J* in Hz)	δ_C, mult.	δ_H mult (*J* in Hz)	δ_C
1	4.12 dd (5.5, 2.4)	64.3 (CH_2)	4.64 dd (11.8, 6.5)	66.7
			4.72 dd (11.8, 4.3)	
2	4.44 m	70.8	4.44 m	70.9
3a	4.64 ddd (11.1, 6.4, 2.4)	66.6 (CH_2)	4.12 d (5.9)	64.1
3b	4.71 ddd (11.1, 4.6, 2.4)			
1'	-	173.3 (C)	-	173.5

2'	2.34 m	34.2 (CH_2)	2.32 t (7.9)	34.4
3'	1.62 m	26.6 (CH_2)	1.65 m	26.5
4'	1.50 m	29.5 (CH_2)	1.50 m	30.1-29.3
5'-25'	1.25 brs	30.1-29.6 (CH_2)	1.28 brs	30.1-29.3
26'	1.49 m	25.0 (CH_2)	1.52 m	25.3
27'	1.74 m	33.5 (CH_2)	1.76 m	33.7
28'	3.87 td (6.6, 2.3)	61.9 (CH_2)	3.84 t (6.6)	62.1

[a](Mukherjee et *al.*, 1994)

II.1.3.8. Sterols

II.1.3.8.1. Elucidation of compound DGTFI4

Compound DGTFI4 was isolated as white needles in the solvent system PE/EtOAc (19:1). It gave a positive green coloration to the Liebermann-Burchard test indicative its steroidic nature. On its ESIMS, a sodiated pseudo molecular ion peak $[M+Na]^+$ at *m/z* 435.4 which is in accordance with the molecular formula $C_{29}H_{48}O$ implying six double bonds is observed.

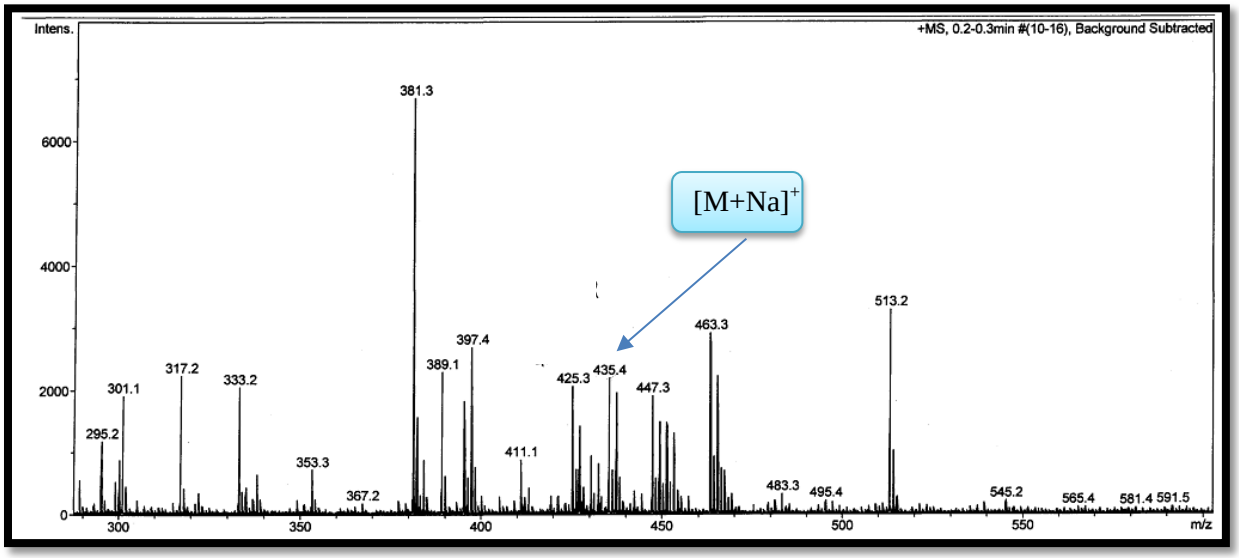

Figure 121: ESI mass spectrum of compound DGTFI4

The ^{1}H NMR spectrum of this compound displayed signals of one olefinic proton at δ_H 5.37 (H-6, brs) and one oxymethine proton at δ_H 4.61 (H-3, m) characteristic of β-sitosterol and signals of three olefinic protons at δ_H 5.37 (H-6, brs) δ_H 5.15 (H-22, dd, J = 14.6, 8.4 Hz) and δ_H 5.02 (H-23, dd, J = 15.6, 8.4 Hz) corresponding to signals of stigmsterol.

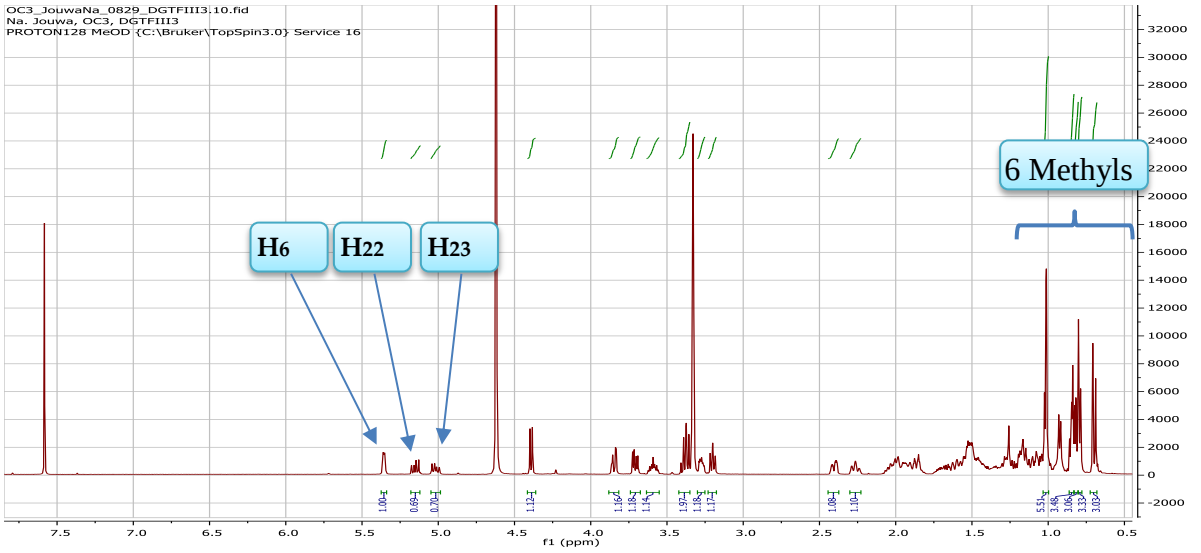

Figure 122: ^{1}H NMR spectrum (500 MHz) of compound DGTFI4 in $CDCl_3$

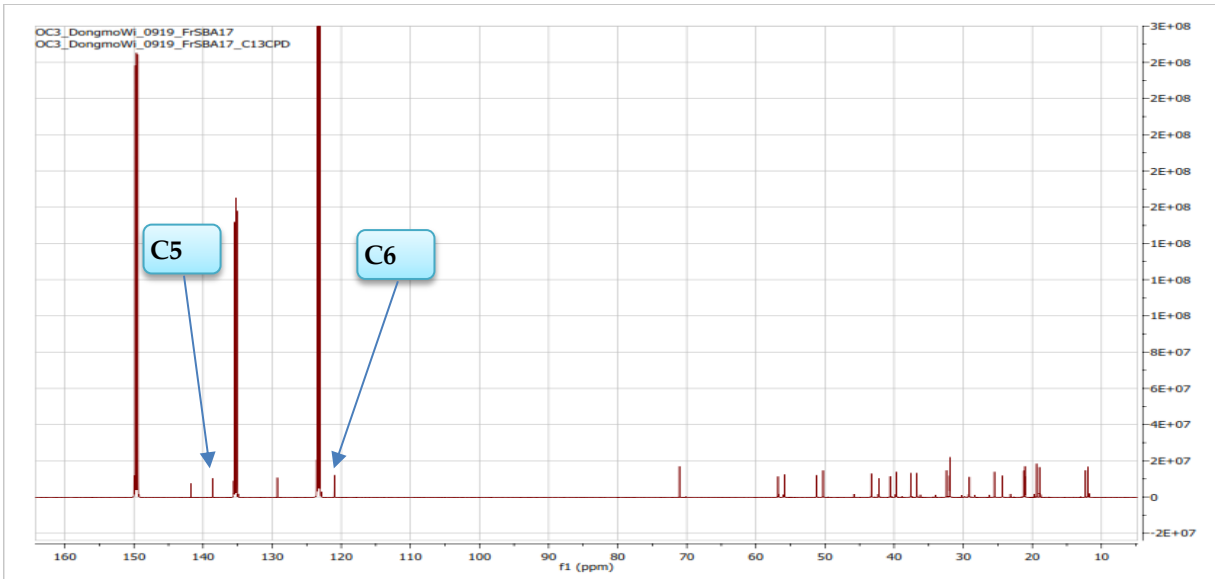

Figure 123: ^{13}C NMR spectrum (125 MHz) of compound DGTFI4 in C_5D_5N

Therefore compound DGTFI4 was identified as a mixture of stigmasterol and *β*-sitosterol, previously isolated from *Rubus suavissimus* by Chaturvedula et Prakashin in 2012.

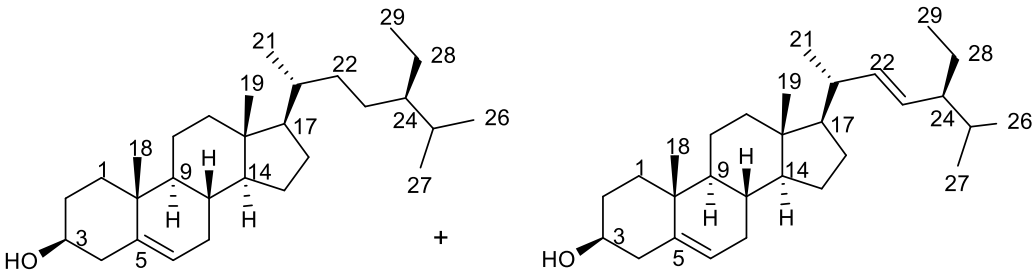

75 a **75 b**

Table 32: ^{1}H (500MHz) and ^{13}C (125MHz) NMR assignments of compound DGTFI4 in $CDCl_3$

	DGTFI4			
	75 a		75 b	
Position	δ_H mult (*J* in Hz)	δ_C, mult.	δ_H mult (*J* in Hz)	δ_C, mult.
1		37.0 CH_2		37.0 CH_2
2		28.2 CH_2		28.2 CH_2
3	4.61 m	73.6 CH	4.61 m	73.6 CH
4		39.7 CH_2		39.7 CH_2
5		139.7 C		139.7 C
6	5.37 brs	122.5 C	5.37 brs	122.5 C
7		31.9 CH_2		31.9 CH_2
8		31.8 C		31.8 C
9		50.0 CH		51.2 CH
10		36.6 C		36.6 C
11		21.0 CH_2		21.0 CH_2
12		38.1 CH_2		38.1 CH_2
13		42.3 CH		42.3 CH
14		56.7 CH		56.7 CH
15		24.3 CH_2		24.3 CH_2
16		26.1 CH_2		26.1 CH_2
17		56.0 CH		56.0 CH
18	0.68 s	11.8 CH_3	0.68 s	11.8 CH_3
19	1.02 s	19.0 CH_3	1.02 s	19.0 CH_3
20		36.1 CH		36.1 CH
21	0.92 d (6.6)	18.8 CH_3	0.92 d (6.6)	18.8 CH_3
22		33.9 CH_2	5.15 dd (14.6, 8.4)	138.3 CH
23		29.7 CH_2	5.02 dd (15.6, 8.4)	129.3 CH
24		45.8 CH		51.2 CH
25		29.1 CH		28.1 CH
26	0.83 m	19.8 CH_3	0.83 m	19.8 CH_3
27	0.81 m	19.3 CH_3	0.81 m	19.3 CH_3
28		23.0 CH_2		23.0 CH_2
29	0.87 m	12.0 CH_3	0.87 m	12.0 CH_3

II.1.3.8.2. Elucidation of DGTFIII3

Compound DGTFIII3 was isolated as a beige powder in the solvent system PE/EtOAc (2:3). It responded positively to the Liebermann Burchard reagent with a green coloration characteristic of steroids. Its ESIMS in negative mode showed the pseudo molecular ion peak $[M-H]^-$ at *m/z* 575.4 which correspond to the molecular formula $C_{35}H_{60}O_6$ implying seven degrees of insaturation. Analysis of its ^1H and ^{13}C NMR data identified DGTFIII3 as a mixture of stigmasterol-3-*O*-*β*-*D*-glucoside **76 b** and *β*-sitosterol-3-*O*-*β*-*D*-glucopyranoside **76 a**, previously isolated from *Viola odorata* by Peshin et Kar in 2017.

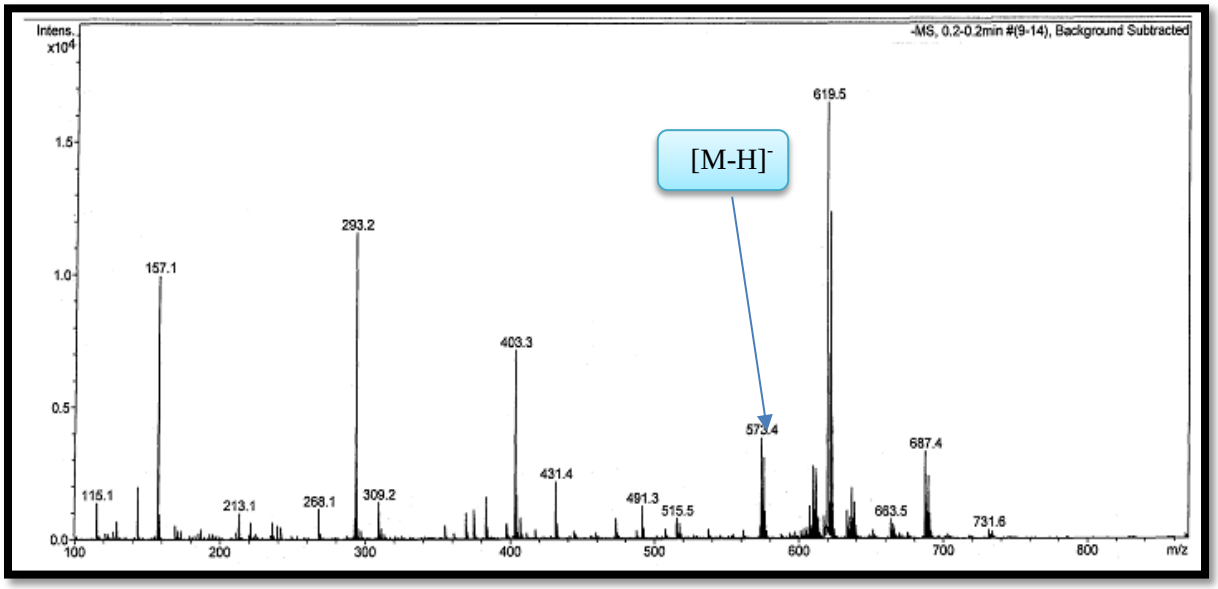

Figure 124: ESI mass spectrum of compound DGTFIII3

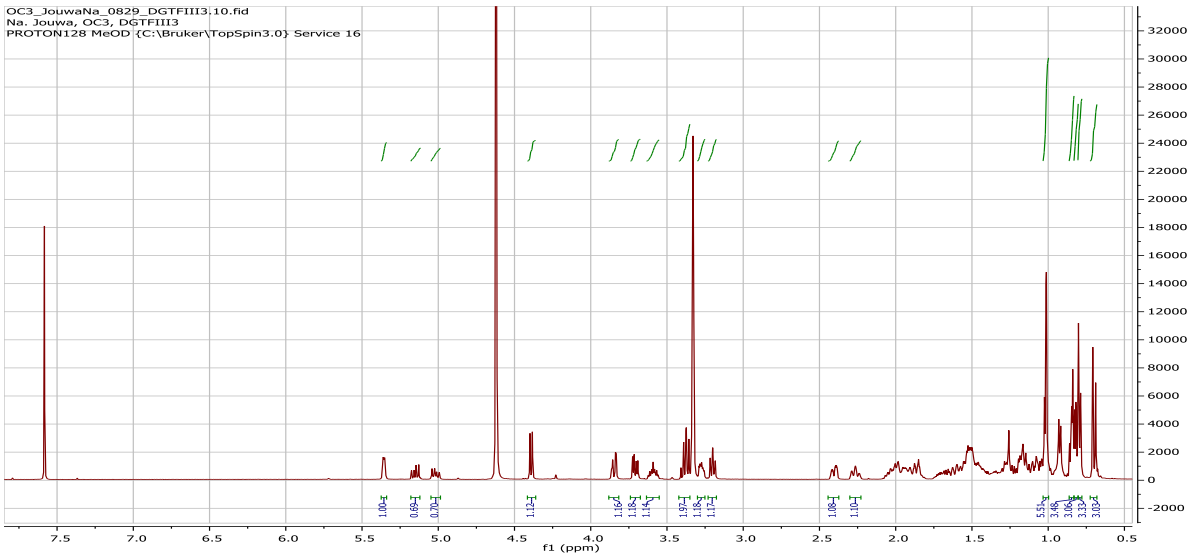

Figure 125: ^1H NMR spectrum (500 MHz) of compound DGTFIII3 in Methanol-d_4 + $CDCl_3$

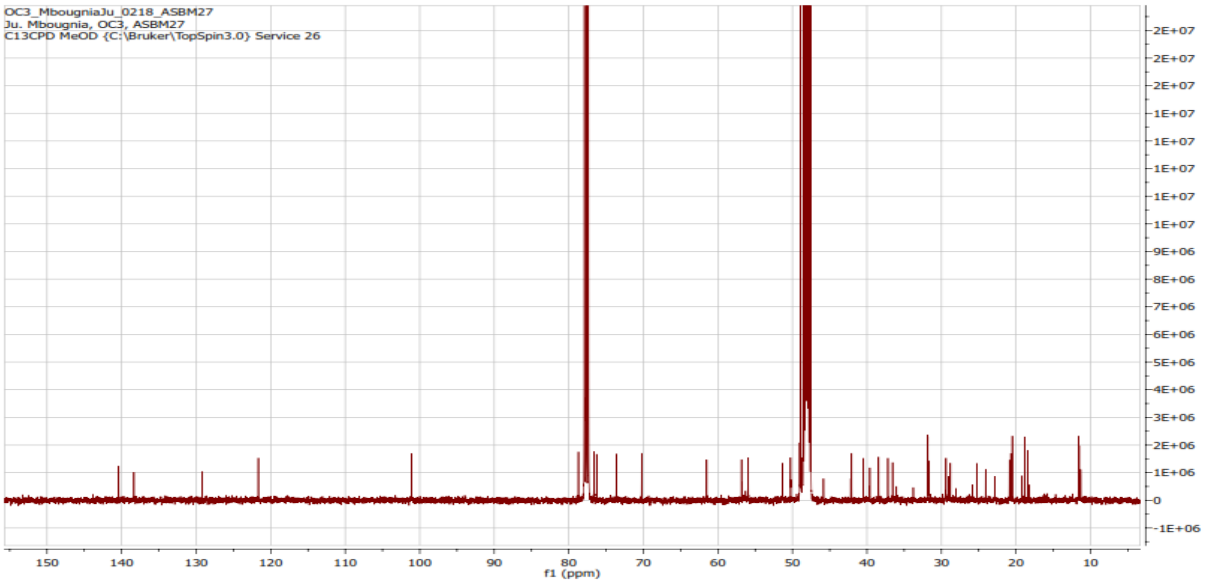

Figure 126: ^{13}C NMR spectrum (125 MHz) of compound DGTFIII3 in Methanol-d_4 + $CDCl_3$

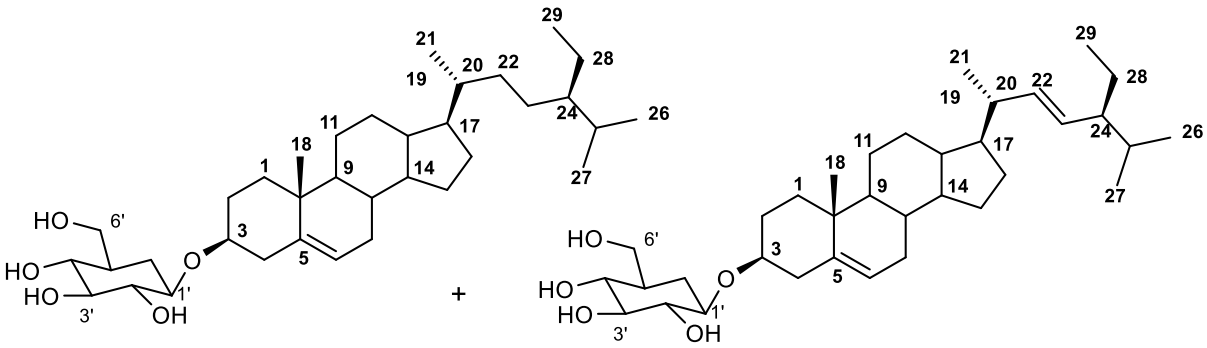

76 a + **76 b**

Table 33: ^{1}H (500MHz) and ^{13}C (125MHz) NMR assignments of compound DGTFIII3 in Methanol-d_4 + $CDCl_3$

Position	DGTFIII3			
	76 a		76 b	
	δ_H mult (*J* in Hz)	δ_C, mult.	δ_H mult (*J* in Hz)	δ_C, mult.
1		38.3 CH_2		38.3 CH_2
2		33.3 CH_2		33.3 CH_2
3	3.47 m	76.9 CH	3.47 m	76.9 CH
4		41.8 CH_2		41.8 CH_2
5		140.4 C		140.4 C
6	5.32 brs	121.1 C	5.32 brs	121.1 C
7		31.4 CH_2		31.4 CH_2
8		31.3 C		31.3 C
9		50.6 CH		50.6 CH
10		36.8 C		36.8 C

11		22.6 CH_2		22.6 CH_2
12		41.8 CH_2		41.8 CH_2
13		45.1 CH		45.1 CH
14		56.1 CH		56.1 CH
15		24.8 CH_2		24.8 CH_2
16		27.8 CH_2		27.8 CH_2
17		55.4 CH		55.4 CH
18	0.65 s	11.6 CH_3	0.65 s	11.6 CH_3
19	0.96 s	19.0 CH_3	0.96 s	19.0 CH_3
20		36.1 CH		36.1 CH
21	0.90 m	18.6 CH_3	0.90 m	18.6 CH_3
22		35.4 CH_2	5.15 dd (8.3, 14.6)	138.0 CH
23		29.2 CH_2	5.03 dd (8.3, 14.6)	121.1 CH
24		49.6 CH		49.6 CH
25		28.7 CH		28.7 CH
26	0.80 m	20.6 CH_3	0.80 m	20.6 CH_3
27	0.78 m	19.7 CH_3	0.78 m	19.7 CH_3
28		23.8 CH_2		23.8 CH_2
29	0.79 m	11.7 CH_3	0.79 m	11.7 CH_3
Glucose				
1'	4.22 d (8.4)	100.7 CH	4.22 d (8.4)	100.7 CH
2'	2.89 m	73.4 CH	2.89 m	73.4 CH
3'	3.10 m	76.7 CH	3.10 m	76.7 CH
4'	3.02 m	70.1 CH	3.02 m	70.1 CH
5'	3.10 m	76.7 CH	3.10 m	76.7 CH
6'	3.64 m	61.0 CH_2	3.64 m	61.0 CH_2
	3.41 m		3.41 m	

II.2. CHEMICAL TRANSFORMATIONS

The second part of our work consisted on the undertaking of chemical transformations on some compounds, in order to confirm their structure and/or increase their biological activities.

II.2.1. Acetylation

II.2.1.1. Acetylation of DGET4

Compound DGET4 underwent an acetylation reaction of all the hydroxyl functions present in its structure to yield the acetylated derivative DGET4Ac with a yield of 67.2 %. This transformation has been performed by stirring at room temperature this compound in the presence of acetic anhydride and pyridine 90%.

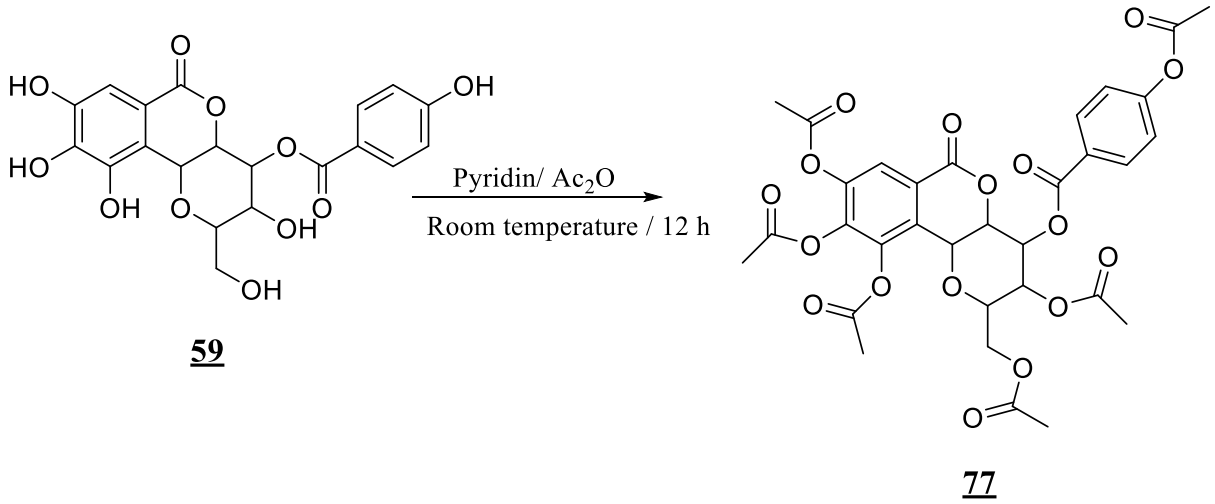

59 **77**

Scheme 12 : Acetylation reaction progress of compound DGET4

HRESIMS of compound DGET4Ac showed in positive mode (Figure 127) the sodium adduct ion peak $[M+Na]^+$ at *m/z* 709.1378.

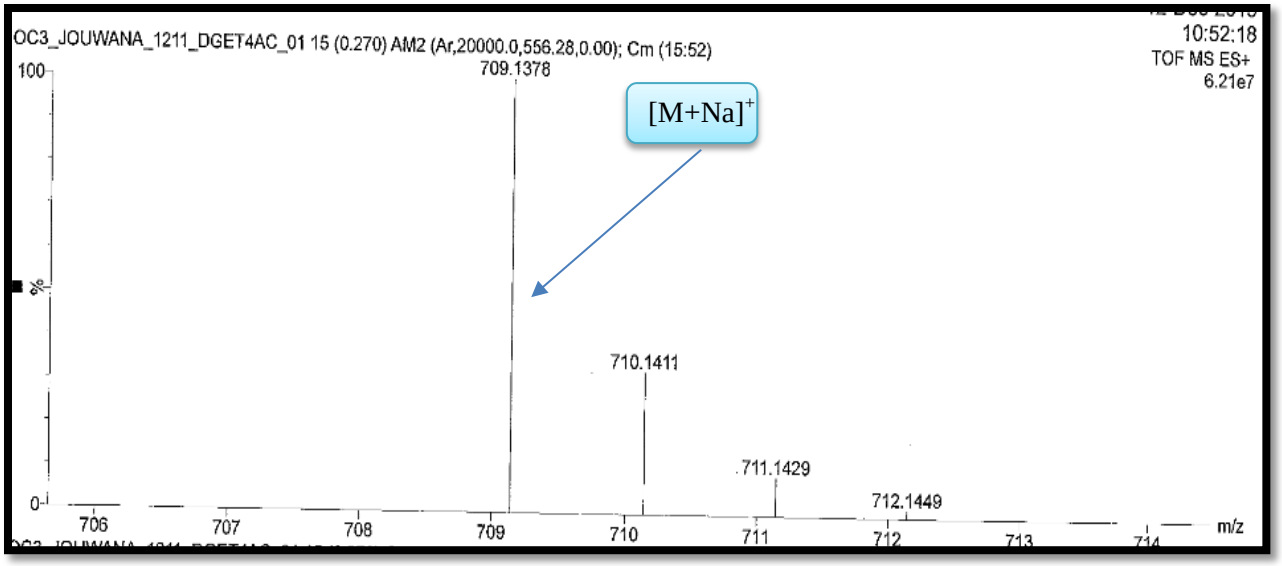

Figure 127: ESI mass spectrum of compound DGET4Ac

The formation of the acetylated derivative DGET4Ac was further confirmed by the appearance on ^{1}H and ^{13}C NMR spectra of this compound of six signals of acetoxy group including six methyls at δ_H 1.96 (3H, s), δ_H 2.08 (3H, s), δ_H 2.30 (9H, s), δ_H 2.33 (3H, s) and six carbonyl of esters at δ_C 170.9, δ_C 169.8, δ_C 169.2, δ_C 167.8, δ_C 166.7 and δ_C 167.2.

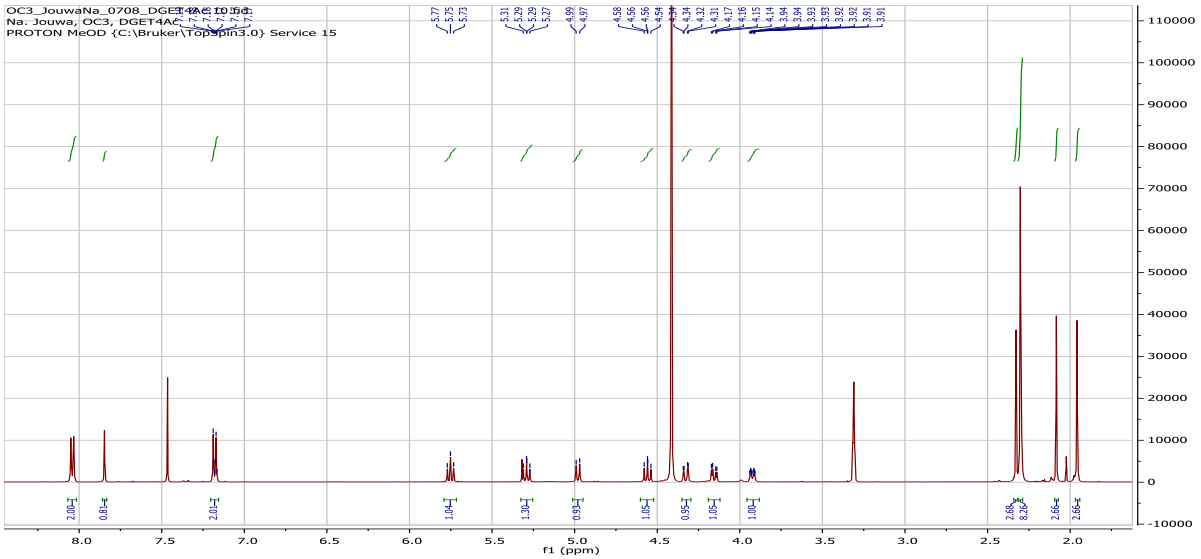

Figure 128: ^{1}H NMR spectrum (500 MHz) of compound DGET4Ac in Methanol-d_4

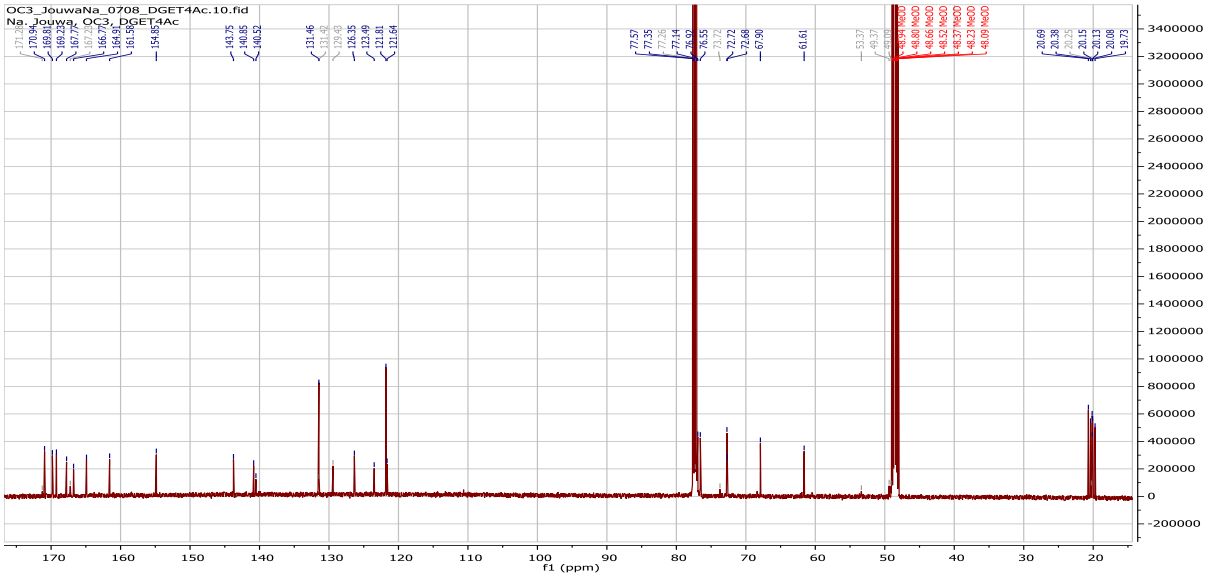

Figure 129: ^{13}C NMR spectrum (125 MHz, Methanol-d_4) of compound DGET4Ac.

Therefore compound DGET4Ac was identified as the new per-acetylated derivative of 4-*O*-*p*-hydroxybenzoylnorbergenin.

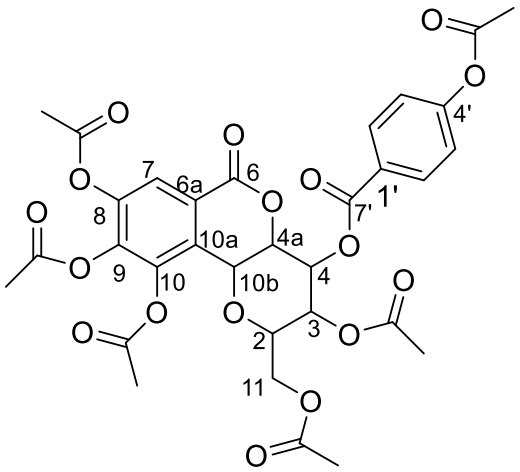

77

Table 34: ^{1}H (500MHz) and ^{13}C (125MHz) NMR assignments of compounds DGET4 (4-*O*-*p*-hydroxybenzoylnorbergenin) in Methanol-d_4 and DGET4Ac (per-acetylated 4-*O*-*p*-hydroxybenzoylnorbergenin) in Methanol-d_4 + $CDCl_3$.

Position	DGET4		DGET4Ac	
	δ_H, mult (*J* in Hz)	δ_C, mult	δ_H, mult (*J* in Hz)	δ_C, mult
2	3.82, m	83.1, CH	3.92, m	76.5, CH
3	3.80, m	70.2, CH	5.29, m	67.9, CH
4	5.60, dd (8.4, 9.8)	76.2, CH	5.75, t (9.5)	72.6, CH
4a	4.42, t (10.4)	79.1, CH	4.56, t (10.6)	76.9, CH
6	-	166.0, C	-	161.7, C
6a	-	114.1, C	-	129.4, C
7	7.08, s	111.1, CH	7.84, s	121.6, CH
8	-	147.4, C	-	143.7, C
9	-	141.5, C	-	140.5, C
10	-	143.7, C	-	140.8, C
10a	-	117.0, C	-	123.4, C
10b	5.14, d (10.4)	74.4, CH	4.98, d (10.6)	72.7, CH
11	4.04, dd (11.6, 1.6)	62.5, CH_2	4.32, dd (2.2 ,12.8)	61.8, CH_2
	3.75, m		4.15, dd (3.6 ,12.8)	
1'	-	122.0, C	-	129.4, C
2'/6'	7.97, d (8.8)	133.2, CH	8.08, d (8.9	121.8, CH
3'/5'	6.84, d (8.8)	116.1, CH	7.18, d (8.9)	131.4, CH
4'	-	163.7, C	-	154.8, C
7'	-	167.5, C	-	164.9, C
OAc				
3	-	-	1.96, s*	19.7, CH_3*
8	-	-	2.30, s*	20.0, CH_3*
9	-	-	2.08, s*	20.3, CH_3*
10	-	-	2.30, s*	20.1, CH_3*
11	-	-	2.33, s*	20.7, CH_3*
4'	-	-	2.30, s*	20.1, CH_3*
CO	-	-		166.7
CO	-	-		167.2
CO	-	-		170.9
CO	-	-		169.8
CO	-	-		167.8
CO	-	-		169.2

* value are exchangeable

II.2.1.2. Acetylation of DFR5

Acetylation of compound **DFR5** was achieved with acetic anhydride in pyridine by following the same conditions reaction used for compound DGET4 to yield the acetylated derivative DFR5Ac (72.1%).

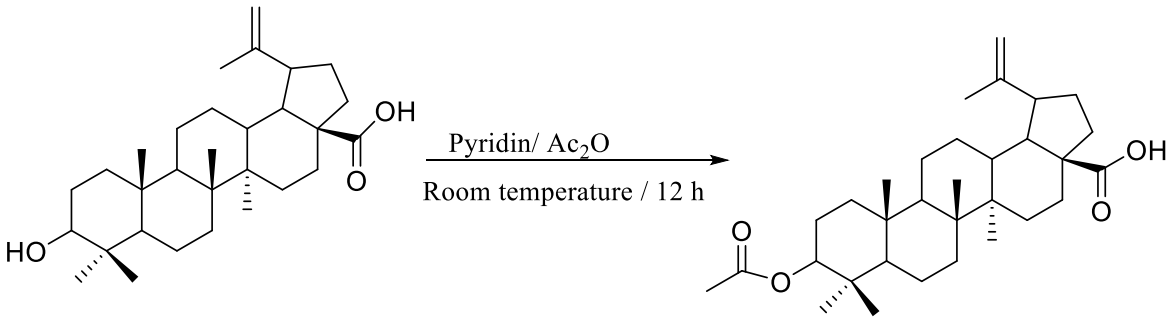

Scheme 13 : Acetylation reaction process of compound DFR5

ESI mass spectrum of compound DFR5Ac showed in negative mode a pseudo molecular ion peak $[M-H]^-$ at *m/z* 497.2 corresponding to the mass of betulinic acid on which one acetoxy group was added.

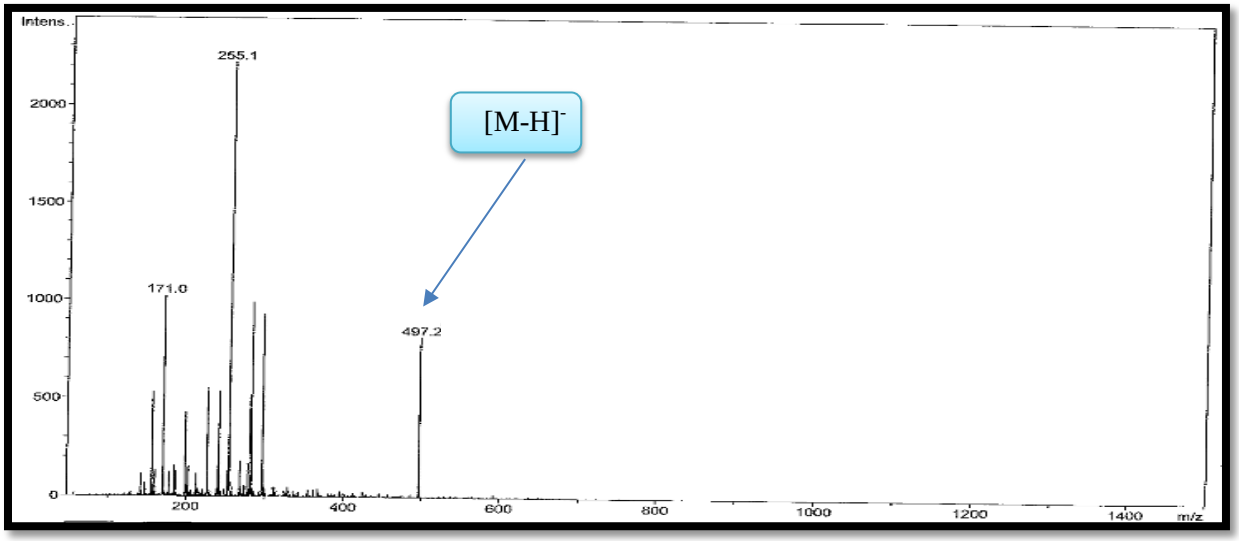

Figure 130: ESI mass spectrum of compound DFR5Ac

The Formation of the acetylated derivative was further confirmed on one hand by the appearence on the ^{1}H NMR spectrum of compound DFR5Ac, in addition to signals observed for betulinic acid, of one additional singlet of methyl at δ_H 1.97 and on the other hand by the change on chemical shift of signal of proton H-3 which appeared downfield at δ_H 4.40 (1H, m).

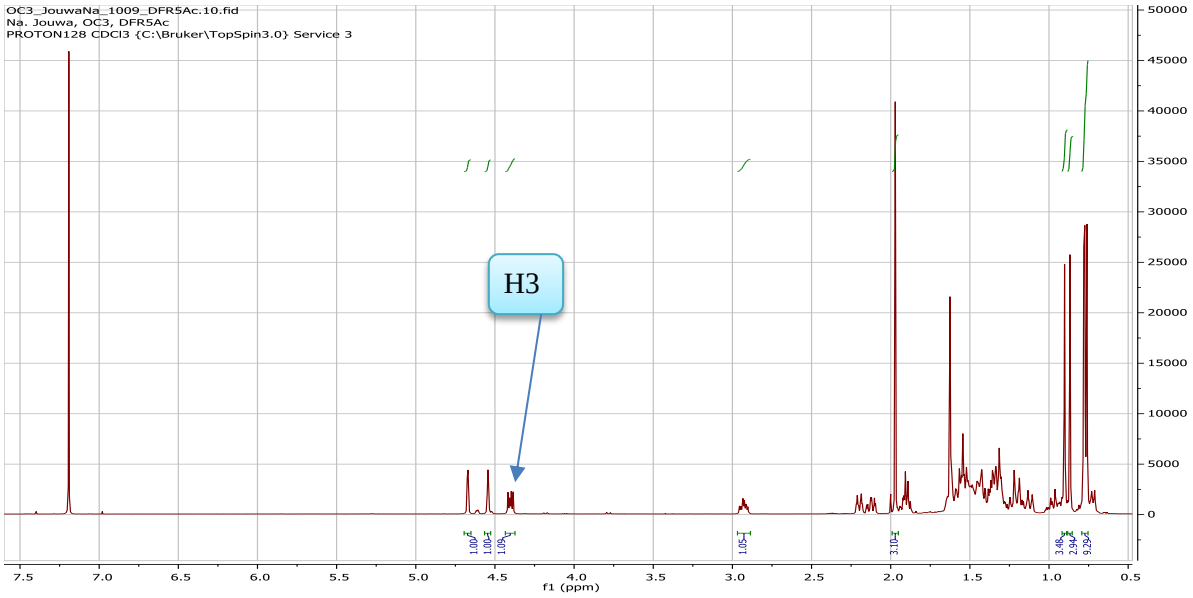

Figure 131: ^{1}H NMR spectrum of compound DFR5Ac (500 MHz, $CDCl_3$).

On the basis of the above spectroscopic data, compound DFR5Ac was identified as betulinic acid acetate.

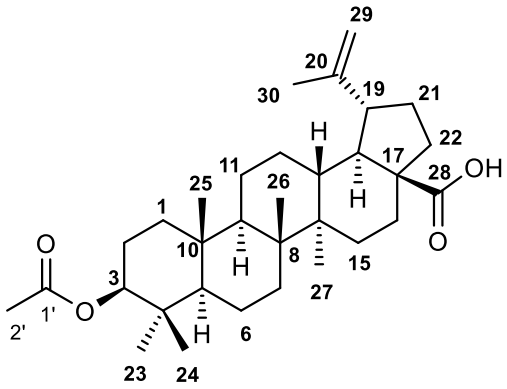

78

Table 35: ^{1}H (500MHz) NMR assignment of compounds DFR5 (betulinic acid) in Methanol-d_4 + $CDCl_3$ and DFR5Ac (betulinic acid acetate) in $CDCl_3$.

Position	DFR5		DFR5Ac	
	δ_H mult (*J* in Hz)	δ_C, mult.	δ_H mult (*J* in Hz)	δ_C
1		39.3 CH_2		39.5
2		28.3 CH_2		28.7
3	3.12 dd (10.9, 5.4)	78.1 CH	4.40 m	78.1
4	-	39.5 C		39.5
5	0.67 m	55.9 CH	0.82 m	56.0
6		18.8 CH_2		18.8
7		34.8 CH_2		34.9
8		41.1 C		41.1
9		50.9 CH		51.0
10		37.6 C		37.6
11		21.2 CH_2		21.2
12		26.1 CH_2		26.2
13		38.6 CH		38.7
14		42.8 C		42.9
15		31.2 CH_2		30.3
16		32.9 CH_2		32.9
17		56.6 C		56.9
18		49.7 CH		49.8
19	3.00 m	47.8 CH	3.52 m	47.8
20		151.3 C		151.3
21		30.3 CH_2		31.2
22		37.5 CH_2		37.6
23	1.21 s	28.6 CH_3	1.22 s	28.7
24	0.99 s	16.3 CH_3	1.00 s	16.3
25	0.81 s	16.4 CH_3	0.83 s	16.4
26	1.04 s	16.4 CH_3	1.06 s	16.4
27	1.06 s	15.0 CH_3	1.07 s	14.9
28	-	178.8 C	-	178.8
29	4.93 brs	109.9 CH_2	4.95 s	109.9
	4.76 brs		4.77 s	
30	1.78 s	19.5 CH_3	1.79 s	19.5
1'	-	-	-	171.6
2'	-	-	1.97	21.3

II.2.1.3. Acetylation of DFFFII13I

Acetylation of compound DFFFII13I followed the same condition reactions than those of compounds DGET4 and DFR5. This reaction yielded compound DFFFII13IA with an efficiency of 61.4 %.

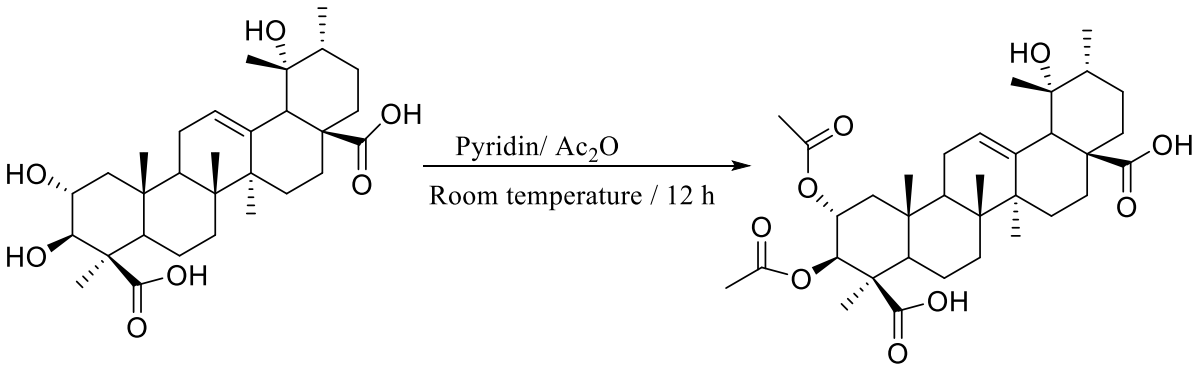

Scheme 14 : Acetylation reaction process of compound DFFFII13I

ESI mass spectrum of compound DFFFII13IA showed in negative mode the pseudo molecular ion peak $[M-H]^-$ at *m/z* 601.2 corresponding to the mass of vismiaefolic acid plus two acetoxy groups.

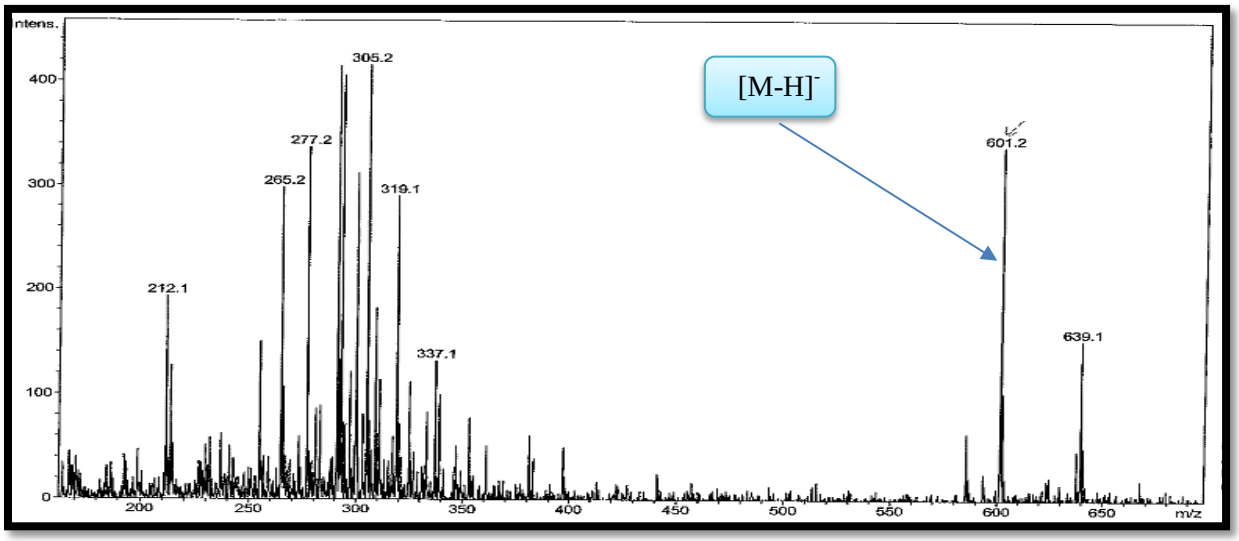

Figure 132: ESI mass spectrum of compound DFFFII13IA

The ^{1}H NMR spectrum of compound DFFFII13IA showed, in addition to signals observed for vismiaefolic acid, two singlets of methyl at δ_H 1.97 and δ_H 2.07. This spectrum also showed the signals of methine protons H-2 and H-3 downfield at δ_H 5.73 (m) and δ_H 4.79 (d, J = 10.4 Hz) respectively, which confirmed the fact that acetoxy groups were fixed at positions C-2 and C-3.

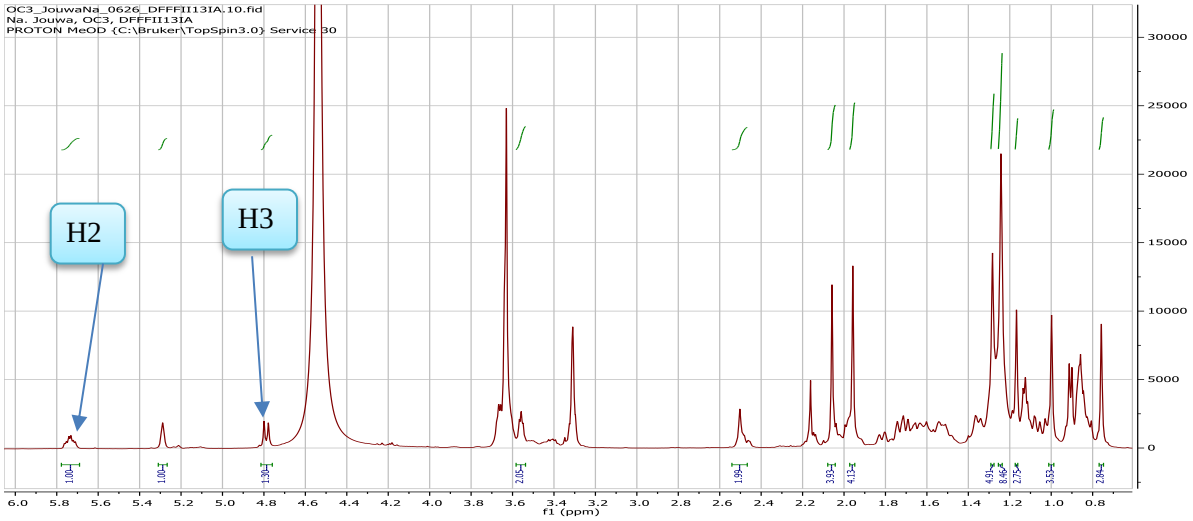

Figure 133: ^{1}H NMR spectra of compound DFFFII13IA (500 MHz) in Methanol-d_4.

The above spectroscopic data established compound DFFFII13IA as per acetylated derivative of vismiaefolic acid.

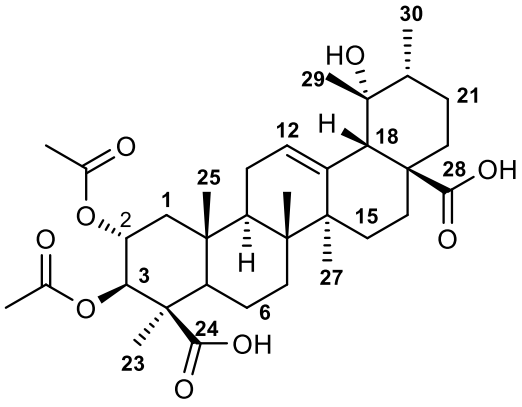

79

Table 36: ^{1}H (500MHz) NMR assignment of compounds DFFFII13I (vismiaefolic acid) in DMSO-d_6 and DFFFII13IA (per-acetylated vismiaefolic acid) in Methanol-d_4.

Position	DFFFII13I		DFFFII13IA	
	δ_H mult (J in Hz)	δ_C, mult.	δ_H mult (J in Hz)	δ_C
1		47.9 CH_2		48.1
2	3.93 m	67.3 CH	5.73 m	68.2
3	2.75 d (9.7)	83.0 CH	4.79 d (10.4)	83.7
4		49.3 C		49.7
5	0.94 m	55.9 CH	1.18 m	56.5
6		19.1 CH_2		20.6

7		32.6 CH_2		33.4
8		40.1 C		39.9
9		46.7 CH	1.87 m	46.8
10		38.3 C		38.6
11		24.2 CH_2		23.9
12	5.18 t (3.7)	127.3 CH	5.51 brs	127.6
13		139.0 C		139.5
14		40.4 C		41.9
15		29.1 CH_2		28.9
16		25.0 CH_2		26.0
17		47.6 C		47.9
18	2.38 s	53.7 CH	2.96 s	54.3
19		72.2 C		72.3
20		41.7 CH		42.0
21		26.6 CH_2		26.5
22		38.8 CH_2		38.1
23	1.29 s	24.8 CH_3	1.68 s	24.7
24		178.3 C		180.3
25	0.85 s	15.0 CH_3	1.11 s	14.9
26	0.70 s	17.0 CH_3	1.05 s	16.8
27	1.29 s	24.4 CH_3	1.65 s	24.2
28		179.5 C		180.5
29	1.08 s	26.9 CH_3	1.39 d (6.5)	26.7
30	0.84 d (6.7)	16.8 CH_3	1.06 d (6.0)	16.4
1'	-	-	-	172.3
2'	-	-	2.02	21.5
3'	-	-	-	171.7
4'	-	-	1.98	22.6

II.2.2. Allylation

II.2.2.1. Allylation of DGET4

Compound DGET4 was subjected to an allylation reaction using allyl bromide and calcium carbonate in anhydrous acetone. This reaction was performed at 70°C during 4 Hours and all the phenolic hydroxide present in the structure of this compound reacted to yield a per allylated derivative named DGET4Al (58.6 %).

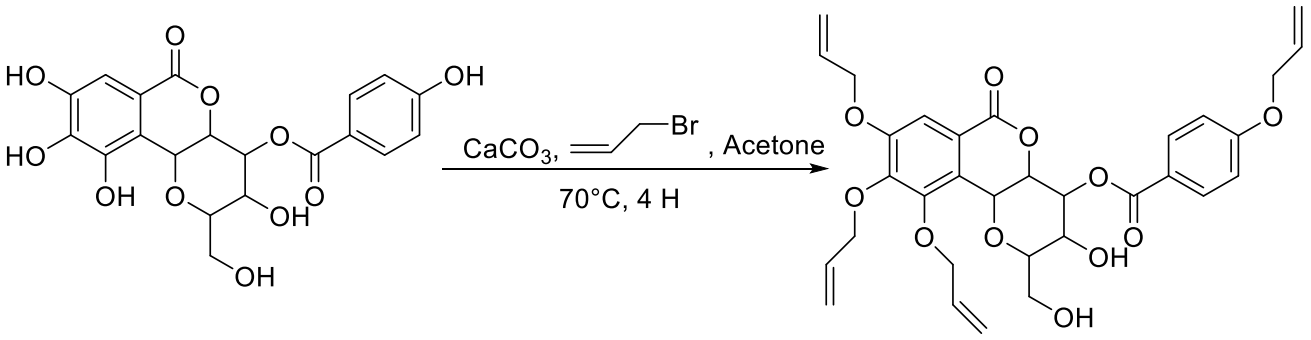

Scheme 15 : Allylation reaction process of compound DGET4

HRESIMS of this compound showed in positive mode the pseudo molecular ion peak $[M+Na]^+$ at *m/z* 617.1998, which corresponded to the mass of 4-*O*-*p*-hydroxybenzoylnorbergenin added to four allyl groups.

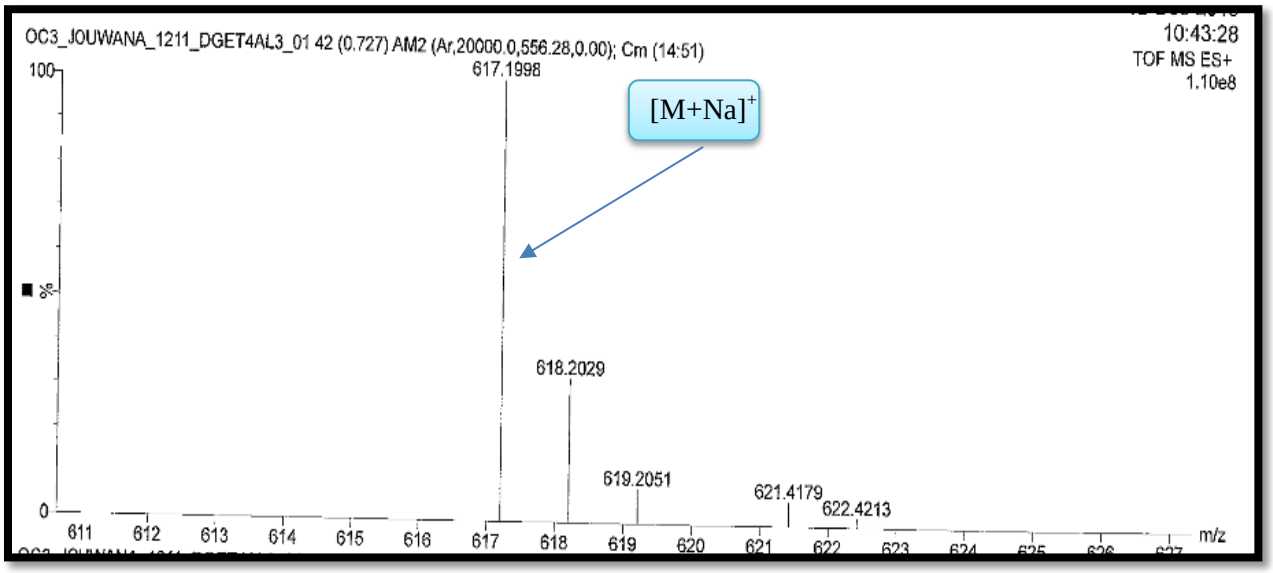

Figure 134: HRESI mass spectrum of compound DGET4Al

This information was supported by the ^{1}H and ^{13}C NMR spectra of compound DGET4Al which showed, in addition to the signal of 4-*O*-*p*-hydroxybenzoylnorbergenin, signals of four allyl groups including four oxymethylenes at δ_H 4.54 (2H, m) / δ_C 68.9, δ_H 4.56 (2H, m) / δ_C 69.9, δ_H 4.58 (2H, m) / δ_C 74.4, δ_H 4.58 (2H, m) / δ_C 74.5, olefinic protons and carbons at δ_H 5.21 (2H, m) / δ_C 117.6, δ_H 5.24 (2H, m) / δ_C 118.2, δ_H 5.26 (2H, m) / δ_C 118.3, δ_H 5.28 (2H, m) / δ_C 118.4, δ_H 6.01 (1H, m) / δ_C 132.2, δ_H 6.01 (1H, m) / δ_C 132.3, δ_H 6.01 (1H, m) / δ_C 133.5 and δ_H 6.01 (1H, m) / δ_C 133.6.

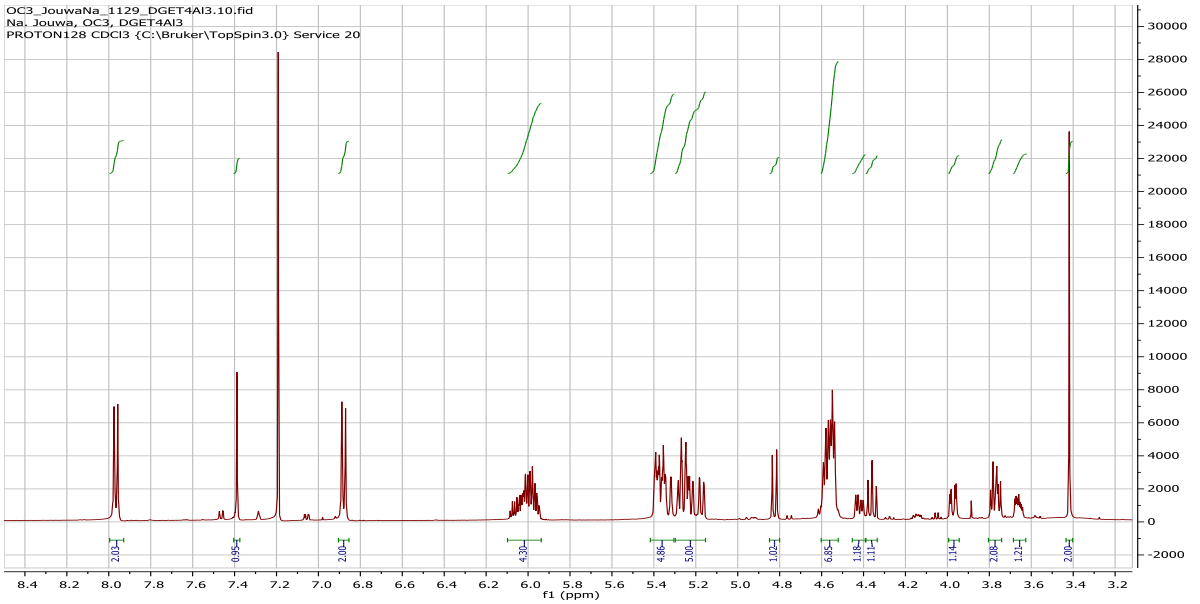

Figure 135: ^{1}H NMR spectrum of compound DGET4Al

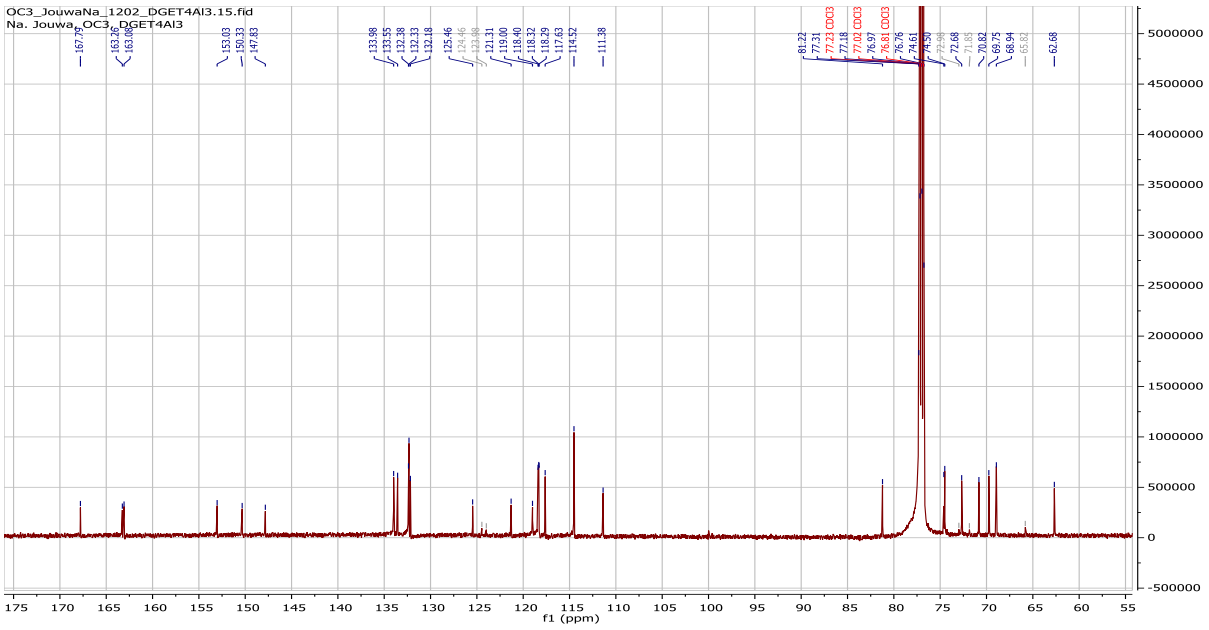

Figure 136: ^{13}C NMR spectrum of compound DGET4Al

Based on those spectroscopic data, compound DGET4Al was identified as the new per allylated derivative of 4-*O*-*p*-hydroxybenzoylnorbergenin.

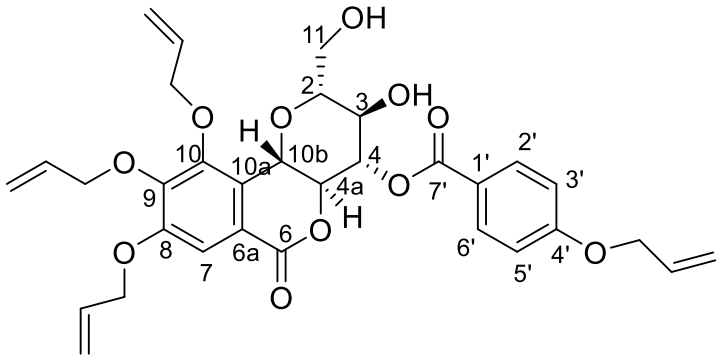

80

Table 37: ^{1}H (500 MHz) and ^{13}C (125MHz) NMR assignment of compounds DGET4 in Methanol-*d_4* and DGET4Al in $CDCl_3$.

Position	DGET4		DGET4Al	
	δ_H, mult (*J* in Hz)	δ_C, mult	δ_H, mult (*J* in Hz)	δ_C, mult
2	3.82, m	83.1, CH	3.92, m	81.2, CH
3	3.80, m	70.2, CH	5.29, m	70.9, CH
4	5.60, dd (8.4, 9.8)	76.2, CH	5.75, t (9.5)	76.7, CH
4a	4.42, t (10.4)	79.1, CH	4.56, t (10.6)	79.2, CH
6	-	166.0, C	-	163.0, C
6a	-	114.1, C	-	114.4, C
7	7.08, s	111.1, CH	7.84, s	111.3, CH
8	-	147.4, C	-	147.0, C
9	-	141.5, C	-	140.5, C
10	-	143.7, C	-	141.9, C
10a	-	117.0, C	-	117.7, C
10b	5.14, d (10.4)	74.4, CH	4.98, d (10.6)	74.1, CH
11	4.04, dd (11.6, 1.6)	62.5, CH_2	4.32, dd (2.2 ,12.8)	61.8, CH_2
	3.75, m		4.15, dd (3.6 ,12.8)	
1'	-	122.0, C	-	122.6, C
2'/6'	7.97, d (8.8)	133.2, CH	8.08, d (8.9	133.7, CH
3'/5'	6.84, d (8.8)	116.1, CH	7.18, d (8.9)	117.6, CH
4'	-	163.7, C	-	163.3, C
7'	-	167.5, C	-	167.7, C
OCH_2				
8	-	-	1.96, s*	19.7, CH_3*
9	-	-	2.30, s*	20.0, CH_3*
10	-	-	2.08, s*	20.3, CH_3*

II.2.2.2. Allylation of DFR5

This reaction was performed at 70°C by using sodium hydroxide and allyl bromide in anhydrous acetone and the allylated derivative DFR5Al (64.9 %) was obtained after 4 Hours of agitation.

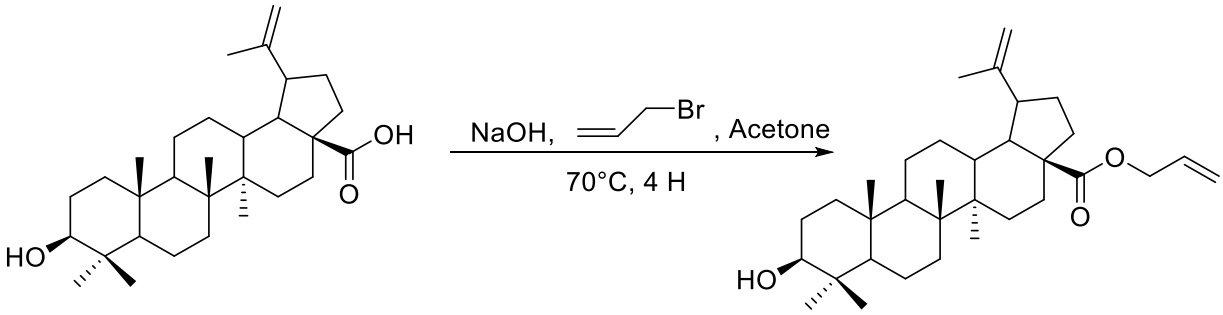

Scheme 16 : Allylation reaction process of compound DFR5Al

ESI mass spectrum of this compound showed in positive mode the pseudo molecular ion peak $[M+Na]^+$ at *m/z* 519.4 corresponding to the mass of betulinic acid on which one allyl group was added.

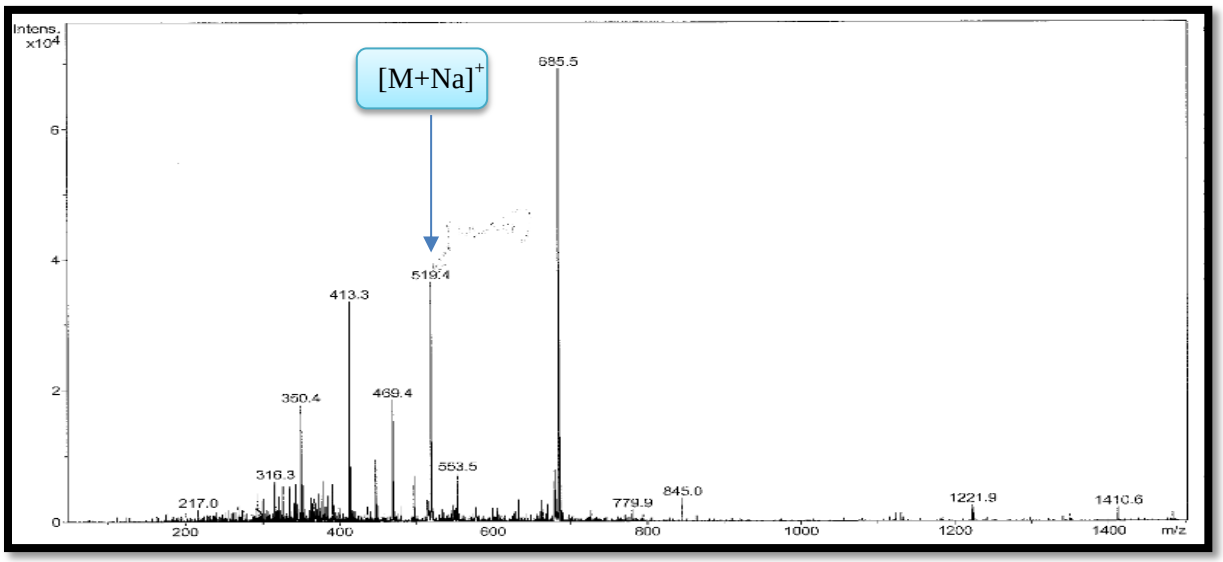

Figure 137: ESI mass spectrum of compound DFR5Al

Its ^{1}H NMR spectrum was in accordance with its mass spectrum by showing in addition to signals of betulinic acid another signals corresponding to an allyl groupement including one oxymethylene at δ_H 4.49 (2H, m) and three olefinic protons at δ_H 5.17 (m), δ_H 5.29 (m) and δ_H 5.85 (m).

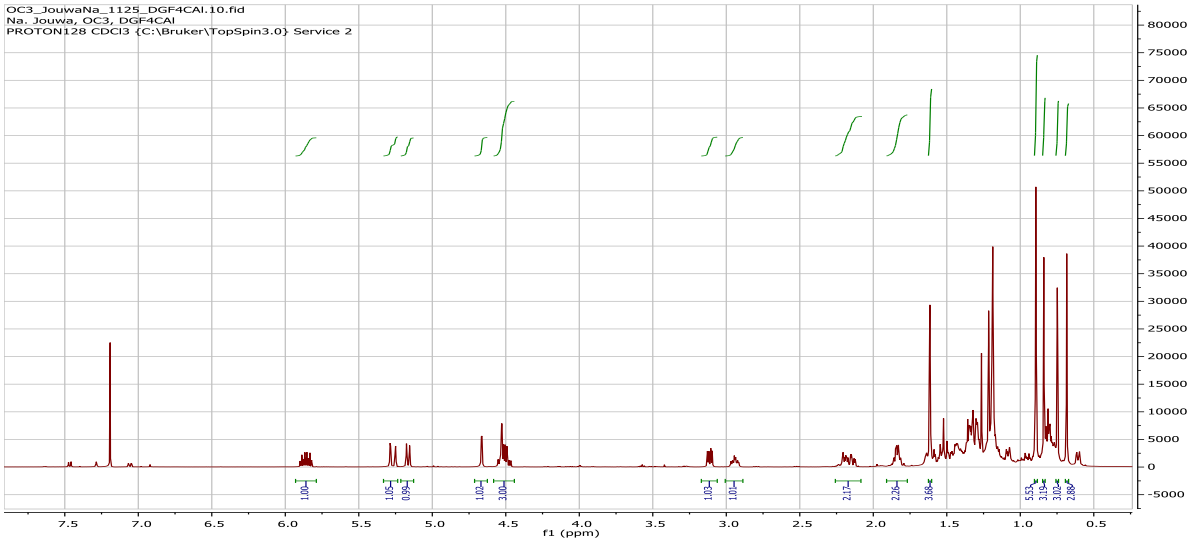

Figure 138: ^{1}H NMR spectrum (500 MHz) of compound DFR5Al in $CDCl_3$

The above spetroscopic data attributed to DFR5Al the structure of betulinic acid 28-allyle

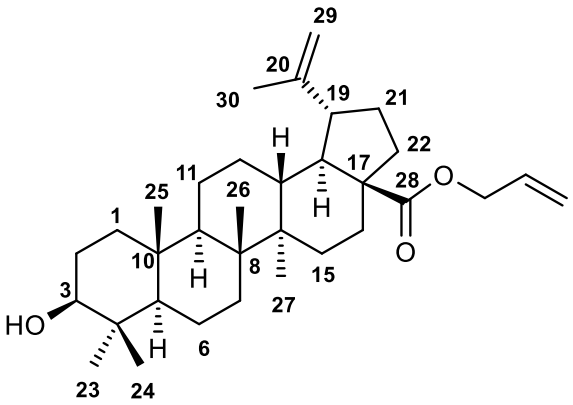

81

II.2.2.3. Allylation of DGF5

Allylation of compound DGF5 followed the same condition reaction than that of compound DFR5. This reaction yielded compound DGF5Al with an efficiency of 53.1 %.

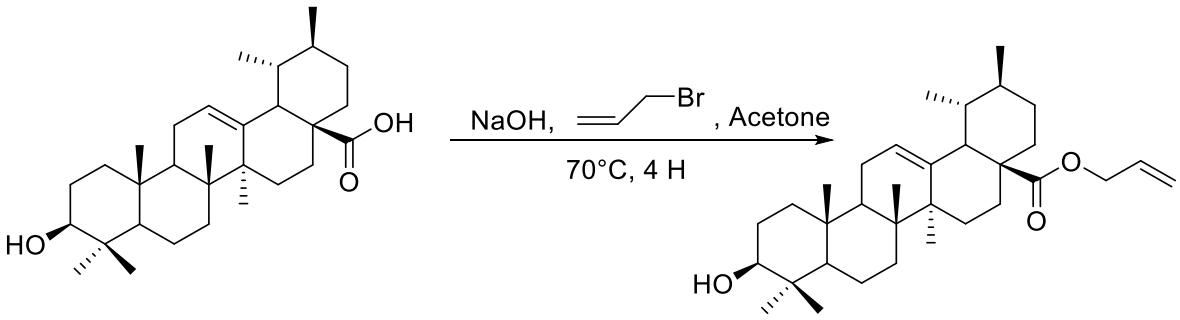

Scheme 17 : Allylation reaction process of compound DGF5

The ESI spectrum of this compound showed in positive mode a pseudo molecular ion peak $[M+Na]^+$ at *m/z* 519.3 which is attributable to the mass of ursolic acid plus an allyl group.

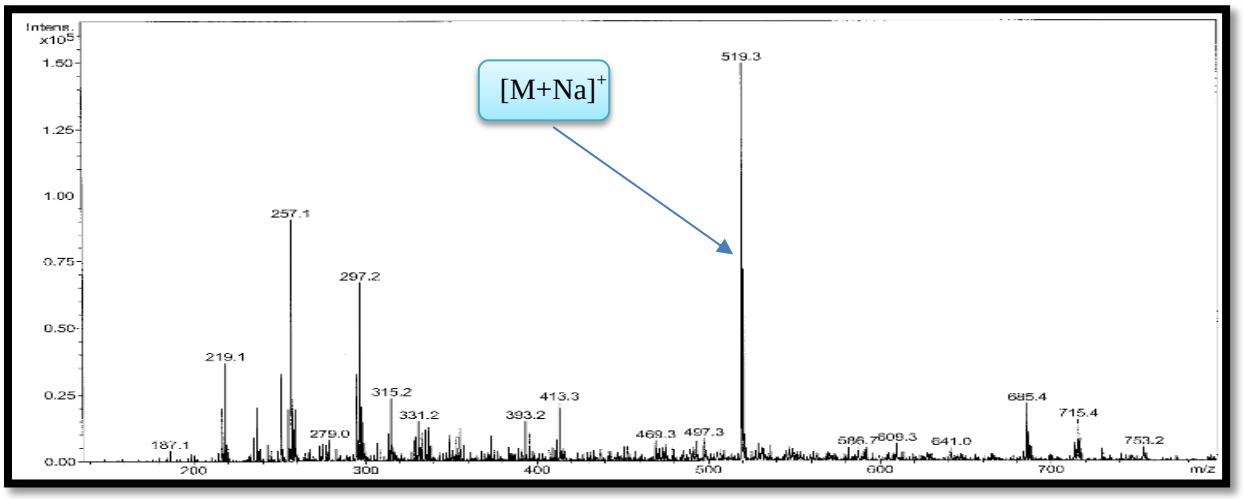

Figure 139: ESI mass spectrum of compound DGF5Al

The allyl group was further confirmed to be a part of this molecule by means of ^1H NMR spectrum of compound DGF5Al which showed signals of an oxymethylene at δ_H 4.43 (2H, m) and three olefinic protons at δ_H 5.13 (m), δ_H 5.24 (m) and δ_H 5.82 (m).

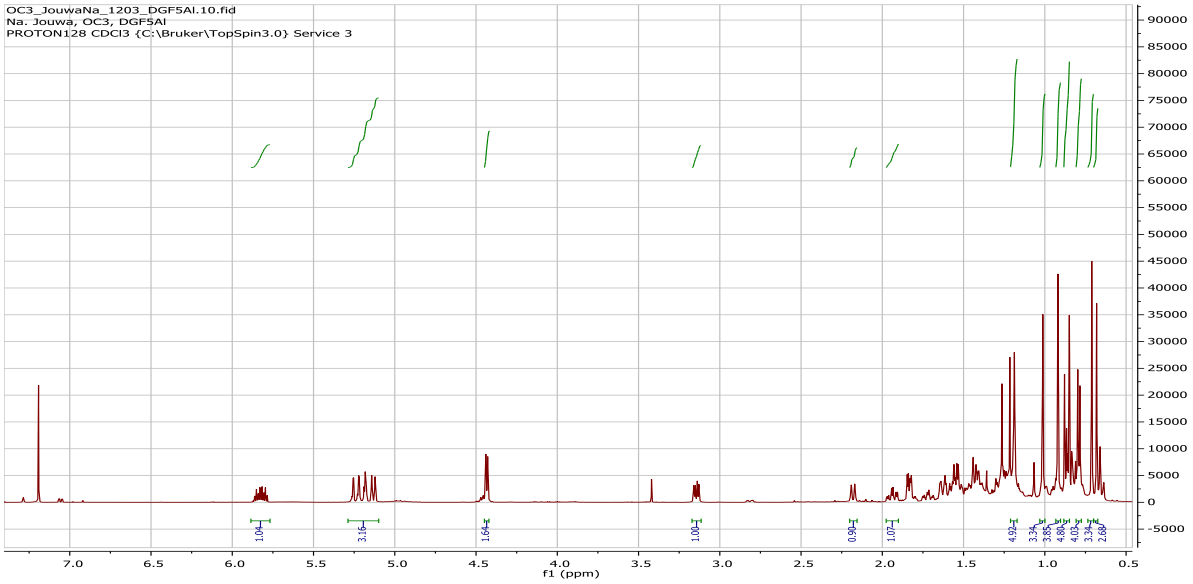

Figure 140: ^{1}H NMR spectrum of compound DGF5Al

Therefore compound DGF5Al was identified as ursolic acid 28-allyle

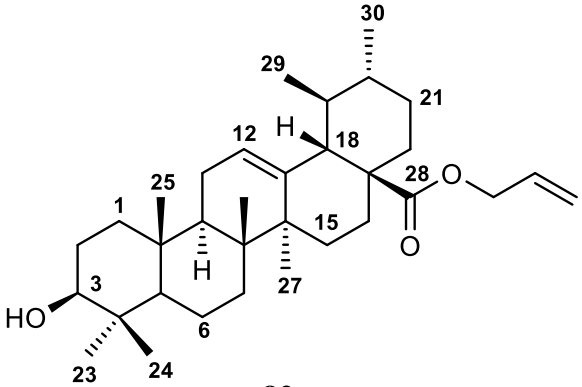

82

II.3. BIOLOGICAL ACTIVITIES OF EXTRACTS AND SOME ISOLATED COMPOUNDS

In order to valorise the compounds isolated in our two selected plant extracts and to justify the uses of these plants in traditional medicine, we were interested in the evaluation of three biological activities: antibacterial, antioxidant and cytotoxic activities.

II.3.1. Cytotoxic activity

The cytotoxicity of some extracts and compounds was evaluated on two cancers cell lines: The human cervix carcinoma cell line KB-3-1 and the human colon cancer cell line HT-29. Methanolic extracts of the leaves, twigs and stem bark of *Diospyros gilletii* as well as methanolic extracts of the leaves and roots of *Diospyros fragans* were evaluated together with twenty-one compounds (ursolic acid, corosolic acid, vismiaefolic acid, lupeol, myrtifolic acid, uvaol, betulinic acid, betulinic acid acetate, betulinic acid 28-allyle, per acetylated vismiaefolic acid, per allylated vismiaefolic acid, norbergenin, 4-*O*-galloylnorbergenin, 4-*O*-p-hydroxybenzoylnorbergenin,11-*O*-*E*-cinnamoylnorbergenin,11-*O*-*p*-hydroxybenzoylnorbergenin, per acetylated 4-*O*-*p*-hydroxybenzoylnorbergenin, per allylated 4-*O*-*p*-hydroxybenzoylnorbergenin, luteine, 1-*O*-(28-Hydroxyoctacosanoyl) glycerol) at the concentration of 0.00025 mol/L for compounds and 0.1 mg/mL for extracts. The results are reported in the **Table 38** below.

Table 38: Cytotoxicity of some compounds and extracts from *D. gilletii* and *D. fragrans*

Compounds	IC_{50} (µM)	
	KB-3-1	HT-29
DGF2	-	-
DGF5	50.9	34.4
DGF5Al	-	-
DGF7	14.7	16.5
DFR5	-	-
DFR5Ac	-	-
DFR5Al	-	-
DFR6	-	-
DFFFI8	-	-
DFFFI8B	-	-
DFFFII13I	-	-
DFFFII13IA	-	-
DFFFII14	-	-
DFFFII17D	-	-
DGET4	-	-
DGET4Ac	24.0	-

DGET4Al	-	-
DGET5B	-	-
DGF8	-	-
DGET1	-	-
DGTFIV1E	-	-
Extracts	IC_{50} (µM)	
Diospyros gilletii leaves	-	-
Diospyros gilletii twigs	-	-
Diospyros gilletii stem	-	-
Diospyros fragrans leaves	-	-
Diospyros fragrans roots	-	-
Reference (Griseofulvin)	17 µM	21 µM

(-) not active

It appeared from this table that ursolic acid and corosolic acid, two triterpenes belonging to the urs-12-ene serie and having carboxylic acid and alcohol functions, exhibited some level of activity on the both cancer cells tested. Corosolic acid which possess one more alcohol function in position 2 than ursolic acid was found to be more active than the reference used. This could mean that the cytotoxic activity of the urs-12-ene triterpenes on cancer cells KB-3-1 and HT-29 increases with the number of hydroxyl functions and their position. But in that case vismiaefolic acid, which is also a triterpene from urs-12-ene serie with three alcohol functions should be more active than corosolic acid, which is not the case. More investigations should be done on these triterpenes in order to find the groupement responsible for the activity observed and their position in the triterpenic skeleton.

Per acetylated derivative of 4-*O*-*p*-hydroxybenzoylnorbergenin from the acetylation reaction of compound 4-*O*-*p*-hydroxybenzoylnorbergenin showed a moderate activity on cancer cells KB-3-1 while compound 4-*O*-*p*-hydroxybenzoylnorbergenin didn't show any activity. This activity observed for the acetylated derivative can be directly linked to the number of ester groups present in the structure of this compound. In fact, most of the compounds presents in the literature and containing either ester or lactone groupements are found to exhibit moderate to good cytotoxic activities against cancers cell line (Kikuchi et *al*., 2011). More investigations should be done to confirm this hypothesis.

None of the extracts showed activity on the cancer cells tested, which would mean that the activity observed in the case of ursolic and corosolic acid was masked within the extracts by the presence of other compounds having antagonistic effects.

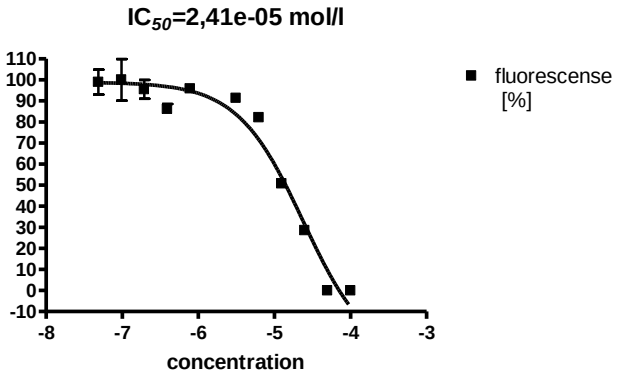

DGET4Ac on KB-3-1 cells

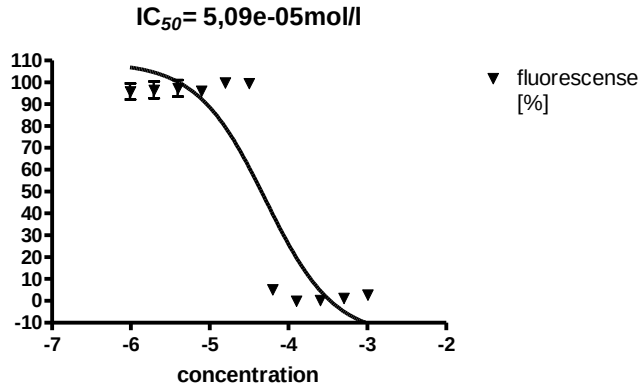

DGF5 on KB-3-1 cells

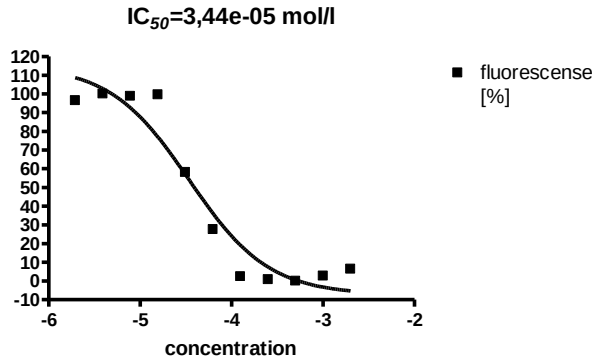

DGF5 on HT-29 cells

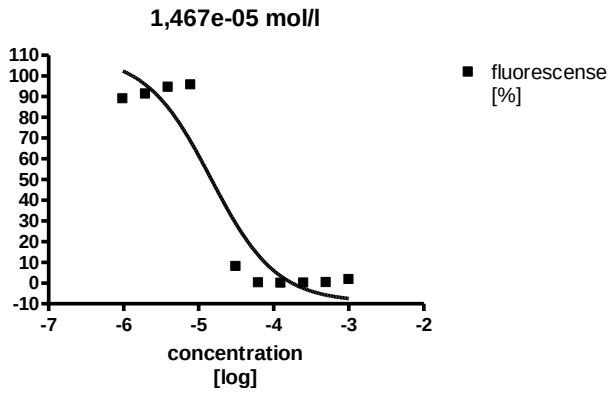

DGF7 on KB-3-1 cells

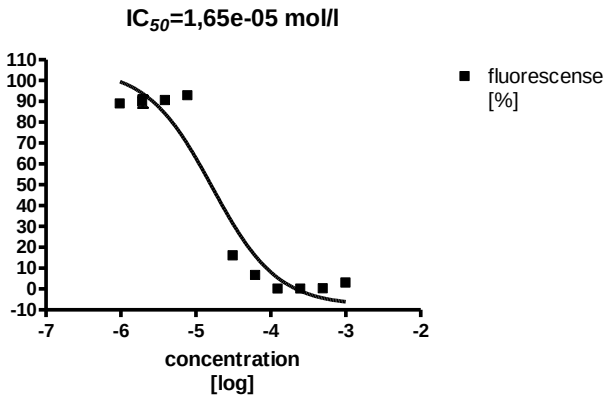

DGF7 on HT-29 cells

Figure 141: IC_{50} values of compounds DGF5, DGF7 and DGET4Ac

II.3.2. Antioxidant activity

The antioxidant activity of some compounds was evaluated using DPPH method based on the hydrogen donating capabilities of antioxidants to a stable free radical such as 2, 2-diphenyl-1-picrylhydrazyl (DPPH$^{\cdot}$). The DPPH radical has a deep violet color in solution, and it becomes colorless or pale yellow when neutralized. Norbergenin, 4-*O*-galloylnorbergenin, 4-*O*-*p*-hydroxybenzoylnorbergenin, 11-*O*-*(E)*-cinnamoylnorbergenin, 11-*O*-*p*-hydroxybenzoylnorbergenin and per acetylated 4-*O*-*p*-hydroxybenzoylnorbergenin were evaluated for their antioxidant capacities over the range of 500 - 0,5 µg/mL concentration. Trolox was used as positive control and the results are shown in the **table 39** below.

Table 39: Antioxidant activities of some isolated compounds

Compound	IC_{50} (μg/mL)
DGET1	41.6
DGET4	8.2
DGET5	22.0
DGF8	23.8
DGTFIV1E	144.0
DGET4Ac	>250
Trolox	37.0

All the compounds have the same basic skeleton with different substituents and they all exhibited good antioxidant activity, except per acetylated 4-*O*-*p*-hydroxybenzoylnorbergenin which showed IC_{50} beyond 250 µg/mL. That can be explained by the loss of its hydrogen donating which were replaced by acetoxy groups during the acetylation reaction. It appeared from this table that the different substituents and their position on the basic skeleton influence the antioxidant activity, and a great variation is observed when the substitution occurs at C-4 of the norbergenin nucleus. In fact, 4-*O*-*p*-hydroxybenzoylnorbergenin exhibited the best activity with an IC_{50} value of 8.2 µg/mL, but its C-11 isomer 11-*O*-*p*-hydroxybenzoylnorbergenin exhibited less activity with an IC_{50} value of 144.0 µg/mL. 4-*O*-galloylnorbergenin, which substituent is also at position C-4 showed less activity than 4-*O*-*p*-hydroxybenzoylnorbergenin, meaning that the 4-*O* substitution in the norbergenin nucleus with a *para*-hydroxybenzoyl moiety exhibited the better DPPH free radical scavenging activity.

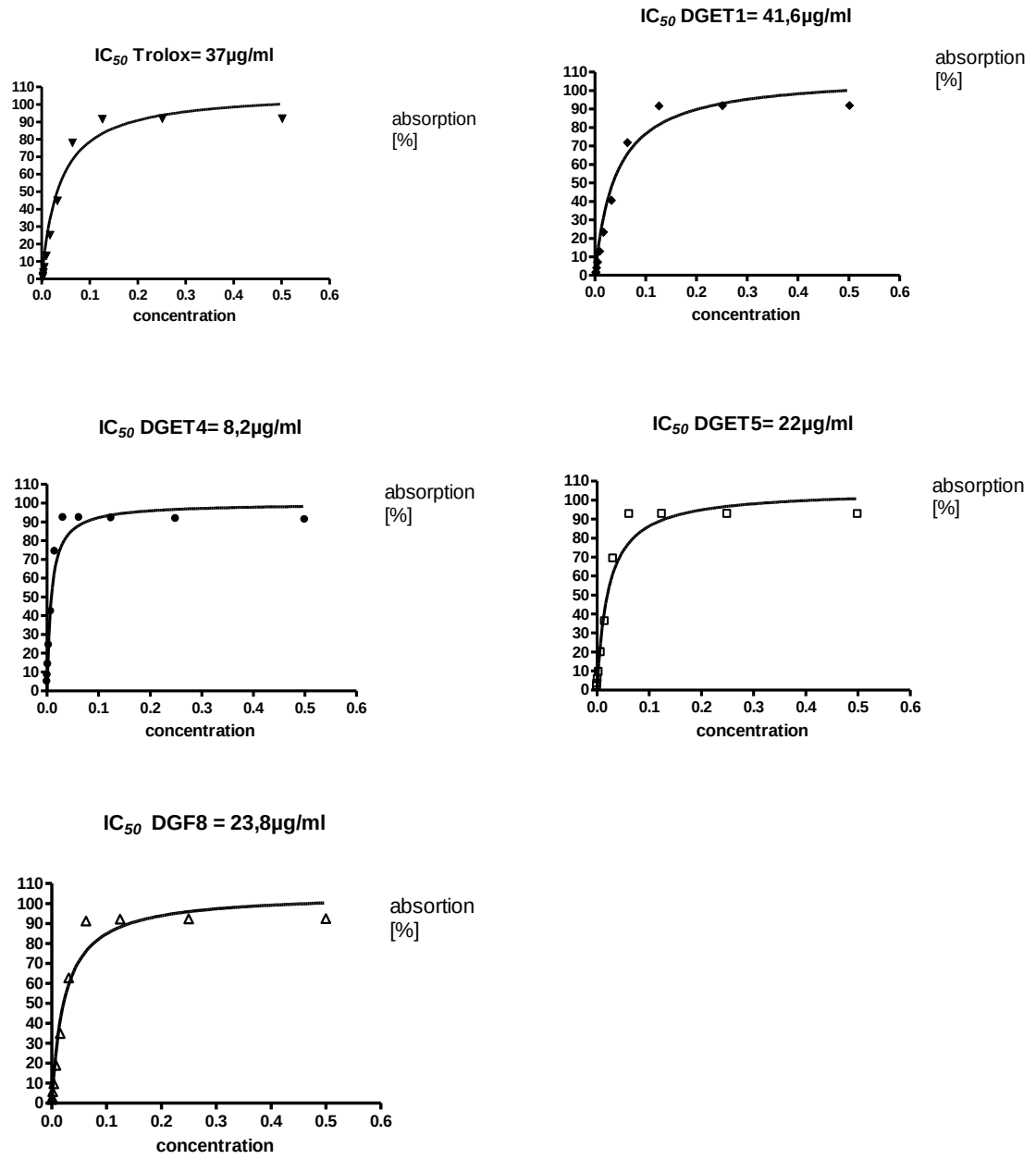

Figure 142: IC_{50} values of antioxidant activities of some isolated compounds

II.3.3. Antibacterial activity

Methanolic extracts of the leaves, twigs, stem bark of *Diospyros gilletii* as well as methanolic extracts of the leaves and roots of *Diospyros fragans* and some compounds were evaluated for their antibacterial activities using the disk diffusion method on three gram positive and two gram negative bacteria: *Escherichia coli* DSMZ 1058, *Bacillus subtilis* DSMZ 704, *Micrococcus luteus* DSMZ 1605, *Pseudomonas agarici* DSMZ 11810 and *Staphylococcus warneri* DSMZ 20036. The compounds tested were ursolic acid, corosolic acid, vismiaefolic acid, lupeol, myrtifolic acid, uvaol, betulinic acid, betulinic acid acetate, per

acetylated vismiaefolic acid, norbergenin, betulinic acid 28-allyle, ursolic acid 28-allyle, 4-*O*-galloylnorbergenin, 4-*O*-*p*-hydroxybenzoylnorbergenin, 11-*O*-*E*-cinnamoylnorbergenin, 11-*O*-*p*-hydroxybenzoylnorbergenin, per acetylated 4-*O*-*p*-hydroxybenzoylnorbergenin, luteine, 1-*O*-(28-Hydroxyoctacosanoyl) glycerol, quercitol and 5-*O*-methyl-*β*-*D*-glucopyranoside. DMSO was used as negative control and Gentamycin as positive one. The concentrations used were 0.5 µg/mL for compounds and 20 µg/mL for extracts and the results are given in the **table 40** below.

Table 40: Antibacterial activities of some isolated and chemical transformed compounds and extracts

Compounds	*Escherichia coli* DSMZ 1058	*Bacillus subtilis* DSMZ 704	*Pseudomonas agarici* DSMZ 11810	*Micrococcus luteus* DSMZ 1605	*Staphylococcus warneri* DSMZ 20036
	Inhibition diameter in mm				
DGET1	-	-	-	-	-
DGET4	-	-	-	-	-
DGET5	-	-	-	-	-
DGF8	-	-	-	-	-
DGTFIV1E	-	-	-	-	-
DGET4Ac	-	-	-	-	-
DGET4Al	-	-	-	-	-
DFR5Ac	-	10	7	-	-
DFR5Al					
DFFFII13I	-	-	-	-	-
DFFFII13IA	-	-	7	-	-
DFFFII14	-	-	-	-	-
DFFFII17D	-	-	-	-	-
DFFFI8	-	9	-	-	-
DFFFI8B	-	7	-	-	-
DGF1	-	-	-	-	-
DGF5	-	-	-	-	-
DGF5Al	-	-	-	-	-
DGF7	-	-	-	-	-
DGF2	-	-	-	-	-
DGF3	-	-	-	-	-
DFR5	-	-	-	-	-
DFR6	-	-	-	-	-
Extracts					
DGET	-	-	-	-	-
DGT	-	7	-	-	-
DFF	-	-	-	-	-
DGF	8	-	7	-	-
DFR	8	7	-	-	-
Gentamycin	16/20	22	19	19	19

- (-) not active

Per acetylated derivatives of betulinic acid and vismiaefolic acid showed low activities against *Pseudomonas agarici* 11810 (7 mm of diameter) while betulinic acid and vismiaefolic acid didn't show any activity. Per acetylated derivative of betulinic acid also showed a good activity against *Bacillus subtilis* DSMZ 704 with a diameter of inhibition of 10 mm. These results suggested that the presence of acetoxy group in the urs-12-ene series may play a role in inhibitory activity. From this table it also appeared that uvaol and myrtifolic acid exhibited respectively low and moderate activities against *Bacillus subtilis* DSMZ 704 with diameter of inhibition of 7 and 9 mm while ursolic acid didn't show any activity. From these results we could suggested that position of double bond which is at 12 in ursolic acid and 7 in myrtifolic acid played a role in inhibitory activity. Minimale inhibitory concentration (MIC) were calculated for myrtifolic acid and per acetylated derivative of betulinic acid regarding their activities observed against *Bacillus subtilis* DSMZ 704 and the results are given in the **table 41** below.

Table 41: Minimale inhibitory concentration (MIC) of myrtifolic acid and per acetylated derivative of betulinic acid against *Bacillus subtilis* DSMZ 704

Compounds	MIC against *Bacillus subtilis* DSMZ 704 (µg/mL)
DFR5Ac	>250
DFFFI8	31.3
Reference (Gentamycin)	1.6

Regarding these results, the most active compound was found to be myrtifolic acid with a significant MIC of 31.3 µg/mL (Kuete, 2010).

CONCLUSION AND OUTLOOK

During our work on the phytochemical study and evaluation of antibacterial, antioxidant and cytotoxic activities of the chemical constituents of two Cameroonian medicinal plants belonging to the Ebenaceae family, *Diospyros gilletii* and *Diospyros fragrans*, twenty-eight compounds were isolated and fully characterized. These compounds belong to several classes of natural substances, among which are five isocoumarins, twelve triterpenes, a naphthalene derivative, a monoglyceride, a polyterpene, a carotenoid, four sterols and three polyols.

From the five isocoumarins obtained, two were identified as new derivatives to which we have assigned the names 4-*O*-*p*-hydroxybenzoylnorbergenin and 11-*O*-*(E)*-cinnamoylnorbergenin. The other three one were identified as norbergenin, 4-*O*-galloylnorbergenin and 11-*O*-*p*-hydroxybenzoylnorbergenin.

The naphthalene derivative was designed as 3,6-dihydroxy-8-methyl-3,4-dihydronaphthalen-1(2H)-one, a new derivative to which we have given the trivial name fragranone.

The twelve triterpenes obtained, all known, were identified as belonging to various classes of pentacyclic triterpenes. These are three lupans named lupeol, betulin, betulinic acid, six ursans named ursolic acid, corosolic acid, uvaol, myrtifolic acid, vismiaefolic acid, rotundic acid and three oleans named oleanolic acid, hederagenin and *β*-amyrin acetate.

The polyterpene was identified as α-tocopherol, the monoglyceride as 1-*O*-(28-Hydroxyoctacosanoyl) glycerol, the carotenoid as luteine, the four sterols as mixture of Stigmasterol + *β*-Sitosterol and mixture of 3-*O*-*β*-*D*-glucopyranoside of Stigmasterol + *β*-Sitosterol, and finally the three polyols as quercitol, 5-*O*-methyl-myo-inositol and methyl-*β*-*D*-glucopyranoside.

Structural elucidation of all these compounds was based on intensive interpretation of their spectral data, in particular, ^{1}H and ^{13}C NMR in one and two dimensions in conjunction with mass spectrometry, IR and UV. The structures of some compounds were further confirmed by their X-ray data.

Acetylation and allylation reactions were performed on 4-*O*-*p*-hydroxybenzoylnorbergenin, ursolic acid, betulinic acid and vismiaefolic acid, leading to their

acetylated and allylated derivatives among which those of 4-*O*-*p*-hydroxybenzoylnorbergenin were identified as new ones.

On the biological level, the crude extracts from the different parts of the two plants, as well as the isolated and hemisynthetic compounds were evaluated for their antibacterial activities against three Gram-positive (*Bacillus subtilis*, *Micrococcus luteus*, *Staphylococcus warneri*) and two Gram-negative (*Escherichia coli* and *Pseudomonas agarici*) bacteria using microdillution method, for their cytotoxic activities against human cervix carcinoma cell line KB-3-1 and human colon cancer cell line HT-29 and for their antioxidant activities using DPPH.

The antibacterial test revealed a moderate activity against *Escherichia coli*, *Bacillus subtilis* and *Pseudomonas agarici* concerning crude extracts from the leaves and twigs of *Diospyros gilletii*, as well as that from the roots of *Diospyros fragrans*. Myrtifolic acid and the acetylated derivative of betulinic acid showed good activity against *Bacillus subtilis* with MIC values of 31.3 and 250 µg/ mL respectively.

Concerning the cytotoxic test, corosolic acid was active on both cancer cells KB-3-1 and HT-29 with IC_{50} values of 14.6 and 16.5 µM respectively. The other compound showed very low activities.

The antioxidant test showed that all the isocoumarins exhibited good activities and were more active over the range of 500 - 0,5 µg/mL concentration than the standard antioxidant trolox, with IC_{50} values ranging from 8.2 µg/ml to 41.6 µg/mL.

Considering all these results, the use of plants of the *Diospyros* genus in traditional medicine in the treatment of cancer and infectious diseases, among others, would be due to the presence within them of molecules presenting biological activities that we have just described above.

For the continuation of our work, we are considering:

- To continue structural elucidation of the remaining compounds.
- To isolate compounds from the remaining extracts (roots extract of *D. gilletii*, stem bark and twigs extracts of *D. fragrans*) and other parts of the plants (fruit, seed, bark).
- To perform chemical transformations on the isocoumarins and the other compounds in view of studying their relation structure–activity.

CHAPTER III:

MATERIAL AND METHODS

III.1. EQUIPMENTS

Melting point was determined on a BÜCHI Melting point B-540 (BUCHI, Switzerland). Optical rotations were measured on a JASCO DIP-3600 digital polarimeter (JASCO, Tokyo, Japan) using a 10 cm cell. UV spectra were recorded on a Hitachi UV 3200 spectrophotometer and IR spectra were determined on a JASCO Fourier transform IR-420 spectrometer (Thermo Scientific, Waltham, MA, USA). 1D and 2D NMR spectra were recorded on a Bruker DRX 500 NMR spectrometers (Bruker, Rheinstetten, Germany) with TMS as an internal standard and chemical shifts shown as δ-values (ppm), while coupling constants (*J*) were measured in Hz. Homonuclear ^{1}H connectivities were determined by using the COSY experiment. One-bond ^{1}H-^{13}C connectivities were determined with HMQC gradient pulse factor selection, and two- and three-bond ^{1}H-^{13}C connectivities by HMBC experiments. EI-MS spectra were recorded on a Finnigan MAT 95 spectrometer (70 eV) (Thermo Fisher Scientific, Darmstadt, Germany) and ESI-MS on Agilent 6220 TOF LCMS mass spectrometer with perfluorokerosene as reference substance for ESI-HR-MS (Agilent Technologies, Santa Clara, CA, USA). Column chromatography was carried out on silica gel 230–400 mesh, silica gel 70–230 mesh (Merck, Darmstadt, Germany) and Sephadex LH-20 gel (Sigma-Aldrich, Munich, Germany). Thin layer chromatography (TLC) were performed on Merck precoated silica gel 60 F_{254} aluminum foil (Merck, Darmstadt, Germany) and were revealed using UV lamp (254–365 nm) and 10% H_2SO_4 reagent followed by heating. All reagents used were of analytical grade.

III.2. PLANTS MATERIAL

The leaves, twigs and stem bark of *Diospyros gilletii* De Wild were collected in March 2018 at Mbalmayo, Centre region-Cameroon. The leaves and roots of *Diospyros fragrans* Gürke were collected in December 2018 at Abang, Centre region-Cameroon. M. Nana victor, a botanist at the Cameroon National Herbarium did the identification of the both species.

III.2.1. Extraction and isolation of the compounds

III.2.1.1 From the leaves of *D. gilletii*

The dried and powdered leaves of *D. gilletii* (0.95 kg) were extracted by maceration using methanol (2x3 L) at room temperature for 3 days. After filtration, white crystals precipitated in the resulting methanolic solution. This crystal was filtered and washed with methanol to afford DGF1 (Quercitol). The methanolic filtrate was further evaporated to dryness under reduced pressure to give 122.10 g of MeOH extract. 120 g of this extract was

dissolved in water and submitted to liquid – liquid fractioning using petroleum ether (PE), dichloromethane (CH_2Cl_2), ethyl acetate (EtOAc) and n-butanol to yield respectively 2.31 g, 9.25 g, 43.18 g and 21.37 g of organic extracts. These differents extracts were subjected to column chromatography to afford pure samples. Below, is summarized the extraction and isolation process.

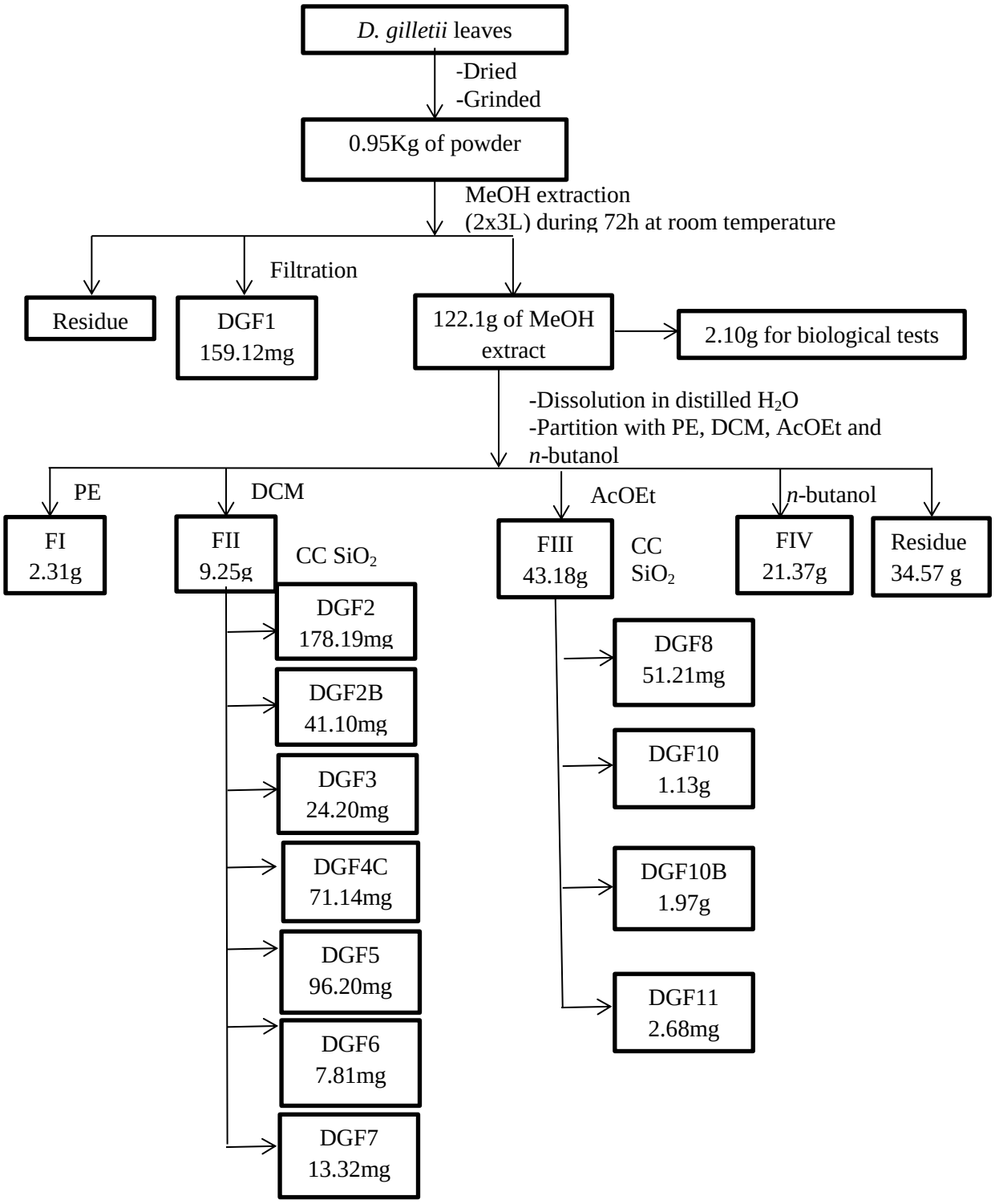

Scheme 7 : Extraction and isolation procedure of compounds from the leaves of *D. gilletii*.

III.2.1.1.1. Purification of the ethyl acetate extract (FIII)

The ethyl acetate extract (40.00 g) was subjected to column chromatography in silica gel eluted sequentially with mixture of PE/EtOAc and EtOAc/MeOH of increasing polarities to yield 153 fractions of 100 mL each. These fractions were combined based on TLC analysis to give 17 subfractions labelled Ai.

Table 42 : Chromatogram of fraction FIII

Column eluent	Fractions	Subfractions	Observation
PE/EtOAc 40%	1-20	1-11 ; **A_1**	Complex mixture
		12-20 ; **A_2**	Complex mixture + drag
PE/EtOAc 50%	21-35	21-28 ; **A_3**	Mixture of five compounds + drag
		29-35 ; **A_4**	Mixture of seven compounds + drag
PE/EtOAc 60%	36-58	36-43 ; **A_5**	Complex mixture
		44-52 ; **A_6**	Mixture of eight compounds
		53-58 ; **A_7**	Mixture of six compounds
PE/EtOAc 75%	59-90	59-60 ; **A_8**	Mixture of three compounds + drag
		61-68 ; **A_9**	**DGF8 +** one spot
		69-70 ; **A_{10}**	**DGF9** + Mixture of four compounds
		71-87 ; **A_{11}**	**DGF10 +** four spots
		88-90 ; **A_{12}**	Complex mixture + drag
EtOAc 100%	91-118	91 ; **A_{13}**	Mixture of five compounds
		92-115 ; **A_{14}**	**DGF10B +** two spots
		116-118 ; **A_{15}**	Mixture of four compounds
EtOAc/MeOH 5%	119-130	119-121 ; **A_{16}**	Mixture of three compounds
EtOAc/MeOH 10%	131-142	122-153 ; **A_{17}**	**DGF11** + drag
EtOAc/MeOH 15%	143-153		

MeOH 100%	Washing	/	Drag

Subfractions A_9 and A_{11} eluted from the column chromatography with a mixture of PE/EtOAc (1:3) precipitated and the precipitates were washed with a mixture of PE/EtOAc (1:1) to yield respectively DGF8 (11-*O*-*(E)*-cinnamoylnorbergenin) and DGF10 (4-*O*-*p*-hydroxybenzoylnorbergenin).

Subfraction A_{14} eluted from the column chromatography with the solvent EtOAc 100% precipitated and was washed after filtration with a mixture of PE/EtOAc (1:3) to yield DGF10B (4-*O*-galloylnorbergenin).

Subfraction A_{17} eluted with a mixture of EtOAc/MeOH (19:1) to EtOAc/MeOH (17:3) afforded after filtration and washing with EtOAc 100% DGF11 (norbergenin).

III.2.1.1.2. Purification of the dichloromethane extract (FII)

The dichloromethane extract (9,00 g) was chromatographed on silica gel and eluted with a gradient of a mixture of PE-EtOAc to yield 299 fractions of 100 mL each. On the basis of TLC analysis, these fractions were combined in 22 subfractions labelled Bi.

Table 43: Chromatogram of fraction FII

Column eluent	Fractions	Subfractions	Observation
PE 100%	1-14	1-14 ; **B_1**	Oily mixtures
PE/EtOAc 2,5%	15-32	15-26 ; **B_2** 27-32 ; **B_3**	Oily mixtures
PE/Ac 5%	33-57	33-41 ; **B_4**	**DGF2** + three spots
		42-57 ; **B_5**	Mixture of three compounds
PE/ EtOAc 7,5%	58-71	58-67 ; **B_6** 68-71 ; **B_7**	Complex mixtures
PE/ EtOAc 10%	72-88	72-77 ; **B_8**	Mixture of four compounds
		78-88 ; **B_9**	**DGF2B** + two spots
PE/ EtOAc 12,5%	89-100	89-93 ; **B_{10}**	Mixture of five compounds

PE/ EtOAc 15%	101-122	101-110 ; **B_{11}**	**DGF3** + two spots
PE/ EtOAc 17,5%	123-136	111-136 ; **B_{12}**	Complex mixture
PE/ EtOAc 20%	137-154	137-154 ; **B_{13}**	**DGF4C +** three spots
PE/ EtOAc 25%	155-178	155-159 ; **B_{14}**	**DGF5** + three spots
		160-178 ; **B_{15}**	**DGF6** + four spots
PE/ EtOAc 30%	179-194	179-194 ; **B_{16}**	**DGF7** + two spots
PE/ EtOAc 35%	195-219	195-219 ; **B_{17}**	Mixture of five compounds
PE/ EtOAc 40%	220-242	220-242 ; **B_{18}**	Mixture of three compounds
PE/ EtOAc 50%	243-259	243-259 ; **B_{19}**	Mixture of four compounds
PE/ EtOAc 60%	260-275	260-275 ; **B_{20}**	Two spots + drag
PE/ EtOAc 75%	276-299	276-287 ; **B_{21}** 288-299 ; **B_{22}**	Complex mixtures + drag
MeOH 100%	washing	/	Drag

Compounds DGF2 (lupeol), DGF2B (mixture of stigmasterol+ β sitosterol), DGF3 (betulin) and DGF4C (betulinic acid) were obtained respectively from subfractions B_4, B_9, B_{11}, B_{13} and after washing with MeOH.

Compounds DGF5 (ursolic acid) and DGF7 (corosolic acid) were obtained after washing with PE/EtOAc (4:1) subfractions B_{14} and B_{16} respectively.

Compound DGF6 (oleanolic acid) was obtained after purification of subfraction B_{15} in silica gel column chromatography eluted with an isochratic solvent system of PE/EtOAc (9:1)

III.2.1.2 From the stem bark of *D. gilletii*

The air dried and powdered stem bark of *Diospyros gilletii* (0.8 kg) were macerated twice with 3L of MeOH at room temperature for 3 days. The result filtered extract was evaporated under reduce pressure to give 158.00 g of brown crude extract. From 150.00 g of that crude extract suspended in distillated water, was filtered a beige powder named DGET1. After filtration of this compound, the water suspension was partitioned successively with PE, DCM, AcOEt and n-butanol to yield respectively 2.20, 17.30, 58.40 and 34.30 g of crude

extract. From these crude extracts were isolated seven pure compounds labelled DGETH1 to DGETH3 and DGET3 to DGET5B. The protocol used is illustrated by the scheme below.

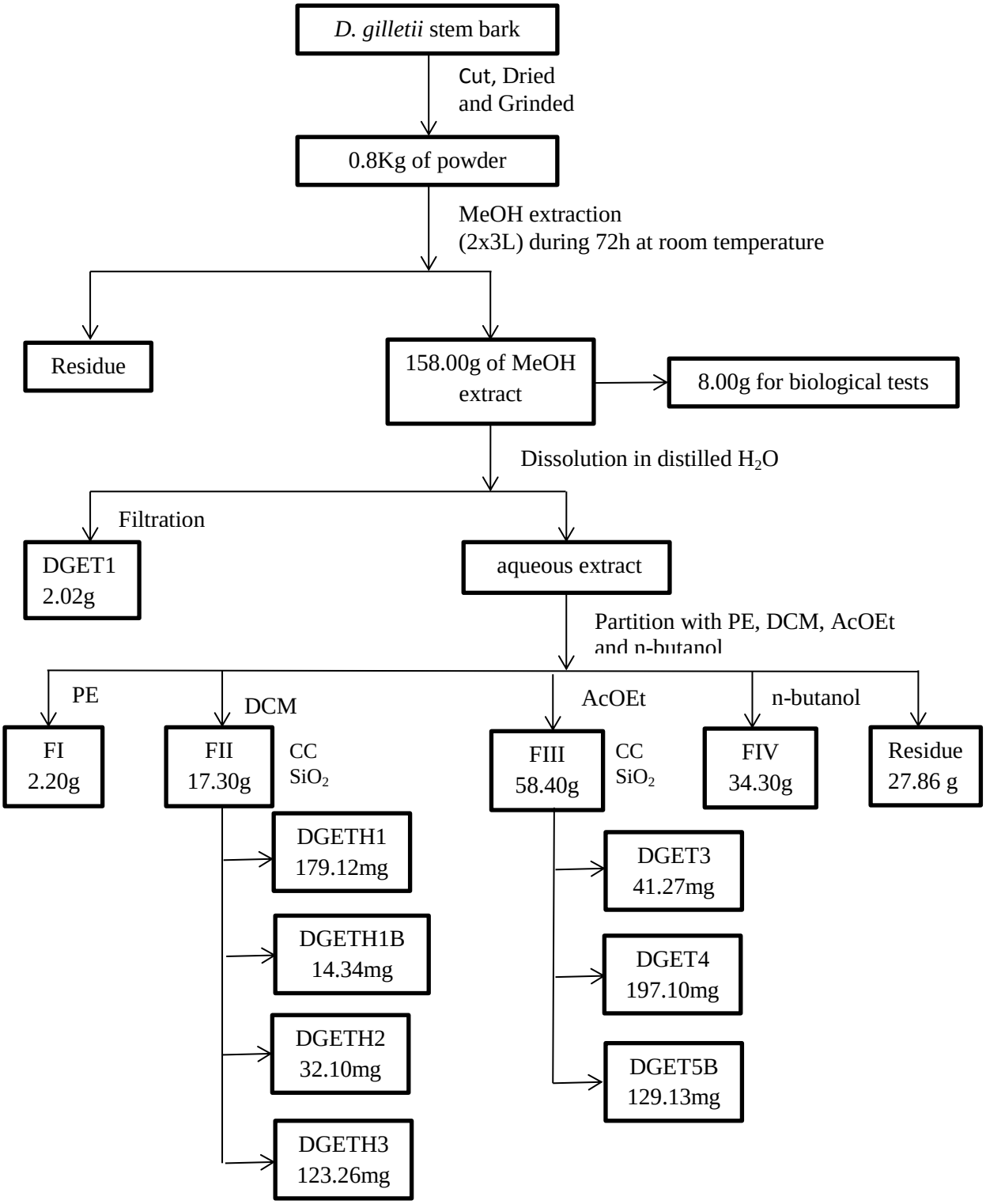

Scheme 8 : Extraction and isolation procedure of compounds from the stem bark of *D. gilletii.*

III.2.1.2.1. Purification of the ethyl acetate extract (FIII)

EtOAc extract of the stem bark of *D. gilletii* (58.40 g) was subjected to silica gel column chromatography using gradient systems PE/EtOAc and EtOAc/MeOH as eluent to afford 132 fractions of 200 mL combined after TLC into twelve subfractions labelled Ci.

Table 44 : Chromatogram of fraction FIII

Column eluent	Fractions	Subfractions	Observation
PE/EtOAc 50%	1-22	1-9 ; **C_1**	Mixture of five compounds + drag
		10-17 ; **C_2**	Mixture of seven compounds + drag
		18-22 ; **C_3**	Complex mixture
PE/EtOAc 60%	23-35	23-25 ; **C_4**	Complex mixture
		26-35 ; **C_5**	**DGET3** + two compounds+ drag
PE/EtOAc 75%	36-54	36-48 ; **C_6**	Mixture of three compounds + drag
		49-54 ; **C_7**	**DGET4** + one compounds
EtOAc 100%	55-78	55-62 ; **C_8**	Mixture of five compounds
		63-73 ; **C_9**	+ two spots
		74-78 ; **C_{10}**	Mixture of four compounds
EtOAc/MeOH 5%	79-90	79-86 ; **C_{11}**	Mixture of five compounds
EtOAc/MeOH 10%	91-115	87-132 ; **C_{12}**	**DGET5B** + drag
EtOAc/MeOH 15%	116-132		
MeOH 100%	washing	/	Drag

Subfraction C_5 afforded DGET3 (mixture of 3-*O*-*β*-glucoside of stigmasterol and *β*-sitosterol) after washing with MeOH.

Subfractions C_7 and C_{12} afforded respectively DGET4 (4-*O*-*p*-hydroxybenzoylnorbergenin) and DGET5B (norbergenin) after washing with PE/EtOAc (1:3).

III.2.1.2.2. Purification of the dichloromethane extract (FII)

Dichloromethane extract (17.30 g) was eluted over silica gel using a gradient system PE/EtOAc to yield 118 fractions of 100 mL. after TLC analysis these fractions were combined into ten subfractions labelled Di.

Table 45: Chromatogram of fraction FII

Column eluent	Fractions	Subfractions	Observation
PE/EtOAc 5%	1-17	1-9 ; **D_1**	Mixture of four compounds
		10-17 ; **D_2**	**DGETH1** +Mixture of two compounds
PE/EtOAc 10%	18-31	18-23 ; **D_3**	Complex mixture
		24-31 ; **D_4**	**DGETH1B** + two compounds+ drag
PE/EtOAc 15%	32-44	32-35 ; **D_5**	Mixture of three compounds + drag
		36-44 ; **D_6**	**DGETH2+** one compound
PE/EtOAc 20%	45-57	45-48 ; **D_7**	Mixture of five compounds
		49-55 ; **D_8**	**+** two spots
PE/EtOAc 25%	58-71	56-90 ; **D_9**	**DGETH3 +** mixture of six compounds
PE/EtOAc 30%	72-90		
PE/EtOAc 40%	91-118	91-118 ; **D_{10}**	Three compounds + drag
AcOEt 100%	washing	/	Drag

From subfractions D_2 and D_9 were filtered and washed with MeOH respectively compounds DGETH1 (lupeol) and DGETH3 (betulinic acid). From subfractions D_4 and D_6 were obtained Compounds DGETH1B (mixture of stigmasterol and *β*-sitosterol) and DGETH2 (betulin) respectively.

III.2.1.3 From the twigs of *D. gilletii*

The dried and powdered twigs of *D. gilletii* (1.5 Kg) were extracted twice with 5L of MeOH at room temperature for 3 days. The filtered extract was concentrated to dryness under reduced pressure to give a brown MeOH extract (99.10g). 95 g of this extract were flash chromatographed over silica gel CC in five fractions: FI (PE/EtOAc (3:1)), FII (CH_2Cl_2), FIII (PE/EtOAc (1:1)), FIV (EtOAc) and FV (EtOAc/MeOH (3:1)). Based on TLC analysis, fractions FII and FIII were grouped together. These fractions were further subjected to column chromatography to yield pure samples. The protocol used for the isolement of the samples is given in the scheme below.

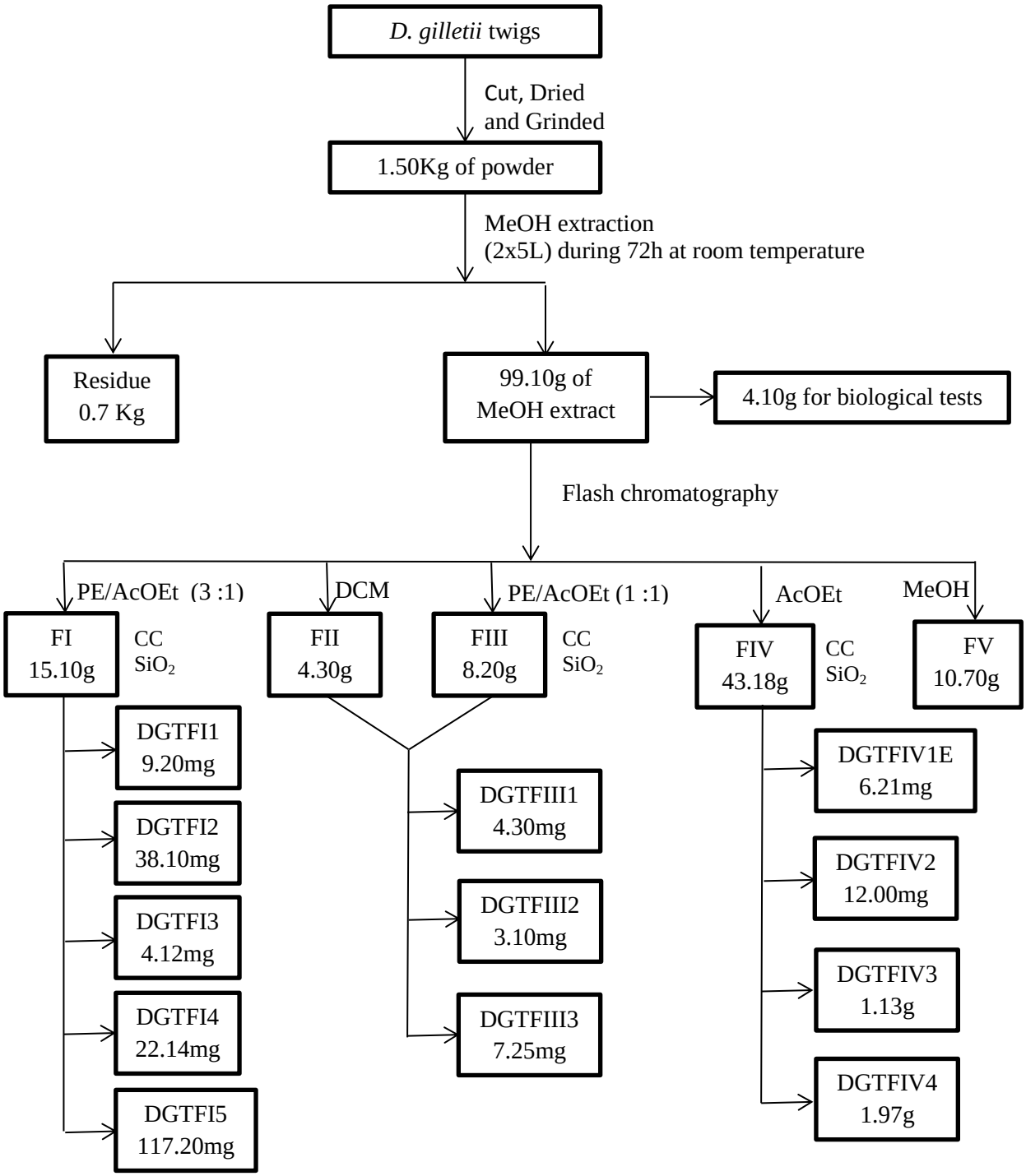

Scheme 9 : Extraction and isolation procedure of compounds from the twigs of *D. gilletii*.

Table 46: Chromatogram of the flash chromatography of the twigs of *D. gilletii*.

Fractions	Column eluent
FI	PE/EtOAc 3:1
FII	DCM
FIII	PE/EtOAc 1:1
FIV	EtOAc
FV	MeOH

III.2.1.3.1 Purification of fraction FI

Fraction FI (15.10g) chromatographed over silica gel with the gradient solvent system PE/EtOAC afforded 115 fractions of 100 mL combined after TLC into twelve subfractions labelled Ei.

Table 47: Chromatogram of fraction FI

Column eluent	Fractions	Subfractions	Observation
PE 100%	1-8	1-8 ; **E_1**	**DGTFI1**+ three compounds
PE/EtOAc 5%	9-20	9-14 ; **E_2**	Oily mixture
		15-20; **E_3**	**DGTFI2**+ three compounds
PE/EtOAc 10%	21-35	21-23 ; **E_4**	**DGTFI3** + five compounds
		24-35 ; **E_5**	**DGTFI4** + two compounds+ drag
PE/EtOAc 15%	36-55	36-45 ; **E_6**	Mixture of three compounds + drag
		46-55 ; **E_7**	Mixture of four compound
PE/EtOAc 20%	56-79	56-68 ; **E_8**	Mixture of five compounds
		69-79 ; **E_9**	**DGTFI5 +** two spots
PE/EtOAc 25%	80-92	80-92 ; **E_{10}**	Mixture of seven compounds

PE/EtOAc 30%	93-103	93-103 ; **E_{11}**	Mixture of three compounds
PE/EtOAc 40%	104-115	104-115 ; **E_{12}**	Three compounds + drag
AcOEt 100%	washing	/	Drag

Compounds DGTFI1 and DGTFI3 were obtained respectively from subfractions E_1 and E_4. Their spectra analysis is still in progress.

Compounds DGTFI2 (lupeol), DGTFI4 (betulin) and DGTFI5 (betulinic acid) were obtained respectively from subfractions E_3, E_5 and E_9.

III.2.1.3.2 Purification of fractions FII and FIII

Fractions FII (4.30 g) and FIII (8.20 g) were grouped together on the basis of comparative TLC and eluted over silica gel using a gradient system PE/EtOAc from (1:3) to (3:1) to yield 110 fractions of 100 mL. After TLC analysis these fractions were combined into twelve subfractions labelled Fi.

Table 48: Chromatogram of fraction FIII

Column eluent	Fractions	Subfractions	Observation
PE/EtOAc 25%	1-14	1-8 ; **F_1**	Complex mixture
PE/EtOAc 30%	15-27	15-22 ; **F_2**	Mixture of five compounds
		23-27; **F_3**	Mixture of six compounds
PE/EtOAc 35%	28-39	28-39 ; **F_4**	**DGTFIII1**+ three compounds
PE/EtOAc 40%	40-55	40-46 ; **F_5**	Mixture of three compounds + drag
		47-55 ; **F_6**	Mixture of four compound
PE/EtOAc 50%	56-78	56-65 ; **F_7**	Mixture of five compounds

		66-78 ; **F_8**	Mixture of six compounds
PE/EtOAc 60%	79-101	79-88 ; **F_9**	**DGTFIII2** +Mixture of three compounds
		89-93 ; **F_{10}**	
		94-101 ; **F_{11}**	**DGTFIII3**
PE/EtOAc 75%	102-110	102-110 ; **F_{12}**	Drag
MeOH100%	washing	/	Drag

Compounds DGTFIII2 was obtained from the subfraction F_9 after washing with MeOH. Its analysis is still on going.

Compounds DGTFIII1 (corosolic acid) and DGTFIII3 (mixture of 3-*O*-*β*-glucoside of stigmasterol and *β*-sitosterol) were obtained from subfractions F_4 and F_{11} respectively.

III.2.1.3.3 Purification of fraction FIV

Fraction FIV (43.18g) was chromatographed over silica gel using gradient solvent system PE/EtOAc and EtOAc/MeOH and 129 fractions of 200mL were obtained. These fractions were grouped together into thirteen subfractions labelled Gi on the basis of TLC analysis.

Table 49: Chromatogram of fraction FIV

Column eluent	Fractions	Subfractions	Observation
PE/EtOAc 50%	1-16	1-5 ; **G_1**	Mixture of seven compounds + drag
		6-12; **G_2**	Mixture of five compounds + drag
		13-16 ; **G_3**	Mixture of three compounds
PE/EtOAc 60%	17-35	17-28 ; **G_4**	Mixture of five compounds
		29-35 ; **G_5**	Mixture of six compounds+ drag
PE/EtOAc 75%	36-64	36-40 ; **G_6**	**DGTFIV1E +** three compounds+ drag

		41-48 ; **G_7**	Mixture of three compounds
		49-64 ; **G_8**	**DGTFIV2 +** one compound
EtOAc 100%	65-88	65-69 ; **G_9**	Mixture of five compounds
		70-82 ; **G_{10}**	**DGTFIV3 +** two compounds
		83-88 ; **G_{11}**	Mixture of four compounds
EtOAc/MeOH 5%	89-99	89-96 ; **G_{12}**	Mixture of five compounds
EtOAc/MeOH 10%	100-112	97-129 ; **G_{13}**	**DGTFIV4** + drag
EtOAc/MeOH 15%	113-129		
MeOH 100%	washing	/	Drag

Compound DGTFIV1E was obtained from the Sephadex LH-20 column chromatography elution of fraction G_6 with MeOH.

Compounds DGTFIV2, DGTFIV3 and DGTFIV4 were obtained after filtration of fractions G_8, G_{10} and G_{13} respectively.

III.2.1.4 From the leaves of *D. fragrans*

The dried and powdered leaves of *D. fragrans* (3.20 kg) were extracted by maceration in methanol (2x7.5L) at room temperature for 3 days. After filtration and evaporation under reduce pressure, a visqueous green methanolic extract (101.70g) was obtained and fractionated using flash chromatography over silica gel cc into four fractions: FI (PE/EtOAc 3:1), FII (PE/EtOAc 1:1), FIII (EtOAc) and FIV (EtOAc/MeOH). On the basis of TLC analysis, fractions FII and FIII were grouped together. The column chromatography of these fractions yielded pure samples. The protocol used is illustrated by the scheme below.

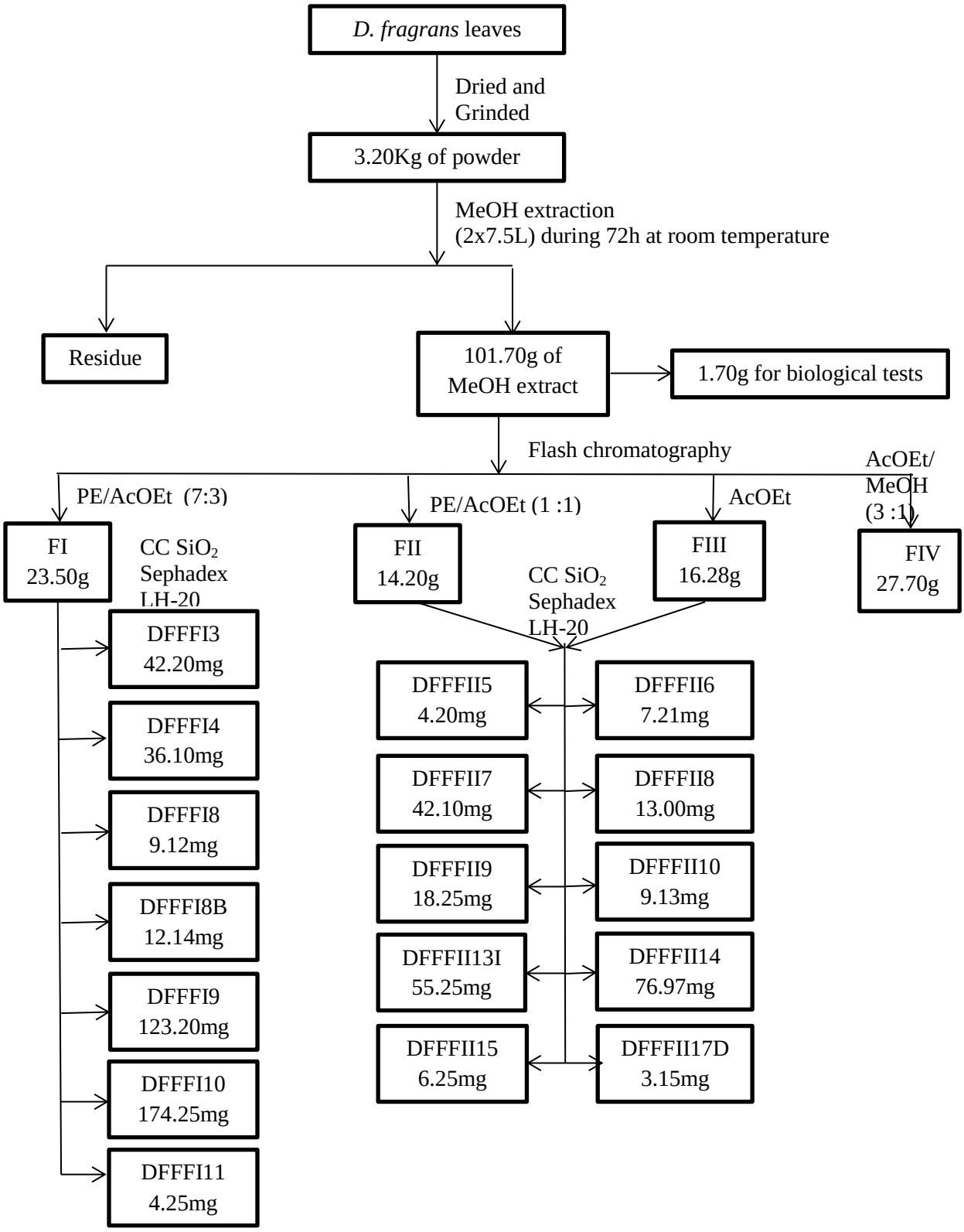

Scheme 10 : Extraction and isolation procedure of compounds from the leaves of *D. fragrans*.

Table 50: Fractions obtained from the leaves

Fractions	Column eluent
FI	PE/EtOAc 7:3
FII	PE/EtOAc 1:1
FIII	EtOAc
FIV	MeOH

III.2.1.4.1 Purification of fraction FI

Fraction FI (23.50g) chromatographed over silica gel with the gradient solvent system PE/EtOAC afforded182 fractions of 100 mL. These fractions were combined after TLC analysis into 18 subfractions labelled Hi.

Table 51: Chromatogram of fraction FI

Column eluent	Fractions	Subfractions	Observation
PE 100%	1-12	1-12 ; **H_1**	Oily mixture
PE/EtOAc 5%	13-29	13-16 ; **H_2**	**DFFFI11** + Oily mixture
		17-22; **H_3**	Mixture of four compounds
		23-29 ; **H_4**	**DFFFI3** + three compounds
PE/EtOAc 10%	30-44	30-37; **H_5**	Mixture of five compounds
		38-44 ; **H_6**	**DFFFI4** + two compounds
PE/EtOAc 15%	45-84	45-51 ; **H_7**	Mixture of six compounds
		52-59 ; **H_8**	**DFFFI8** +Mixture of three compounds + drag
		60-63 ; **H_9**	Mixture of three compounds
		64-70 ; **H_{10}**	**DFFFI8B+**Mixture of four compound
		71-74 ; **H_{11}**	Mixture of three compounds
		75-84 ; **H_{12}**	**DFFFI9 +** Mixture of two compounds
PE/EtOAc 20%	85-99	85-89 ; **H_{13}**	Mixture of five compounds

		90-99 ; **H_{14}**	Mixture of seven compounds
PE/EtOAc 25%	100-135	100-135 ; **H_{15}**	**DFFFI10 +** Mixture of seven compounds
PE/EtOAc 30%	136-152	136-152 ; **H_{16}**	Mixture of five compounds
PE/EtOAc 40%	153-165	153-165 ; **H_{17}**	Mixture of three compounds + drag
PE/EtOAc 50%	166-182	166-182 ; **H_{18}**	Drag
AcOEt 100%	washing	/	Drag

Compounds DFFFI3 (lupeol), DFFFI4 (betulin), DFFFI8 (Myrtifolic acid), DFFFI9 (betulinic acid) and DFFFI10 (ursolic acid) were obtained respectively from subfractions H_4, H_6, H_8, H_{12} and H_{15}. Compounds DFFFI8B (uvaol) and DFFFI11 (β-amyrin acetate) were obtained from the Sephadex LH-20 column chromatography elution of fractions H_2 and H_{10} respectively with the mixture CH_2Cl_2/MeOH (3:1).

III.2.1.4.2 Purification of fraction FII and FIII

These fractions grouped together (30.48g) were chromatographed over silica gel and eluted with PE/EtOAc and EtOAc/MeOH at increasing polarities to yield 229 fractions of 100 ml. based on TLC analysis, these fractions were combined into 24 subfractions labelled Ii.

Table 52: Chromatogram of fraction FII and FIII

Column eluent	Fractions	Subfractions	Observation
PE/EtOAc 20%	1-17	1-10 ; **I_1**	Complex mixture
		11-17 ; **I_2**	**DFFFII17D** + Three compounds
PE/EtOAc 25%	18-33	18-24 ; **I_3**	**DFFFII5 +** two compounds
		25-33 ; **I_4**	Mixture of four compounds
PE/EtOAc 30%	34-49	34-39 ; **I_5**	**DFFFII6 +** one compound
		40-49 ; **I_6**	Complex mixture + drag
PE/EtOAc 35%	50-76	50-62 ; **I_7**	Mixture of five compounds + drag

		63-76 ; **I_8**	Mixture of seven compounds + drag
PE/EtOAc 40%	77-92	77-92 ; **I_9**	**DFFFII15** + Mixture of two compounds
PE/EtOAc 50%	93-117	93-102 ; **I_{10}**	**DFFFII7** + Mixture of five compounds
		103-117 ; **I_{11}**	Mixture of four compounds
PE/EtOAc 60%	118-137	118-124 ; **I_{12}**	**DFFFII13I** + Mixture of three compounds
		125-131 ; **I_{13}**	Mixture of eight compounds
		132-137 ; **I_{14}**	**DFFFII8** + Mixture of six compounds
PE/EtOAc 75%	138-171	138-143 ; **I_{15}**	Mixture of three compounds + drag
		144-152 ; **I_{16}**	**DFFFII9** + two compounds
		153-160 ; **I_{17}**	Mixture of four compounds
		161-166 ; **I_{18}**	**DFFFII10 +** four spots
		167-171 ; **I_{19}**	Complex mixture + drag
EtOAc 100%	172-190	172-177 ; **I_{20}**	Mixture of five compounds
		178-183 ; **I_{21}**	Mixture of five
EtOAc/MeOH 5%	191-205	184-205 ; **I_{22}**	**DFFFII14** +Mixture of four compounds Mixture of three compounds
EtOAc/MeOH 10%	206-217	206-217 ; **I_{23}**	drag
EtOAc/MeOH 15%	218-229	218-229 ; **I_{24}**	drag
MeOH 100%	washing	/	Drag

Compounds DFFFII5 (oleanolic acid), DFFFII6 (corosolic acid), DFFFII8 (mixture of 3-*O*-*β*-glucoside of stigmasterol and *β*-sitosterol), DFFFII9 (5-*O*-methylinositol) and DFFFII14 (methyl- *β*-*D*-glucopyranoside) were obtained from subfractions I_3, I_5, I_{14}, I_{16} and I_{22} respectively.

Silica gel column chromatography of subfraction I_{12} with isochratic mixture of PE/EtOAc 35% yielded compound DFFFII13I (vismiaefolic acid).

Subfraction I_9 was eluted over silica gel with isochratic system PE/EtOAc 25 % to yield compound DFFFII15 (caulosapogenin).

Compound DFFFII17D (luteine) was obtained after silica gel column chromatography with isochratic system PE/EtOAc 10% and Sephadex LH-20 column chromatography with CH_2Cl_2/MeOH 50% of subfraction I_2.

Compounds DFFFII7 and DFFFII10 were obtained from subfractions I_{10} and I_{18} respectively. Their structure elucidations are still on going.

III.2.1.5 From the roots of *D. fragrans*

The air dried and powdered roots of *Diospyros fragrans* (2.8 kg) were macerated twice with 5L of MeOH at room temperature during 3 days. The resulting methanolic filtrate was concentrated to dryness under reduced pressure to give 78.9 g of a brown methanolic extract. 77 g of this extract was subjected to column chromatography in silica gel eluted sequentially with mixture of PE/EtOAc and EtOAc/MeOH of increasing polarities to afford pure samples. Below, are summarized extraction and isolation procedures for this part of the plant studied.

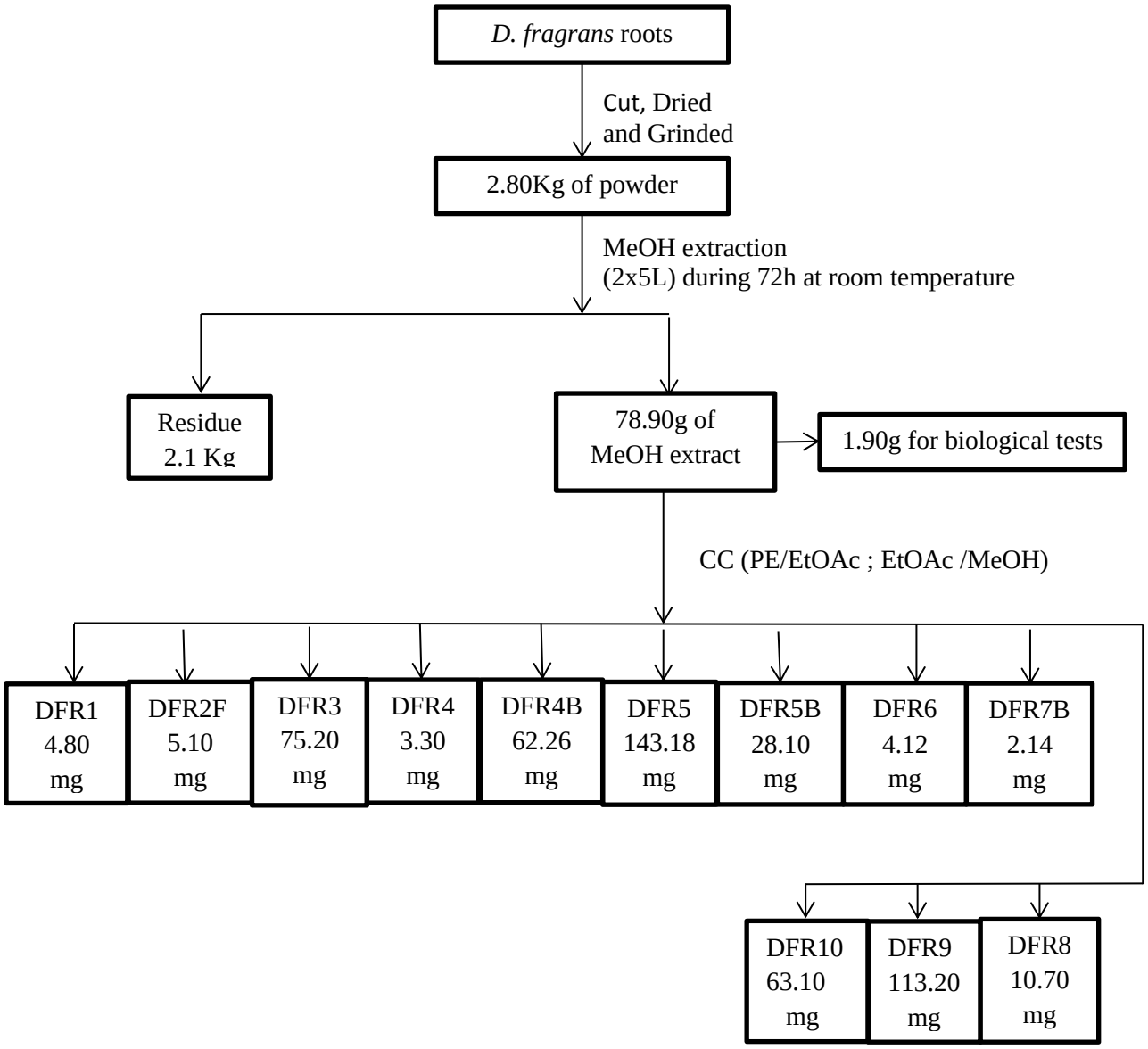

Scheme 11: Extraction and isolation procedure of compounds from the roots of *D. fragrans*.

429 fractions of 200 mL were obtained and combined in 26 subfractions labelled Ji on the basis of TLC analysis.

Table 53: Chromatogram of the roots extract of *Diospyros fragrans*

Column eluent	Fractions	Subfractions	Observation
PE 100%	1-12	1-14 ; **J_1**	Oily mixtures + **DFR1**
PE/EtOAc 2,5%	13-39	13-26 ; **J_2**	Oily mixtures
		27-39 ; **J_3**	Oily mixtures + **DFR2F**
PE/Ac 5%	40-67	40-49 ; **J_4**	Mixture of five compounds
		50-57 ; **J_5**	**DFR3** + three spots
		58-67 ; **J_6**	**DFR4** + Mixture of six compounds
PE/ EtOAc 7,5%	68-82	68-77 ; **J_7**	Complex mixtures
		78-82 ; **J_8**	**DFR4B** + Mixture of two compounds
PE/ EtOAc 10%	83-95	83-89 ; **J_9**	Mixture of five compounds
		90-95 ; **J_{10}**	Mixture of four compounds
PE/ EtOAc 12,5%	96-119	96-119 ; **J_{11}**	Mixture of seven compounds
PE/ EtOAc 15%	120-138	120-138; **J_{12}**	Mixture of four compounds
PE/ EtOAc 17,5%	139-171	139-151 ; **J_{13}**	Mixture of six compounds
		152-171 ; **J_{14}**	**DFR5** + five compounds
PE/ EtOAc 20%	172-193	172-221 ; **J_{15}**	**DFR5B** + Mixture of six compounds
PE/ EtOAc 25%	194-221		
PE/ EtOAc 30%	222-253	222-253 ; **J_{16}**	Complex mixture
PE/ EtOAc 35%	254-271	254-271 ; **J_{17}**	Mixture of five compounds
PE/ EtOAc 40%	272-294	272-278 ; **J_{18}**	**DFR6** + Mixture of three compounds

		279-290 ; **J_{19}**	Mixture of six compounds
		291-294 ; **J_{20}**	**DFR7B** + Mixture of two compounds
PE/ EtOAc 50%	295-315	295-315 ; **J_{21}**	**DFR8** + Mixture of four compounds
PE/ EtOAc 60%	316-338	316-357 ; **J_{22}**	**DFR9** + drag + Complex mixtures
PE/ EtOAc 75%	339-357		
EtOAc 100%	358-377	358-369 ; **J_{23}**	Mixture of seven compounds + drag
		370-393 ; **J_{24}**	**DFR10** + two compounds
EtOAc/MeOH 5%	378-393		
EtOAc/MeOH 10%	394-409	394-409 ; **J_{25}**	Mixture of four compounds + drag
EtOAc/MeOH 15%	410-429	410-429 ; **J_{26}**	drag
MeOH 100%	washing	/	Drag

Compounds DFR3 (lupeol), DFR4B (mixture of stigmasterol and *β*-sitosterol), DFR5 (betulinic acid), DFR5B (ursolic acid), DFR8 (vismiaefolic acid), DFR9 (mixture of 3-*O*-*β*-glucoside of stigmasterol and *β*-sitosterol) and DFR10 (methyl- *β*-*D*-glucopyranoside) were obtained from subfractions J_5, J_8, J_{14}, J_{15}, J_{21}, J_{22} and J_{24} respectively.

Subfractions J_{18} and J_{20} were subjected each to sephadex LH-20 eluted with MeOH and yielded compounds DFR6 (1-*O*-(28-Hydroxyoctacosanoyl) glycerol) and DFR7B (fragranone) respectively.

Subfraction J_6 was subjected successively to sephadex LH-20 eluted with CH_2Cl_2/MeOH (1:1) to yield compound DFR4 (*α*-tocopherol).

Structure elucidations of compounds DFR1 and DFR2F are still on going.

III.2.2. Physical and spectral data of compounds isolated from *Diospyros gilletii* and *Diospyros fragrans*

- DGET4; DGF10; DGTFIV2

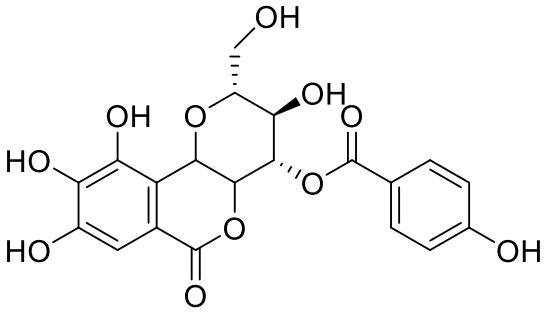

Name: 4-*O*-*p*-hydroxybenzoylnorbergenin; White powder; $[\alpha]_D^{20}$: -53 (*c* 0.68, MeOH); **m.p.** 286-287°C; **IR** υ_{max} 3730, 3392, 1714, 1699, 1607, 1470 cm^{-1}; **HRESIMS**: *m/z* 457.0738 (calculated for $C_{20}H_{18}O_{11}Na$: *m/z* 457.0741); **$FeCl_3$ test**: Positive**;** **^1H** and **^{13}C NMR** : see Table. 9

- DGF8

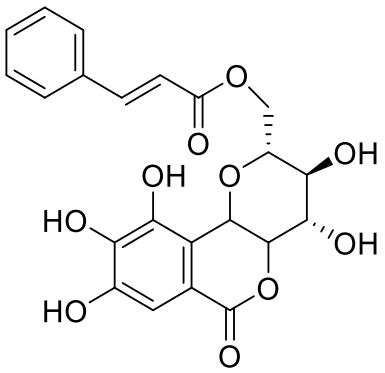

Name: 11-*O*-*(E)*-cinnamoylnorbergenin; White powder; $[\alpha]_D^{20}$**:** 58,3 (*c* 1, MeOH); **IR** υ_{max} 3354, 1698, 1635, 1314, 1087 cm^{-1}; **MF**: $C_{22}H_{20}O_{10}$; **HRESIMS**: *m/z* 467.0949 (calculated for $C_{22}H_{20}O_{10}Na$: *m/z* 467.09487); **$FeCl_3$ test**: Positive; **^1H** and **^{13}C NMR** : see Table. 11

- DGET1; DGF10B; DGTFIV3

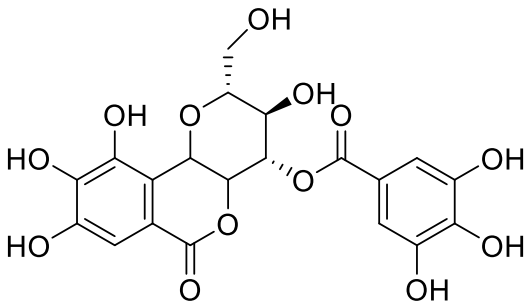

Name: 4-*O*-galloylnorbergenin; White powder; **MF**: $C_{20}H_{18}O_{13}$; **mp**: 219-220°C; **HRESIMS**: *m/z* 489.0696 (calculated for $C_{20}H_{18}O_{13}Na$: *m/z* 489.06396); **$FeCl_3$ test**: Positive; **^{1}H** and **^{13}C NMR:** see Table. 12

- DGTFIV1E

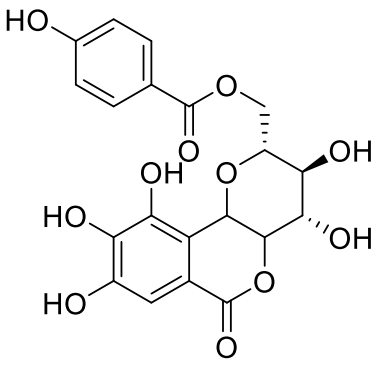

Name: 11-*O*-p-hydroxybenzoylnorbergenin; White powder; **MF**: $C_{20}H_{18}O_{11}$; **ESIMS**: *m/z* 457.1 $[M+Na]^+$; **$FeCl_3$ test**: Positive**; ^{1}H** and **^{13}C NMR:** see Table. 10

- DGET5B; DGTFIV4; DGF11

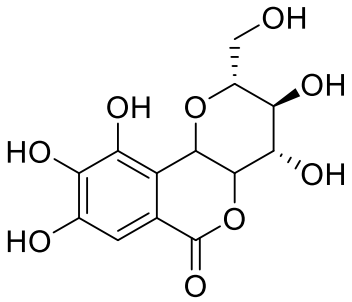

Name: norbergenin; White powder; **MF**: $C_{13}H_{14}O_9$; **mp**: 178-180°C**; ESIMS**: *m/z* 312.9 $[M-H]^-$; **$FeCl_3$ test**: Positive; **^{1}H** and **^{13}C NMR:** see Table. 8

- DFR7B

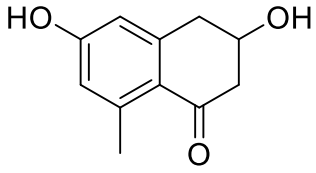

Name: Fragranone**;** Brown oil; **$[\alpha]_D^{20}$:** -8.1 (*c* 0.166, MeOH); **IR** υ_{max} 3270, 2955, 2925, 1732, 1646, 1601 cm^{-1}; **MF**: $C_{11}H_{12}O_3$; **HRESIMS**: *m/z* 193.08605 (calculated for $C_{11}H_{12}O_3H$: *m/z* 193.08592); **$FeCl_3$ test**: Positive; **^{1}H** and **^{13}C NMR** : see Table. 13

- DGF5; DFFFI10; DFR5B

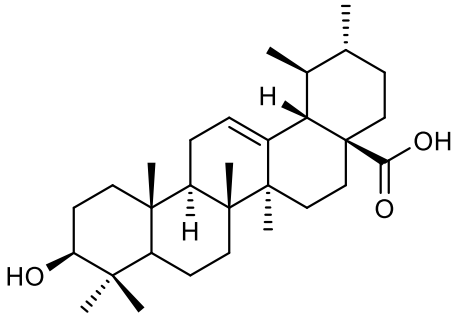

Name: Ursolic acid; White powder; **MF**: $C_{30}H_{48}O_3$; **mp**: 285-288°C**; ESIMS**: *m/z* 479.4 $[M+Na]^+$; **Liebermann Burchard test**: positive; **^{1}H** and **^{13}C NMR** : see Table. 14

- DGF7; DGTFIII1; DFFFII6

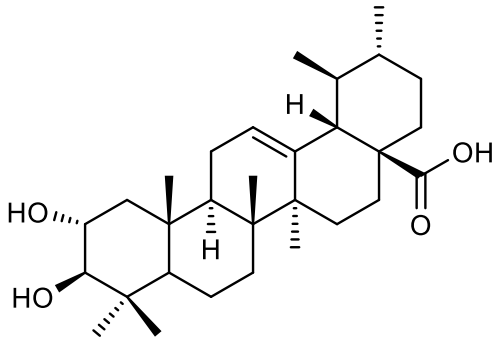

Name: Corosolic acid; White powder; **MF**: $C_{30}H_{48}O_4$; **mp**: 243-245°C**; ESIMS**: *m/z* 495.3 $[M+Na]^+$; **Liebermann Burchard test**: positive; **^{1}H** and **^{13}C NMR** : see Table. 15.

- DFFFI8B

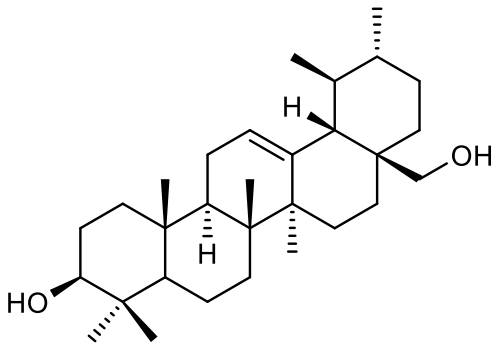

Name: Uvaol; White powder; **MF**: $C_{30}H_{50}O_2$; **mp**: 223-225°C**; ESIMS**: *m/z* 465.3 $[M+Na]^+$; **Liebermann Burchard test**: positive; **^{1}H** and **^{13}C NMR** : see Table. 16

- DFFFI8

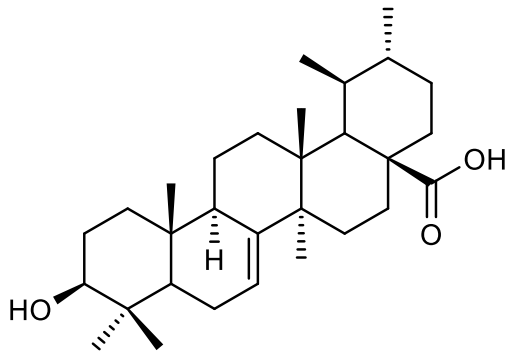

Name: Myrtifolic acid; White powder; **MF**: $C_{30}H_{48}O_3$; **mp**: 305-308°C; **ESIMS**: *m/z* 479.3 $[M+Na]^+$; **Liebermann Burchard test**: positive; **^{1}H** and **^{13}C NMR** : see Table. 17

- DGTFIII2

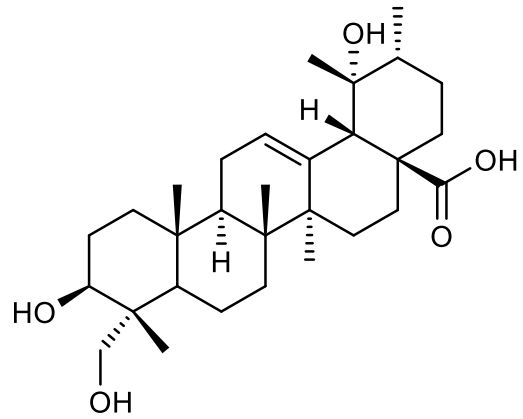

Name: Rotundic acid; White powder; **MF**: $C_{30}H_{48}O_5$; **mp**: 272-274°C; **ESIMS**: *m/z* 487 $[M-H]^-$; **Liebermann Burchard test**: positive; **^{1}H** and **^{13}C NMR**: see Table. 18

- DFFFII13I; DFR8

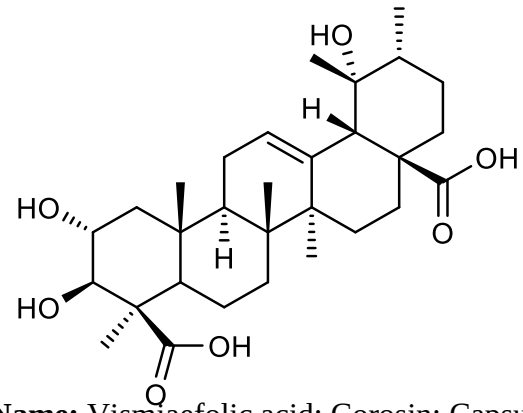

Name: Vismiaefolic acid; Corosin; Capsularone; Trachelosperogenin A; White powder; **MF**: $C_{30}H_{46}O_7$; **mp**: > 300°C; **ESIMS**: *m/z* 541.4 $[M+Na]^+$; **Liebermann Burchard test**: positive; **^{1}H** and **^{13}C NMR** : see Table. 19

- DGF2; DGTFI2; DGETH1; DFFFI3; DFR3

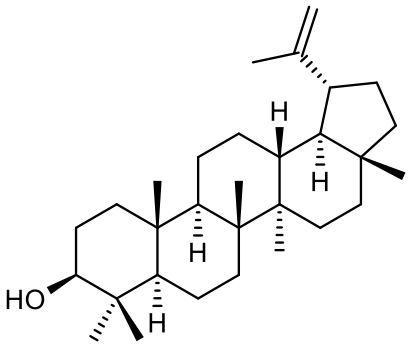

Name: Lupeol; White powder; **MF**: $C_{30}H_{50}O$; **mp**: 208-210°C**; ESIMS**: *m/z* 449.4 $[M+Na]^+$; **Liebermann Burchard test**: positive; **^{1}H** and **^{13}C NMR** : see Table. 20

- DGF3; DGETH2

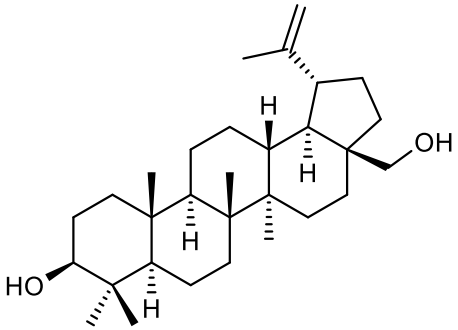

Name: Betulin; White powder; **MF**: $C_{30}H_{50}O$; **mp**: 256-258°C; **HRESIMS**: *m/z* 443.3881 (calculated for $C_{30}H_{50}OH$: *m/z* 443.38836); **Liebermann Burchard test**: positive; **^{1}H** and **^{13}C NMR**: see Table. 21

- DFR5; DGF4C; DGTFI5; DGETH3; DFFFI9

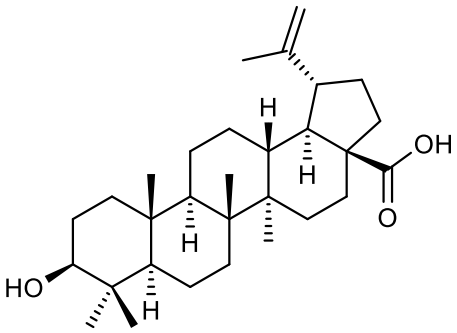

Name: Betulinic acid; White powder; **MF**: $C_{30}H_{48}O_3$; **mp**: 316-318°C; **ESIMS**: *m/z* 479.3 $[M+Na]^+$; **Liebermann Burchard test**: positive; **^{1}H** and **^{13}C NMR** : see Table. 22

- DGF6; DFFFII5

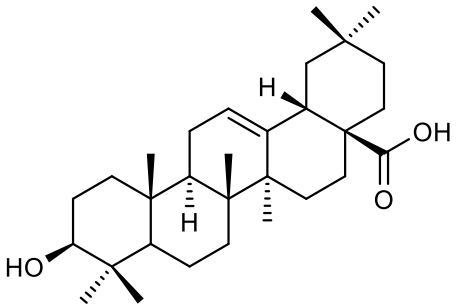

Name: Oleanolic acid; White powder; **MF**: $C_{30}H_{48}O_3$; **mp**: 300-310°C; **ESIMS**: *m/z* 479.4 $[M+Na]^+$; **Liebermann Burchard test**: positive; **^{1}H** and **^{13}C NMR** : see Table. 23

- DFFFI11

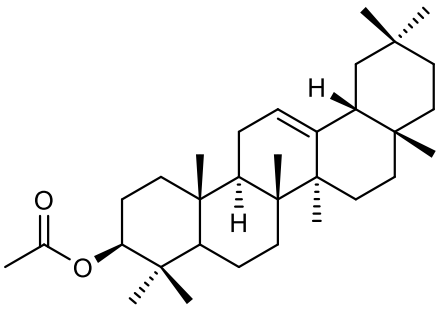

Name: *β*-amyrin acetate; White powder; **MF**: $C_{32}H_{52}O_2$; **mp**: 238-245°C; **ESIMS**: *m/z* 491.4 $[M+Na]^+$; **Liebermann Burchard test**: positive; **^{1}H** and **^{13}C NMR** : see Table. 25

- DFFFII15

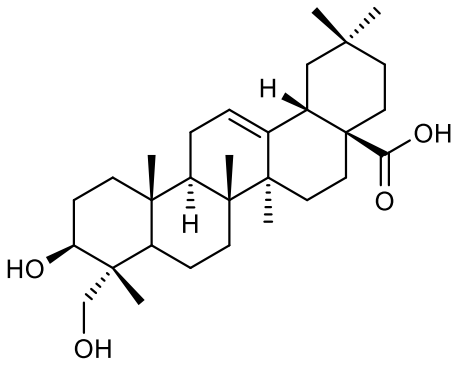

Name: Hederagenin; caulosapogenin; White powder; **MF**: $C_{30}H_{48}O_4$; **mp**: 332-334°C; **ESIMS**: *m/z* 495.3 $[M+Na]^+$; **Liebermann Burchard test**: positive; **^{1}H** and **^{13}C NMR** : see Table. 24

- DGF1

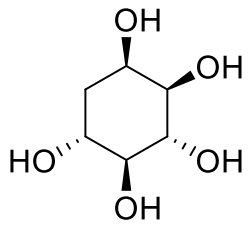

Name: *D*-Quercitol; 5-Deoxyinositol; beige crytals; **MF**: $C_6H_{12}O_5$; **mp:** 233 - 235 °C; **ESIMS**: *m/z* 163.4 $[M-H]^-$; **^{1}H** and **^{13}C NMR**: see Table. 26

- DFFFII14; DFR10

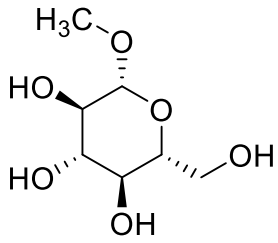

Name: methyl-*β*-*D*-glucopyranoside; White crystals; **MF**: $C_7H_{14}O_6$; **mp**: 103-105°C; **^{1}H** and **^{13}C NMR**: see Table. 27

- DFFFII9

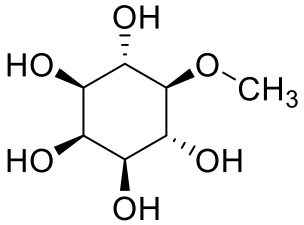

Name: 5-*O*-methyl-myo-inositol; Sequoyitol; brown powder; **MF**: $C_7H_{14}O_6$; **mp**: 241-244°C; **^{1}H** and **^{13}C NMR**: see Table. 28

- DGTFI4; DGF2B; DGETH1B; DFFFI4; DFR4B

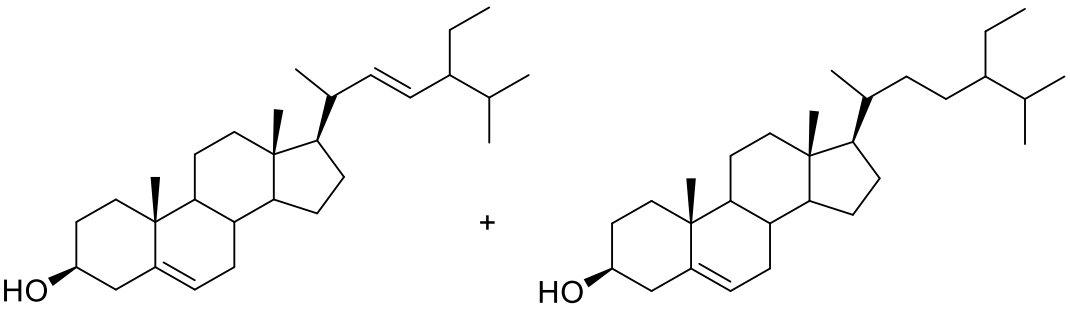

Name: Stigmasterol + *β*-sitosterol; White needles; **MF**: $C_{29}H_{48}O$ and $C_{29}H_{50}O$; **mp**: 165-167°C; **ESIMS:** *m/z* 435.4 $[M+Na]^+$; **Salkowski test**: positive; **^{1}H** and **^{13}C NMR** : see Table. 31

- DGTFIII3; DGET3; DFFFII8; DFR9

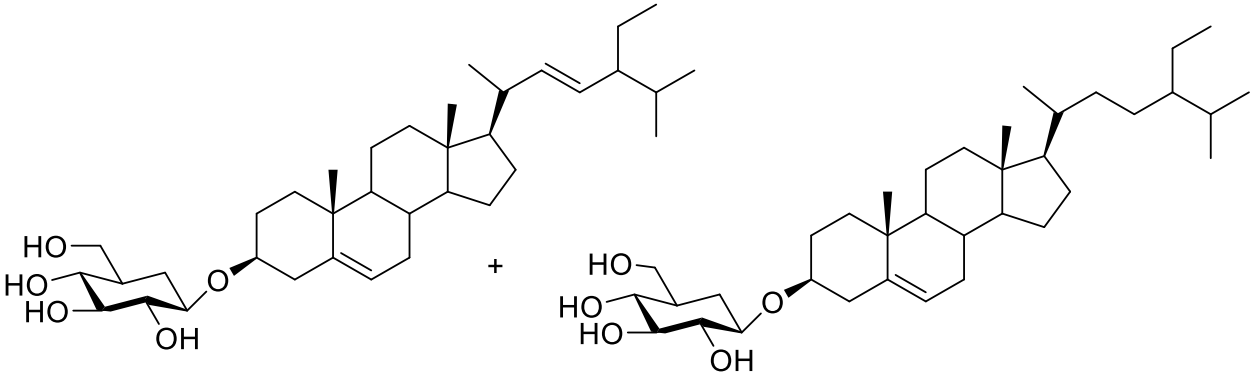

Name: 3-*O*-*β*-*D*-glucopyranoside of stigmasterol + *β*-sitosterol. Beige powder; **MF**: $C_{35}H_{60}O_6$; **mp:** 270 – 272 °C; **ESIMS:** *m/z* 575.4 $[M-H]^-$; **Salkowski test**: positive; **Molish test**: Positive; **^{1}H** and **^{13}C NMR**: see Table. 32

- DFR4

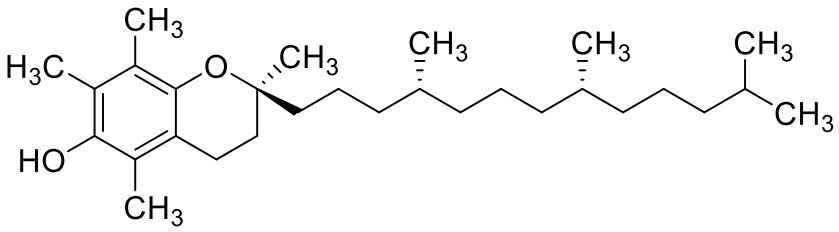

Name: *α*-tocopherol; incolor oil; **MF**: $C_{29}H_{50}O_2$; **mp**: 76-77°C; **ESIMS:** *m/z* 429.2 $[M+Na]^+$; **^{1}H** and **^{13}C NMR** : see Table. 29

- DFFFII17D

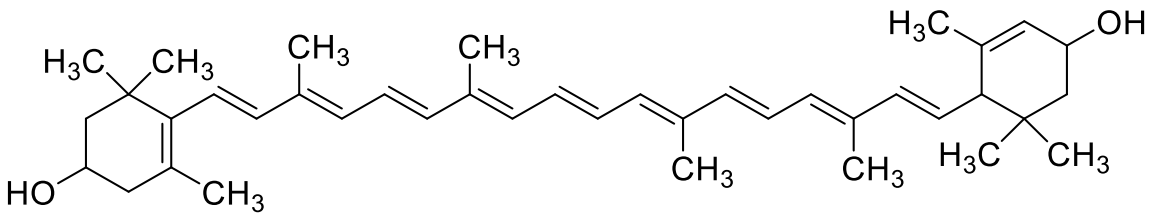

Name: Lutein; Red powder; **MF**: $C_{40}H_{56}O_2$; **mp**: 190-191°C; **ESIMS:** *m/z* 569.4 $[M+H]^+$; **^{1}H** and **^{13}C NMR** : see Table. 30

- DFR6

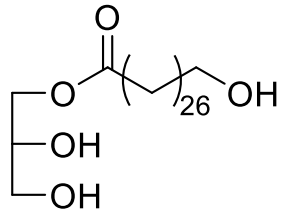

Name: 1-*O*-(28-hydroxyoctacosanoyl) glycerol; Brown oil; **MF**: $C_{31}H_{62}O_5$; **mp**: 190-191°C; **HRESIMS:** *m/z* 537.4487 $[M+Na]^+$; **^{1}H** and **^{13}C NMR** : see Table. 31

- DGET4Ac

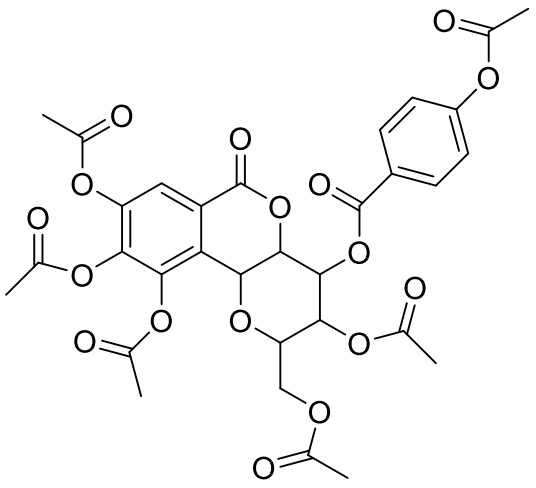

Name: per-acetylated derivative of 4-*O*-*p*-hydroxybenzoylnorbergenin; White powder; **MF**: $C_{32}H_{30}O_{17}$; **HRESIMS:** *m/z* 709.1378 (calculated for $C_{32}H_{30}O_{17}Na$: *m/z* 709.1380); **^{1}H** and **^{13}C NMR**: see Table. 34

- DGET4Al

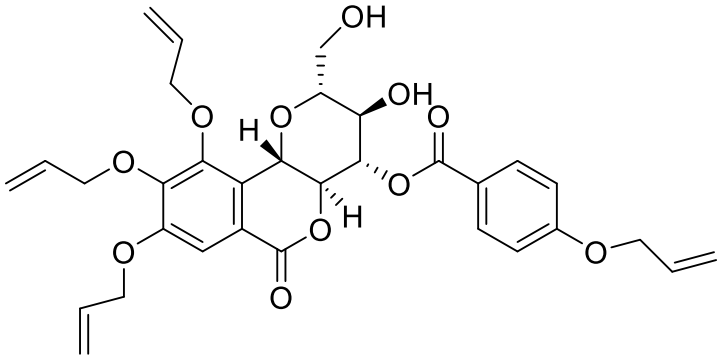

Name: per-allylated derivative of 4-*O*-*p*-hydroxybenzoylnorbergenin; colorless oil; **MF**: $C_{32}H_{34}O_{11}$; **HRESIMS:** *m/z* 617.1998 (calculated for $C_{32}H_{34}O_{11}Na$: *m/z* 617.1999); **^{1}H** and **^{13}C NMR**: see Table. 37

- DFFFII13IA

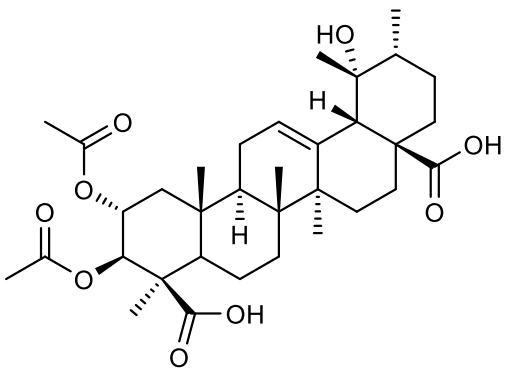

Name: per acetylated derivative of vismiaefolic acid; white powder; **MF**: $C_{34}H_{50}O_9$; **ESIMS:** *m/z* 601.2 $[M-H]^-$; **^{1}H** and **^{13}C NMR**: see Table. 36

- DFR5Ac

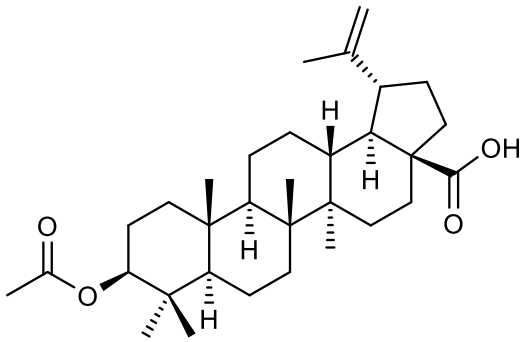

Name: Betulinic acid acetate; white powder; **MF**: $C_{32}H_{50}O_4$; **ESIMS:** *m/z* 497.2 $[M-H]^-$; **^{1}H** and **^{13}C NMR**: see Table. 36

- DFR5Al

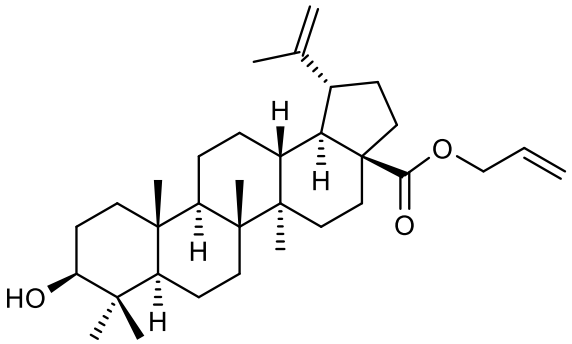

Name: Betulinic acid 28-allyle; colorless oil; **MF**: $C_{33}H_{52}O_3$; **ESIMS:** *m/z* 497.2 $[M-H]^-$.

- DGF5Al

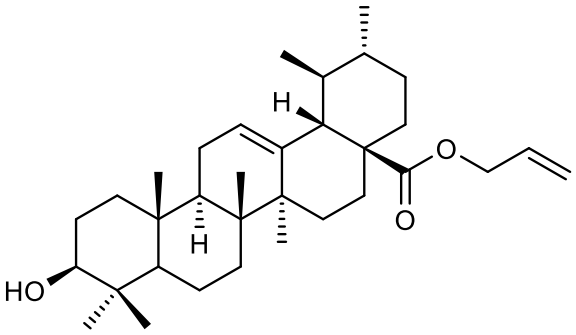

Name: Ursolic acid 28-allyle; colorless oil; **MF**: $C_{33}H_{52}O_3$; **ESIMS:** *m/z* 519.3 $[M+Na]^+$.

III.3. CHEMICAL TRANSFORMATIONS

III.3.1. Acetylation

III.3.1.1. Acetylation of DGET4

Compound DGET4 (20 mg) was dissolved in pyridine (2 mL) and 2 mL of acetic anhydride was added to the mixture and leave under agitation at room temperature during 12 hours. After stopping agitation, the reaction mixture was dissolved in distilled water and partitioned with dichloromethane and this dichloromethane concentrate further gave DGET4Ac (per-acetylated derivative of 4-*O*-*p*-hydroxybenzoylnorbergenin) as a white powder (12 mg).

III.3.1.2. Acetylation of DFFFII13I

10 mg of compound DFFFII13I was introduced into a conical flask together with 1 mL of pyridine and 1 mL of acetic anhydride. The mixture obtained was agitated at room temperature during 12 Hours. After that, 20 mL of distilled water was added to the reaction mixture and the organic part was extracted with dichloromethane to give after evaporation on an rotatif evaporator compound DFFFII13IAc (per-acetylated derivative of vismiaefolic acid) as a white powder (7 mg).

III.3.1.3. Acetylation of DFR5

The acetylation scheme of DFR5 (20 mg) followed the same conditions than that of DGET4. We obtained compound DFR5Ac at the end of the process as a white powder (11 mg).

III.3.2. Allylation

III.3.2.1. Allylation of DGET4

Compound DGET4 (25 mg) was dissolved in anhydrous acetone (12 mL) and 500 mg of calcium carbonate was added to the medium. After complete dissolution, 4.0 mL of allyl bromide was introduced in the reaction mixture and submitted to agitation at 70°C during 4 hours. Then, the solvent was removed by evaporation on an rotatif evaporator under reduce pressure and 20 ml of distilled water was added to the reaction mixture. The organic part was extracted with dichloromethane and the oily medium obtained was chromatographed over

silica gel eluted with an isochratic solvent system PE/EtOAc 9:1 to afford DGET4Al (per-allylated derivative of 4-*O*-*p*-hydroxybenzoylnorbergenin) as an incolor oil (9 mg).

III.3.2.2. Allylation of DFR5

20 mL of DFR5 was dissolved in 10 mL of anhydrous acetone and 500 mg of sodium hydroxide was added to the mixture. Then 4 ml of allyl bromide was introduced to the medium and the reaction mixture was agitated during 4 hours at 70°C. 20 ml of distilled water was added after stopping the reaction and the mixture was extracted with dichloromethane. After evaporation on a rotatif evaporator, the obtained dry sample was adsorbed onto silica gel and separated using gravity CC on a column packed with silica gel using PE/EtOAc 17:3 as eluent to afford DFR5Al (betulinic acid-28-allyle) as incolor oil (7 mg).

III.3.2.3. Allylation of DGF5

The allylation scheme of DGF5 (20 mg) was achieved following the same conditions than that of the above compound DFR5. The organic part afforded DGF5Al (ursolic acid-28-allyle) as incolor oil (8 mg).

III.4. BIOLOGICAL TESTS

III.4.1. Cytotoxic activity

The test is based on the irreversible reduction of the colour indicator resazurin to strongly fluorescent resorufin in the presence of viable cells. Indeed, non-viable cells rapidly lose their metabolic capacity to reduce resazurin and thus no longer produce fluorescent signals. In the presence of NADPH dehydrogenase or NADH dehydrogenase, NADH and NADPH convert resorufin to resofurin in the mitochondria in a manner proportional to aerobic respiration according to the following scheme 23.

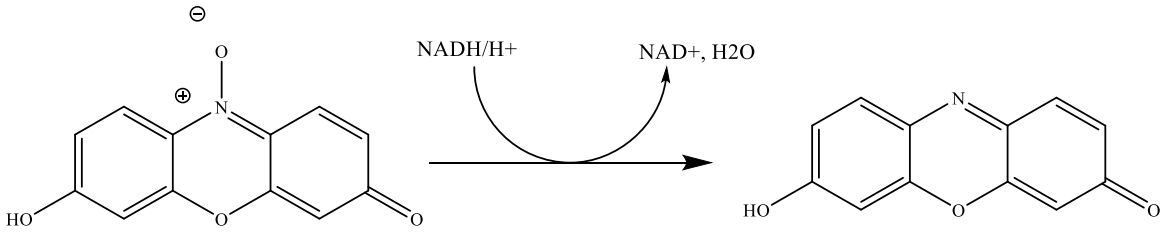

Scheme 23: Reduction of resazurin into resorufin

Operationally, the cytotoxic tests on human cervix carcinoma cell line KB-3-1 and human colon cancer cell line HT-29 were conducted with griseofulvin as reference and with dimethylsulfoxide as the solvent for solubility of the samples. Aliquots of 1.10^4 cells per well

were seeded in 96 well dishes in a total volume of 100 µL. The compounds to be studied were added immediately in varying concentrations in an additional 100 µL of culture medium to give a total volume of 200 µL/well. After 72 hours, 30 µL of a 175 µM resazurin solution diluted in distilled water was added to each well and the plates were incubated at 37°C for 6 hours. Fluorescence was measured in an Infinite M2000 ProTM plate reader (Tecan, Crailsheim, Germany) using excitation and emission wavelengths of 530 nm and 588 nm respectively. Each test was performed at least six times. Cell viability was assessed by comparison to untreated cells. IC_{50} values represent the concentrations of compounds required to inhibit 50% of cell proliferation and are calculated from the dose-response calibration curve on GRAPHPAD PRIWM 4.03 software.

III.4.2. Antioxidant activity

The radical scavenging activities of pure compounds were evaluated spectrophotometrically using the 2,2-diphenyl-1- picrylhydrazyl (DPPH) free radical. When DPPH reacts with an antioxidant compound, which can donate hydrogen, it is reduced and its purple color fades rapidly, as shown in the following scheme 24.

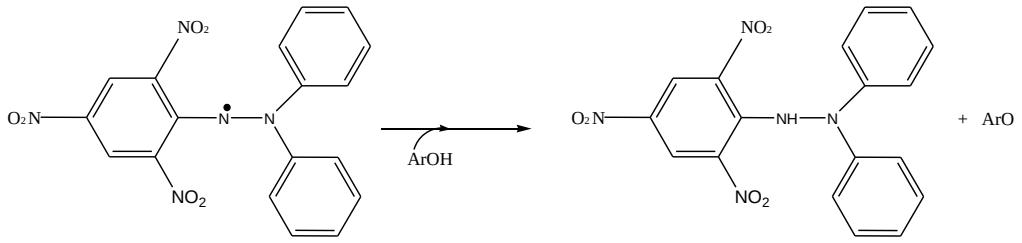

DPPH
Couleur violette

DPPHH
Couleur jaune

Scheme 24: Reduction of free radical DPPH

The changes in colour were measured at 517 nm under UV/Visible light spectrophotometer. Pure compounds were dissolved and diluted in MeOH at different concentrations (500, 250, 125, 60.25 and 30.125 µg/mL). Then, Fifty-five microliters of each diluted compound was mixed with fifty-five µL of 0.2 mg/mL solution of DPPH radical in MeOH. The mixture was incubated for 30 min in the dark at room temperature. The scavenging capacity was determined spectrophotometrically by monitoring the decrease in absorbance at 517 nm against a blank. Trolox was used as reference. Each assay was done in triplicate and the results, recorded as the mean ± standard deviation (SD) of the three findings, were presented in tabular form. The radical scavenging activity (RSA, in %) was calculated as follows:

%RSA= [(Absorbance of DPPH – Absorbance of sample) / Absorbance of DPPH] x 100

The radical scavenging percentages were plotted against the logarithmic values of concentration of test samples and a linear regression curve was established in order to calculate the RSA_{50} or IC_{50}, which is the concentration of sample necessary to decrease by 50% the total free DPPH radical.

III.4.3. Antibacterial activity

The antibacterial activity of extracts and pure compounds were evaluated on three gram positive and two gram negative bacteria which were stored at 4°C on nutrient agar: *Bacillus subtilis* (Bs), *Micrococcus luteus* (MI), *Staphylococcus warneri* (Stw), *Escherichia coli* (Ecoli) and *Pseudomonas agarici* (Psa). In a petri dish with Nutrient Broth agar (or trypticase soy broth in the case of *Staphylococcus warneri*), 0,2 mL of a bacterial solution were plated, then Whatmann filter paper disks of 6 mm in diameter previously impregnated with 25 µL of crude extract at 20 mg/mL or isolated compounds at 0.5 mg/mL (in DMSO) were placed on the bacteria plate and incubated at 37°C in a 5% enriched atmosphere of CO_2 for 24 hours. After that, inhibition zones around the paper disk were measured in millimeters three times. 25µL of Genatamycin at 0.5 mg/mL was taken as reference. For inhibitory zones more than 9 mm, MIC was measured following the microdilution method (Zgoda et Porter, 2001).

III.5. QUALITATIVE TESTS OF THE ISOLATED COMPOUNDS

III.5.1. Liebermann Burchard test

This test is characteristic of triterpenes and sterols. Liebermann Burchard's reagent is constituted of acetic anhydride [$(CH_3CO)_2O$], sulfuric acid (H_2SO_4) and chloroform ($CHCl_3$).
Protocol: Dissolve a small amount of the compound to test in 50 mL of $CHCl_3$ and then add 20 mL of acetic anhydride and few drops of concentrated sulfuric acid.

Interpretation: The presence of triterpenes is manifested by the appearance of a purplish red color and that of sterols by the appearance of a greenish blue color.

III.5.2. Ferric chloride test

The aim of this test is to identify phenolic hydroxyl groups. The ferric chloride's reagents are ferric chloride ($FeCl_3$) and methanol (MeOH).

Protocol: dissolve a small amount of the compound to test in methanol and add few drops of $FeCl_3$.

Interpretation: depending on the structure of the compound, a blue, red or green complex type $[Fe(OAr)_6]^{3-}$ is formed.

III.5.3. Molish test

This test consists on the characterization of sugars. The reagents used are ethanol, α-naphtol and sulfuric acid.

Protocol: Prepare a mixture of 1% α-naphtol in ethanol and use this mixture to dissolve a small amount of the compound to test. Then add few drops of H_2SO_4.

Interpretation: in the presence of sugar, a purplish red ring is formed at the interphase.

REFERENCES

1) **AACR**, "Cancer Progress Report 2012". Clinical cancer research (2012).
2) **Abraham R. J., Ghersi A., Pertillo G., Sancassan F.**, "Conformational Analysis. Part 30. The Conformational Analysis of some Lactones by the Lanthanide Induced Shift (LIS) Technique". *Journal of the Chemical Society Perkin Trans*, 2, 1279 (1997).
3) **Adzu B., Amos S., Dzarma S., Muazzam I., Gamaniel K., "**Pharmacological evidence favouring the folkloric use of *Diospyros mespiliformis* Hochst in the relief of pain and fever". *Journal of ethnopharmacology*, 82, 191-195 (2002).
4) **Akak C. M., Djama C. M., Nkengfack A. E., Tu P. F., Lei L. D., "**New coumarin glycosides from the leaves of *Diospyros crassiflora* (Hiern)". *Fitoterapia*, 81, 873-877 (2010).
5) **Anand P., Kunnumakkara A. B., Sundaram C., Harikumar K. B., Tharakan S. T., Lai O. S., Sung B., Aggarwal B. B**., "Cancer is a preventable disease that requires major lifestyle changes". *Pharmaceutical Research*, 25, 2097–116 (2008).
6) **Araújo F. W. L.** and **Souza M. P.,** "vismiaefolic acid, a new triterpene from *vochysia vismiaefolia*". *Journal of Natural Products*, 53, 1436-1440 (1990).
7) **Aro A. O., Dzoyem J. P., Awouafack M. D., Selepe A. M., Eloff N. J., McGaw L. J**., "Fractions and isolated compounds from *Oxyanthus speciosus* subsp. stenocarpus (Rubiaceae) have promising antimycobacterial and intracellular activity". *BMC Complementary and Alternative Medicine*, 19, 1-11 (2019).
8) **Auamcharoen W., Kijjoa A., Chandrapatya A., Pinto M. M., Silva A. M.S., Naengchomnong W., Herz W**., "A New Tetralone from *Diospyros cauliflora*". *Biochemical Systematics and Ecology*, 37, 690-692 (2009).
9) **Baker J. K.** and **Myers C. W**., "One dimensional and two dimensional 1H and 13C-Nuclear magnetic resonance (NMR) analysis of vitamin E raw materials or analytical reference standards". *Pharmaceutical research*, 8, 763-770 (1991).

10) **Baravalia Y., Kaneria M., Yaghasiya Y., Parekh J., Chanda S.**, "Antioxidant and antibacterial activity of *Diospyros ebenum* roxb. leaf extracts". *Turkish Journal of Biology*, 33, 159-164 (2009).
11) **Bhattacharyya A., Chattopadhyay R., Mitra S., Crowe S. E**., "Oxidative stress: an essential factor in the pathogenesis of gastrointestinal mucosal diseases". *Physiological Reviews*, 94, 329-354 (2014).
12) **Boiteau P., Pasich B., Ratsimamanga A., «** Les triterpènoïdes en physiologie animale et végétale ». *Gauthier Villars*, 1, 50-60 (1964).
13) **Bouquet A**., "Féticheurs et Médécine Traditionnelles du Congo (Brazzaville)". *Office de la Recherche Scientifique et Technique Outre-Mer, Paris*, 107 (1969).
14) **Bouquet A.** and **Debray M**., « Plantes médicinales de la Côte d'Ivoire ». Travaux et documents de l'ORSTOM. *Office de la Recherche Scientifique et Technique Outre-Mer, Paris*; 232 (1974).
15) **Brisson R**., « Utilisation des plantes par les pygmées Baka Etudes pygmées ». Paris, France (1999).
16) **Bruneton J., «** Pharmacognosie, Phytochimie et Plantes médicinales ». *Techniques et Documentation-Lavoisier*, 3, 410-670 (1999).
17) **Burton G. W.** and **Ingold K. U.,** "Vitamin E as an in vitro and in vivo antioxidant". *Annals of the New York Academy of Sciences*, 570, 7-22 (1989).
18) **Cai L., Wei G. X., van der Bijl P., Wu C. D**., "Namibian Chewing Stick, *Diospyros lycioides*, Contains Antibacterial Compounds Against Oral Pathogens". *Journal of Agricultural and Food Chemistry*, 48, 909-914 (2000).
19) **Cai Y. Z., Sun M., Corke H.,** "Antioxidant activity of betalains from plants of the amaranthaceae". *Journal of Agricultural and Food Chemistry*, 51, 2288–2294 (2003).
20) **Chang H. W., Jang K. H., Lee D., Kang H. R., Kim T.-Y., Lee B. H., Shin J**., "Monoglycerides from the brown alga *Sargassum sagamianum*: Isolation, synthesis, and biological activity". *Bioorganic & Medicinal Chemistry Letters*, 18, 3589-3592 (2008).
21) **Chaturvedula V. S. P.** and **Prakash I**., "Isolation of Stigmasterol and *β*-Sitosterol from the dichloromethane extract of *Rubus suavissimus". International Current Pharmaceutical Journal*, 1, 239-242 (2012).
22) **Chhabra S. C., Mahunnah R. L. A., Mshiu E. N., "**Plants used in traditional medicine in Eastern Tanzania. II. Angiospersm (Capparidaceae to Ebenaceae)". *Journal of Ethnopharmacology*, 25, 339-359 (1989).

23) **Chorghade S. M.,** "Drug Discovery and Development, Volume 2: Drug development" *John Wiley & Sons*, Chap. 17, 1-6 (2007).

24) **Cichewicz R. H.** and **Kouzi S. A.**, "Chemistry, Biological Activity, and Chemotherapeutic Potential of Betulinic Acid for the Prevention and Treatment of Cancer and HIV Infection". *Medicinal Research Reviews*, 24, 90-114 (2004).

25) **Cotelle N., Bernier J. L., Catteau J. P., Pommery J., Wallet J. C., Gaydou E. M**., "Antioxidant properties of hydroxyflavones". *Free Radical Biology and Medicine*, 20, 35–43 (1996).

26) **Cragg G. M.** and **Newman D. J**., "Biodiversity: a continuing source of novel drug leads". *Pure and Applied chemistry*, 77, 7-24 (2005).

27) **Darley-Usmar V.** and **Halliwell B**., "Blood radicals: reactive nitrogen species, reactive oxygen species, transition metal ions, and the vascular system". *Pharmaceutical Research*, 13, 649-662 (1996).

28) **Dimitriadis, Georgios K; Angelousi, Anna; Weickert, Martin O; Randeva, Harpal S; Kaltsas, Gregory; Grossman, Ashley**., "Paraneoplastic endocrine syndromes". *Endocrine-Related Cancer*. 24, R173–R190 (2017).

29) **Dongmo, J. D. D., Akak, C. M., Tala, M. F., Kedi, P. B. E., Azebaze, A. G. B., Vardamides, J. C., Laatsch, H**., "Longiflorol, a bergenin *α-d*-apioside from the stem bark of *Diospyros longiflora* and its antioxidant activity". *Zeitschrift für Naturforschung*. B. 73, 539-543 (2018).

30) **Duangjai S., Samuel R., Munzinger J., Forest F., Wallnofer B., Barfuss M. H. J., Fischer G., Chase M. W.**, "A Multi-locus Plastid Phylogenetic Analysis of the Pantropical Genus *Diospyros* (Ebenaceae), with an Emphasis on the Radiation and Biogeographic Origins of the New Caledonian Endemic Species ". *Molecular Phylogenetics and Evolution*, 52, 602-620 (2009).

31) **Duangjai S., Wallnöfer B., Samuel R., Munzinger J., Chase M. W.,** "Generic Delimitation and Relationships in Ebenaceae sensu lato: Evidence from six plastid DNA regions". *American Journal of Botany*, 93, 1808-1827 (2006).

32) **Dzoyem J. P., Tangmouo J. G., Lontsi D., Etoa F. X., Lohoue P. J.**, "In vitro antifungal activity of extract and plumbagin from the stem bark of *Diospyros crassiflora* Hiern (Ebenaceae)". *Phytotherapy Research*, 21, 671-674 (2007).

33) **Emerit J. M.** and **Edeas F. B**., "Neurodegenerative diseases and oxidative stress". *Biomedicine & Pharmacotherapy*, 58, 39-46 (2004).

34) **Fong Y., Gonen M., Rubin D., Radzyner M., Brennan M. F.,** "Long-term survival is superior after resection for cancer in high-volume centers". *Annals of Surgery*, 242, 234-241 (2005).

35) **Ganapaty S., Pannakal S. T., Fotso S., Hartmut L., "**Antitermitic quinones from *Diospyros sylvatica"*. *Phytochemistry* ,65, 1265-1271 (2004).

36) **Geeraerts A., Raeymaekers J.A.M., Vinckier S., Pletsers A., Smets E., Huysmans S.**, "Systematic Palynology in Ebenaceae with Focus on Ebenoideae: Morphological Diversity and Character Evolution", *Review of Palaeobotany and Palynology*, 153, 336-353 (2009).

37) **Gunasekera S. P.** and **Sultanbawa M. U. S.,** "Chemical investigation of Ceylonese plants. Part 20. Extractives of Mesua myrtifolia. Isolation and structure of a new triterpene hydroxy-acid, myrtifolic acid". *Journal of the chemical society, perkin transactions 1*, 1, 6-10 (1977).

38) **Halliwell B.,** "Free radicals, antioxidants, and human disease: curiosity, cause, or consequence?" *Lancet*, 344, 721-724 (1994).

39) **Halliwell B.** and **Gutteridge J. M.,** "Role of free radicals and catalytic metal ions in human disease: an overview". *Methods in Enzymology*, 186, 1-85 (1990).

40) **Han Z., Luo J., Kong L.-Y**., "Two new tocopherol polymers from the seeds of Euryale ferox". *Journal of Asian Natural Products Research*, 14, 743-747 (2012).

41) **Hanahan D.** and **Weinberg R. A**., "The hallmarks of cancer". *Cell*, 100, 57–70 (2000).

42) **Harris D. J., Moutsamboté J.-M., Kami, E., Florence, J., Bridgewater S., Wortley A. H**., "An introduction to the trees from the north of the Republic Congo". Published by Royal Botanic Garden Edinburgh, 1st edition (2011).

43) **Harris E. D.**, "Percival SS: A role for ascorbic acid in copper transport". *The American Journal of Clinical Nutrition*, 54, 1193S-1197S (1991).

44) **Hay J. E.** and **Haynes L.** J., "Bergenin, a C-Glycopyranosyl derivative of 4-O-methylgallic acid", *Journal of the Chemical Society*, 2231-2238 (1958).

45) **Hazra S., Ghosh S., Kumar A., Pandey B. N., Hazra B.**, "Acetylamine derivative of diospyrin a plant-derived binaphthylquinonoid, inhibits human colon cancer growth in Nod-Scid mice". *Investigational New Drugs*, 33, 22-31 (2015).

46) **Herzner H., Palmacci E. R., Seeberger P. H.,** "Short total synthesis of 8,10-di-*O*-methylbergenin". *Organic Letters*, 4, 2965–7 (2002).

47) **Higa M., Takashima Y., Yokaryo H., Harie Y., Suzuka T., Ogihara K**., "Naphthoquinone Derivatives from *Diospyros maritime"*. *Chemical & pharmaceutical bulletin*, 65, 739-745 (2017).

48) **Hill R. A.,** "Naturally Occurring Isocoumarins". *Fortschritte der Chemie organischer Naturstoffe*, 49, 1-78 (1986).

49) **Huang M. H., Wu S. N., Wang J. P., Lin C. H., Lu S. I., Liao L. F., Shen A. Y**., "Biological Study of Naphthalene Derivatives with Antiinflammatory Activities". *Drug Development Research*, 60, 261-269 (2003).

50) **Huang S. W., Qiao J. W., Sun X., Gao P. Y., Li L. Z., Liu Q. B., Sun B., Wu D. L., Song S. J.,** "Secoiridoids and lignans from the leaves of *Diospyros kaki* Thunb. with antioxidant and neuroprotective activities". *Journal of Functional Foods*, 24, 183–195 (2016).

51) **Inoue M., Sato E. F., Nishikawa M., Park A. M., Kira Y., Imada I., Utsumi K.,** "Mitochondrial generation of reactive oxygen species and its role in aerobic life". *Current Medicinal Chemistry*, 10, 2495-2505 (2003).

52) **Jintasirikul A.** and **Thebtaranonth Y**., "Chemical Investigation of *Diospyros mollis* Griff [Ebenaceae]; Chemical Constituents of the Black Heartwood. The Final Chapter ". *Journal of the Science Society of Thailand*, 22, 111-116 (1996).

53) **Joshi B. S., Singh K. L., Roy R.,** "Complete assignments of ^{1}H and ^{13}C NMR spectra of the pentacyclic triterpene hederagenin from *Nigella sativa* Linn". *Magnetic resonance in Chemistry*, 3, 295-298 (1999).

54) **Kantamreddi V. S. S.** and **Wright C. W.**, "Investigation of Indian *Diospyros* species for antiplasmodial properties". *Evidence-based Complementary and Alternative Medicine*, 5, 187-190 (2008).

55) **Kawase M., Motohashi N., Satoh K.**, "Biological activity of persimmon (*Diospyros kaki*) peel extracts". *Phytotherapy Research*, 17, 495-500 (2003).

56) **Kengne O. A. B., Tene M., Tchinda T. A., Tane** P., **Frédérich M., "**Terpenoids from *Phaulopsis imbricata* (Acanthaceae)". *Journal of medicinal plant research*, 10,122-129, (2016).

57) **Khalidhar S. B., Parthasarathy M. R., Sharma P.,** "Norbergenin, a new C-glycoside from *Woodfordia fruticosa* Kurz." *Indian Journal of Chemistry*, 20B, 720-721 (1981).

58) **Kikuchi T., Ishii K., Noto T., Takahashi A., Tabata K., Suzuki T., Akihisa T.**, "Cytotoxic and Apoptosis-Inducing Activities of Limonoids from the Seeds of *Azadirachta indica* (Neem)". *Journal of Natural Products*, 74, 866–870 (2011).

59) **King A. T.** and **Primrose J. N.,** "Principles of cancer treatment by surgery". *Surgery* 21, 284-288 (2003).

60) **Klaunig J. E.,** "Oxidative Stress and Cancer". *Current Pharmaceutical Design*, 24, 4771-4778 (2018).

61) **Kohen R.** and **Nyska A.**, "Oxidation of biological systems: oxidative stress phenomena, antioxidants, redox reactions, and methods for their quantification". *Toxicologic Pathology*, 30, 620-650 (2002).

62) **Krohn K., Bahramsari R., Florke U., Ludewig K., Kliche-Spory C., Michel A., Aust H. J., Draeger S., Schulz B., Antus S**., "Dihydroisocoumarins from fungi: isolation, structure elucidation, circular dichroism and biological activity". *Phytochemistry*, 45, 313-320 (1997).

63) **Kuete V.,** "Potential of Cameroonian Plants and Derived Products against Microbial Infections: A Review". *Planta Medica*, 76, 1479–1491 (2010).

64) **Kufe D. W., Pollock R. E., Weichselbaum R. R., Bast R. C., Gansler T. S., Holland J. F., Frei E**., "Holland-Frei Cancer Medicine. 6th edition". Hamilton (ON): BC Decker (2003).

65) **Kull D. R.** and **Pfander H.,** "Isolation and Structure Elucidation of Two (Z)-Isomers of Lutein from the Petals of Rape (*Brassica napus*)". *Journal of Agricultural and Food Chemistry*, 45, 4201−4203 (1997).

66) **Kumagai Y., Shinkai Y., Miura T., Cho A. K., "**The chemical biology of naphthoquinones and its environmental implications". *Annual Review Pharmacology Toxicology*, 52, 221-247 (2012).

67) **Kuper H., Adami H. O., Boffetta P.** "Tobacco use, cancer causation and public health impact". *Journal of Internal Medicine*. 251, 455–66 (2002).

68) **Lee T. H., Juang S. H., Hsu F. L., Wu C. Y.,** "Triterpene Acids from the Leaves of *Planchonella duclitan* (Blanco) Bakhuizan". *Journal of the Chinese Chemical Society*, 52, 1275-1280 (2005).

69) **Lee Y. A., Cho E. J., Yokozawa T.**, "Protective effect of persimmon (*Diospyros kaki*) peel proanthocyanidin against oxidative damage under H_2O_2-induced cellular senescence". *Biological and Pharmaceutical Bulletin*, 31, 1265-1269 (2008).

70) **Letouzey R.** and **White F.,** « Flore du Cameroun, les Ebénaceaes et les Ericacées » *Muséum National d'Histoire Naturelle*, 11, 3-73 (1970).

71) **Magid A. A., Nazabadioko L. V., Moroy G., Moretti C., Lavaud C.,** "Dihydroisocoumarin Glucosides from Stem Bark of *Caryocar glabrum*". *Phytochemistry*, 68, 2439-2443 (2007).

72) **Mahato S. B.** and **Kundu A. P.**, "^{13}C NMR Spectra of Pentacyclic Triterpenoids-a Compilation and some Salient Features". *Phytochemistry*, 37, 1517-1575 (1994).

73) **Mallabaev A.** and **Sidyakin G. P.**, "Some Features of the IR Spectra of Isocoumarins". *Chemistry of Natural Compounds*, 8, 276-277 (1972).

74) **Mallavadhani U. V., Panda A. K., Rao Y. R.**, "Pharmacology and Chemotaxonomy of *Diospyros*". *Phytochemistry*, 49, 901-951 (1998).

75) **Maroyi A., "***Diospyros lycioides Desf.:* Review of its botany, medicinal uses, pharmacological activities and phytochemistry". *Asian Pacific Journal of Tropical Biomedicine*, 8, 130-136 (2018).

76) **Mathers C. D.** and **Loncar D**., "Projections of global mortality and burden of disease from 2002 to 2030". *PLOS Medicine*, 3, 442-443 (2006).

77) **Mattson M. P**., "Metal-catalyzed disruption of membrane protein and lipid signaling in the pathogenesis of neurodegenerative Disorders". *Annals of the New York Academy of Sciences*, 1012, 37-50 (2004).

78) **Maurya R., Srivastava A., Shah P., Siddiqi M. I., Rajendran S. M., Puri A., Yadav P. P.,** "*β*-Amyrin acetate and *β*-amyrin palmitate as antidyslipidemic agents from *Wrightia tomentosa* leaves". *Phytomedicine*, 19, 682-685 (2012).

79) **Meksuriyen D., Nanayakkara N. P. D., Phoebe Jr. C. H., Cordell G. A.,** "Two triterpenes from *Davidsonia pruriens"*. *Phytochemistry*, 25, 1685-1689 (1986).

80) **Mohamed L. E., El Nur E. B. E., Choudhary M. I., Khan. S. N., "**Bioactive Natural Products from Two Sudanese Medicinal Plants: *Diospyros mespiliformis* and *Croton zambesicus". Records of Natural Products*, 3:4, 198-203 (2009).

81) **Mohamed S. A. N., Gandhidasan R., Charles J. A**., "Two 2-Naphthoic Acids from *Diospyros paniculata*". *Indian Journal of Chemistry*, 45B, 1544-1546 (2006).

82) **Moss G. P.,** "Carbon-13 NMR spectra of carotenoids". *Carotenoids*, 4, 97-102 (1976).

83) **Mukherjee R. K., Fujimoto Y., Kakinuma K.,** "1-(omega-hydroxyfattyacyl)glycerols and two flavanols from *cinnamomum camphora*". *Phytochemistry*, 37, 1641-1643 (1994).

84) **Mukherjee R.** and **De Medeiros C. L. C.,** "Stereoconfiguration of sequoyitol by high resolution ^{1}H NMR ". *Phytochemistry*; 27, 279–281 (1988).

85) **Mustapha T**., « Synthèse de dérivés d'isocoumarines naturelles, métabolites du champignon pathogène Ceratocystis fimbriata sp » Thèse de Doctorat, Université de Neuchâtel- France, 7-126 (2005).

86) **Newman D. J., Cragg G. M., Snader K. M.,** "The influence of natural products upon drug discovery". *Natural Product Reports*, 17, 215-234 (2000).

87) **Nijs J, Meeus M, De Meirleir K**., "Chronic musculoskeletal pain in chronic fatigue syndrome: recent developments and therapeutic implications". *Manual Therapy*, 11, 187-91 (2006).

88) **Noor A. O., Almasri D. M., Bagalagel A. A., Abdallah H. M., Mohamed S. G. A., Mohamed G. A., Ibrahim S. R. M.,** "Naturally Occurring Isocoumarins Derivatives from Endophytic Fungi: Sources, Isolation, Structural Characterization, Biosynthesis, and Biological Activities". *Molecules*, 25, 395 (2020)

89) **Okoye N. N., Ajaghaku D. L., Okeke H. N., Ilodigwe E. E., Nworu C. S., Okoye F. B. C., "**beta-Amyrin and alpha-amyrin acetate isolated from the stem bark of *Alstonia boonei* display profound anti-inflammatory activity". *Pharmaceutical Biology*, 52, 1478–1486 (2014).

90) **Oluremi B. B., Osungunna M. O., Ogbole O. O., "**Phytochemical and Antimicrobial Screening of the Leaf Extract of *Diospyros barteri* Gurke". *Pharmacognosy journal*, 2, 405-408 (2010).

91) **Oyama T., Aoyama H., Yamada K., Mitsuhashi T., Sugiyama N.,** "Isolation of a new triterpene, rotundic acid, from ilex rotunda". *Tetrahedron Letters*, 9, 4639–4641, (1968).

92) **Pal S.** and **Pal M.,** "Isocoumarin, Thiaisocoumarin and Phosphaisocoumarin: Natural Occurrences, Synthetic Approaches and Pharmaceutical Applications". Elsevier, 1-216 (2018).

93) **Pasupuleti V. R., Elawarasi K., Indireddy R. M. R., Malepati D. N., Siew H. G**., "Phytochemical Analysis and in vitro Evaluation of Antidiabetic Activity of *Diospyros buxifolia". American Journal of Biochemistry and Molecular Biology*. 6, 95-101 (2016).

94) **Peshin T.** and **Kar H. K.,** "Isolation and Characterization of *β*-Sitosterol-3-*O*-*β*-*D*-glucoside from the extract of the Flowers of *Viola odorata". British Journal of Pharmaceutical Research*, 16, 1-8 (2017).

95) **Pilane M. C., Bagla V. P., Mokgotho M. P., Mbazima V., Matsebatlela T. M., Ncube I., Mampuru L**., "Free radical scavenging activity: antiproliferative and proteomic Analyses of the differential expression of apoptotic proteins in MCF-7 cells

treated with acetone leaf extract of *Diospyros lycioides* (Ebenaceae)". *Evidence-based Complementary and Alternative Medicine*, 534808 (2015).

96) **Pinho B. R., Sousa C., Oliveira J. M. A., Valentão P., Andrade P. B**., "Naphthoquinones' biological activities and toxicological effects. In: Bitterlich A, Fischl S. (Eds.) Bioactive compounds: Type, biological activities and health effects". *New York: Nova Science Publishers*. 181-218 (2012).

97) **Rasamison V. E., Rakotondraibe H. L., Razafintsalama V., Rakotonandrasana S., Rakotondrafara A., Ratsimbason M. A., Rafidinarivo E.**, "Chemical constituents from stems and leaves of *Diospyros gracilipes* Hiern and the antimicrobial and cytotoxic principles". *Journal of Pharmacognosy and Phytochemistry*, 5, 109-113 (2016).

98) **Rathore K., Singh V. K., Jain P.**, "In-vitro and in-vivo antiadipogenic, hypolipidemic and Anti-diabetic activity of *Diospyros melanoxylon* (Roxb)". *Journal of Ethnopharmacology*, 155, 1171-1176 (2014).

99) **Rauf A., Uddin G., Patel S., Khan A., Halim S. A., Bawazeer S., Ahmad K., Muhammad N., Mubarak M. S., "***Diospyros*, an under-utilized, multi-purpose plant genus: A review". *Biomedecine and pharmacotherapy*, 91, 714-730 (2017).

100) **Ravikumar A., Vengalrao P., Shobhana K., Kishore S., "**An Overview on *Diospyros malabarica". International Journal of Novel Trends in Pharmaceutical Sciences*, 4, 93-96 (2014).

101) **Riham A. El-shiekh, Dalia A. Al-Mahdy, Mohamed S. Hifnawy, Tzvetomira Tzanova,** Bana, Stéphanie Philippot, Denyse Bagrel, Essam A. -Emilie Evain Abdelsattar., "Chemical and Biological Investigation of *Ochrosia elliptica* Labill. Cultivated in Egypt". *Records of Natural Products*, 11, 552-557 (2017).

102) **Rokade Y. B.** and **Sayyed R. Z**., "Naphthalene Derivatives: a New Range of Antimicrobials with High Therapeutic Value", *Rasāyan Journal of Chemistry*, 2, 972-980 (2009).

103) **Ruano-Ravina A., Figueiras A., Freire-Garabal M., Barros-Dios J. M**., "Antioxidant vitamins and risk of lung cancer". *Current Pharmaceutical Design*, 12, 599-613 (2006).

104) **Saeed A.**, "A Short Synthesis of Natural Isocoumarin Glucoside Delphoside". *Chinese Journal of Chemistry*, 23, 762-766 (2005).

105) **Sagar S., Kaur M., Minneman K. P., Bajic V. B.,** "Protective role of *Diospyros lotus* on cisplatin-induced changes in sperm characteristics, testicular damage and oxidative stress in rats". *Andrologia,* 48, 308-317 (2016).

106) **Saijo R., Nonaka G. I., Nishioka I.**,"Gallic Acid Esters of Bergenin and Norbergenin from Mallotus japonicus". *Phytochemistry*, 29, 267-270 (1990).

107) **Saikat D., Anup K. D., Ranabir S., Moumita G.**, "Antidiabetic activity of *Diospyros peregrine* fruit: Effect on hyperglycemia, hyperlipidemia and augmented oxidative stress in experimental type 2 diabetes". *Food and Chemical Toxicology*, 47, 2679–2685 (2009).

108) **Sameera R. S., Meran K. E., Lakshan W., Nisala F., Luxmiga T., Kamani H. T., Poorna P., Achyut A**., "Isolation of cytotoxic triterpenes from the mangrove plant, *Scyphiphora hydrophyllacea* C.F.Gaertn (Rubiaceae)". *Tropical Journal of Pharmaceutical Research*, 17, 475-481 (2018).

109) **Samuel R., Turner B., Duangjai S., Munzinger J., Paun O., Barfuss M. H. J., Chase M. W.,** "Systematics and evolution of the Old World Ebenaceae, a review with emphasis on the large genus *Diospyros* and its radiation in New Caledonia". *Botanical Journal of the Linnean Society*, 189, 99-114 (2019).

110) **Setu J., Akhter A., Rahman R., Islam M., Koly M., Amran M., Foyzun T.,** "Study on Antioxidant and Cytotoxic Activities of Methanolic and Ethyl Acetate Extracts of Peel and Seed of *Diospyros blancoi"*. *Annual Research & Review in Biology*, 21, 1-9 (2017).

111) **Shaik D., Malika F. A., Rafi S. M., Naqui B**., "Studies of antibacterial activity of ethanolic extract from Nericumindicum and Hibiscus rosasinensis". *Medical journal of Islamic world academy of sciences*, 7,167-168 (1994).

112) **Shih T. L., Lin Y. L., Kuo W. S.,** "Highly stereoselective and stereospecific syntheses of a variety of quercitols from D- (-)-quinic acid". *Tetrahedron*, 61, 1919–1924 (2005).

113) **Shu L., Cheug K. L., Khor T. O., Chen C., Kong A. N.,** "Phytochemicals: cancer chemoprevention and suppression of tumor onset and metastasis". *Cancer Metastasis Revue*, 29, 483-502 (2010).

114) **Sies H., Berndt C., Jones D. P.,** "Oxidative Stress". *Annual Review of Biochemistry*, 86, 715-748 (2017).

115) **Sun L., Zhang J., Lu X., Zhang L., Zhang Y**., "Evaluation to the antioxidant activity of total flavonoids extract from persimmon (*Diospyros kaki* L.) leaves". *Food and Chemical Toxicology*, 49, 2689-2696 (2011).

116) **Taneja S. C.** and **Qazi G. N**., "In: Bioactive Molecules in Medicinal Plants: A perspective in their therapeutic action, in Drug discovery and development". Chorghade MS, editor. John Wiley and Sons, Inc, 1-50 (2007).

117) **Taneyama M., Yoshida S., Kobayashi M., Hasegawa M.,** "Isolation of Norbergenin from *Saxifraga Stolonifera*". *Phytochemistry,* 22, 1053-1054 (1983).

118) **Tangmouo J. G., Lontsi D., Ngounou F. N., Kuete V., Meli A. L., Manfouo R. N., Kamdem, H. W., Tane P., Beng V. P., Sondengam B. L., Connolly J. D**., "Diospyrone, a new coumarinylbinaphthoquinone from *Diospyros canaliculata* (Ebenaceae): structure and antimicrobial activity". *Bulletin of Chemical Society Ethiopia*, 19, 81-88 (2005).

119) **Tangmouo J. G., Meli A. L., Komguem J., Kuete V., Ngounou F. N., Lontsi D., Beng V. P., Choudhary M. I., Sondengam B. L.,** "Crassiflorone, a new naphthoquinone from *Diospyros crassiflora* (Hien)". *Tetrahedron Letters*. 47, 3067-3070 (2006).

120) **Tangmouo J. G., Ho R., Lannang A. M., Komguem J., Messi B. B., Lontsi A. T., Lontsi D., Hostettmann K., "**Norbergenin derivatives from the stem bark of *Diospyros sanza-minika* (Ebenaceae) and their radical scavenging activity". *Phytochemistry Letters,* 2, 192-195 (2009).

121) **Thnakijcharoenpath W.** and **Theanphong O., "**Triterpenoids from the stem of *Diospyros glandulosa"*. *Thaï Journal of Pharmacology Sciences*, 31, 1-8 (2007).

122) **Titto Varughese, Mozahidur Rahaman, No-Soo Kim, Soon-Chang Cho, and Surk-Sik Moon.,** "Gamnamoside, a Phenylpropanoid Glycoside from Persimmon Leaves (Diospyros kaki) with an Inhibitory Effect against an Alcohol Metabolizing Enzyme". *The Bulletin of the Korean Chemical Society*, 30, 1035-1038 (2009).

123) **Venkateswara R. G., Sahoo M. R., Madhavi M. S. L., Mukhopadhyay T.,** "Phytoconstituents from the leaves and seeds of *Manilkara zapota* Linn". *Der Pharmacia Letter*, 6, 69–73 (2014).

124) **Verma S. C., Jain C. L., NIGAM S., PADHI M. M.,** "Rapid Extraction, Isolation, and Quantification of Oleanolic Acid from *Lantana camara* L. Roots Using Microwave and HPLC–PDA Techniques". *Acta Chromatographica*, 25, 181-199 (2013).

125) **Wallnöfer B.,** "The Biology and Systematics of *Ebenaceae*: a Review". *Annalen des Naturhistorischen Museums in Wien*, 102B, 485-512 (2001).

126) **Wei Z.** and **Guangyuan Z**., "Corosolic acid isolation from the leaves of *Eriobotrta japonica* showing the effects on carbohydrate metabolism and differentiation of 3T3-L1 adipocytes". *Asia Pacific Journal of Clinical Nutrition*, 16, 346-352 (2007).

127) **Wiseman H.** and **Halliwell B.,** "Damage to DNA by reactive oxygen and nitrogen species: role in inflammatory disease and progression to cancer". *Biochemical Journal*, 313 (Pt 1) 17-29 (1996).

128) **World Health Organization**. "Cancer".12 September 2018. Retrieved 19 December (2018).

129) **World Health Organization**. "New report calls for urgent action to avert antimicrobial resistance crisis". 29 April 2019 (2019).

130) **World Health Organization**. "Cancer". 21 september 2021 (2021).

131) **World Health Organization**, "IARC classifies radiofrequency electromagnetic fields as possibly carcinogenic to humans" (PDF) (2011).

132) **Yamagishi M., Matsumoto S., Nakatsuka A., Itamura H.,** "Identification of persimmon (*Diospyros kaki*) cultivars and phenetic relationships between *Diospyros* species by more effective RAPD analysis". *Scientia Horticulturae*, 105, 283–290 (2005).

133) **Zanatta A. C., Vilegas W., Edrada-Ebel R.,**" UHPLC-(ESI)-HRMS and NMR-based metabolomics approach to access the seasonality of byrsonima intermedia and serjania marginata from brazilian cerrado flora diversity". Frontiers in Chemistry, 9, 1-17 (2021).

134) **Zgoda J. R.** and **Porter J. R.,** "A convenient microdilution method for screening natural products against bacteria and fungi". *Pharmaceutical Biology*, 39, 221-225 (2001).

135) **Zhang Q. Y., Zhao Y. Y., Cheng T. M., Cui Y. X., Liu X. H.,** "A new triterpenoid from *stelmatocrypton khasianum*". *Journal of Asian natural products research*, 2, 81-86 (1999).

136) **Zhou Z., Huang Y., Liang J., Ou M., Chen J., Li G.,** "Extraction, purification and anti-radiation activity of persimmon tannin from *Diospyros kaki". Journal of Environmental Radioactivity*, 162, 182-188 (2016).

LIST OF PUBLICATIONS

1) **Jouwa N. S. T., Akak C. M., Happi G. M., Frese M., Stammler H.-G., Neumann B., Lenta B. N., Sewald N., Nkengfack A. E.,** "Antioxidant norbergenin derivatives from the leaves of *Diospyros gilletii* De Wild (Ebenaceae)". *Phytochemistry Letters*, 36, 63-67 (2020).
2) **Jouwa N. S. T., Akak C. M., Tabekoueng G. B., Mkounga P., Bitchagno G. T., Lenta B. N., Sewald N., Nkengfack A. E.,** "Chemical constituents from *Diospyros fragrans* Gürke (Ebenaceae)". *Biochemical Systematics and Ecology*, 100, 1-7 (2021).

Phytochemistry Letters 36 (2020) 63–67

Contents lists available at ScienceDirect

Phytochemistry Letters

journal homepage: www.elsevier.com/locate/phytol

Antioxidant norbergenin derivatives from the leaves of *Diospyros gilletii* De Wild (Ebenaceae)

Nathalie S. Jouwa Tameye[a,b], Carine Mvot Akak[a,*], Gervais Mouthé Happi[b,c], Marcel Frese[b], Hans-Georg Stammler[d], Beate Neumann[d], Bruno Ndjakou Lenta[c], Norbert Sewald[b], Augustin E. Nkengfack[a]

[a] Department of Organic Chemistry, Faculty of Science, University of Yaounde I, P.O. Box 812, Yaounde, Cameroon
[b] Organic and Bioorganic Chemistry, Faculty of Chemistry, Bielefeld University, D-33501 Bielefeld, Germany
[c] Department of Chemistry, Higher Teacher Training College, University of Yaounde I, P.O. Box 47, Yaounde, Cameroon
[d] Department of Chemistry, Inorganic and Structural Chemistry, Bielefeld University, D-33501 Bielefeld, Germany

ARTICLE INFO

Keywords:
Diospyros gilletii
Ebenaceae
Norbergenin
Antioxidant
X-ray crystal structure

ABSTRACT

Two new norbergenin derivatives, 4-*O*-*p*-hydroxybenzoylnorbergenin (**1**) and 11-*O*-(*E*)-cinnamoylnorbergenin (**2**), were isolated from the leaves of *Diospyros gilletii* De Wild along with nine known compounds, including norbergenin (**3**), 4-*O*-galloylnorbergenin (**4**), betulin (**5**), betulinic acid (**6**), lupeol (**7**), ursolic acid (**8**), corosolic acid (**9**), β-sitosterol (**10**) and quercitol (**11**). Their structures were elucidated from the analysis of their 1D and 2D ^{1}H and ^{13}C NMR spectral data in conjunction with mass spectrometry. Single-crystal X-ray diffraction technique unambiguously established the structure of compound (**1**). The antimicrobial properties of the eleven compounds isolated were investigated as well as the antioxidant activity of the norbergenin derivatives (**1–4**). The results obtained showed that none of those compounds displayed antimicrobial activity at 0.5 μg/ml whereas norbergenin derivatives exhibited noteworthy antioxidant property with IC_{50} values ranging from 8.2 μg/ml to 41.6 μg/ml.

1. Introduction

Plants of the genus *Diospyros* (Ebenaceae), which include several species that produce ebony, consist of trees and shrubs found in Africa, Asia–Pacific region, Neotropics, Australia, New Caledonia, Madagascar and Comoros (Geeraerts et al., 2009; Duangja et al., 2009). From the 500 species belonging to this genus distributed over the world, about 36 species are found in Cameroon (Letouzey and White, 1970). *Diospyros* species are widely used in African folk medicine for the treatment of various diseases including leprosy, fungal infections, dysentery, whooping cough, hemorrhages, incontinence, rheumatoid arthritis, cardiovascular disorder and various cancer types (Maroyi, 2018; Rauf et al., 2017; Ravikumar et al., 2014). Previous phytochemical studies carried out on some Cameroonian *Diospyros* species led to the isolation and the characterization of a wide range of secondary metabolites including triterpenes (Feusso et al., 2016, 2017), naphthoquinones (Tangmouo et al., 2005, 2006; Lenta et al., 2015), coumarins (Akak et al., 2010), bergenin and norbergenin derivatives (Dongmo et al., 2018; Akak et al., 2013; Tangmouo et al., 2009); some of which exhibited diverse biological activities such as antimycobacterial and antigonorrhoeal (Kuete et al., 2009), antioxidant (Tangmouo et al., 2009), and antitrypanosomal (Fouokeng et al., 2019). As part of our ongoing search for secondary metabolites of biological importance from Cameroonian medicinal plants, the methanolic extract of the leaves of *Diospyros gilletii* was investigated. In this paper, we report the isolation, structural elucidation, as well as the biological activity; especially, the antimicrobial and antioxidant activities of the isolates.

2. Results and discussion

The dried aerial parts of *Diospyros gilletii* were extracted by maceration in methanol. The crude extract obtained was suspended in distilled water and further extracted with various solvents. The fractionation of the ethyl acetate and dichloromethane soluble fractions using various chromatographic techniques afforded two new norbergenin derivatives (1–2) with nine known compounds. (Fig. 1). The known compounds were identified, by comparison of their spectroscopic data with those reported in the literature, as norbergenin (**3**), 4-

* Corresponding author.
E-mail address: mvotcarine@yahoo.fr (C. Mvot Akak).

https://doi.org/10.1016/j.phytol.2020.01.012
Received 6 November 2019; Received in revised form 16 January 2020; Accepted 16 January 2020

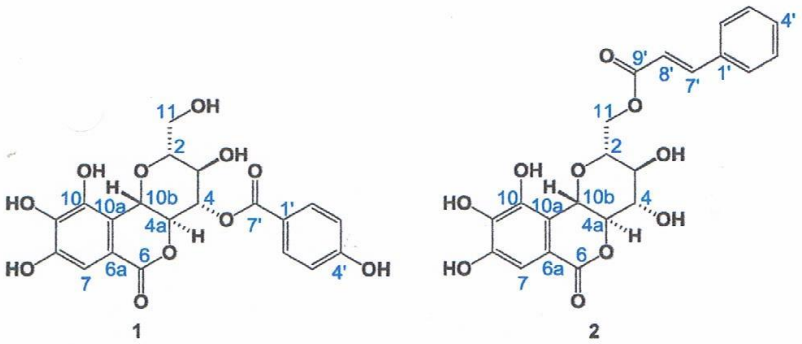

Fig. 1. Chemical structures of new norbergenin **1** and **2**.

O-galloylnorbergenin (**4**) (Saijo et al., 1990), betulin (**5**) (Joshi et al., 2013), betulinic acid (**6**) (Haque et al., 2013), lupeol (**7**) (Jamal et al., 2008), ursolic acid (**8**) (Seebacher et al., 2003), corosolic acid (**9**) (Hou et al., 2009), β-sitosterol (**10**) (Chaturvedula and Prakash, 2012) and quercitol (**11**) (Shih et al., 2005).

2.1. Structure elucidation of 4-*O*-*p*-hydroxybenzoylnorbergenin (1)

Compound **1** was obtained as a white powder. Its molecular formula, $C_{20}H_{18}O_{11}$, implying twelve double bond equivalents, was determined from its HR-TOF-ESIMS spectrum which showed in positive mode the sodiated molecular ion peak $[M+Na]^+$ at *m/z* 457.0738 (calcd for $C_{20}H_{18}O_{11}Na$: *m/z* 457.0741). The UV spectrum of compound **1** exhibited absorption bands at λ_{max} 218 and 262 nm while the IR spectrum indicated vibration bands characteristic of hydroxyl group (−OH) at 3392 cm^{-1}; carbonyl esters (C=O) at 1714, 1699 cm^{-1} and aromatic at 1608, 1470 cm^{-1}. The analysis of the ^1H NMR and HSQC spectra of this compound (Table 1) showed a set of signals constituted of one aromatic proton singlet at δ_H 7.08 (1H, s) / δ_C 111.1; five oxymethines signals at δ_H 5.60 (1H, dd, *J* = 8.4, 9.8 Hz) / δ_C 76.2, δ_H 5.14 (1H, d, *J* = 10.4 Hz) / δ_C 74.4, δ_H 4.42 (1H, dd, *J* = 10.0, 10.4 Hz) / δ_C 79.1, δ_H 3.82 (1H, m) / δ_C 83.1 and δ_H 3.80 (1H, m) / δ_C 70.2; and two diastereotopic oxymethylene signals at δ_H 4.04 (1H, dd, *J* = 1.6; 11.6 Hz) / δ_C 62.5 and δ_H 3.75 (1H, m) / δ_C 62.5 characteristic of a norbergenin skeleton (Saijo et al., 1990). This was supported, on one hand, by COSY spectrum in which correlations were observed between aliphatic oxymethine H-4a (δ_H 4.42) and protons H-10b (δ_H 5.14) and H-4 (δ_H 5.60); oxymethine H-3 (δ_H 3.80) and protons H-4 (δ_H 5.60) and H-2 (δ_H 3.82) which also correlated with the diastereotopic oxymethylene protons H-11 (δ_H 4.04 / δ_H 3.75) and on the other hand by HMBC correlations observed between the oxymethine proton H-10b (δ_H 5.14) and carbons C-2 (δ_C 83.1), C-10a (δ_C 117.0), C-6a (δ_C 114.1); proton H-4a (δ_H 4.42) and carbons C-6 (δ_C 166.0) and C-10a (δ_C 117.0); aromatic methine H-7 (δ_C 7.08) and carbons C-6 (δ_C 166.0), C-6a (δ_C 114.1), C-10a (δ_C 117.0), C-8 (δ_C 147.4), C-9 (δ_C 141.5) (Fig. 2). Further analysis of the ^1H NMR spectrum of compound **1** indicated an AA'BB' spin system at δ_H 7.97 (2H, d, *J* = 8.8 Hz) / δ_C 133.2 and δ_H 6.84 (2H, d, *J* = 8.8 Hz) / δ_C 116.1 characteristic of a *para*-disubstituted benzene ring. The correlations observed in the HMBC spectrum of this compound between the aromatic proton at δ_H 7.97 with downfield carbons at δ_C 167.5 (C=O ester) and δ_C 163.7, on one hand, and between the other aromatic proton at δ_H 6.84 and carbons at δ_C 122.0 and at δ_C 163.7, on the other hand, indicated that the *para*-aromatic moiety correspond to a *para*-hydroxybenzoyl group. It remained to us to establish the linkage between the *para*-hydroxybenzoyl moiety and the norbergenin fragment. To this end, the HMBC correlation observed between the aliphatic oxymethine proton H-4 at δ_H 5.60 and the carbonyl of the benzoyl group at δ_C 167.5 led to the conclusion that the *para*-hydroxybenzoyl moiety was linked to the norbergenin fragment at C-4 position through an oxygen atom.

In order to confirm the proposed structure and to establish unambiguously the relative stereochemistry at C-2, C-3, C-4, C-4a and C-10a along the tetrahydropyran ring of the norbergenin core, a single-crystal X-ray diffraction analysis was performed. Recrystallization of **1** by slow evaporation from methanol gave a very small and weakly diffracting crystals. Two molecules of **1** crystalized together with two solvent water molecules in the unit cell of the space group P1 resulting in a three-dimensional network bonded by hydrogen bonds and π–π interactions (See SI for further information). The X-ray structure, indicated a *trans* diaxial relationship between the aliphatic methines in the tetrahydropyran ring of the norbergenin core as shown in Fig. 3. The assigned relative stereochemistry was in full agreement with the value of the coupling constant *J* (8−10 Hz) of the oxymethines protons and the NOESY spectrum which showed correlations (Fig. 2) between protons H-10b, H-4 and H-2, and between protons H-4a, H-3 and H-11.

Accordingly, compound **1** was characterized as 4-*O*-*p*-hydroxybenzoylnorbergenin, a new norbergenin derivative with the structure as shown.

Table 1
NMR spectroscopic data[a] of compounds **1** and **2**.

Position	1		2	
	δ_H, mult (*J* in Hz)	δ_C, mult	δ_H, mult (*J* in Hz)	δ_C, mult
2	3.82, m	83.1, CH	3.93, ddd (2.2, 7.0, 9.9)	80.5, CH
3	3.80, m	70.2, CH	3.52, t (8.7, 9.9)	71.9, CH
4	5.60, dd (8.4, 9.8)	76.2, CH	3.84, brt (9.0)	75.5, CH
4a	4.42, dd (10.0, 10.4)	79.1, CH	4.08, dd (9.4, 10.5)	81.3, CH
6	–	166.0, C	–	166.3, C
6a	–	114.1, C	–	114.2, C
7	7.08, s	111.1, CH	7.09, s	111.1, CH
8	–	147.4, C	–	147.4, C
9	–	141.5, C	–	141.2, C
10	–	143.7, C	–	143.5, C
10a	–	117.0, C	–	117.0, C
10b	5.14, d (10.4)	74.4, CH	5.01, d (10.5)	74.5, CH
11	4.04, dd (1.6, 11.6) 3.75, m	62.5, CH_2	4.80, dd (2.2, 12.2) 4.36, dd (7.0, 12.2)	64.8, CH_2
1'	–	122.0, C	–	135.6, C
2'/6'	7.97, d (8.8)	133.2, CH	7.63, m	129.4, CH
3'/5'	6.84, d (8.8)	116.1, CH	7.41, m	130.0, CH
4'	–	163.7, C	7.41, m	131.7, CH
7'	–	167.5, C	7.76, d (16.0)	147.0, CH
8'	–	–	6.59, d (16.0)	118.2, CH
9'	–	–	–	168.4, C

[a] Chemical shift measured in CD_3OD, at 500 MHz for ^1H and 125 MHz for ^{13}C using TMS as internal standard (δ in ppm, *J* in Hz).

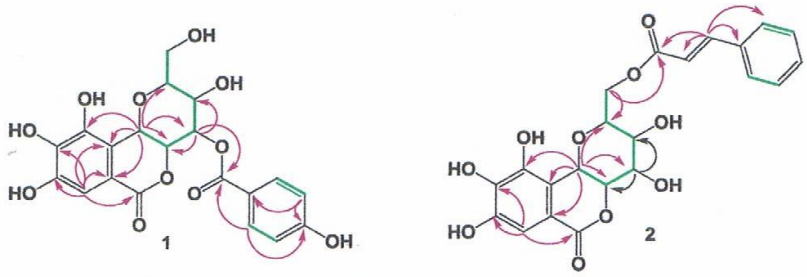

Fig. 2. Key HMBC (Purple) and COSY (Green) correlations of compounds **1** and **2**.

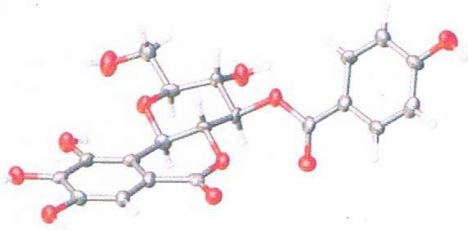

Fig. 3. ORTEP-like view of compound **1** at 50 % probability level. The second molecule and water solvent molecules are omitted.

2.2. Structure elucidation of 11-O-(E)-cinnamoylnorbergenin (2)

Compound **2** was obtained as a white powder. Its molecular formula, $C_{22}H_{20}O_{10}$, was assigned from its HR-TOF-ESIMS which exhibited in positive mode, the sodium adduct ion peak $[M+Na]^+$ at *m/z* 467.0949 (calcd for $C_{22}H_{20}O_{10}Na$: *m/z* 467.09487). The UV spectrum of this compound showed maxima absorption bands at 217 and 279 nm while in its IR spectrum, the vibration bands due to hydroxyl group (3354 cm^{-1}) and carbonyl function (1698 and 1635 cm^{-1}) were observed. The comparison of ^1H and ^{13}C NMR spectra of compound **2** (Table 1) showed close similarities with those of compound **1**. These data indicated the presence in compound **2** of a norbergenin core through the aromatic singlet at δ_H 7.09 (1H, s, H-7) / δ_C 111.1, the five norbergenin types oxymethines at δ_H 5.01 (1H, d, *J* = 10.5 Hz, H-10b) / δ_C 74.5, δ_H 4.08 (1H, dd, *J* = 9.4, 10.5 Hz, H-4a) / δ_C 81.3, δ_H 3.93 (1H, ddd, *J* = 2.2, 7.0, 9.9 Hz, H-2) / δ_C 80.5, δ_H 3.84 (1H, brt, *J* = 9.0 Hz, H-4) / δ_C 75.5, δ_H 3.52 (1H, t, *J* = 8.7, 9.9 Hz, H-3) / δ_C 71.9, the diastereotopic oxymethylene protons at δ_H 4.80 (1H, dd, *J* = 2.2, 12.2 Hz, H-11) / δ_C 64.8 and δ_H 4.36 (1H, dd, *J* = 7.0, 12.2 Hz, H-11) / δ_C 64.8, the carbonyl ester at δ_C 166.3 (C-6) and the aromatic carbons at δ_C 147.4 (C-8), δ_C 143.5 (C-10), δ_C 141.2 (C-9), δ_C 117.0 (C-10a) and δ_C 114.2 (C-6a). The differences between the two compounds were the nature of the substituent and its position on the norbergenin skeleton. Indeed, whereas in compound **1**, the substituent was a *para*-hydroxybenzoyl moiety, in compound **2**, this substituent was a cinnamoyl group which was characterized from the set of signals observed in the ^1H and ^{13}C NMR spectra, constituted by two olefinic methines which appeared as an AB spin system with a *trans* coupling at δ_H 6.59 (1H, d, *J* = 16 Hz, H-8') / δ_C 118.2 (C-8') and δ_H 7.76 (1H, d, *J* = 16 Hz, H-7') / δ_C 147.0 (C-7'), five aromatic protons at δ_H 7.63 (2H, m, H-2', H-6') / δ_C 129.4 (C-2'/C-6') and δ_H 7.41 (2H, m, H-3', H-5') / δ_C 130.0 (C-3'/ C-5'), δ_H 7.41 (1H, m, H-4') / δ_C 131.7 (C-4'), δ_C 135.6 (C-1') and signal of one carbonyl ester at δ_C 168.4 (C-9'). The deshielding of the diastereotopic oxymethylene protons (H-11) of norbergenin appearing at δ_H 4.80 and δ_H 4.36 in compound **2** compared to their values in compound **1** indicated that the cinnamoyl moiety was located at C-11 position of the norbergenin backbone. This was confirmed by the HMBC correlations observed between diastereotopic protons H-11 and carbonyl of the cinnamoyl group C-9' at δ_C 168.4. As in compound **1**, the relative stereochemistry of the oxymethine protons in compound **2** was established as *trans* diaxial from the value of the coupling constant *J* (8−10 Hz) and the NOESY experiment. From the above spectroscopic data, compound **2** was identified as 11-*O*-(*E*)-cinnamoylnorbergenin isolated from natural source and described for the first time (Deng and Huang, 2006).

2.3. Antimicrobial and antioxidant activities of extract and isolated compounds

Extract and isolated compounds from *Diospyros gilletii*, were evaluated for their antimicrobial and antioxidant properties.

The crude methanol extract of the leaves of *D. gilletii* and compounds (**1–11**) were tested against three Gram-positive (*Bacillus subtilis DSMZ 704, Micrococcus luteus DSMZ 1605, Staphylococcus warneri DSMZ* 20036) and two Gram-negative (*Escherichia coli DSMZ 1058* and *Pseudomonas agarici DSMZ* 11810) bacteria using agar disk diffusion method with gentamicin taken as reference. The results obtained indicated that the crude extract exhibited some level of activity at concentration 20 µg/ml against the Gram-negative bacteria with inhibition zone values of, respectively, 8 mm for *Escherichia coli* and 7 mm for *Pseudomonas agarici*, while none of the tested bacterial strains were sensitive to compounds (**1–11**) at concentration 0.5 µg/ml.

Furthermore, the antioxidant activity of compounds (**1–4**) was evaluated throughout their ability to scavenge the DPPH radical. Ascorbic acid was used as positive control. The four compounds have the same basic skeleton and were more effective as antioxidant over the range of 500–0,5 µg/ml concentration than the standard antioxidant ascorbic acid, with IC_{50} values ranging from 8.2 µg/ml to 41.6 µg/ml (Table 2). The different substituents and their position on the basic skeleton influence the antioxidant activity, and a great variation is observed when the substitution occurs at C-4 of the norbergenin nucleus. Thus, the 4-*O* substitution in the norbergenin nucleus with a *para*-hydroxybenzoyl moiety (compound **1**) exhibited the better DPPH free radical scavenging activity.

Table 2
Free Radical Scavenging Activity of compounds (**1–4**) determined by the DPPH Assay.

Compounds	IC_{50} [µg/ml]
1	8.2
2	23.8
3	22.0
4	41.6
Ascorbic acid	50.5

3. Experimental

3.1. General experimental procedures

Melting point was determined on a BÜCHI Melting point B-540. Optical rotations were measured on a JASCO DIP-3600 digital polarimeter u0sing a 10 cm cell. UV spectra were recorded on a Hitachi UV 3200 spectrophotometer. IR spectra were determined on a JASCO Fourier transform IR-420 spectrometer.1D and 2D NMR spectra were recorded on a Bruker DRX 500 NMR spectrometers with TMS as an internal standard and chemical shifts shown as δ-values (ppm), while coupling constants (*J*) were measured in Hz. Homonuclear ^{1}H connectivities were determined by using the COSY experiment. One-bond ^{1}H-^{13}C connectivities were determined with HMQC gradient pulse factor selection, and two- and three-bond ^{1}H-^{13}C connectivities by HMBC experiments. ESI-MS spectra were recorded on Agilent 6220 TOF LCMS mass spectrometer with perfluorokerosene as reference substance for ESI-HR-MS. Column chromatography was carried out on silica gel 230–400 mesh and silica gel 70–230 mesh, Merck. Thin layer chromatography (TLC) were performed on Merck precoated silica gel 60 F_{254} aluminum foil and were revealed using UV lamp (254–365 nm) and 10 % H_2SO_4 reagent followed by heating.

3.2. Plant material

The leaves of *D. gilletii* De Wild were collected at Mbalmayo, Centre region-Cameroon, in March 2018 and identified at the National Herbarium of Cameroon where a voucher specimen of the species is deposited under number N° 15418 HNC.

3.3. Extraction and isolation

The dried and powdered leaves of *D. gilletii* (0.95 kg) were extracted by maceration in methanol (2 × 3L) at room temperature for 3 days. After filtration, white crystals precipitated in the resulting methanolic solution. This crystal was filtered and washed with methanol to afford Quercitol [(**11**), 159.12 mg]. The methanolic filtrate was further evaporated to dryness under reduced pressure to give 122.10 g of a methanolic residue. This residue was suspended in distilled water, and the suspension obtained was successively fractionated with petroleum ether (PE), dichloromethane (CH_2Cl_2), ethyl acetate (EtOAc) and *n*-butanol (*n*-BuOH) to yield respectively 2.31 g, 9.25 g, 43.18 g and 21.37 g of organic extracts. The ethyl acetate extract (40.00 g) was subjected to column chromatography in silica gel 60 C (0.04–0.063 mm) eluted sequentially with mixture of PE - EtOAc and EtOAc - MeOH of increasing polarities. 153 fractions of 100 ml each were collected and concentrated under reduced pressure on a rotary evaporator. These fractions were combined based on TLC analysis to give 17 subfractions labelled A1–A17. From subfractions A9 and A11 eluted from the column with a mixture of PE - EtOAc 1:3, were obtained, respectively, 11-*O*-(*E*)-cinnamoylnorbergenin [(**2**), 51.21 mg] and 4-*O*-*p*-hydroxybenzoylnorbergenin [(**1**), 1.13 g]. From subfraction A14 eluted from the column with EtOAc, was obtained 4-*O*-galloylnorbergenin [(**4**), 1.97 g] while subfraction A17 eluted with a mixture of EtOAc-MeOH 19:1 to EtOAc-MeOH 17:3 afforded norbergenin [(**3**), 2.68 g]. The dichloromethane extract (9.00 g) was equally chromatographed on silica gel 60 C (0.04–0.063 mm) eluted with a gradient of a mixture of PE-EtOAc to yield lupeol [(**7**), 178.14 mg] at PE-EtOAc 19:1, β-sitosterol [(**10**), 41.10 mg] at PE-EtOAc 9:1, betulin [(**5**), 24.20 mg] at PE-EtOAc 17:3, betulinic acid [(**6**), 71.14 mg] at PE-EtOAc 4:1, ursolic acid [(**8**), 96.21 mg] at PE-EtOAc 3:1 and corosolic acid [(**9**), 13.32 mg] at PE-EtOAc 7:3.

3.4. Spectroscopic data

3.4.1. 4-O-p-hydroxybenzoylnorbergenin (1)

White powder; $[\alpha]_D^{20}$: −53 (c 0.68, MeOH); m.p. 286−287 °C; IR υ_{max} 3730, 3392, 1714, 1699, 1608, 1470 cm^{-1}; UV λ_{max} nm (log ε) 218 (3.41), 262 (3.19); ^{1}H NMR (500 MHz) and ^{13}C NMR (125 MHz) data in CD_3OD, see Table 1; HRESIMS: *m/z* 457.0738 (calcd for $C_{20}H_{18}O_{11}Na$: *m/z* 457.0741).

3.4.2. 11-O-(E)-cinnamoylnorbergenin (2)

White powder; $[\alpha]_D^{20}$: 58,3 (c 1, MeOH); IR υ_{max} 3354, 1698, 1635, 1314, 1087 cm^{-1}: UV λ_{max} nm (log ε) 217 (3.82), 279 (3.54); ^{1}H NMR (500 MHz) and ^{13}C NMR (125 MHz) data in CD_3OD, see Table 2; HRESIMS: *m/z* 467.0949 (calcd for $C_{22}H_{20}O_{10}Na$: *m/z* 467.09487).

3.5. X-ray diffraction of 4-O-p-hydroxybenzoylnorbergenin (1)

A single crystal of compound **1** x H_2O ($C_{20}H_{20}O_{12}$) was examined on a Rigaku Supernova diffractometer using Cu Kα (λ = 1.54184 Å) radiation. The crystal was kept at 100.0(1) K during data collection. Using Olex2, the structure was solved with the ShelXT structure solution program using Intrinsic Phasing and refined with the ShelXL refinement package using Least Squares minimisation. The very poor-diffracting crystal was refined as non-merohedral two-component twin, ratio (76:24), hydrogen atoms were taken into account using a riding model. Details of the X-ray investigation are given in the SI. CCDC 1958054 contains the supplementary crystallographic data for this paper. These data can be obtained free of charge from The Cambridge Crystallographic Data Centre via www.ccdc.cam.ac.uk/conts/retrieving.html.

Declaration of Competing Interest

The authors declare no conflict of interest.

Acknowledgments

Authors are grateful to the German Academic Exchange Service (DAAD) for financial support to the Yaounde-Bielefeld Graduate School of Natural Products with Antiparasite and Antibacterial activities (YaBiNaPA), project N° 57316173. We thank Carmela Michalek for the biological tests.

Appendix A. Supplementary data

Supplementary material related to this article can be found, in the online version, at doi:https://doi.org/10.1016/j.phytol.2020.01.012.

References

Akak, C.M., Djama, C.M., Nkengfack, A.E., Tu, P.F., Lei, L.D., 2010. New coumarin glycosides from the leaves of *Diospyros crassiflora* (Hiern). Fitoterapia 81, 873–877. https://doi.org/10.1016/j.fitote.2010.05.011.

Akak, C.M., Nkengfack, A.E., Tu, P.F., 2013. Norbergenin derivatives from *Diospyros crassiflora* (Ebenaceae). Nat. Prod. Commun. 8, 1575–1578. https://doi.org/10.1177/1934578X1300801119.

Chaturvedula, V.S.P., Prakash, I., 2012. Isolation of stigmasterol and β-sitosterol from the dichloromethane extract of *Rubus suavissimus*. Int. Curr. Pharm. J. 1, 239–242.

Deng, L., Huang, H., Preparation of bergeninum derivatives as antitussives and expectorants, From Faming Zhuanli Shenqing, Chinese patent n° CN 1733766 A, 15 February 2006.

Dongmo, J.D.D., Akak, C.M., Tala, M.F., Kedi, P.B.E., Azebaze, A.G.B., Vardamides, J.C., Laatsch, H., 2018. Longiflorol, a bergenin α-d-apioside from the stem bark of *Diospyros longiflora* and its antioxidant activity. Z. Naturforsch. B 73, 539–543. https://doi.org/10.1515/znb-2018-0019.

Duangja, S., Samuel, R., Munzinger, J., Forest, F., Wallnöfer, B., Barfuss, M.H.J., Chase, M.W., 2009. A multi-locus plastid phylogenetic analysis of the pantropical genus *Diospyros* (Ebenaceae), with an emphasis on the radiation and biogeographic origins of the New Caledonian endemic species. Mol. Phylogenet. Evol. 52, 602–620. https://doi.org/10.1016/j.ympev.2009.04.021.

Feusso, H.M.F., Akak, C.M., Tala, M.F., Azebaze, A.G.B., Tsabang, N., Vardamides, J.C., Laatsch, H., 2016. Conocarpol, a new cycloartane triterpenoid from *Diospyros conocarpa*. Z. Naturforsch. B 71, 935–940. https://doi.org/10.1515/znb-2016-0059.

Feusso, H.M.F., Akak, C.M., Tala, M.F., Azebaze, A.G.B., Vardamides, J.C., Laatsch, H., 2017. Mannic acid, a new *ent*-kaurane dimer diterpenoid and other chemical constituents from different parts of *Diospyros mannii*. Biochem. Syst. Ecol. 74, 51–56. https://doi.org/10.1016/j.bse.2017.09.001.

Fouokeng, Y., Feusso, H.M.F., Mbosso, T.J.E., Siwe, N.X., Wintjens, R., Isaacs, M., Hoppe, H.C., Krause, R.W.M., Azebaze, A.G.B., Vardamides, J.C., 2019. In vitro antimalarial, antitrypanosomal and HIV-1 integrase inhibitory activities of two Cameroonian medicinal plants: *Antrocaryon klaineanum* (Anacardiaceae) and *Diospyros conocarpa* (Ebenaceae). S. Afr. J. Bot. 122, 510–517. https://doi.org/10.1016/j.sajb.2018.10.008.

Geeraerts, A., Raeymaekers, J.A.M., Vinckier, S., Pletsers, A., Smets, E., Huysmans, S., 2009. Systematic palynology in Ebenaceae with focus on Ebenoideae: morphological diversity and character evolution. Rev. Palaeobot. Palynol. 153, 336–353. https://doi.org/10.1016/j.revpalbo.2008.10.001.

Haque, A., Siddiqi, M.M.A., Rahman, A.F.M.M., Hasan, C.M., Chowdhury, A.M.S., 2013. Isolation of betulinic acid and 2,3-dihydroxyolean-12-en-28-oic acid from the leaves of *Callistemon linearis*. Dhaka Univ. J. Sci. 61, 211–212. https://doi.org/10.3329/dujs.v61i2.17073.

Hou, W., Li, Y., Zhang, Q., Wie, X., Peng, A., Chen, L., Wie, Y., 2009. Triterpene acids isolated from *Lagerstroemia speciosa* leaves as α-glucosidase inhibitors. Phytother. Res. 23, 614–618. https://doi.org/10.1002/ptr.2661.

Jamal, A.K., Yaacob, W.A., Din, L.B., 2008. A chemical study on *Phyllanthus reticulatus*. J. Phys. Sci. 19, 45–50.

Joshi, H., Saxena, G.K., Singh, V., Arya, E., Singh, R.P., 2013. Phytochemical investigation, isolation and characterization of betulin from bark of *Betula utilis*. J. Pharmacogn. Phytochem. 2, 145–151.

Kuete, V., Tangmouo, J.G., Meyer, J.J.M., Lall, N., 2009. Diospyrone, crassiflorone and plumbagin: three antimycobacterial and antigonorrhoeal naphthoquinones from two *Diospyros* spp. Int. J. Antimicrob. Agents 34, 322–325. https://doi.org/10.1016/j.ijantimicag.2009.04.008.

Lenta, B.N., Ngamgwe, R.F., Kamdem, L.M., Ngatchou, J., Tantangmo, F., Antheaume, C., Kaiser, M., Ngouela, S., Tsamo, E., Sewald, N., 2015. Compounds from *Diospyros canaliculata* (Ebenaceae) and their antiparasitic activities. IRJPAC 6, 56–65. https://doi.org/10.9734/IRJPAC/2015/15267.

Letouzey, R., White, F., 1970. Flore du Cameroun, Ebénacées et Ericacées. Muséum Nationale d'Histoire Naturelle, 16 rue Buffon Paris.

Maroyi, A., 2018. *Diospyros lycioides Desf.*: review of its botany, medicinal uses, pharmacological activities and phytochemistry. Asian Pac. J. Trop. Biomed. 8, 130–136. https://doi.org/10.4103/2221-1691.225617.

Rauf, A., Uddin, G., Patel, S., Khand, A., Halim, S.A., Bawazeer, S., Ahmad, K., Muhammad, N., Mubarak, M.S., 2017. *Diospyros*, an under-utilized, multi-purpose plant genus: a review. Biomed. Pharmacother. 91, 714–730. https://doi.org/10.1016/j.biopha.2017.05.012.

Ravikumar, A., Vengalrao, P., Shobhana, K., Kishore, S., 2014. An overview on *Diospyros malabarica*. IJNTPS 4, 93–96.

Saijo, R., Nonaka, G.I., Nishioka, I., 1990. Gallic acid esters of bergenin and norbergenin from *Mallotus japonicus*. Phytochemistry 29, 267–270. https://doi.org/10.1016/0031-9422(90)89047-D.

Seebacher, W., Simic, N., Weis, R., Saf, R., Kunert, O., 2003. Complete assignments of ^{1}H and ^{13}C NMR resonances of oleanolic acid, 18α-oleanolic acid, ursolic acid and their 11-oxo derivatives. Magn. Reson. Chem. 41, 636–638. https://doi.org/10.1002/mrc.1214.

Shih, T.L., Lin, Y.L., Kuo, W.S., 2005. Highly stereoselective and stereospecific syntheses of a variety of quercitols from D- (-)-quinic acid. Tetrahedron 61, 1919–1924. https://doi.org/10.1016/j.tet.2004.11.084.

Tangmouo, J.G., Ho, R., Lannang, A.M., Komguem, J., Messi, B.B., Lontsi, A.T., Lontsi, D., Hostettmann, K., 2009. Norbergenin derivatives from the stem bark of *Diospyros sanza-minika* (Ebenaceae) and their radical scavenging activity. Phytochem. Lett. 2, 192–195. https://doi.org/10.1016/j.phytol.2009.07.001.

Tangmouo, J.G., Lontsi, D., Ngounou, F.N., Kuete, V., Meli, A.L., Manfouo, R.N., Kamdem, H.W., Sup, W.Y., Tane, P., Beng, V.P., Sondengam, B.L., Connolly, J.D., 2005. Diospyrone, a new coumarinylbinaphthoquinone from *Diospyros canaliculata* (Ebenaceae): structure and antimicrobial activity. Bull. Chem. Soc. Ethiopia 19, 81–88.

Tangmouo, J.G., Meli, A.L., Komguem, J., Kuete, V., Ngounou, F.N., Lontsi, D., Beng, P.V., Choudhary, M.I., Sondengam, B.L., 2006. Crassiflorone, a new naphthoquinone from *Diospyros crassiflora* (Hien). Tetrahedron Lett. 47, 3067–3070. https://doi.org/10.1016/j.tetlet.2006.03.006.

Biochemical Systematics and Ecology 100 (2022) 104373

Contents lists available at ScienceDirect

Biochemical Systematics and Ecology

journal homepage: www.elsevier.com/locate/biochemsyseco

Chemical constituents from *Diospyros fragrans* Gürke (Ebenaceae)

Nathalie S. Jouwa Tameye [a,b], Carine Mvot Akak [a,**], Georges Bellier Tabekoueng [b,c,*], Pierre Mkounga [a], Gabin Thierry M. Bitchagno [d], Bruno N Lenta [e], Norbert Sewald [b], Augustin E. Nkengfack [a]

[a] Department of Organic Chemistry, Faculty of Science, University of Yaoundé I, P.O. Box: 812, Yaoundé, Cameroon
[b] Organic and Bioorganic Chemistry, Faculty of Chemistry, Bielefeld University, D-33501, Bielefeld, Germany
[c] Department of Chemistry, Faculty of Science, University of Douala, 24157, Douala, Cameroon
[d] Department of Organic Chemistry, Faculty of Science, University of Dschang, P.O. Box 67, Dschang, Cameroon
[e] Department of Chemistry, Higher Teacher Training College, University of Yaoundé I, P. O. Box 47, Yaoundé, Cameroon

ARTICLE INFO

Keywords:
Diospyros fragrans
Ebenaceae
Naphtalenone
Chemotaxonomic relevance
Cytotoxicity
Antibacterial

ABSTRACT

A new naphtalenone derivative named fragranone, alongside seventeen known compounds: ten triterpenoids, one monoglycerol, one polyterpenoid, one carotenoid, two steroids and two polyols were isolated from the leaves and roots of *Diospyros fragrans*. Four semi-synthetic derivatives obtained from the acetylation and allylation of betulinic acid, allylation of ursolic acid and acetylation of vismiaefolic acid are also reported. The structures of the compounds were established using their MS and NMR spectral data. The chemotaxonomic relevance of the compounds is also discussed in this paper. The extracts, as well as the isolates and the semi-synthetic compounds were evaluated for their antibacterial and cytotoxic activities. The obtained results showed a moderate antibacterial activity for myrtifolic acid and the semi-synthetic compound betulinic acid acetate against *Bacillus subtilis* DSMZ 704 with a diameter zone of inhibition of 9 and 10 mm, respectively. Ursolic acid and corosolic acid exhibited a moderate cytotoxicity against human colorectal adenocarcinoma cells HT-29 and the cervix carcinoma cells KB-3-1 with inhibitory concentration 50 values of 34.4 and 50.9 μM for ursolic acid, and 16.5 and 14.6 μM for corosolic acid, respectively.

1. Subject and source

Diospyros fragrans is a small tree reaching a height of 15 m. This species is one of the 36 species of *Diospyros* found in the wettest areas of dense forests (Letouzey and White, 1970). The *Diospyros* genus belongs to the Ebenaceae family, consisting of approximately 500 species of trees and shrubs, distributed in tropical and subtropical regions of the world (Duangjai et al., 2006). Plants of this genus have various ethnomedicinal applications, including treatment of dysentery, whooping cough, hemorrhages, leprosy, fungal infections, incontinence, rheumatoid arthritis, cardiovascular disorders, and various types of cancers (Maroyi, 2018; Rauf et al., 2017). They are a rich source of bioactive compounds belonging to triterpenoids, naphthoquinones, benzopyrones, naphthalene-based aromatics, polyphenols, and carotenoids (Jouwa et al., 2020; Rauf et al., 2017; Mallavadhani et al., 1998). In continuation of our search for bioactive substances from *Diospyros*, the leaves and roots of *D. fragrans* were collected for analysis in December 2018 at Abang, Centre region of Cameroon. It was identified at the Cameroon National Herbarium where a voucher specimen was conserved with reference number 60166 HNC.

2. Previous work

Pentacyclic triterpenoids, specifically the lupane, ursane, and oleanane types, as well as 1,4- naphthoquinones have long served as the chemotaxonomic markers of the *Diospyros* genus (Mallavadhani et al., 1998). However, a few 1,4-naphtoquinone derivatives have been isolated from Cameroonian *Diospyros* species (Lenta et al., 2015; Tangmouo et al., 2006), while several pentacyclic triterpenoids (Dongmo et al., 2018; Feusso et al., 2017) and norbergenin and bergenin derivatives were also obtained (Akak et al., 2013; Jouwa et al., 2020; Tangmouo et al., 2009). Extracts and secondary metabolites isolated from *Diospyros*

* Corresponding author. Organic and Bioorganic Chemistry, Faculty of Chemistry, Bielefeld University, D-33501, Bielefeld, Germany.
** Corresponding author.
E-mail addresses: mvotcarine@yahoo.fr (C. Mvot Akak), bellier_tab@yahoo.fr (G.B. Tabekoueng).

https://doi.org/10.1016/j.bse.2021.104373
Received 11 May 2021; Received in revised form 30 November 2021; Accepted 2 December 2021
0305-1978/

species have shown remarkable antimicrobial and cytotoxic activities (Cai et al., 2000; Hazra et al., 2014; Tangmouo et al., 2006; Kuete et al., 2009; Quintal-Novelo et al., 2013; Rauf et al., 2017; Jouwa et al., 2020). The great diversity of the chemistry and pharmacology of *Diospyros* species has tilted our attention towards *D. fragrans*, which has not yet been subjected to chemical and pharmacological investigations. The present work thus reports the isolation and structural elucidation of one unreported naphtalenone derivative, fragranone **1**, together with seventeen known compounds, and four semi-synthetic derivatives obtained from the acetylation and allylation of betulinic acid, as well as the antibacterial and cytotoxic activities.

3. Present study

3.1. General experimental procedures

Optical rotations were measured on a JASCO DIP-3600 digital polarimeter (JASCO, Tokyo, Japan) using a 10 cm cell. IR spectra were recorded using a JASCO Fourier transform IR-420 spectrometer. UV spectra were recorded using a Hitachi UV 3200 spectrophotometer (Thermo Scientific, Waltham, MA, USA). NMR spectra were recorded on a Bruker DRX-500, 600 MHz spectrometer (Bruker, Rheinstetten, Germany). Chemical shifts are reported in δ (ppm) using tetramethylsilane (TMS) (Sigma-Aldrich, Munich, Germany) as internal standard, while coupling constants (J) were measured in Hz. ESI-MS spectra were recorded on an Agilent 6220 TOF LCMS mass spectrometer with perfluorokerosene as reference substance for ESI-HR-MS. Column chromatography was carried out on silica gel of 70–230 mesh (Merck, Darmstadt, Germany) and sephadex LH-20 (Sigma-Aldrich, Munich, Germany). Thin layer chromatography (TLC) was performed on Merck precoated silica gel 60 F_{254} aluminium foil and were revealed under UV light at 254 or 365 nm, followed by spraying with 10% H_2SO_4 and heating.

3.2. Extraction and isolation

The shade-dried and powdered leaves (3.2 kg) and roots (2.8 kg) of *D. fragrans* were macerated separately twice with 7.5 and 5.0 L of MeOH, respectively, at room temperature for 3 days. The resulting methanolic filtrates were concentrated to dryness under reduced pressure to give 101.7 g and 78.9 g of methanolic residues for the leaves and roots, respectively.

The root extract (77.0 g) was chromatographed over silica gel using open column eluted with a gradient of petroleum ether – ethyl acetate and ethyl acetate-methanol. 429 fractions of 200 mL were collected and concentrated under reduced pressure on a rotary evaporator and then combined based on thin layer chromatography (TLC) into 26 subfractions labelled J_1–J_{26}. Fraction J_{20} (PE-EtOAc 3:2) was chromatographed over sephadex LH-20 and eluted with MeOH to afford a mixture of three compounds. Preparative TLC eluting with PE-EtOAc 1:1 was then further used to obtain fragranone [(**1**), 2.1 mg] as a light brown oil. Fraction J_6 (PE-EtOAc 19:1) was further chromatographed over sephadex LH-20 with an isocratic solvent system of CH_2Cl_2–MeOH 1:1 to afford α-tocopherol [(**14**), 3.3 mg] as a colourless oil. Using MeOH as eluent, 1-*O*-(28-hydroxyoctacosanoyl)-glycerol [(**12**), 4.1 mg] was obtained in like manner as α-tocopherol (**14**) from fraction J_{18} (PE-EtOAc 3:2). Lupeol [(**2**), 75.2 mg], the mixture of β-sitosterol and stigmasterol [(**17**), 62.2 mg], betulinic acid [(**3**), 143.1 mg], ursolic acid [(**4**), 28.1 mg], vismiaefolic acid [(**5**), 12.7 mg], and the mixture of β-sitosterol-3-*O*-β-*D*-glucopyranoside and stigmasterol-3-*O*-β-*D*-glucopyranoside [(**18**), 113.2 mg] precipitated as white powders from fractions J_5 (PE-EtOAc 19:1), J_8 (PE-EtOAc 37:3), J_{14} (PE-EtOAc 33:7), J_{15} (PE-EtOAc 4:1), J_{21} (PE-EtOAc 1:1) and J_{22} (PE-EtOAc 2:3) respectively. Finally, methyl-β-D-glucopyranoside [(**15**), 63.1 mg] was obtained as clear crystals from fraction J_{24} (EtOAc-MeOH 9:1).

A portion of the leaf extract (100.0 g) was fractionated using open silica gel column to yield fractions F_1 (PE-EtOAc 3:1, 23.5 g), F_2 (PE-EtOAc 1:1, 14.2 g), F_3 (EtOAc, 16.2 g) and F_4 (EtOAc-MeOH 3:1, 27.7 g). Fraction F_1 was dissolved in methanol, adsorbed onto silica gel (70–230 mesh) and subjected to purification using open column chromatography, eluting with petroleum ether and ethyl acetate in increasing polarity. A total of 182 fractions of 100 mL each were collected, monitored by thin layer chromatography (TLC), and then pooled into 18 subfractions labelled H_1–H_{18}. Subfraction H_4 was eluted from the column with a mixture of PE-EtOAc 19:1 to yield lupeol [(**2**), 42.2 mg]. Subfraction H_{15} was eluted with a mixture of PE-EtOAc 3:1 to afford ursolic acid [(**4**), 174.3 mg]. Subfractions H_8 and H_{12} were eluted with PE-EtOAc 17:3 to yield myrtifolic acid [(**7**), 9.1 mg] and betulinic acid [(**3**), 123.2 mg] respectively. Subfraction H_6 eluting with PE-EtOAc 9:1, afforded a mixture of β-sitosterol and stigmasterol [(**17**), 36.1 mg]. Subfraction H_2 was subjected to column chromatography over silica gel with an isocratic solvent system of PE-EtOAc 19:1 to give β-amyrin acetate [(**11**), 4.1 mg]. Uvaol [(**8**), 12.3 mg] was obtained by purification of subfraction H_{10} over silica gel column with PE-EtOAc 9:1.

Fractions F_2 and F_3 (30.4 g) were combined on the basis of their TLC profiles and further subjected to silica gel open CC, eluting with a gradient of PE-EtOAc, followed by EtOAc-MeOH to afford 229 fractions of 100 mL each. On the basis of their TLC profiles, these fractions were combined into 24 subfractions (I_{1-24}). Subfractions I_5 (PE-EtOAc 7:3), I_{14} (PE-EtOAc 2:3), I_{16} (PE-EtOAc 1:3), and I_{22} (EtOAc-MeOH 19:1) directly precipitated to afford corosolic acid [(**6**), 7.2 mg], a mixture of stigmasterol-3-*O*-β-*D*-glucopyranoside, and β-sitosterol-3-*O*-β-*D*-glucopyranoside [(**18**), 13.0 mg], 5-*O*-methylinositol [(**16**), 18.1 mg], and methyl- β-*D*-glucopyranoside [(**15**), 76.8 mg], respectively. Subfraction I_2 (PE-EtOAc 4:1) was chromatographed over silica gel with an isocratic solvent system of PE-EtOAc 9:1 to afford a mixture of two compounds, which were subsequently eluted with methanol over sephadex LH-20 to yield a red powder identified as lutein [(**13**), 3.1 mg]. Oleanolic acid [(**9**), 2.3 mg] was obtained after purification of subfraction I_3 (PE-EtOAc 3:1) over silica gel with PE-EtOAc 9:1. Similarly, subfractions I_9 and I_{12} were purified with PE-EtOAc 3:1 to yield hederagenin [(**10**), 6.2 mg], and vismiaefolic acid [(**5**), 55.4 mg], respectively.

3.3. Identification of compounds

Compound **1** was isolated as a brown oil. Its positive mode HR-ESIMS showed the pseudo-molecular ion peak $[M+H]^+$ at m/z 193.0860 (calcd. for $C_{11}H_{13}O_3^+$ m/z 193.0859), which is in agreement with the molecular formula $C_{11}H_{12}O_3$, implying six double bond equivalents. The UV spectrum of **1** exhibited two absorption maxima at 231 and 279 nm, typical of naphthalene derivatives (Ganapaty et al., 2006). Its IR spectrum showed vibration bands due to hydroxy group (3270 cm^{-1}), benzylic ketone (1646 cm^{-1}) and benzene ring (1577, 1465 cm^{-1}). The ^1H NMR and HSQC spectra of compound **1** displayed an AX type spin-system ascribable to two *meta* coupled aromatic protons at δ_H 6.56 (d, J = 2.5 Hz)/δ_C 114.8 and δ_H 6.54 (d, J = 2.5 Hz)/δ_C 118.9, and a low field aromatic methyl signal at δ_H 2.54 (s)/δ_C 23.9. The spectra also displayed a hydroxymethine proton and carbon resonance at δ_H 4.22 (m)/δ_C 67.0, and four diastereotopic protons of two methylene groups at δ_H 2.58 (dd, J = 16.5 and 8.4 Hz); 2.83 (ddd, J = 16.5, 4.0 and 1.4 Hz)/δ_C 49.9 and δ_H 2.91 (dd, J = 15.9 and 7.9 Hz); 3.15 (dd, J = 15.9 and 4.0 Hz)/δ_C 40.5. In addition, three other aromatic quaternary carbons at δ_C 145.6, 146.9, and 124.3, alongside a hydroxylated aromatic carbon at δ_C 163.1 and a benzylic ketone at δ_C 199.5 were present on the ^{13}C NMR spectrum of **1**. All the spin systems mentioned herein, especially those of the hydroxymethine with the two methylene groups have been highlighted on the ^1H–^1H COSY spectrum (Fig. 2) of **1**. Indeed, homonuclear correlations of the hydroxymethine proton at δ_H 4.22 with both methylene groups at δ_H 2.91/3.15 and δ_H 2.58/2.83 were suggestive of a 1, 3-disubstituted propan-2-ol moiety. Their vicinities were unambiguously established using HMBC cross peaks (Fig. 2) of the methylene protons at δ_H 2.91 and 3.15 with the aromatic quaternary carbons at δ_C

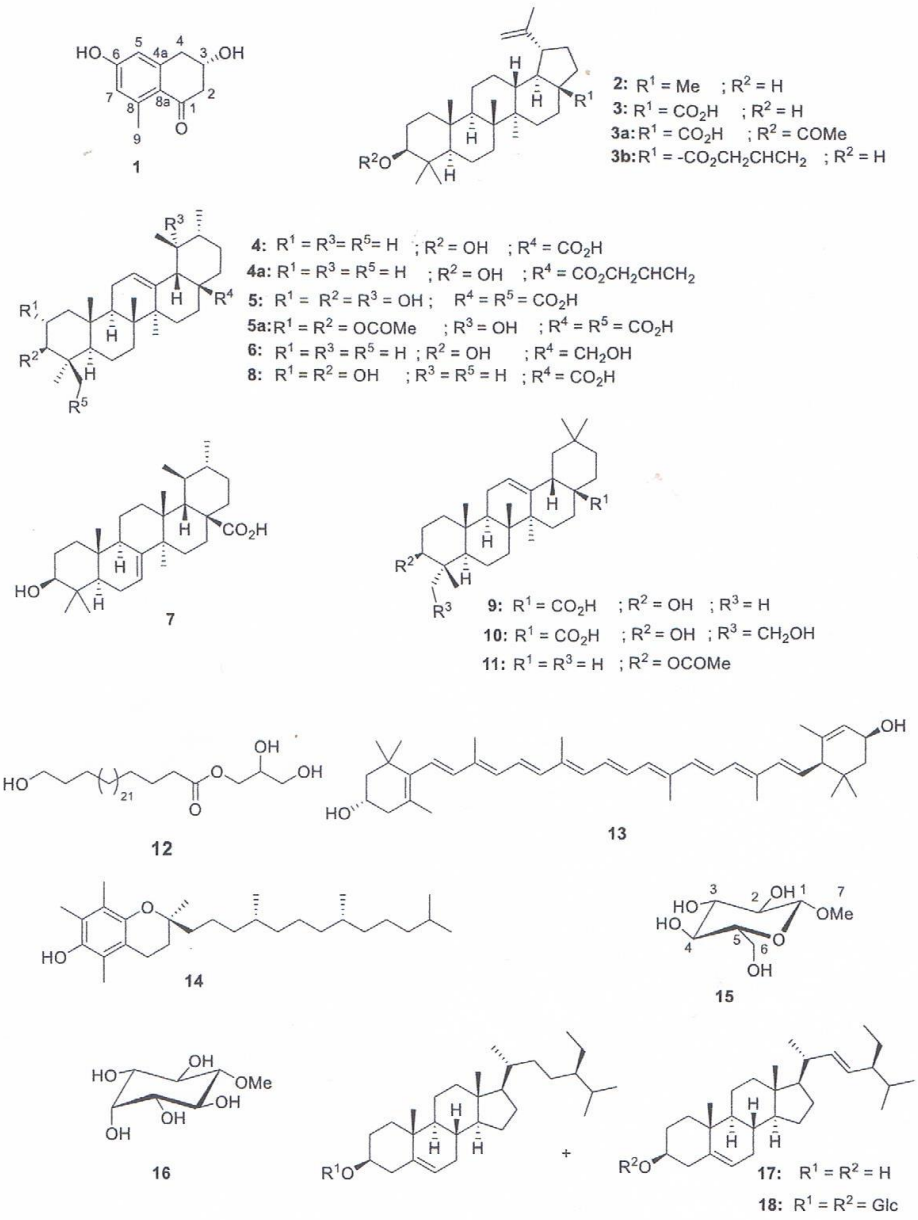

Fig. 1. Structures of compounds 1–18.

124.3 and 146.9, and also of the other methylene protons at δ_H 2.58 and 2.83 with the ketone at δ_C 199.5, supporting a ring fusion of both the aromatic and the aliphatic chain leading to a naphtalenone skeleton. A methyl and a hydroxy group were located respectively at C-8 and C-6 positions on the naphtalenone ring based on the HMBC cross peaks observed between the aromatic proton at δ_H 6.54 and the carbons at δ_C 124.3, 114.8 and 23.9; the aromatic proton at δ_H 6.56 and the carbons at δ_C 124.3, 118.9, 163.1 and 40.5, and the methyl proton at δ_H 2.54 and the carbons at δ_C 124.3, 145.6 and 118.9. The equatorial orientation of the hydroxyl group on the chiral carbon C-3 in **1** (Fig. 3) was established from the observed axial-axial coupling constants of both methylene protons H-2 (δ_H 2.58) and H-4 (δ_H 2.91) with the hydroxymethine proton H-3 (δ_H 4.22) (Table 1, Fig. 3). From the above spectroscopic data, compound **1** was identified as the new derivative 3,6-dihydroxy-8-methyl-3,4-dihydro-1(2*H*)-naphthalenone, trivially named fragranone.

By comparison of their spectroscopic data with those reported in the literature (Fig. 1), the seventeen known compounds were identified as

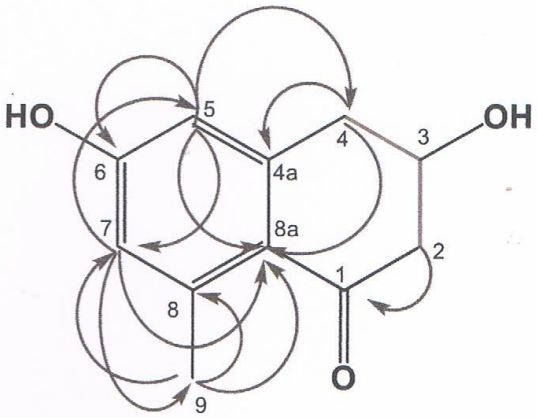

Fig. 2. Key HMBC (Fuchsia) and COSY (Green) correlations of compound 1. **(For interpretation of the references to colour in this figure legend, the reader is referred to the Web version of this article.)**

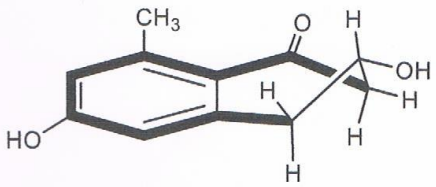

Fig. 3. Spatial conformation of fragranone (1).

Table 1
NMR spectroscopic data[a] of fragranone (1).

Position	δ_H, mult (*J* in Hz)	δ_C, mult
1	–	199.5, C
2	2.58, dd (16.5, 8.4) 2.83, ddd (16.5, 4.0, 1.4)	49.9, CH_2
3	4.22, m	67.0, CH
4	2.91, dd (15.9, 7.9) 3.15, dd (15.9, 4.0)	40.5, CH_2
4a	–	146.9, C
5	6.56, d (2.5)	114.8, CH
6	–	163.1, C
7	6.54, d (2.5)	118.9, CH
8	–	145.6, C
8a	–	124.3, C
9	2.54, s	23.9, CH_3

[a] Chemical shift measured in CD_3OD, at 600 MHz for ^1H and 150 MHz for ^{13}C using TMS as internal standard(δ in ppm, *J* in Hz).

lupeol (**2**) (Jamal et al., 2008), betulinic acid (**3**) (Haque et al., 2013), ursolic acid (**4**) (Seebacher et al., 2003), vismiaefolic acid (**5**) (Araújo et al., 1990), corosolic acid (**6**) (Hou et al., 2009), myrtifolic acid (**7**) (Meksuriyen et al., 1986), uvaol (**8**) (El-Shiekh et al., 2017), oleanolic acid (**9**) (Verma et al., 2013), hederagenin (**10**) (Joshi et al., 1999), β-amyrin acetate (**11**) (Maurya et al., 2012), 1-*O*-(28-hydroxyoctacosanoyl)glycerol (**12**) (Mukherjee et al., 1994), lutein (**13**) (Aro et al., 2019), α-tocopherol (**14**) (Han et al., 2012), 5-*O*-methyl--myo-inositol (**16**) (Mukherjee and De Medeiros, 1988), mixture of β-sitosterol and stigmasterol (**17**) (Sadikun et al., 1996), mixture of β-sitosterol-3-*O*-β-D-glucopyranoside and stigmasterol-3-*O*-β-D-glucoside (**18**) (Sadikun et al., 1996), and methyl-β-D-glucopyranoside (**15**) (Aubert et al., 2004). In addition, the ^{13}C NMR data of methyl-β-D-glucopyranoside (**15**) are reported here for the first time (Table 2).

3.4. Fragranone (1)

Brownish oil; $[\alpha]_D^{20}$: −8.1 (c 0.166, MeOH); IR $\bar{\upsilon}_{max}$ 3270, 2955, 2925, 1732, 1646, 1601 cm^{-1}; UV λ_{max} nm (log ε) 231 (4.06), 279 (4.10); ^1H NMR (600 MHz) and ^{13}C NMR (150 MHz) data in CD_3OD, see Table 1; HRESIMS: *m/z* 193.08605 (calcd. for $C_{11}H_{13}O_3$: *m/z* 193.08647).

3.5. Acetylation of betulinic acid and vismiaefolic acid

20.0 mg (0.044 mmol) of betulinic acid (**3**) were dissolved in 2 mL (24.9 mmol) of pyridine and introduced into a conical flask together with 2 mL (21.2 mmol) of acetic anhydride. The mixture obtained was subjected to stirring at room temperature for 12 h. After that, 20.0 mL of distilled water was added to the reaction mixture and the organic part was extracted using dichloromethane. Evaporation of the organic portion on a rotative evaporator yielded an oily mixture. This mixture was further separated by column chromatography using silica gel and an isocratic solvent system of PE-EtOAc 9:1 to afford betulinic acid acetate (**3a**) as a white powder (10.9 mg, 0.0218 mmol). Using the same procedure and an isocratic solvent system of PE-EtOAc 3:1, 3.3 mg (0.0054 mmol) of vismiaefolic acid diacetate (**5a**) was obtained from 10 mg (0.0193 mmol) of vismiaefolic acid (**5**).

3.6. Allylation of betulinic acid and ursolic acid

Betulinic acid [(**3**), 20.0 mg, 0.0438 mmol] and 500 mg (12.5 mmol) of sodium hydroxide were dissolved in 10.0 mL of anhydrous acetone. Then 4.0 mL (46.7 mmol) of allyl bromide was introduced to the medium and the reaction mixture was agitated for 4 h at 70 °C. 20.0 mL of distilled water were added and the mixture was extracted with dichloromethane. After evaporation on a rotative evaporator, the dry sample obtained was adsorbed onto silica gel and separated using silica gel CC with PE-EtOAc 17:3 as eluent to afford 28-allyl betulinic acid [(**3b**), 7.1 mg, 0.0143 mmol] as a colourless oil. The same procedure was used to obtain 28-allyl ursolic acid [(**4a**), 4.1 mg, 0.00825 mmol] from 10.0 mg (0.0219 mmol) of ursolic acid (**4**).

3.7. Antibacterial assay

The leaves and root extracts of *D. fragrans* as well as compounds **1–8**, **12–13**, **15** and the semi-synthetic compounds **3a**, **3b**, **4a**, and **5a** were evaluated for their antibacterial activity against three Gram-positive bacteria (*Bacillus subtilis* DSMZ 704, *Micrococcus luteus* DSMZ 1605, and *Staphylococcus warneri* DSMZ 20036) and two Gram-negative bacteria (*Escherichia coli* DSMZ 1058 and *Pseudomonas agarici* DSMZ 11810) using agar disk diffusion method with gentamicin as reference. A certain level of activity was observed for the root extract at a concentration of

Table 2
NMR spectroscopic data[a] of methyl-β-D-glucopyranoside (**15**).

Position	δ_H, mult (*J* in Hz)	δ_C, mult
1	4.19, d (7.8)	105.5, CH
2	3.18, dd (7.8, 9.2)	75.1, CH
3	3.37, m	78.0, CH
4	3.30, m	78.1, CH
5	3.29, m	71.6, CH
6	3.69, d (4.4, 9.5) 3.89, m	62.9, CH_2
7	3.55, s	57.4, CH_3

[a] Chemical shift measured in CD_3OD, at 500 MHz for ^1H and 125 MHz for ^{13}C using TMS as internal standard(δ in ppm, *J* in Hz).

20 μg/mL against *Escherichia coli* DSMZ 1058 and *Bacillus subtilis* DSMZ 704 with inhibition zone values of 8 mm and 7 mm, respectively, while the leaf extract did not exhibit any activity. The most active compounds at a concentration of 0.5 μg/mL were found to be myrtifolic acid (**7**) and the semi-synthetic derivative betulinic acid acetate (**3a**) against *Bacillus subtilis* DSMZ 704, with inhibition zone values of 9 mm and 10 mm, respectively. Uvaol (**8**) also exhibited a certain level of activity against *Bacillus subtilis* DSMZ 704 with inhibition zone values of 7 mm. In addition, the acetylated derivative of vismiaefolic acid (**5a**) as well as the acetylated derivative of betulinic acid (**3a**) also exhibited some level of activity at a concentration of 0.5 μg/mL against *Pseudomonas agarici* DSMZ 11810, with inhibition zone values of 7 mm each (see Table 3). A comparison of the antibacterial activity of the semi-synthetic compounds **3a** and **5a** with their respective precursors **3** and **5** suggested that acetylation at C-3 of betulinic acid and C-2 of vismiaefolic acid was favorable for the antibacterial activity. In contrast, allylation at C-28 of betulinic acid and ursolic acid did not improve the activity.

3.8. Cytotoxic assay

The same samples were subjected to cytotoxic activity assay against cervix carcinoma cells KB-3-1 and human colorectal adenocarcinoma cells HT-29 using griseofulvin as positive control. Only ursolic acid and corosolic acid exhibited moderate activities (Kuete et al., 2017) on both cells over the range of 1–2000 μM concentration, with IC_{50} values of 34.4 μM and 50.9 μM for ursolic acid, and 16.5 μM and 14.6 μM for corosolic acid, respectively, against HT-29 and KB-3-1. Furthermore, corosolic acid was more active than the positive control griseofulvin. These results provide evidence that ursane-type triterpene acid can be used as lead compounds in the production of anti-cancerous compounds. Both acetylation and allylation reactions performed on compounds **3**, **4**, and **5** did not improve the cytotoxicity. A loss of activity was observed for compound **4a**, suggesting that allylation at C-28 was not favorable for the cytotoxicity (see Table 4).

4. Chemotaxonomic significance

In this paper, we report the isolation and structure elucidation of a new naturally occurring naphtalenone derivative (**1**), together with seventeen known compounds including two lupane (**2–3**), five ursane (**4–8**), and three oleanane (**9–11**) type triterpenoids, one polyterpene (**14**), one monoglyceride (**12**), one carotenoid (**13**), two polyols (**15–16**) and two steroids (**17–18**) from *Diospyros fragrans*. All the isolates (**1–18**) are newly isolated from this species while myrtifolic acid (**7**) as well as 1-*O*-(28-hydroxyoctacosanoyl)glycerol (**12**), β-amyrin acetate (**11**), 5-*O*-methyl-myo-inositol (**16**) and methyl-β-D-glucopyranoside (**15**) are herein reported for the first time from the Ebenaceae family. Considering previous studies, some compounds isolated from this species have already been isolated from other Ebenaceae species. Lupeol (**2**) was previously isolated from *D. canaliculata* (Dzoyem et al., 2011), *D. gilletii* (Jouwa et al., 2020), *D. maritima* (Chang et al., 2009), *D. conocarpa* (Feusso et al., 2016), *D. glandulosa* (Thanakijcharoenpath and Theanphong, 2007), *D. cuneata* (Quintal-Novelo et al., 2013), *D. mespiliformis* (Mohamed et al., 2009), *D. longiflora* (Dongmo et al., 2018), and *D crassiflora* (Tangmouo et al., 2006). Betulinic acid (**3**) was found to be present in *D. longiflora* (Dongmo et al., 2018), *D. maritima* (Chang et al., 2009), *D. gilletii* (Jouwa et al., 2020), *D. canaliculata* (Lenta et al., 2015), *D. mannii* (Feusso et al., 2017), *D. conocarpa* (Feusso et al., 2016), *D. mespiliformis* (Mohamed et al., 2009), *D. crassiflora* (Akak et al., 2010; Tangmouo et al., 2006), *D. kaki* (Guang et al., 2000), and *D. filipendula* (Wisetsai et al., 2019). Ursolic acid (**4**) was previously reported in *D. gracilipes* (Rasamison et al., 2016), *D. crassiflora* (Akak et al., 2010), *D. gilletii* (Jouwa et al., 2020), and *D. glandulosa* (Thanakijcharoenpath and Theanphong, 2007). Vismiaefolic acid (**5**) was previously isolated from *D. decandra* (Nareeboon et al., 2006). Corosolic acid (**6**) was previously reported from *D. gracilipes* (Rasamison et al., 2016), *D. gilletii* (Jouwa et al., 2020). Uvaol (**8**) was previously reported from *D. iturensis* (Feusso et al., 2020), *D. melanoxylon* (Mallavadhani et al., 2001), and *D. kaki* (Guang et al., 2000). Oleanolic acid (**9**) was previously reported from *D. melanoxylon* (Mallavadhani et al., 2001), *D. glandulosa* (Thanakijcharoenpath and Theanphong, 2007), and *Diospyros kaki* (Guang et al., 2000). Hederagenin (**10**) was previously reported from *D. mannii* (Feusso et al., 2017), while lutein (**13**) was obtained from *D. digyna* (Yahia et al., 2011). α-tocopherol (**14**) was reported from *D. maritima* (Chang et al., 2009). Previous phytochemical studies revealed that lupane, ursane, and oleanane-type triterpenoids are the major pentacyclic triterpenes found in the *Diospyros* genus (Chen et al., 2009; Feusso et al., 2017; Mallavadhani et al., 1998). Thus, the isolation of ten pentacyclic triterpenes from *D. fragrans* confirms the fact that these metabolites are chemotaxonomic markers of the genus *Diospyros*. Furthermore, from these ten pentacyclic triterpenes, seven were found to be acid triterpenes. Regarding these results and those previously reported in the literature, evidence appears that *Diospyros* species synthetize and accumulate in large amount acid triterpenes, and led us to suggest that acid triterpenes are chemical markers of the genus *Diospyros*. Moreover, it is noteworthy that ursane-type triterpenoids isolated from *Diospyros* species were mostly urs-12-ene type scaffolds, except for bauerenol, an urs-7-ene acid triterpene previously isolated from *D. ebenum, D. kirkii, D. melanoxylon, D. mespiliformis*, and *D. sylvatica* (Mallavadhani et al., 1998), closely related to myrtifolic acid (**7**) isolated from *D. fragrans*. In addition, myrtifolic acid (**7**) has so far been reported in only four other plants, namely *Mesua myrtifolia* (Clusiaceae) (Gunasekera and Sultanbawa, 1977), *Davidsonia pruriens* (Cunoniaceae) (Meksuriyen et al., 1986), *Ophiorrhiza grandibracteolata* (Rubiaceae) (Jing et al., 2009), and *Biophytum petersianum* (Oxalidaceae) (Sembiring and Darwati, 2014; Darwati et al., 2019). A few naphthalene-based aromatics have been isolated from *Diospyros* species and some of them were found to be dimers or trimers of naphthalene

Table 3
Diameter zone of inhibition in mm of extracts and some isolated compounds from *D. fragrans* against bacteria.

Samples	Conc. (mg/mL)	Ec	Bs	Pa	Ml	St
Leaves crude extract	20	–	–	–	–	–
Roots crude extract	20	8	7	–	–	–
1	0.5	–	–	–	–	–
2	0.5	–	–	–	–	–
3	0.5	–	–	–	–	–
4	0.5	–	–	–	–	–
5	0.5	–	–	–	–	–
6	0.5	–	–	–	–	–
7	0.5	–	9	–	–	–
8	0.5	–	7	–	–	–
12	0.5	–	–	–	–	–
13	0.5	–	–	–	–	–
15	0.5	–	–	–	–	–
3a	0.5	–	10	7	–	–
3b	0.5	–	–	–	–	–
4a	0.5	–	–	–	–	–
5a	0.5	–	–	7	–	–
Gentamycin[c]	0.5	20	23	17	19	19

Ec: *E. coli*, Bs: *B. subtillis*, Pa: *P. agarici*, Ml: *M. luteus*, St: *S. warneri*, -: not active.
[c] Positive control.

Table 4
Cytotoxic activities of ursolic acid and corosolic acid against KB-3-1 and HT-29 cell lines.

Compounds	IC_{50} (μM)	
	KB-3-1	HT-29
4	50.9	34.4
6	14.7	16.5
Griseofulvin[c]	17.0	21.0

[c] Positive control.

(Mallavadhani et al., 1998). An example of a naphthalenone monomer reported in *Diospyros* species is 3,4-dihydro-4β,6-dihydroxy-5-methoxy-2α-methyl-1(2*H*)-naphthalenone, isolated from *D. cauliflora* (Auamcharoen et al., 2009). Various naphthalene-based aromatics are assumed to be precursors of naphthoquinones, which is one of the most isolated classes of compounds from *Diospyros* species (Mallavadhani et al., 1998). Thus, the isolation of fragranone (**1**) from *D. fragrans* is of great biosynthetic significance as it confirms that *Diospyros* species synthesize and accumulate a large number of 1,4-naphthoquinone, which are amongst the chemotaxonomic markers of the genus.

In conclusion, this chemical study of the leaves and roots of *Diospyros fragrans* is valuable for the chemotaxonomy of the genus *Diospyros*. Indeed, it provides precious information regarding the chemical composition of a previously unstudied *Diospyros* species, confirming its position within the genus. The isolation of an urs-7-ene type triterpenoid (**7**) in *D. fragrans* established the presence of this skeleton in *Diospyros* species, thus highlighting its connection with other species within this genus.

Declaration of competing interest

The author declares that they have no known competing financial interests or personal relationships that could have appeared to influence the work reported in this paper.

Acknowledgments

The authors are thankful to the German Academic Exchange Service (DAAD) for financial support to the Yaoundé-Bielefeld Graduate School of Natural Products with Antiparasite and Antibacterial activities (YaBiNaPA), project N° 57316173. We thank Carmela Michalek for the biological tests.

Appendix A. Supplementary data

Supplementary data to this article can be found online at https://doi.org/10.1016/j.bse.2021.104373.

References

Akak, C.M., Djama, C.M., Nkengfack, A.E., Tu, P.F., Lei, L.D., 2010. New coumarin glycosides from the leaves of *Diospyros crassiflora* (Hiern). Fitoterapia 81, 873–877. https://doi.org/10.1016/j.fitote.2010.05.011.

Akak, C.M., Nkengfack, A.E., Tu, P.F., 2013. Norbergenin derivatives from *Diospyros crassiflora* (Ebenaceae). Nat. Prod. Commun. 8, 1575–1578. https://doi.org/10.1177/1934578X1300801119.

Araújo, F.W.L., Souza, M.P., Filbo, R.B., 1990. Vismiaefolic Acid, a new triterpene from *Vochysia vismiaefolia*. J. Nat. Prod. 53, 1436–1440. https://doi.org/10.1021/np50072a006.

Aro, A.O., Dzoyem, J.P., Awouafack, M.D., Selepe, A.M., Eloff, N.J., McGaw, L.J., 2019. Fractions and isolated compounds from *Oxyanthus speciosus* subsp. stenocarpus (Rubiaceae) have promising antimycobacterial and intracellular activity. BMC Compl. Alternative Med. 19, 1–11.

Auamcharoen, W., Kijjoa, A., Chandrapatya, A., Pinto, M.M., Silva, A.M.S., Naengchomnong, W., Herz, W., 2009. A new tetralone from *Diospyros cauliflora*. Biochem. Systemat. Ecol. 37, 690–692. https://doi:10.1016/j.bse.2009.10.004.

Aubert, S., Choler, P., Pratt, J., Douzet, R., Gout, E., Bligny, R., 2004. Methyl-β-D-glucopyranoside in higher plants: accumulation and intracellular localization in *Geum montanum* L. leaves and in model systems studied by ^{13}C nuclear magnetic resonance. J. Exp. Bot. 55, 2179–2189. https://doi.org/10.1093/jxb/erh235.

Cai, L., Wei, G.X., Van der Bijl, P., Wu, C.D., 2000. Namibian chewing stick, *Diospyros lycioides*, contains antibacterial compounds against oral pathogens. J. Agric. Food Chem. 48, 909–914. https://doi.org/10.1021/jf9909914.

Chang, C.-I., Chen, C.-R., Chiu, H.-L., Kuo, C.-L., Kuo, Y.-H., 2009. Chemical constituents from the stems of *Diospyros maritima*. Molecules 14, 5281–5288. https://doi.org/10.3390/molecules14125281.

Chen, G., Wang, Z.Q., Jia, J.M., 2009. Three minor novel triterpenoids from the leaves of *Diospyros kaki*. Chem. Pharm. Bull. 57, 532–535. https://doi.org/10.1248/cpb.57.532.

Darwati, I., Nurcahyanti, A., Trisilawati, O., Nurhayati, H., Bermawie, N., Wink, M., 2019. Anticancer potential of kebar grass (*Biophytum petersianum*), an Indonesian traditional medicine. IOP Conf. Ser. Earth Environ. Sci. 292, 1–8. https://doi:10.1088/1755-1315/292/1/012063.

Dongmo, J.D.D., Akak, C.M., Tala, M.F., Kedi, P.B.E., Azebaze, A.G.B., Vardamides, J.C., Laatsch, H., 2018. Longiflorol, a bergenin α-*d*-apioside from the stem bark of *Diospyros longiflora* and its antioxidant activity. Z. Naturforsch. B Chem. Sci. 73, 539–543. https://doi.org/10.1515/znb-2018-0019.

Duangjai, S., Wallnöfer, B., Samuel, R., Munzinger, J., Chase, M.W., 2006. Generic delimitation and relationships in Ebenaceae sensu lato: evidence from six plastid DNA regions. Am. J. Bot. 93, 1808–1827. https://doi.org/10.3732/ajb.93.12.1808.

Dzoyem, J.P., Kechia, F.A., Kuete, V., Pieme, A.C., Akak, C.M., Tangmouo, J.G., Lohoue, P.J., 2011. Phytotoxic, antifungal activities and acute toxicity studies of the crude extract and compounds from *Diospyros canaliculata*. Nat. Prod. Res. 25, 741–749. https://doi.org/10.1080/14786419.2010.531392.

El-Shiekh, R.A., AL-Mahdy, D.A., Hifnawy, M.S., Tzonova, T., Evain-Bana, E., Philippot, S., Bagrel, D., Abdelsattar, E.A., 2017. Chemical and biological investigation of *Ochrosia elliptica* Labill. cultivated in Egypt. Record Nat. Prod. 11, 552–557. https://doi.org/10.25135/rnp.70.17.03.049.

Feusso, H.M.F., Akak, C.M., Tala, M.F., Azebaze, A.G.B., Tsabang, N., Vardamides, J.C., Laatsch, H., 2016. Conocarpol, a new cycloartane triterpenoid from *Diospyros conocarpa*. Z. Naturforsch. 71, 935–940. https://doi.org/10.1515/znb-2016-0059.

Feusso, H.M.F., Akak, C.M., Tala, M.F., Azebaze, A.G.B., Vardamides, J.C., Laatsch, H., 2017. Mannic acid, a new *ent*-kaurane dimer diterpenoid and other chemical constituents from different parts of *Diospyros mannii*. Biochem. Systemat. Ecol. 74, 51–56. https://doi.org/10.1016/j.bse.2017.09.001.

Feusso, H.M.F., Dongmo, J.D.D., Djomkam, H.L.M., Akak, C.M., Lateef, M., Ahmed, A., Azebaze, A.G.B., Waffo, A.F.K., Ali, M.S., Vardamides, J.C., 2020. Chemicals constituents from leaves of *Diospyros iturensis* (Gürke) letouzey & F. White and their biological activities. Nat. Prod. Sci. 26, 311–316. https://doi.org/10.20307/nps.2020.26.4.311.

Ganapaty, S., Thomas, P.S., Karagianis, G., Waterman, P.G., Brun, R., 2006. Antiprotozoal and cytotoxic naphthalene derivatives from *Diospyros assimilis*. Phytochemistry 67, 1950–1956. https://doi.org/10.1016/j.phytochem.2006.05.039.

Guang, C., Suixu, X., Yi, S., 2000. Studies on the constituents of *Diospyros kaki* leaves (I). Chin. J. Med. Chem. 10, 298–299.

Gunasekera, S.P., Sultanbawa, M.U.S., 1977. Chemical investigation of Ceylonese plants. Part 20. Extractives of *Mesua myrtifolia*. Isolation and structure of a new triterpene hydroxy-acid, myrtifolic acid. J. Chem. Soc., Perkin Trans. 1, 6–10. https://doi.org/10.1039/P19770000006.

Han, Z., Luo, J., Kong, L.-Y., 2012. Two new tocopherol polymers from the seeds of *Euryale ferox*. J. Asian Nat. Prod. Res. 14, 743–747. https://doi.org/10.1080/10286020.2012.688956.

Haque, A., Siddiqi, M.M.A., Rahman, A.F.M.M., Hasan, C.M., Chowdhury, A.M.S., 2013. Isolation of betulinic acid and 2,3-dihydroxyolean-12-en-28-oic acid from the leaves of *Callistemon linearis*. Dhaka Univ. J. Sci. 61, 211–212. https://doi.org/10.3329/dujs.v61i2.17073.

Hazra, S., Ghosh, S., Kumar, A., 2014. Acetylamine derivative of diospyrin, a plant-derived binaphthylquinonoid, inhibits human colon cancer growth in *Nod*-Scid mice. Invest. N. Drugs 33, 22–31. https://doi.org/10.1007/s10637-014-0165-7.

Hou, W., Li, Y., Zhang, Q., Wie, X., Peng, A., Chen, L., Wie, Y., 2009. Triterpene acids isolated from *Lagerstroemia speciosa* leaves as α-glucosidase inhibitors. Phytother Res. 23, 614–618. https://doi.org/10.1002/ptr.2661.

Jamal, A.K., Yaacob, W.A., Din, L.B., 2008. A chemical study on *Phyllanthus reticulatus*. J. Phys. Sci. 19, 45–50.

Jing, L., Qi-shi, S., Wei, X., Shu-min, Y., 2009. Chemical studies on Ophiorrhiza grandibracteolata. NPRD 21, 433–434.

Joshi, B.S., Singh, K.L., Roy, R., 1999. Complete assignments of ^{1}H and ^{13}C NMR spectra of the pentacyclic triterpene hederagenin from *Nigella sativa* Linn. Magn. Reson. Chem. 3, 295–298. https://doi.org/10.1002/(SICI)1097-458X(199904)37:4<295::AID-MRC457>3.0.CO;2-Z.

Jouwa, N.S.T., Akak, C.M., Happi, G.M., Frese, M., Stammler, H.-G., Neumann, B., Lenta, B.N., Sewald, N., Nkengfack, A.E., 2020. Antioxidant norbergenin derivatives from the leaves of *Diospyros gilletii* De wild (Ebenaceae). Phytochem. Lett. 36, 63–67. https://doi.org/10.1016/j.phytol.2020.01.012.

Kuete, V., Mafodong, F.L.D., Celik, I., Fobofou, S.A.T., Ndontsa, B.L., Karaosmanoglu, O., Weissjohann, L.A., Tane, P., Koparal, A.T., Sivas, H., 2017. In *vitro* cytotoxicity of compounds isolated from *Desbordesia glaucescens* against human carcinoma cell lines. South Afr. J. Bot. 111, 37–43. https://doi.org/10.1016/j.sajb.2017.03.031.

Kuete, V., Tangmouo, J.G., Meyer, J.J.M., Lall, N., 2009. Diospyrone, crassiflorone and plumbagin: three antimycobacterial and antigonorrhoeal naphthoquinones from two *Diospyros* spp. Int. J. Antimicrob. Agents 34, 322–325. https://doi.org/10.1016/j.ijantimicag.2009.04.008.

Lenta, B.N., Ngamgwe, R.F., Kamdem, L.M., Ngatchou, J., Tantangmo, F., Antheaume, C., Kaiser, M., Ngouela, S., Tsamo, E., Sewald, N., 2015. Compounds from *Diospyros canaliculata* (Ebenaceae) and their antiparasitic activities. Int. Res. J. Pure Appl. Chem. 6, 56–65. https://doi.org/10.9734/IRJPAC/2015/15267.

Letouzey, R., White, F., 1970. Flore du Cameroun, Ebénacées et Ericacées, museum nationale d'histoire naturelle, vol. 16. Buffon, Paris.

Mallavadhani, U.V., Panda, A.K., Rao, Y.R., 1998. Pharmacology and chemotaxonomy of *Diospyros*. Phytochemistry 49, 901–951. https://doi.org/10.1016/S0031-9422(97)01020-0.

Mallavadhani, U.V., Panda, A.K., Rao, Y.R., 2001. *Diospyros melanoxylon* Leaves: a rich source of pentacyclic triterpenes. Pharm. Biol. 39, 20–24. https://doi.org/10.1076/phbi.39.1.20.5941.

Maroyi, A., 2018. *Diospyros lycioides* Desf.: review of its botany, medicinal uses, pharmacological activities and phytochemistry. Asian Pac. J. Trop. Biomed. 8, 130–136. https://doi.org/10.4103/2221-1691.225617.

Maurya, R., Srivastava, A., Shah, P., Siddiqi, M.I., Rajendran, S.M., Puri, A., Yadav, P.P., 2012. β-Amyrin acetate and β-amyrin palmitate as antidyslipidemic agents from *Wrightia tomentosa* leaves. Phytomedicine 19, 682–685. https://doi.org/10.1016/j.phymed.2012.03.013.

Meksuriyen, D., Nanayakkara, N.P.D., Phoebe, C.H., Cordell, G.A., 1986. Two triterpenes from *Davidsonia pruriens*. Phytochemistry 25, 1685–1689. https://doi.org/10.1016/S0031-9422(00)81236-4.

Mohamed, I.E., El Nur, E.B.E., Choudhary, M.I., Khan, S.N., 2009. Bioactive natural products from two sudanese medicinal plants: *Diospyros mespiliformis* and *Croton zambesicus*. Record Nat. Prod. 3, 198–203.

Mukherjee, K., Fujimoto, R.Y., Kakinuma, K., 1994. 1-(ω-Hydroxyfattyacyl)glycerols and two flavanols from Cinnamomum camphora. Phytochemistry 37, 1641–1643. https://doi.org/10.1016/S0031-9422(00)89583-7.

Mukherjee, R., De Medeiros, C.L.C., 1988. Stereoconfiguration of sequoyitol by high resolution ^{1}H NMR. Phytochemistry 27, 279–281. https://doi.org/10.1016/0031-9422(88)80633-2.

Nareeboon, P., Kraus, W., Beifuss, U., Conrad, J., Klaiber, I., Sutthivaiyakit, S., 2006. Novel 24-nor-, 24-nor-2,3-seco-, and 3,24-dinor-2,4-seco-ursane triterpenes from *Diospyros decandra*: evidences for ring A biosynthetic transformations. Tetrahedron 62, 5519–5526. https://doi.org/10.1016/j.tet.2006.03.034.

Quintal-Novelo, C., Moo-Puc, R.E., Chale-Dzul, J., Cáceres-Farfán, M., Mendez-Gonzalez, M., Borges-Argáez, R., 2013. Cytotoxic constituents from the stem bark of *Diospyros cuneata* Standl. Nat. Prod. Res. 27, 1594–1597. https://doi.org/10.1080/14786419.2012.738201.

Rasamison, V.E., Rakotondraibe, H.L., Razafintsalama, V., Rakotonandrasana, S., Rakotondrafara, A., Ratsimbason, M.A., Rafidinarivo, E., 2016. Chemical constituents from stems and leaves of *Diospyros gracilipes* Hiern and the antimicrobial and cytotoxic principles. J. Pharmacogn. Phytochem. 5, 109–113.

Rauf, A., Uddin, G., Patel, S., Khand, A., Halim, S.A., Bawazeer, S., Ahmad, K., Muhammad, N., Mubarak, M.S., 2017. *Diospyros*, an under-utilized, multi-purpose plant genus: a review. Biomed. Pharmacother. 91, 714–730. https://doi.org/10.1016/j.biopha.2017.05.012.

Sadikun, A., Aminah, I., Ismail, N., Ibrahim, P., 1996. Sterol and sterol glycosides from the leaves of *Gynura procumbens*. Nat. Prod. Sci. 2, 19–23.

Seebacher, W., Simic, N., Weis, R., Saf, R., Kunert, O., 2003. Complete assignments of ^{1}H and ^{13}C NMR resonances of oleanolic acid, 18α-oleanolic acid, ursolic acid and their 11-oxo derivatives. Magn. Reson. Chem. 41, 636–638. https://doi.org/10.1002/mrc.1214.

Sembiring, B., Darwati, I., 2014. Identification of chemical component of kebar grass accession (*Biophytum petersianum*) from Papua and Java. Bul. Penelit. Tanam. Rempah Obat. 24, 37–44. https://doi.org/10.21082/bullittro.v25n1.2014.37-44.

Tangmouo, J.G., Meli, A.L., Komguem, J., Kuete, V., Ngounou, F.N., Lontsi, D., Beng, P. V., Choudhary, M.I., Sondengam, B.L., 2006. Crassiflorone, a new naphthoquinone from *Diospyros crassiflora* (Hien). Tetrahedron Lett. 47, 3067–3070. https://doi.org/10.1016/j.tetlet.2006.03.006.

Tangmouo, J.G., Ho, R., Lannang, A.M., Komguem, J., Messi, B.B., Lontsi, A.T., Lontsi, D., Hostettmann, K., 2009. Norbergenin derivatives from the stem bark of *Diospyros sanza-minika* (Ebenaceae) and their radical scavenging activity. Phytochem. Lett. 2, 192–195. https://doi.org/10.1016/j.phytol.2009.07.001.

Thanakijcharoenpath, W., Theanphong, O., 2007. Triterpenoids from the stem of *Diospyros glandulosa*. Thai. J. Pharm. Sci. 31, 1–8.

Verma, S.C., Jain, C.L., Nigam, S., Padhi, M.M., 2013. Rapid extraction, isolation, and quantification of oleanolic acid from *Lantana camara* L. roots using microwave and HPLC-PDA techniques. Acta Chromatogr. 25, 181–199. https://doi:10.1556/achrom.25.2013.1.12.

Wisetsai, A., Schevenels, F.T., Lekphrom, R., 2019. Chemical constituents and their biological activities from the roots of *Diospyros filipendula*. Nat. Prod. Res. 35, 2739–2743. https://doi.org/10.1080/14786419.2019.1656630.

Yahia, E.M., Gutierrez-Orozco, F., Leon, C.A., 2011. Phytochemical and antioxidant characterization of the fruit of black sapote (*Diospyros digyna* Jacq.). Food Res. Int. 44, 2210–2216. https://doi:10.1016/j.foodres.2010.11.025.